

RECEIVED

MAR 24 1997

DOE/CE/23810-80

OSTI

THERMOPHYSICAL PROPERTIES OF HCFC ALTERNATIVES

Final Report

1 April 1994 - 31 October 1996

W.M. Haynes

Physical and Chemical Properties Division
National Institute of Standards and Technology
325 Broadway
Boulder, Colorado 80303

November 1996

Prepared for
The Air-Conditioning and Refrigeration Technology Institute
Under
ARTI MCLR Project Number 660-50800

This research project was supported in part by a grant from the U.S. Department of Energy, Office of Building Technology (Grant number DE-FG02-91CE23810: Materials Compatibilities and Lubricants Research on CFC-Refrigerant Substitutes). Federal funding supporting this project constitutes 93.57% of allowable costs. Funding from the air conditioning and refrigeration industry supporting the project consists of direct cost sharing of 6.43% of allowable costs; and significant in-kind contributions.

DISTRIBUTION OF THIS DOCUMENT IS UNLIMITED



MASTER

DISCLAIMER

U.S. Department of Energy and the air-conditioning and refrigeration industry support for the Materials Compatibility and Lubricants Research (MCLR) program does not constitute an endorsement by the U.S. Department of Energy, or by the air-conditioning and refrigeration industry, of the views expressed herein.

NOTICE

This report was prepared on account of work sponsored by the United States Government. Neither the United States Government, nor the Department of Energy, nor the Air Conditioning and Refrigeration Technology Institute, nor any of their employees, nor any of their contractors, subcontractors, or their employees, makes any warranty, expressed or implied, or assumes any legal liability or responsibility for the accuracy, completeness, or usefulness of any information, apparatus, product or process disclosed or represents that its use would not infringe privately-owned rights.

COPYRIGHT NOTICE

(for journal publication submissions)

By acceptance of this article, the publisher and/or recipient acknowledges the right of the U.S. Government and the Air-Conditioning and Refrigeration Technology Institute, Inc. (ARTI) to retain a nonexclusive, royalty-free license in and to any copyrights covering this paper.

DISCLAIMER

This report was prepared as an account of work sponsored by an agency of the United States Government. Neither the United States Government nor any agency thereof, nor any of their employees, make any warranty, express or implied, or assumes any legal liability or responsibility for the accuracy, completeness, or usefulness of any information, apparatus, product, or process disclosed, or represents that its use would not infringe privately owned rights. Reference herein to any specific commercial product, process, or service by trade name, trademark, manufacturer, or otherwise does not necessarily constitute or imply its endorsement, recommendation, or favoring by the United States Government or any agency thereof. The views and opinions of authors expressed herein do not necessarily state or reflect those of the United States Government or any agency thereof.



DISCLAIMER

**Portions of this document may be illegible
in electronic image products. Images are
produced from the best available original
document.**

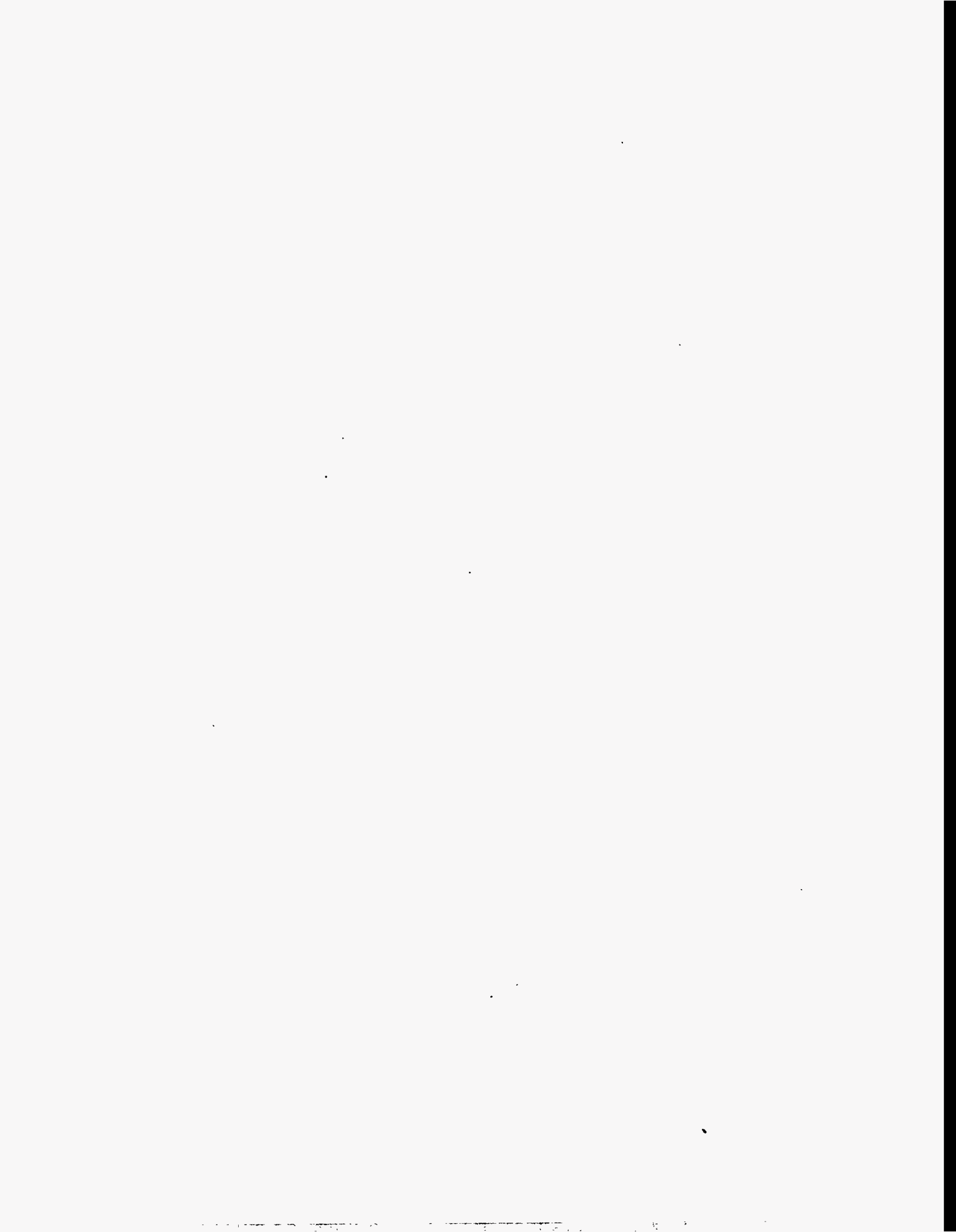


TABLE OF CONTENTS

	<u>Page</u>
LIST OF FIGURES	iii
LIST OF TABLES	vi
ABSTRACT	1
SCOPE	1
INTRODUCTION	2
SIGNIFICANT RESULTS	2
Thermophysical Properties of R32/125/134a and Its Constituent Binaries	2
R32/134a	3
R32/125	3
R125/134a	4
R32/125/134a	4
Mixtures with HFC-143a	5
R32/143a	5
R125/143a	6
R143a/134a	6
Mixtures with HC-290	7
R32/290	7
R125/290	8
R134a/290	8
HFC-41 and R41/744	9
HFC-41	9
R41/744	11
REFPROP 6.0 and the Lemmon-Jacobsen Model	12
COMPLIANCE WITH AGREEMENT	14
PRINCIPAL INVESTIGATOR EFFORT	14
REFERENCES	15
FIGURES	17
APPENDIX A: TABLES OF THERMOPHYSICAL PROPERTY DATA	A-1
APPENDIX B: EXPERIMENTAL APPARATUS	B-1
Vapor-Liquid Equilibrium Apparatus	B-2
Bubble-Point and Near-Saturation (p, ρ ,T) Apparatus	B-2
Isochoric (p, ρ ,T) Apparatus	B-2
Adiabatic Constant Volume Calorimeter	B-3
Spherical Resonator Sound Speed Apparatus	B-4
APPENDIX C: ESTIMATES OF STATE-POINT UNCERTAINTIES	C-1
APPENDIX D: GAS CHROMATOGRAPH CALIBRATION PROCEDURES	D-1

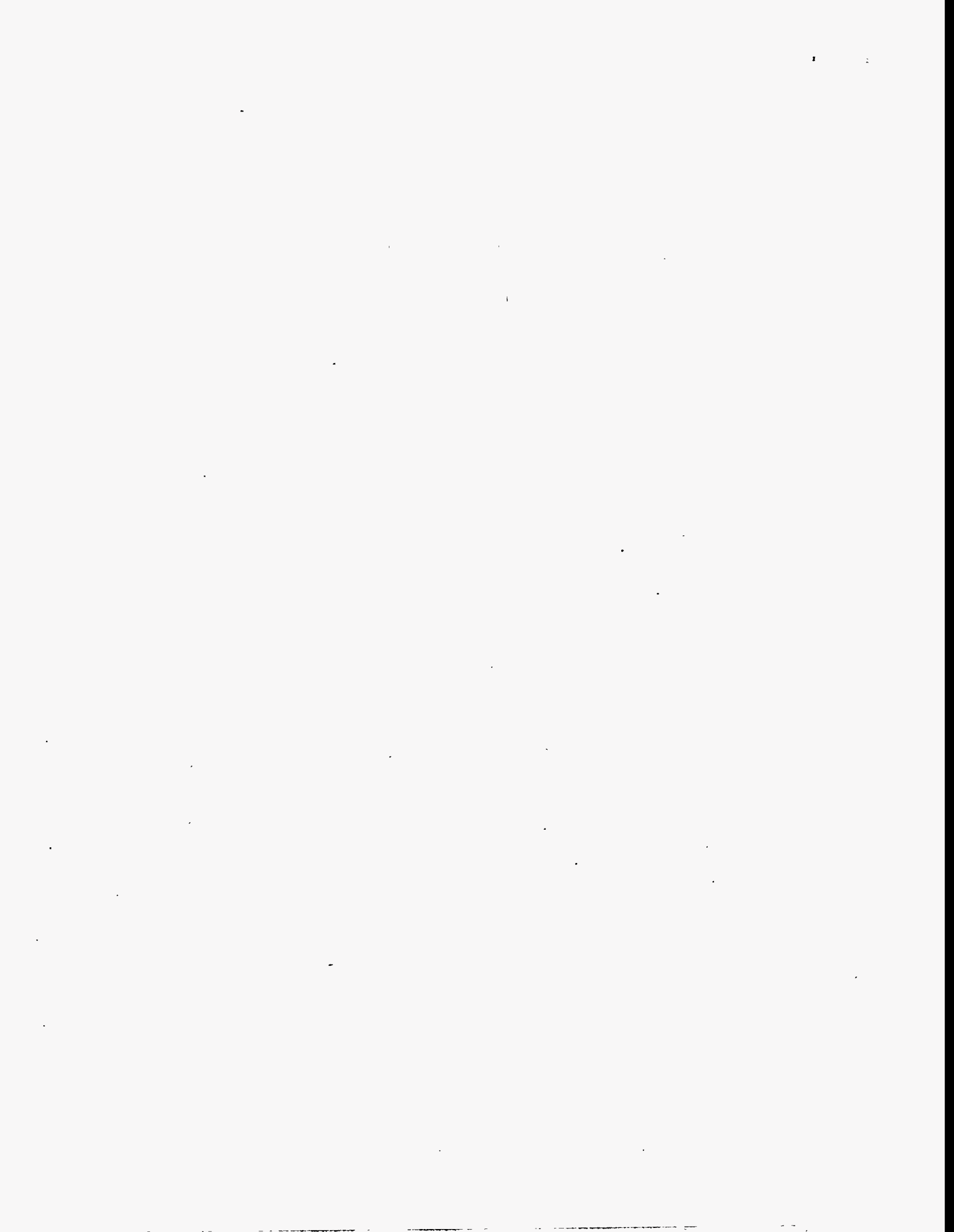


LIST OF FIGURES

	<u>Page</u>
Figure 1. Types of Phase Behavior for the Refrigerant Mixtures Studied in This Project.	18
Figure 2. Comparison of Bubble-Point Pressures for the R32/134a System; the Baseline is from the Lemmon-Jacobsen Model in REFPROP 6.0.	19
Figure 3. Comparison of Vapor Compositions for the R32/134a System; the Baseline is from the Lemmon-Jacobsen Model in REFPROP 6.0.	20
Figure 4. Comparison of Densities for the R32/134a System; the Baseline is from the Lemmon-Jacobsen Model in REFPROP 6.0.	21
Figure 5. Comparison of Bubble-Point Pressures for the R32/125 System; the Baseline is from the Lemmon-Jacobsen Model in REFPROP 6.0.	22
Figure 6. Comparison of Vapor Compositions for the R32/125 System; the Baseline is from the Lemmon-Jacobsen Model in REFPROP 6.0.	23
Figure 7. Comparison of Densities for the R32/125 System; the Baseline is from the Lemmon-Jacobsen Model in REFPROP 6.0.	24
Figure 8. Comparison of Bubble-Point Pressures for the R125/134a System; the Baseline is from the Lemmon-Jacobsen Model in REFPROP 6.0.	25
Figure 9. Comparison of Vapor Compositions for the R125/134a System; the Baseline is from the Lemmon-Jacobsen Model in REFPROP 6.0.	26
Figure 10. Comparison of Densities for the R125/134a System; the Baseline is from the Lemmon-Jacobsen Model in REFPROP 6.0.	27
Figure 11. Comparison of Bubble-Point Pressures for the R32/125/134a System; the Baseline is from the Lemmon-Jacobsen Model in REFPROP 6.0.	28
Figure 12. Comparison of Vapor Compositions for the R32/125/134a System; the Baseline is from the Lemmon-Jacobsen Model in REFPROP 6.0.	29
Figure 13. Comparison of Densities for the R32/125/134a System; the Baseline is from the Lemmon-Jacobsen Model in REFPROP 6.0.	30
Figure 14. Comparison of Bubble-Point Pressures for the R32/143a System; the Baseline is from the Lemmon-Jacobsen Model in REFPROP 6.0.	31
Figure 15. Comparison of Vapor Compositions for the R32/143a System; the Baseline is from the Lemmon-Jacobsen Model in REFPROP 6.0.	32
Figure 16. Comparison of Densities for the R32/143a System; the Baseline is from the Lemmon-Jacobsen Model in REFPROP 6.0.	33
Figure 17. Comparison of Bubble-Point Pressures for the R125/143a System; the Baseline is from the Lemmon-Jacobsen Model in REFPROP 6.0.	34
Figure 18. Comparison of Vapor Compositions for the R125/143a System; the Baseline is from the Lemmon-Jacobsen Model in REFPROP 6.0.	35

Figure 19. Range of Measured Temperatures and Pressures for Isochoric (p, ρ ,T) Data for a Mixture of R125/143a with $x(R125)=0.49996$ Mole Fraction (0.58812 Mass Fraction).	36
Figure 20. Comparison of Densities for the R125/143a System; the Baseline is from the Lemmon-Jacobsen Model in REFPROP 6.0.	37
Figure 21. Comparison of Bubble-Point Pressures for the R143a/134a System; the Baseline is from the Lemmon-Jacobsen Model in REFPROP 6.0.	38
Figure 22. Comparison of Vapor Compositions for the R143a/134a System; the Baseline is from the Lemmon-Jacobsen Model in REFPROP 6.0.	39
Figure 23. Comparison of Densities for the R143a/134a System; the Baseline is from the Lemmon-Jacobsen Model in REFPROP 6.0.	40
Figure 24. Comparison of Bubble-Point Pressures for the R32/290 System; the Baseline is from the Lemmon-Jacobsen Model in REFPROP 6.0.	41
Figure 25. Comparison of Vapor Compositions for the R32/290 System; the Baseline is from the Lemmon-Jacobsen Model in REFPROP 6.0.	42
Figure 26. Comparison of Densities for the R32/290 System; the Baseline is from the Lemmon-Jacobsen Model in REFPROP 6.0.	43
Figure 27. Comparison of Bubble-Point Pressures for the R125/290 System; the Baseline is from the Lemmon-Jacobsen Model in REFPROP 6.0.	44
Figure 28. Comparison of Vapor Compositions for the R125/290 System; the Baseline is from the Lemmon-Jacobsen Model in REFPROP 6.0.	45
Figure 29. Comparison of Densities for the R125/290 System; the Baseline is from the Lemmon-Jacobsen Model in REFPROP 6.0.	46
Figure 30. Comparison of Bubble-Point Pressures for the R134a/290 System; the Baseline is from the Lemmon-Jacobsen Model in REFPROP 6.0.	47
Figure 31. Comparison of Vapor Compositions for the R134a/290 System; the Baseline is from the Lemmon-Jacobsen Model in REFPROP 6.0.	48
Figure 32. Comparison of Densities for the R134a/290 System; the Baseline is from the Lemmon-Jacobsen Model in REFPROP 6.0.	49
Figure 33. Comparison of Vapor Pressures for HFC-41; the Baseline is from the Ancillary Equation for Vapor Pressure.	50
Figure 34. Range of Measured Temperatures and Pressures for Isochoric (p, ρ ,T) Data for HFC-41.	51
Figure 35. Comparison of Densities for HFC-41; the Baseline is from the MBWR Model in REFPROP 6.0.	52
Figure 36. Deviations of the MBWR Equation of State for HFC-41 from Ancillary Equations for Vapor Pressure, Saturated Liquid Density, and Saturated Vapor Density.	53

Figure 37. Deviations of the MBWR Equation of State for HFC-41 from Experimental (p, ρ ,T) Data.....	54
Figure 38. Deviations of the MBWR Equation of State for HFC-41 from Experimental Isochoric Heat Capacity Data at Saturation and in the Single-Phase Liquid Region.....	55
Figure 39. Comparison of Bubble-Point Pressures for the R41/744 System; the Baseline is from the Lemmon-Jacobsen Model in REFPROP 6.0.....	56
Figure 40. Comparison of Vapor Compositions for the R41/744 System; the Baseline is from the Lemmon-Jacobsen Model in REFPROP 6.0.....	57
Figure 41. Range of Measured Temperatures and Pressures for Isochoric (p, ρ ,T) Data for a Mixture of R41/744 with $x(R41)=0.49982$ Mole Fraction (0.43591 Mass Fraction)....	58
Figure 42. Comparison of Isochoric (p, ρ ,T) Data for the Equimolar Mixture of R41/744; the Baseline is from the Lemmon-Jacobsen Model in REFPROP 6.0.....	59

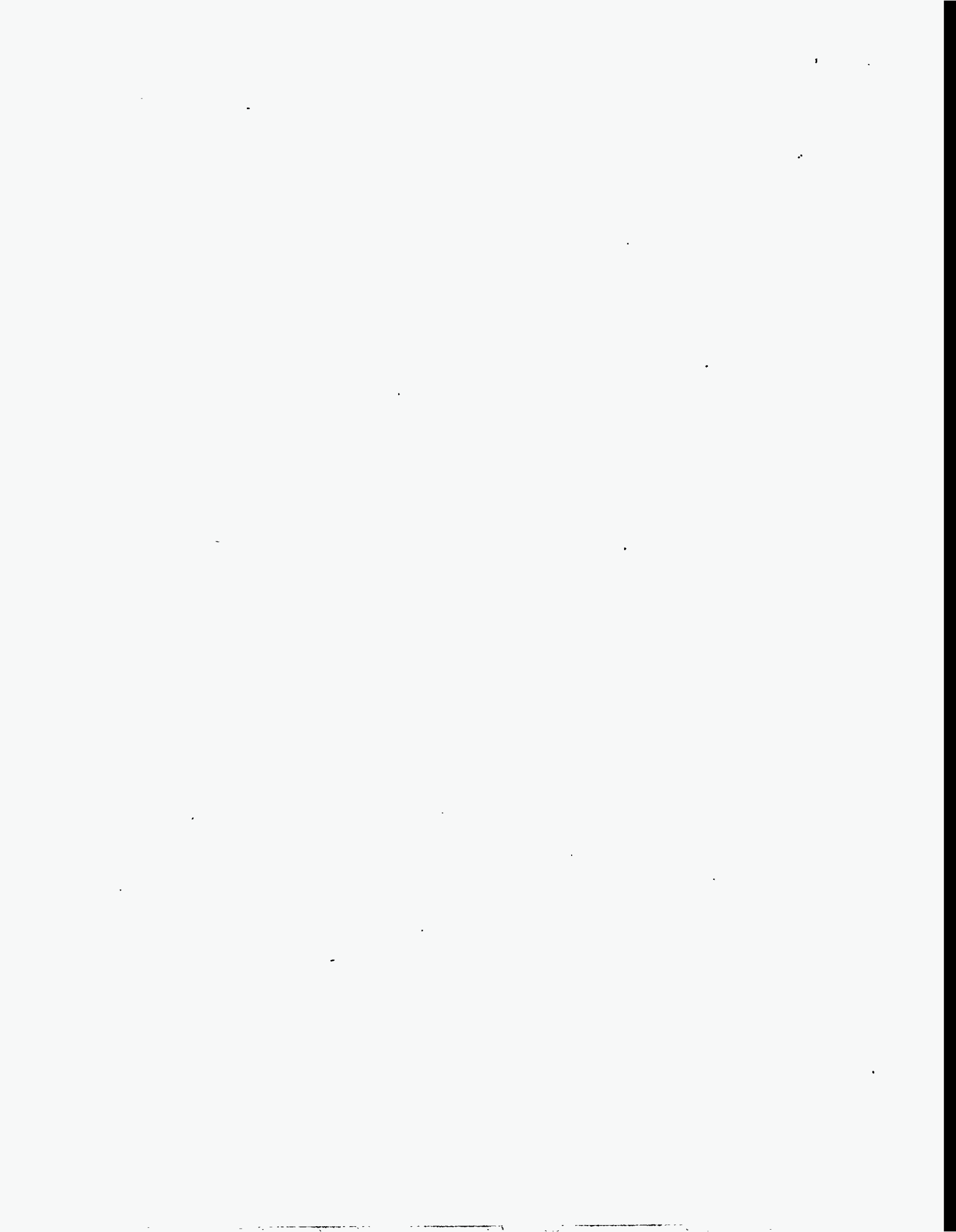


LIST OF TABLES

	<u>Page</u>
Table 1. Summary of the Refrigerant Systems Studied, the Properties Measured for Each System, and the Molecular Weights of the Pure Components.	A-2
Table 2. Summary of the Experimental Uncertainties for the Apparatus Used in This Project.	A-3
Table 3. Vapor-Liquid Equilibrium Data for R32/134a Mixtures from 280 to 340 K (44 to 152°F).	A-4
Table 4. Near-Saturation (p,p,T) Data for R32/134a Mixtures from 279 to 340 K (43 to 152°F).	A-6
Table 5. Vapor-Liquid Equilibrium Data for R32/125 Mixtures from 280 to 340 K (44 to 152°F).	A-8
Table 6. Near-Saturation (p, ρ ,T) Data for R32/125 Mixtures from 279 to 341 K (43 to 154°F).	A-9
Table 7. Vapor-Liquid Equilibrium Data for R125/134a Mixtures from 280 to 340 K (44 to 152°F).	A-11
Table 8. Bubble-Point Pressures for R125/134a Mixtures from 280 to 340 K (45 to 153°F).	A-12
Table 9. Near-Saturation (p, ρ ,T) Data for R125/134a Mixtures from 280 to 342 K (44 to 157°F).	A-13
Table 10. Vapor-Liquid Equilibrium Data for R32/125/134a Mixtures from 280 to 340 K (44 to 152°F).	A-14
Table 11. Bubble-Point Pressures for R32/125/134a Mixtures from 221 to 345 K (-62 to 162°F).	A-15
Table 12. Near-Saturation (p, ρ ,T) Data for R32/125/134a Mixtures from 244 to 346 K (-21 to 163°F).	A-16
Table 13. Vapor-Liquid Equilibrium Data for R32/143a Mixtures from 280 to 340 K (44 to 152°F).	A-18
Table 14. Near-Saturation (p, ρ ,T) Data for R32/143a Mixtures from 279 to 340 K (43 to 152°F).	A-19
Table 15. Vapor-Liquid Equilibrium Data for R125/143a Mixtures from 280 to 326 K (44 to 127°F).	A-21
Table 16. Bubble-Point Pressures for R125/143a Mixtures from 280 to 325 K (45 to 125°F).	A-22
Table 17. Near-Saturation (p, ρ ,T) Data for R125/143a Mixtures from 280 to 328 K (44 to 131°F).	A-23

Table 18. Isochoric (p, ρ ,T) Data from 200 to 400 K (-100 to 260°F) for a Mixture of R125/143a with $x(R125) = 0.49996$ Mole Fraction (0.58812 Mass Fraction).	A-24
Table 19. Isochoric Heat Capacities (C_v) from 205 to 344 K (-90 to 160°F) for a Mixture of R125/143a with $x(R125) = 0.49996$ Mole Fraction (0.58812 Mass Fraction).	A-33
Table 20. Vapor-Liquid Equilibrium Data for R143a/134a Mixtures from 280 to 340 K (45 to 152°F).	A-37
Table 21. Bubble-Point Pressures for R143a/134a Mixtures from 281 to 340 K (46 to 153°F).	A-38
Table 22. Near-Saturation (p, ρ ,T) Data for R143a/134a Mixtures from 280 to 343 K (45 to 158°F).	A-39
Table 23. Vapor-Liquid Equilibrium Data for R32/290 Mixtures from 280 to 341 K (44 to 154°F).	A-40
Table 24. Near-Saturation (p, ρ ,T) Data for R32/290 Mixtures from 278 to 341 K (42 to 153°F).	A-43
Table 25. Vapor-Liquid Equilibrium Data for R125/290 Mixtures from 280 to 364 K (44 to 195°F).	A-45
Table 26. Near-Saturation (p, ρ ,T) Data for R125/290 Mixtures from 280 to 326 K (44 to 128°F).	A-47
Table 27. Vapor-Liquid Equilibrium Data for R134a/290 Mixtures from 279 to 357 K (43 to 182°F).	A-48
Table 28. Near-Saturation (p, ρ ,T) Data for R134a/290 Mixtures from 278 to 357 K (40 to 183°F).	A-51
Table 29. Vapor Pressures for HFC-41 from 219 to 312 K (-66 to 102°F) Using the Vapor-Liquid Equilibrium Apparatus.	A-53
Table 30. Vapor Pressures for HFC-41 from 132 to 317 K (-222 to 111°F) Using the Isochoric (p, ρ ,T) Apparatus.	A-54
Table 31. Vapor Pressures for HFC-41 Calculated from the Vapor Pressure Equation.	A-56
Table 32. Near-Saturation (p, ρ ,T) Data for HFC-41 from 274 to 296 K (34 to 73°F).	A-57
Table 33. Comparisons of Critical Point Parameters for HFC-41.	A-58
Table 34. Isochoric (p, ρ ,T) Data for HFC-41 from 132 to 400 K (-222 to 260°F).	A-59
Table 35. Saturated Liquid Densities for HFC-41 from 131 to 309 K (-224 to 96°F) Extrapolated from Isochoric (p, ρ ,T) Data.	A-72
Table 36. Isochoric Heat Capacities (C_v) for HFC-41 from 148 to 343 K (-193 to 157°F). ...	A-73
Table 37. Two-Phase Heat Capacities for HFC-41 from 136 to 314 K (-215 to 106°F).	A-77

Table 38. Vapor Phase Sound Speed Data for HFC-41 from 249.5 to 350 K (-11 to 170°F).	A-81
Table 39. Coefficients of the MBWR Equation of State for HFC-41.	A-82
Table 40. Vapor-Liquid Equilibrium Data for R41/744 Mixtures from 218 to 290 K (-68 to 62°F).	A-83
Table 41. Isochoric (p, ρ ,T) Data from 192 to 400 K (-114 to 260°F) for a Mixture of R41/744 with $x(\text{R41}) = 0.49982$ Mole Fraction (0.43591 Mass Fraction).	A-85
Table 42. Summary of the Interaction Parameters for the Lemmon-Jacobsen Model for the Binary Systems Studied in This Project.	A-92



THERMOPHYSICAL PROPERTIES OF HCFC ALTERNATIVES

ARTI MCLR Project Number 660-50800

W.M. Haynes

Physical and Chemical Properties Division
National Institute of Standards and Technology

ABSTRACT

Numerous fluids and fluid mixtures have been identified as promising alternatives to the HCFC refrigerants, but, for many of them, reliable thermodynamic data do not exist. In particular, reliable thermodynamic properties data and models are needed to predict the performance of the new refrigerants in heating and cooling equipment and to design and optimize equipment to be reliable and energy efficient. The objective of the project is to measure, with high accuracy, selected thermodynamic properties data for one pure refrigerant and nine refrigerant blends; these data will be used to fit equations of state and other property models which can be used in equipment design. The new data will fill in gaps in the existing data and resolve problems and differences that exist in and between existing data sets. Most of the studied fluids and blends are potential replacements for HCFC-22 and/or R-502; in addition, one pure fluid and one blend are potential replacements for CFC-13 in low temperature refrigerant applications.

SCOPE

This project involved the measurement of primary thermodynamic data for eight binary mixtures and one ternary mixture (R125/134a; R32/143a; R125/143a; R143a/134a; R32/290; R125/290; R134a/290; R41/744; and R32/125/134a) over wide ranges of temperature and composition. These data consist of measurements of the coexisting liquid and vapor compositions and bubble-point pressures, as well as near-saturation pressure-density-temperature (p, ρ, T) measurements. In addition to the primary data for the R41/744 system, single-and two-phase heat capacity data and isochoric (p, ρ, T) data were obtained for this system. The mixture data for these systems have been used to determine mixing parameters for the Lemmon-Jacobsen model. Primary data were also measured for the pure fluid HFC-41. These measurements for HFC-41 included the determination of vapor pressures; liquid densities; liquid, two-phase, and ideal gas heat capacities; vapor sound speeds and virial coefficients; and critical point parameters. These data cover wide ranges of temperature and pressure and have been used (together with available literature data) to fit an equation of state and other models of the thermodynamic properties. The original proposal called for similar measurements of primary data for HFC-245ca; since work on this fluid had been funded by another sponsor, heat capacity and isochoric (p, ρ, T) measurements on the R125/143a system were substituted. A full summary of the data taken on each system is presented in Table 1; tables of the thermophysical property data are presented in Appendix A. The experimental uncertainties of these measurements are reported in Table 2. The descriptions of the apparatus used for the measurements in this project are presented in Appendix B.

The types of models originally specified for representing the mixture data were changed when better models became available. The mixture data in this report were used to optimize the parameters of the Lemmon-Jacobsen model. This model which will be used in REFPROP Version 6.0, has been shown to be more accurate in representing refrigerant mixture properties than previous models. All comparisons in this report use the values calculated from the Lemmon-Jacobsen model as the

baseline. The pure fluid data for HFC-41 have been fit to a modified Benedict-Webb-Rubin (MBWR) equation of state.

INTRODUCTION

Alternative refrigerants have become increasingly important to industrial applications as the ozone-depleting refrigerants are being phased out under the requirements of the Montreal Protocol. The main objective of this project was to measure the data needed to refine the models used by engineers for evaluating new refrigerants and refrigerant mixtures and for designing refrigeration cycles. To meet this objective, several tasks were addressed: 1) to measure properties of pure fluids or mixtures identified as replacements for specific fluids, 2) to investigate the behavior of propane-containing mixtures (propane has been suggested as an additive to enhance oil solubility, and 3) to provide data needed to test the ability of models to predict multicomponent mixture properties and complex phase behavior. The data from this project have been measured to provide property information on previously unstudied systems, to supplement existing data sets, to resolve problems and differences between existing data sets, and to refine models used in equipment design. Eight binary mixtures, one ternary, and one pure fluid were studied in this project.

The phase behavior of a fluid is important in determining if that system will be a suitable replacement for a pure refrigerant or refrigerant mixture. Azeotropic mixtures are important because they are mixtures that behave more like pure fluids. A system exhibiting liquid-liquid immiscibility and an azeotrope may also be exploited in a refrigeration cycle. It was important to gather information on systems that might exhibit liquid-liquid immiscibility for two reasons. The first reason was to provide the data needed to examine the behavior of these systems in a refrigeration cycle. The second reason was to test the capabilities of the Lemmon-Jacobsen model to handle this type of system.

The phase behavior for the systems measured in this report are classified as either Type I or Type II systems. Figure 1 shows generic examples of these two types of phase behavior. Type I systems have a continuous critical line and can have an azeotrope; the azeotrope can be either a positive pressure or a negative pressure azeotrope. All three subclasses of Type I systems were observed in this study. R32/134a, R125/134a, R32/143a, and R41/744 are nonazeotropic systems with the simplest type of phase behavior. R32/125 and R143a/134a are Type I systems with positive pressure azeotropes. R125/143a is a Type I system with a negative pressure azeotrope. Type II systems have a continuous critical line with liquid-liquid immiscibility. Type II systems also can have azeotropes, and the liquid-liquid region can either encompass the azeotrope or the azeotrope can be outside the liquid-liquid region. R32/290, R125/290, and R134a/290 are all believed to be Type II systems where the liquid-liquid immiscibility region encompasses the azeotrope. The azeotrope persists into the critical region, but the liquid-liquid region disappears around 310 K (98°F).

SIGNIFICANT RESULTS

Thermophysical Properties of R32/125/134a and Its Constituent Binaries

Property measurements of the ternary R32/125/134a system are important in meeting the objectives of this project. This ternary is a possible replacement for HCFC-22 and/or R-502, and the ternary results can be used to test the capability of the Lemmon-Jacobsen model to predict the thermophysical properties for a ternary system based on the interaction parameters of its constituent binaries. The constituent binaries of R32/125/134a are also potential replacements for HCFC-22 and/or R-502. Results for two of the constituent binaries were supported under another project, but will be reported here because of their importance in the model development and in predictions for the ternary mixture.

R32/134a

R32/134a is a Type I mixture with no azeotrope. It is one of the least complicated systems to model, but an important mixture for ternary calculations. The data for the R32/134a system cover 5 isotherms from 279 to 340 K (43 to 152°F). A total of 48 vapor-liquid equilibrium and 44 near-saturation (p, ρ, T) measurements was made. The data are presented in Tables 3 and 4. The data were compared to four other data sets available in the literature. The deviations between the data and the values predicted from the Lemmon-Jacobsen model are presented in Figures 2 - 4. In Figure 2, the deviations between the bubble-point pressures and the predicted values are presented. The data from this work agree with the data of Nagel and Bier (1995) within $\pm 1\%$. Most of the data of Higashi (1995) and of Widiatmo et al. (1994) also agree with the data of this work within $\pm 1\%$ except for a few points. The data of Fujiwara et al. (1992) are 3% lower than any of the other data sets.

The scatter in the data might appear large compared to the experimental uncertainties quoted in Table 2. But a distinction must be made between the experimental uncertainty of a specific parameter measurement (such as temperature, pressure, or composition) and the state-point uncertainty. The state point is system dependent and is defined as the equilibrium bubble-point pressure and vapor composition at a given liquid composition and temperature. Each of the parameters (P, T, x, y) has an experimental uncertainty associated with the measurement of that property. However, the state-point uncertainty is a function of the uncertainties of each of these four parameters as well as the dependencies between them. The experimental uncertainty of the bubble-point pressure state point is a function of the uncertainty of the temperature measurement, of the liquid composition measurement, of the pressure measurement, and of the relation of the bubble-point pressure with temperature and liquid composition for the specific system under study. The state-point uncertainties are different for each system and vary with temperature and composition. A detailed discussion on estimates of the state-point uncertainties is presented in Appendix C. The bubble-point pressure state-point uncertainty for the R32/134a system at temperatures from 280 to 340 K (44 to 152°F) ranges from ± 0.22 to $\pm 0.30\%$.

In Figure 3, the vapor compositions of the data sets are compared. In general, the four data sets agree within ± 0.015 mole or mass fraction HFC-32. The data of Fujiwara et al. (1992) are systematically 0.015 mole or mass fraction HFC-32 lower than the data of Nagel and Bier (1995). The vapor-composition state-point uncertainty ranges from ± 0.006 to ± 0.013 mole or mass fraction HFC-32 for the R32/134a system at temperatures from 280 to 340 K (44 to 152°F). As with the bubble-point pressure state-point uncertainty, a similar estimate of the state-point uncertainty of the vapor composition can be calculated. A detailed discussion of the estimate of the vapor-composition state-point uncertainty is presented in Appendix C.

The deviations for the near-saturation (p, ρ, T) data for R32/134a are presented in Figure 4. The liquid densities agree within $\pm 0.5\%$ of the predicted values from the Lemmon-Jacobsen model in REFPROP 6.0. The vapor densities agree within $\pm 1\%$. The liquid-density state-point uncertainty for the R32/134a system at temperatures from 279 to 340 K (43 to 152°F) ranges from ± 0.22 to $\pm 0.26\%$. The vapor-density state-point uncertainty for the R32/134a system at temperatures from 309 to 340 K (97 to 152°F) ranges from ± 0.32 to $\pm 0.79\%$. As with the bubble-point pressure state-point uncertainty, a similar estimate of the state-point uncertainty of the liquid and vapor densities can be calculated. A detailed discussion of the estimate of the density state-point uncertainties is presented in Appendix C.

R32/125

R32/125 is a Type I mixture with a slight positive pressure azeotrope. The data for the R32/125 system cover 5 isotherms from 279 to 341 K (43 to 154°F). A total of 30 vapor-liquid equilibrium and 45 near-saturation (p, ρ, T) measurements was made. The data are presented in Tables 5 and 6. The data were compared to four other data sets available in the literature. The deviations between the data and the values predicted from the Lemmon-Jacobsen model in REFPROP 6.0 are presented in Figures 5 - 7. In Figure 5, the deviations between the bubble-point pressures and the predicted values

are presented. The data from this work agree with the data of Nagel and Bier (1995) and of Widiatmo et al. (1993) within $\pm 1\%$ except for one point on the 325 K (125°F) isotherm. Except for two points, the data of Higashi (1995a) also agree with the data of this work within $\pm 1\%$. The data of Fujiwara et al. (1992) are 2% higher than any of the other data sets. The bubble-point pressure state-point uncertainty for the R32/125 system at temperatures from 280 to 340 K (44 to 152°F) ranges from ± 0.15 to $\pm 0.19\%$.

In Figure 6, the vapor compositions of the data sets are compared. In general, the four data sets agree within ± 0.013 mole or mass fraction HFC-32. The vapor-composition state-point uncertainty ranges from ± 0.008 to ± 0.009 mole or mass fraction HFC-32 for the R32/125 system at temperatures from 280 to 340 K (44 to 152°F).

The deviations for the near-saturation (p, ρ, T) data for R32/125 are presented in Figure 7. The liquid densities agree within $\pm 1\%$ of the predicted values from the Lemmon-Jacobsen model in REFPROP 6.0. The vapor densities agree within $\pm 2\%$. The liquid-density state-point uncertainty for the R32/125 system at temperatures from 279 to 340 K (43 to 152°F) ranges from ± 0.22 to 0.25% . The vapor-density state-point uncertainty for the R32/125 system at temperatures from 294 to 341 K (70 to 154°F) ranges from ± 0.34 to $\pm 0.90\%$.

R125/134a

R125/134a is a Type I mixture with no azeotrope. The data for the R125/134a system cover 5 isotherms from 280 to 342 K (44 to 157°F). A total of 30 vapor-liquid equilibrium and 17 near-saturation (p, ρ, T) measurements was made. Ten bubble-point pressure measurements on standard mixtures were also made. The data are presented in Tables 7 - 9. Bubble-point pressure measurements on standard mixtures were included for this system because of difficulties involved with the gas chromatograph (GC) calibration. The bubble-point pressure measurements eliminate the uncertainty introduced by sampling and analysis to determine the liquid composition. These measurements represent an independent verification of the bubble-point measurements from the vapor-liquid equilibrium measurements, and can be used to check the validity of the GC calibration. The data were compared to two other data sets available in the literature. The deviations between the data and the predicted values from the Lemmon-Jacobsen model are presented in Figures 8 - 10. In Figure 8, the deviations between the bubble-point pressures and the predicted values are presented. The data from this work agree with the data of Nagel and Bier (1995) within $\pm 2\%$. Most of the data of Higuchi and Higashi (1995) also agree with the data of this work within $\pm 2\%$ except for two points. The bubble-point pressure state-point uncertainty for the R125/134a system at temperatures from 280 to 340 K (44 to 152°F) ranges from ± 0.23 to $\pm 0.30\%$.

In Figure 9, the vapor compositions of the data sets are compared. In general, the four data sets agree within ± 0.018 mole or mass fraction HFC-125. The vapor-composition state-point uncertainty ranges from ± 0.006 to ± 0.012 mole or mass fraction HFC-125 for the R125/134a system at temperatures from 280 to 340 K (44 to 152°F).

The deviations for the near-saturation (p, ρ, T) data for R125/134a are presented in Figure 10. The liquid densities agree within $\pm 1\%$ of the predicted values from the Lemmon-Jacobsen model in REFPROP 6.0. The vapor densities agree within $\pm 2\%$. The liquid-density state-point uncertainty for the R125/134a system at temperatures from 280 to 340 K (44 to 153°F) ranges from ± 0.21 to $\pm 0.24\%$. The vapor-density state-point uncertainty for the R125/134a system at temperatures from 296 to 342 K (73 to 157°F) ranges from ± 0.51 to $\pm 1.08\%$.

R32/125/134a

The data for the R32/125/134a system cover 5 isotherms from 280 to 340 K (44 to 152°F) with some additional measurements at temperatures from 221 to 345 K (-62 to 162°F) that were obtained under a project funded by ICI. A total of 24 vapor-liquid equilibrium and 43 near-saturation (p, ρ, T) measurements was made. Thirty-four bubble-point measurements on standard mixtures were

performed to determine the reliability of the GC calibration procedure for a ternary mixture. The data are presented in Tables 10 - 12. The data were compared to the other data set available in the literature. The deviations between the data and the predicted values from the Lemmon-Jacobsen model are presented in Figures 11 - 13. In Figure 10, the deviations between the experimental bubble-point pressures and predicted values are presented. The data from this work agree with the data of Nagel and Bier (1995) and of Higashi (1996) within $\pm 3\%$. The bubble-point pressure state-point uncertainty for the R32/125/134a system at temperatures from 280 to 340 K (44 to 152°F) ranges from ± 0.15 to $\pm 0.30\%$.

In Figure 12, the vapor compositions of the data sets are compared. In general, the four data sets agree within ± 0.018 mole or mass fraction HFC-32. The vapor-composition state-point uncertainty ranges from ± 0.006 to ± 0.013 mole or mass fraction HFC-32 for the R32/125/134a system at temperatures from 280 to 340 K (44 to 152°F).

The deviations for the near-saturation (p, ρ, T) data for R32/125/134a are presented in Figure 13. The liquid densities agree with the predicted values from the Lemmon-Jacobsen model in REFPROP 6.0 within $\pm 1\%$. The vapor densities agree within $\pm 2\%$. The liquid-density state-point uncertainty for the R32/125/134a system at temperatures from 244 to 346 K (-21 to 163°F) ranges from ± 0.21 to $\pm 0.26\%$. The vapor-density state-point uncertainty for the R32/125/134a system at temperatures from 313 to 343 K (103 to 158°F) ranges from ± 0.32 to $\pm 1.08\%$.

The Lemmon-Jacobsen model accurately predicted the phase behavior and densities of the ternary using only the binary interaction parameters. The model did not require any additional parameters specifically required for the ternary mixture. This result confirms that, for this system, the Lemmon-Jacobsen model can be used to predict multicomponent mixture properties as long as the model has been optimized to the binary mixture data.

Mixtures with HFC-143a

Three mixtures with HFC-143a were studied to address the objectives of this work. These mixtures are potential substitutes for HCFC-22 and /or R-502, and the data for these systems with different types of phase behavior can be used to test mixture models.

R32/143a

R32/143a is a Type I system with no azeotrope. The data for the R32/143a system cover 5 isotherms from 279 to 340 K (43 to 152°F). A total of 29 vapor-liquid equilibrium and 49 near-saturation (p, ρ, T) measurements was made. The data are presented in Tables 13 and 14. In Figure 14, the bubble-point pressures are compared. The bubble-point pressures of this work agree with the predicted values from the Lemmon-Jacobsen model within $\pm 0.7\%$. The data of Fujiwara et al. (1992) are 2 to 3% higher than the data from this work. The bubble-point pressure state-point uncertainty for R32/143a at temperatures from 280 to 340 K (44 to 152°F) ranges from ± 0.14 to $\pm 0.20\%$.

In Figure 15, the vapor compositions are compared. The data of Fujiwara et al. (1992) and this work agree within ± 0.025 mole or mass fraction HFC-32 of the predicted values of the Lemmon-Jacobsen model in REFPROP 6.0. The vapor-composition state-point uncertainty for R32/143a at temperatures from 280 to 340 K (44 to 152°F) ranges from ± 0.007 to ± 0.010 mole or mass fraction HFC-32.

In Figure 16, the liquid and vapor near-saturation (p, ρ, T) data are compared to the predicted values from the Lemmon-Jacobsen model in REFPROP 6.0. The liquid densities agree within $\pm 1\%$ except for the 340 K (152°F) isotherm which is close to the critical point of HFC-143a. The vapor densities for the two isotherms closest to the critical region also show larger deviations. The liquid-density state-point uncertainty for the R32/143a system at temperatures from 279 to 340 K (43 to 152°F) ranges from ± 0.21 to $\pm 0.24\%$. The vapor-density state-point uncertainty for the R32/143a system at temperatures from 294 to 340 K (70 to 152°F) ranges from ± 0.27 to $\pm 0.69\%$.

R125/143a

R125/143a is a Type I system with a weak negative pressure azeotrope. The data for the R125/143a system cover 4 isotherms from 280 to 328 K (44 to 131°F). A total of 25 vapor-liquid equilibrium and 14 near-saturation (p, ρ, T) measurements were made. Eleven bubble-point measurements on standard mixtures were performed to determine the reliability of the GC calibration procedure for this binary mixture. The data are presented in Tables 15 - 17. The single-phase data for the R125/143a system cover 15 isochores from 200 to 400 K (-100 to 260°F) at pressures up to 35 MPa (5100 psi). Both gas- and liquid-phase (p, ρ, T) data were measured, as well as liquid-phase heat capacity data. The data are presented in Tables 18 and 19. A total of 281 isochoric (p, ρ, T) data points and 120 isochoric heat capacity measurements was made.

Figure 17 shows the comparison of the bubble-point pressures for R125/143a to the predicted values from the Lemmon-Jacobsen model. The compositions were difficult to measure because the vapor pressure curves of these two components are very similar. The experimental uncertainty of the composition measurements for this system is approximately twice that of the other systems in this study. The experimental uncertainty of the measured composition is ± 0.008 mole or mass fraction HFC-143a. The data from this work fall between the data of Takashima and Higashi (1995) and that of Nagel and Bier (1996). The bubble-point pressure state-point uncertainty for R125/143a at temperatures from 280 to 326 K (44 to 127°F) ranges from ± 0.15 to $\pm 0.18\%$.

Figure 18 shows the comparison of the vapor compositions for R125/143a to the values predicted from the Lemmon-Jacobsen model. The vapor-composition state-point uncertainty for the R125/143a system at temperatures from 280 to 326 K (44 to 127°F) ranges from ± 0.011 to ± 0.012 mole or mass fraction HFC-143a.

The ranges of temperature and pressure for the isochoric (p, ρ, T) data are shown in Figure 19. Figure 20 shows the comparison of the liquid and vapor near-saturation (p, ρ, T) and the isochoric (p, ρ, T) data to the predicted values from the Lemmon-Jacobsen model. The near-saturation (p, ρ, T) liquid densities agree with the model within $\pm 0.8\%$, and the near-saturation (p, ρ, T) vapor densities agree with the model within $\pm 0.75\%$. The liquid-phase isochoric (p, ρ, T) data agree with the model within $\pm 0.25\%$, and the vapor-phase isochoric (p, ρ, T) data agree with the model within $\pm 0.85\%$. The liquid-density state-point uncertainty for the near-saturation (p, ρ, T) data for the R125/143a system at temperatures from 280 to 325 K (44 to 125°F) ranges from ± 0.24 to $\pm 0.27\%$. The vapor-density state-point uncertainty for the near-saturation (p, ρ, T) data for the R125/143a system at temperatures from 296 to 328 K (74 to 131°F) ranges from ± 0.48 to $\pm 0.60\%$.

R143a/134a

R143a/134a is a Type I system with no azeotrope. The data for the R143a/134a system cover 5 isotherms from 280 to 343 K (45 to 158°F). A total of 29 vapor-liquid equilibrium and 17 near-saturation (p, ρ, T) measurements was made. Eleven bubble-point measurements on standard mixtures were performed to determine the reliability of the GC calibration procedure for this binary mixture. The data are presented in Tables 20 - 22.

Figure 21 shows comparisons of the bubble-point pressures for R143a/134a with the predicted values from the Lemmon-Jacobsen model. The bubble-point pressures agree with those of Nagel and Bier (1996) within $\pm 2\%$. The bubble-point pressure state-point uncertainty for the R143a/134a system at temperatures from 280 to 340 K (44 to 152°F) ranges from ± 0.20 to $\pm 0.25\%$.

Figure 22 shows comparisons of the vapor compositions for R125/143a with the predicted values from the Lemmon-Jacobsen model. The vapor compositions agree with those of Nagel and Bier (1996) within ± 0.018 mole or mass fraction HFC-143a. The vapor-composition state-point uncertainty for the R143a/134a system at temperatures from 280 to 340 K (45 to 152°F) ranges from ± 0.006 to ± 0.011 mole or mass fraction HFC-143a.

Figure 23 shows comparisons of the liquid and vapor near-saturation (p, ρ, T) data with the values predicted from the Lemmon-Jacobsen model. The liquid densities agree with the predicted values within $\pm 1\%$. The liquid-density state-point uncertainty for the R143a/134a system at temperatures from 280 to 340 K (45 to 153°F) ranges from ± 0.22 to $\pm 0.24\%$. The vapor-density state-point uncertainty for the R143a/134a system at temperatures from 312 to 343 K (102 to 158°F) ranges from ± 0.38 to $\pm 0.73\%$. There were very few vapor-phase (p, ρ, T) data available to optimize the model. Some preliminary vapor-phase (p, ρ, T) data at much higher temperatures and pressures were used in the fit. There were significantly more data available than the six near-saturation (p, ρ, T) points obtained in this work. Because the two data sets were in different regions and the higher pressure set had significantly more data, the fit has been carried out with a higher weight on the data at the higher temperatures and pressures. Additional data in the moderate temperature and pressure range are needed to determine the accuracy of the near-saturation vapor-phase (p, ρ, T) data and to better optimize the fit.

Mixtures with HC-290

There are two main reasons for studying refrigerant mixtures containing HC-290 (propane). One of the difficulties with the chlorine-free alternative refrigerants is their immiscibility with the oils used in refrigeration cycles. The possibility of adding propane to the mixture to enhance oil solubility is under investigation. In order to model multicomponent systems that contain propane, the mixture parameters for binary systems containing propane are required. Another reason for studying propane is to test mixture models for systems exhibiting complex phase behavior. These systems have very strong positive azeotropes and possible liquid-liquid immiscibility. They provide a very stringent test for the Lemmon-Jacobsen model and its ability to handle polar/nonpolar mixtures.

Although the Lemmon-Jacobsen model is capable of predicting liquid-liquid immiscibility, the algorithms implementing it in REFPROP 6.0 do not consider this behavior. Because of the complexity of this phase behavior, more experimental data are required to model the two separate liquid phases. Accurate liquid- and gas-phase (p, ρ, T) data and a knowledge of the compositions of the two liquid phases and gas phase in equilibrium are necessary for accurately determining the interaction parameters that can be used to model this phase behavior. Unfortunately, the measurements scheduled for these systems included near-saturation (p, ρ, T) data, but not isochoric (p, ρ, T) data. The vapor-liquid equilibrium apparatus was not designed to separate and to measure two distinct liquid phases. In the region where the liquid-liquid immiscibility occurs, no stable liquid densities or compositions can be recorded. The data available in the literature for these systems are limited, maybe because all three systems are in the process of being patented. The overall uncertainty of the measurements and the lack of data to optimize the model have resulted in deviations between the model and the data that are larger than for the other refrigerant systems.

R32/290

R32/290 is a Type II system with a strong positive pressure azeotrope. It shows the most extreme phase behavior of the three propane systems studied. It is a mixture of a small, spherical, very polar molecule with a rod-shaped, nonpolar molecule. The two molecules have strong repulsive interactions and exhibit a strong positive pressure azeotrope. At temperatures below 310 K (98°F), the liquid separates into two phases that were observed visually. The vapor-liquid equilibrium apparatus was not designed to measure two separate liquid phases, but can indicate the presence of two liquid phases by an unstable liquid composition and density for a constant vapor composition, bubble-point pressure, and vapor density. Measurements were made outside the liquid-liquid region where the liquid composition could be measured more accurately. A few measurements were taken to determine the vapor composition in equilibrium with the two liquid phases.

The data for the R32/290 system cover 5 isotherms from 278 to 341 K (42 to 154°F). A total of 75 vapor-liquid equilibrium and 50 near-saturation (p, ρ, T) measurements was made. The data are presented in Tables 23 and 24. There were no other data available for comparison for any of the properties measured for this system.

Figure 24 shows the comparison of the bubble-point pressures to the predicted values of the Lemmon-Jacobsen model in REFPROP 6.0. The data agree with the model within $\pm 5\%$. The bubble-point pressure state-point uncertainty for the R32/290 system at temperatures from 280 to 340 K (44 to 153°F) ranges from ± 0.14 to $\pm 0.63\%$. The uncertainties for the systems with propane are greater than for the other refrigerant systems studied because of the greater sensitivity of the bubble-point pressure to changes in composition. This sensitivity means that small uncertainties in the composition measurement correspond to much larger uncertainties in the bubble-point pressure.

Figure 25 shows the comparison of the vapor compositions to the predicted values from the Lemmon-Jacobsen model in REFPROP 6.0. The vapor compositions agree with the model within ± 0.05 mole or mass fraction HFC-32. The vapor-composition state-point uncertainty for the R32/290 system at temperatures from 280 to 340 K (44 to 153°F) ranges from ± 0.015 to ± 0.025 mole or mass fraction HFC-32. The state-point uncertainties are much larger because of the sensitivity of the equilibrium vapor composition to both temperature and liquid composition.

Figure 26 shows the comparison of the liquid and vapor near-saturation (p, ρ ,T) data to the predicted values from the Lemmon-Jacobsen model in REFPROP 6.0. The liquid and vapor densities agree with the predicted values within $\pm 7\%$. The liquid-density state-point uncertainty for the R32/290 system at temperatures from 278 to 340 K (42 to 153°F) ranges from ± 0.23 to $\pm 0.33\%$. The vapor-density state-point uncertainty for the R32/290 system at temperatures from 296 to 341 K (73 to 153°F) ranges from ± 0.28 to $\pm 3.10\%$.

R125/290

R125/290 is a Type II system with a strong positive pressure azeotrope that may exhibit liquid-liquid immiscibility at temperatures below 280 K (44°F). The data for the R125/290 system cover 8 isotherms from 280 to 364 K (44 to 195°F). A total of 63 vapor-liquid equilibrium and 27 near-saturation (p, ρ ,T) measurements was made. The data are presented in Tables 25 and 26.

In Figure 27, the comparison of the bubble-point pressures for the R125/290 system with the predicted values from the Lemmon-Jacobsen model in REFPROP 6.0 is shown. The bubble-point pressures agree with values from the model within $\pm 4.5\%$. The bubble-point pressure state-point uncertainty for the R125/290 system at temperatures from 280 to 364 K (44 to 195°F) ranges from ± 0.15 to $\pm 0.42\%$.

In Figure 28, the comparison of the vapor compositions for the R125/290 system to the predicted values of the Lemmon-Jacobsen model in REFPROP 6.0 is shown. The vapor compositions agree with the predicted values within ± 0.04 mole or mass fraction HFC-125. The vapor-composition state-point uncertainty for the R125/290 system at temperatures from 280 to 364 K (44 to 195°F) ranges from ± 0.006 to ± 0.015 mole or mass fraction HFC-125.

In Figure 29, the comparison of the liquid and vapor near-saturation (p, ρ ,T) data to the predicted values of the Lemmon-Jacobsen model in REFPROP 6.0 is shown. The liquid densities agree with the model within $\pm 2\%$, and the vapor densities agree within $\pm 3.5\%$. The liquid-density state-point uncertainty for the R125/290 system at temperatures from 280 to 325 K (44 to 125°F) ranges from ± 0.26 to $\pm 0.34\%$. The vapor-density state-point uncertainty for the R125/290 system at temperatures from 294 to 326 K (69 to 128°F) ranges from ± 0.26 to $\pm 2.30\%$.

R134a/290

R134a/290 is a Type II system with a strong positive pressure azeotrope. The data for the R134a/290 system cover 6 isotherms from 278 to 357 K (42 to 183°F). A total of 72 vapor-liquid equilibrium and 52 near-saturation (p, ρ ,T) measurements was made. The data are presented in Tables 27 and 28. Because of the liquid-liquid immiscibility, only qualitative comparisons can be made with the Lemmon-Jacobsen model.

Figure 30 shows the comparison of the bubble-point pressures to the predicted values of the Lemmon-Jacobsen model in REFPROP 6.0. The data of Kleiber (1994) agree with the data from this work within a few percent. The data of Jadot and Frere (1993) appears to be qualitatively different from our data and from the data of Kleiber (1994). The bubble-point pressure state-point uncertainty for the R134a/290 system at temperatures from 280 to 357 K (44 to 183°F) ranges from ± 0.13 to $\pm 0.57\%$.

Figure 31 shows the comparison of the vapor compositions to the predicted values of the Lemmon-Jacobsen model in REFPROP 6.0. The three data sets agree within ± 0.09 mole or mass fraction HFC-134a. The vapor-composition state-point uncertainty for the R134a/290 system at temperatures from 280 to 357 K (44 to 183°F) ranges from ± 0.005 to ± 0.019 mole or mass fraction HFC-134a.

Figure 32 shows the comparison of the liquid and vapor near-saturation (p,p,T) data to the predicted values from the Lemmon-Jacobsen model in REFPROP 6.0. The liquid densities agree with the model within $\pm 5\%$, and the vapor densities show increasing deviations as the temperature increases. The liquid-density state-point uncertainty for the R134a/290 system at temperatures from 278 to 356 K (40 to 181°F) ranges from ± 0.29 to $\pm 0.42\%$. The vapor-density state-point uncertainty for the R125/290 system at temperatures from 311 to 357 K (100 to 183°F) ranges from ± 0.24 to $\pm 2.06\%$.

HFC-41 and R41/744

HFC-41 is a possible substitute for CFC-13. While HFC-23 is most often considered for these applications, the long atmospheric lifetime and high global warming potential of HFC-23 leaves open the search for a more environmentally desirable fluid. Unfortunately, HFC-41 is a flammable fluid. R-744 (carbon dioxide) is a nonflammable fluid, but its freezing point is too high to be used as a replacement for CFC-13. The expectations that a mixture of R41/744 would have reduced flammability relative to pure HFC-41 and a lower freezing point than pure R-744 make this mixture an attractive possibility. Although accurate equations of state exist for R-744, only a preliminary equation of state for HFC-41 was available. Measurements on HFC-41 were performed, and a new MBWR model was developed. Measurements were then performed on R41/744, and the Lemmon-Jacobsen model was optimized to the mixture to allow evaluation of this mixture as a replacement for CFC-13.

HFC-41

A variety of single-phase and two-phase data was collected for HFC-41. A total of 23 vapor pressure measurements was made in the vapor-liquid equilibrium apparatus. Vapor pressure data were also measured in the isochoric (p,p,T) apparatus. A total of 39 vapor pressure measurements was obtained with this apparatus. The vapor pressure data are presented in Tables 29 and 30. The vapor pressure data from this work were combined with the data of Oi et al. (1983), and a vapor pressure correlation that is valid from the triple point to the critical point was developed. This equation is of the form,

$$P_\sigma = P_c \left[\frac{a_1\tau + a_2\tau^{1.5} + a_3\tau^3 + a_4\tau^6}{1 - \tau} \right], \quad (1)$$

where

$$\begin{aligned}\tau &= 1 - T/T_c, \\ T &= \text{temperature,} \\ T_c &= \text{critical temperature,} \\ P_\sigma &= \text{vapor pressure, and} \\ P_c &= \text{critical pressure.}\end{aligned}$$

The critical temperature used in the fit is 317.28 K (111.4°F). The critical pressure used in the fit is 5.897 MPa (855.3 psia). The coefficients a_i are dimensionless and are as follows:

$$\begin{aligned}a_1 &= -7.01707106 \\ a_2 &= 1.33436478 \\ a_3 &= -1.78330695 \\ a_4 &= -1.84394112\end{aligned}$$

Table 31 presents vapor pressures calculated with Equation (1) from the triple point to the critical point at even temperatures. Equation (1) was used as the ancillary equation for the vapor pressure in the MBWR model. Figure 33 shows comparisons of the two data sets from this work and the vapor pressures of Oi et al. (1983) with the calculated values from the MBWR equation in REFPROP 6.0. The data agree within $\pm 0.3\%$. The vapor pressure data at the three lowest temperatures from the VLE apparatus are at such low pressures that the uncertainty of the pressure measurement is relatively large. The vapor pressures at the lowest four temperatures from the isochoric (p,ρ,T) measurements also show increasing uncertainty.

The critical point parameters used in Equation (1) were determined from the near-saturation vapor and liquid (p,ρ,T) data and the vapor pressure data collected in this work. A total of 24 near-saturation vapor and liquid (p,ρ,T) data points was obtained. The data are presented in Table 32. The vapor pressure data and near-saturation (p,ρ,T) data were used to estimate the critical point parameters of HFC-41 using the method of Van Poolen et al. (1994). The critical point temperature is estimated to be 317.28 ± 0.08 K (111.43 ± 0.24 °F). This temperature agrees with those of Bominaar et al. (1987) and of Biwas et al. (1989) within ± 0.12 K (± 0.22 °F). The critical pressure is estimated to be 5.897 ± 0.01 MPa (855.3 ± 1.4 psia). This critical pressure agrees within ± 0.27 MPa (± 4.3 psia) with the critical pressures of Bominaar et al. (1987) and of Biwas et al. (1989). The critical density is estimated to be 316.5 ± 1.5 kg/m³ (19.74 ± 0.9 lb/ft³). The critical density agrees within ± 5.1 kg/m³ (± 0.34 lb/ft³) of the critical densities of Bominaar et al. (1987) and of Biwas et al. (1989). A summary of the critical point parameters is presented in Table 33.

Liquid- and gas-phase (p,ρ,T) measurements for HFC-41 were taken along 17 isochores at temperatures from 132 to 400 K (-222 to 260°F) at pressures up to 35 MPa (5100 psi). A total of 445 isochoric (p,ρ,T) measurements was obtained. The data are presented in Table 34. Saturated liquid densities for HFC-41 were estimated by extrapolating the isochoric (p,ρ,T) data to the vapor pressures calculated from Equation (1). These calculated saturated liquid densities are presented in Table 35. Figure 34 shows the range of temperatures and pressures covered by the isochoric (p,ρ,T) data. Figure 35 compares the near-saturation (p,ρ,T) liquid densities, the isochoric (p,ρ,T) data, and the calculated saturated liquid densities from the isochoric (p,ρ,T) data with calculated values from the new MBWR equation. The densities agree with the predicted values within $\pm 0.3\%$.

Liquid- and gas-phase heat capacity measurements were taken for HFC-41 along 17 isochores at temperatures from 148 to 343 K (-193 to 157°F) at pressures up to 33 MPa (4800 psi). A total of 122 isochoric heat capacity measurements and 133 saturated-liquid heat capacity measurements was obtained. The data are presented in Tables 36 and 37.

Vapor phase sound speed measurements were made from 249.5 to 350 K (-10.6 to 170.3°F). A total of 37 measurements was obtained. The data are presented in Table 38. The heat capacity and sound speed data were included in the optimization of the MBWR equation of state for HFC-41.

Ancillary equations (and their derivatives) for vapor pressure and for saturated liquid and vapor densities are used by the MBWR fitting routine to calculate values for other thermodynamic properties. These ancillary equations are used only in the fitting process and are independent of the final MBWR equation. Figure 36 shows deviations of vapor pressure and of saturated liquid and vapor densities calculated with the MBWR equation of state from those properties as calculated from the ancillary equations. Above 194 K (-100°F) vapor pressures calculated with the MBWR equation have a maximum deviation of $\pm 0.68\%$ from vapor pressures calculated with the ancillary equation. The MBWR equation shows good agreement with the ancillary equation for saturated liquid density with a maximum deviation of approximately $\pm 1.2\%$. Deviations between the MBWR and the ancillary equation for saturated vapor densities are generally within $\pm 2.0\%$ except above 300 K (80°F) and below 174 K (-146°F).

Figure 37 shows density deviations of experimental (p, ρ ,T) data used to optimize the MBWR equation from values calculated with the MBWR equation. All of the data were fit to within $\pm 0.66\%$ and the majority was fit to within approximately 0.2% except in close proximity to the triple point temperature and the critical temperature. The overall fit of the (p, ρ ,T) data has an average absolute deviation of $\pm 0.048\%$ and a bias of 0.002%.

The formulation of the MBWR equation includes the isochoric and saturated heat capacities from this work. Ideal heat capacities were obtained from values reported by Chase et al. (1985) calculated from spectroscopic data. Figure 38 shows deviations of the experimental heat capacity data used to optimize the MBWR equation from heat capacities calculated from the MBWR equation. The experimental isochoric heat capacities are fit with a maximum deviation of $\pm 8.0\%$, and the heat capacities at saturation are fit with a maximum deviation of $\pm 8.0\%$ with the exception of the point at 134 K (-218°F).

The MBWR equation for R41 presented here shows good agreement with experimental data. The equation gives reasonable results upon extrapolation to 500 K (440°F) and to pressures of 40 MPa (5800 psia). However, the accuracies are not as good below 170 K (-154°F). The coefficients for the MBWR equation of state are presented in Table 39.

R41/744

R41/744 is a Type I system with no azeotrope. The data for the R41/744 systems cover 6 isotherms from 218 to 290 K (-68 to 62°F). A total of 37 vapor-liquid equilibrium points was recorded. The data are presented in Table 40. In Figure 39, the deviations between the bubble-point pressures and the predicted values are presented. In Figure 40, the vapor compositions are compared to the predicted values of the Lemmon-Jacobsen model. No other data sets were available for comparison. The bubble-point pressure data agreed with the predicted values from the Lemmon-Jacobsen model within $\pm 1.5\%$. The bubble-point pressure state-point uncertainty for R41/744 at temperatures from 218 to 290 K (-68 to 62°F) ranges from ± 0.19 to $\pm 0.22\%$. The vapor compositions agree with the predicted values from the Lemmon-Jacobsen model within ± 0.018 mole or mass fraction of HFC-41. The vapor-composition state-point uncertainty for the R41/744 system at temperatures from 218 to 290 K (-68 to 62°F) ranges from ± 0.006 to ± 0.011 mole or mass fraction HFC-41.

Isochoric (p, ρ ,T) data were also obtained for the R41/744 system. Measurements were taken in both the gas and liquid phases. The data are reported in Table 41. Figure 41 shows the range of temperatures and pressures covered by the isochoric (p, ρ ,T) data. Figure 42 shows the comparison of the isochoric (p, ρ ,T) data to the predicted values from the Lemmon-Jacobsen model in REFPROP 6.0. The isochoric (p, ρ ,T) data agreed with the predicted values from the Lemmon-Jacobsen model within $\pm 1.0\%$ except for two vapor-phase points.

The R41/744 system is a possible replacement for CFC-13 if the freezing point of the mixture is significantly lower than the freezing point of pure R-744. Prior to this study, no published data were available for the solid-liquid equilibria of R41/744 mixtures. Based on known behavior of similar

mixtures, we expected the freezing points of R41/744 mixtures to fall below that of pure R-744 whose triple point temperature is 216.59 K (-69.83°F). Previously, we reported the triple point temperature of HFC-41 to be 129.82 ± 0.04 K (-226.01 ± 0.07 °F), as observed in the adiabatic calorimeter. The calculated freezing point of our equimolar mixture is approximately 186 K(-125°F), which is 13 K (23.4°F) above the average of the triple point temperatures of HFC-41 and R-744.

To determine some bounds on the freezing point temperature for the equimolar R41/744 mixture (0.499823 mole fraction HFC-41) (0.43591 mass fraction HFC-41), we condensed the sample into a precooled PVT cell. In such experiments, the sample would condense to either a liquid or to a solid after it enters the cell, depending on the initial temperature of the PVT cell. This test required only minimal additional effort, since the PVT cell had to be filled to carry out PVT experiments. We carried out two filling experiments. The initial cell temperatures were 180 K and 170 K (-135.6 and -153.7°F), both at a final pressure of 2 MPa (290 psia). We determined that both samples were liquid phase by heating the samples and observing a steady rise of pressure of approximately 2 MPa/K (161 psia/°F). This technique has established that the freezing point of an equimolar mixture is less than 182.5 K (-131.2°F).

We then employed an adiabatic calorimeter to accurately measure the temperature at which solid precipitates from a liquid sample of the R41/744 mixture. The calorimeter bomb was filled with a liquid sample (57.907 g) (0.1277 lb) at a final temperature and pressure of (292.68 K, 7.50 MPa) (67.14°F, 1088 psia). This quantity of material leaves only a small vapor space above the liquid when it was subsequently cooled. The sample was cooled rapidly to 225 K (-55°F), then slowly to 95 K (-289°F). We observed the formation of a solid phase at a temperature of 125 K (-235°F), as indicated by a sharp break in a graph of the recorded temperatures vs. times. We then heated the sample from 95 K (-289°F) to about 115 K (-253°F), then allowed the sample to equilibrate and measured the small heat leak. The heater power was then lowered to about 15% of the normal level, and we continued to heat the sample to 135 K (-217°F). The freezing temperature was observed where the temperature reached a plateau value for the elapsed time needed to melt the solid phase. Three experiments were carried out. The elapsed time at the plateau temperature was about 640 minutes. The observed freezing temperatures were 124.98 ± 0.02 K (-234.72 ± 0.036 °F), 124.97 ± 0.02 K (-234.74 ± 0.036 °F), and 125.00 ± 0.02 K (-234.69 ± 0.036 °F). Though two heater power levels were selected, no dependence on the applied power was seen. The observed enthalpies of fusion were 2.069 ± 0.01 kJ•mol⁻¹ (22.79 ± 0.11 BTU•lb⁻¹) and 2.074 ± 0.01 kJ•mol⁻¹ (22.84 ± 0.11 BTU•lb⁻¹), after corrections for energy to heat the empty calorimeter and for energy lost to parasitic heat leaks were applied.

The average freezing temperature of 124.98 K (-234.72°F) is 48 K (86.4°F) below the mole fraction average of the pure component triple point temperatures, and also is 5 K (9°F) lower than that of the lowest-melting pure substance in the mixture. This evidence implies that this binary mixture will have at least one eutectic composition. More extensive experimental and theoretical studies of solid-liquid transitions are needed to further elucidate this phenomenon.

REFPROP 6.0 and the Lemmon-Jacobsen Model

The REFPROP computer database from the National Institute of Standards and Technology (NIST) (Huber et al. 1995) has been one of the more widely used tools designed to provide data for the alternative refrigerants. In the initial versions of REFPROP (Gallagher et al. 1993), the intent was to provide data on a wide variety of fluids to allow screening studies of possible replacements for the CFC or HFC refrigerants. For many of these fluids, only sparse data were available, and, consequently, the database relied primarily on a simple model with few adjustable parameters - the Carnahan-Starling-DeSantis (CSD) equation of state and/or the extended corresponding states model (Huber and Ely 1994). As the alternative refrigerants have moved from the laboratory to use in commercial equipment, highly accurate properties are required for a more limited set of fluids. We are now using a new version of the REFPROP program (designated as Version 6.0) which is currently under development and which is based on the most accurate pure fluid and mixture models currently

available. REFPROP 6.0 calculates the thermodynamic properties using comprehensive equations of state for the pure fluids.

The MBWR and Helmholtz free energy equations of state have been used to represent pure fluids in this work. HFC-32 and HFC-125 were represented by MBWR equations of state formulated by Outcalt and McLinden (1995). HFC-134a was represented by a Helmholtz free energy equation of state formulated by Tillner-Roth and Baehr (1994). HFC-143a was represented by a MBWR equation of state formulated by Outcalt and McLinden (1994). HC-290 was represented by a MBWR equation of state formulated by Younglove and Ely (1987). R-744 was represented by a MBWR equation of state formulated by Ely et al. (1987).

The thermodynamic properties of mixtures are calculated with a new model which was developed, in slightly different form, independently by Tillner-Roth (1993) and Lemmon (1996). It applies mixing rules to the Helmholtz energy of the mixture components:

$$a_{\text{mix}} = \frac{A_{\text{mix}}}{RT} = \sum_{j=1}^n x_j (a_j^{id} + a_j^r) + x_j \ln x_j + \sum_{i=1}^{n-1} \sum_{j=i+1}^n x_i x_j F_{ij} a_{ij}^{\text{excess}}. \quad (2)$$

The first summation in Equation (2) represents the ideal solution; it consists of ideal gas (superscript *id*) and residual or real fluid (superscript *r*) terms for each of the *j* pure fluids in the *n* component mixture. The $x_j \ln x_j$ terms arise from the entropy of mixing of ideal gases where x_j is the mole fraction of component *j*. The double summation accounts for the "excess" free energy of "departure" from ideal solution. The F_{ij} 's are generalizing parameters which relate the behavior of one binary pair with another; F_{ij} multiplies the a_{ij}^{excess} term(s), which are empirical functions fitted to experimental binary mixture data. The a^r and a^{excess} functions in Equation (2) are not evaluated at the temperature and density of the mixture T_{mix} and p_{mix} but, rather, at a reduced temperature and density τ and δ . These τ and δ are very much in the spirit of the conformal temperature and density of the extended coresponding states method and are a key innovation in this model. The mixing rules for the reducing parameters are:

$$\tau = \frac{T}{T_{\text{mix}}}, \text{ with } T = \sum_{i=1}^n x_i T_j^{\text{crit}} + \sum_{i=1}^{n-1} \sum_{j=i+1}^n x_i x_j (k_{T,ij} - 1) \frac{1}{2} (T_i^{\text{crit}} + T_j^{\text{crit}}), \text{ and} \quad (3)$$

$$\delta = \frac{\rho_{\text{mix}}}{\rho_*}, \text{ with } \frac{1}{\rho_*} = \sum_{i=1}^n x_i / \rho_j^{\text{crit}} + \sum_{i=1}^{n-1} \sum_{j=i+1}^n x_i x_j (k_{v,ij} - 1) \frac{1}{2} (1/\rho_i^{\text{crit}} + 1/\rho_j^{\text{crit}}). \quad (4)$$

If only limited vapor-liquid equilibrium (VLE) data are available, the a_{ij}^{excess} term is taken to be zero, and only the $k_{T,ij}$ and/or $k_{v,ij}$ parameters are fitted. The $k_{T,ij}$ parameter is most closely associated with bubble-point pressures, and it is necessary to describe systems exhibiting azeotropic behavior. The $k_{v,ij}$ parameter is associated with volume changes on mixing. (Ternary and higher order mixtures are modeled in terms of the constituent binary pairs. If extensive data, including single-phase pressure-volume-temperature and heat-capacity data, are available, the a_{ij}^{excess} function can be determined. The F_{ij} parameter is used (either alone or in combination with $k_{T,ij}$ and $k_{v,ij}$) to generalize the detailed mixture behavior described by the a_{ij}^{excess} function to other, similar binary pairs. Lemmon (1996) has determined the a_{ij}^{excess} function based on data for 28 binary pairs of hydrocarbons, inorganics, and HFC's. This model is referred to as the Lemmon-Jacobsen model in this report. The parameters β and γ are a means to account for composition dependence; they were found not to be needed for the refrigerant mixtures studied here and have been set to unity. Table 42 summarizes the mixing parameters determined in this work.

The Lemmon-Jacobsen model provides a number of advantages. By applying mixing rules to the Helmholtz energy of the mixture components, it allows the use of high-accuracy equations of state for the components, and the properties of the mixture will reduce exactly to the pure components as the composition approaches a mole fraction of 1. Different components in a mixture may be modeled with different forms; for example, a MBWR equation may be mixed with a Helmholtz equation of state. If the components are modeled with the ECS method, this mixture model allows the use of a different reference fluid for each component. The mixture is modeled in a fundamental way, and, thus, the departure function is a relatively small contribution to the total Helmholtz energy for most refrigerant mixtures. The great flexibility of the adjustable parameters in this model allows an accurate representation of a wide variety of mixtures, provided sufficient experimental data are available. A more detailed explanation of the models used in REFPROP 6.0 and the new graphical user interface incorporated in REFPROP 6.0 was reported by McLinden and Klein (1996).

COMPLIANCE WITH AGREEMENT

NIST has complied with all terms of the grant agreement modulo small shifts in the estimated level of effort from one property and/or fluid to another.

PRINCIPAL INVESTIGATOR EFFORT

Dr. W.M. Haynes is the NIST Principal Investigator for the MCLR program. During the thirty one months of the project, Dr. Haynes devoted approximately ten weeks to planning this project, monitoring and reviewing the research, and preparing quarterly and final reports. The project involves multiple researchers and capabilities in Gaithersburg, MD and Boulder, CO.

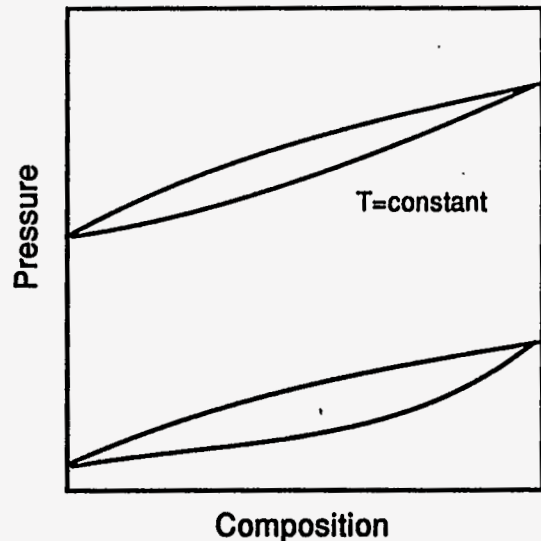
REFERENCES

- Biswas, S.N., Ten Seldam, C.A., Bominaar, S.A.R.C., and Trappeniers, N.J., *Fluid Phase Equilibria* **49**, 1 (1989).
- Bominaar, S.A.R.C., Biswas, S.N., Trappeniers, N.J., and Ten Seldam, C.A., *J. Chem. Thermodynamics* **19**, 959 (1987).
- Chase, M.W., Davies, C.A., Downey, J.R., Frurip, D.J., McDonald, R.A. and Syverd, A.N. JANAF Thermochemical Tables, Third Edition., *J. Phys. Chem. Ref. Data* **14** (suppl. 1): 1-1856 (1985).
- Ely, J.F., Magee, J.W., and Haynes, W.M., Research Report RR-110, Gas Processors Association, Tulsa, OK (1987).
- Fujiwara, K., Momota, H., and Noguchi, M., 13th Japanese Symposium Thermophysical Properties **A116**, 61 (1992).
- Gallagher, J., Huber, M., Morrison, G., and McLinden, M., NIST Standard Reference Database 23, Version 4.0. Standard Reference Data Program, National Institute of Standards and Technology, Gaithersburg, MD. (1993).
- Higashi, Y., Presented at the AIChE Spring Meeting, New Orleans, February (1996).
- Higashi, Y., Proc. 19th Int. Congress of Refrig., The Netherlands, **4a**, 297 (1995).
- Higashi, Y., *Int. J. Thermophysics* **16**, 1175 (1995a).
- Higuchi, M. and Higashi, Y., Proc. 16th Symp. Thermophysical Properties, Hiroshima, Japan **16**, 5 (1995).
- Huber, M., Gallagher, J., McLinden, M., and Morrison, G. NIST Standard Reference Database 23, Version 5.0. Standard Reference Data Program, National Institute of Standards and Technology, Gaithersburg, MD. (1995)
- Huber, M.L. and Ely, J.F., *Int. J. Refrig.* **17**, 18 (1994).
- Jadot, R. and Frere, M., *High Temperatures - High Pressures* **25**, 491 (1993).
- Kleiber, M., *Fluid Phase Equilibria* **92**, 149 (1994).
- Klein, S.A., McLinden, M.O., and Laesecke, A., *Int. J. Refrig.*, submitted.
- Lemmon, E.W., Ph. D. Thesis, Department of Mechanical Engineering, University of Idaho, Moscow, ID. (1996).
- McLinden, M.O. and Klein, S.A., Proc. 6th Int. Refrig. Conf. at Purdue, West Lafayette, IN, July 23-26, 409 (1996).
- Michels, A., Visser, A., Lunbeck, R.J., and Wolkers, G.J., *Physica* **XVIII**, 114 (1952).
- Nagel M. and Bier, K., *Int. J. Refrig.* **18**, 534 (1995).
- Nagel M. and Bier, K., *Int. J. Refrig.* **19**, 264 (1996).

- Oi, T., Shulman, J., Popowicz, A., and Ishida, J., *J. Phys. Chem.* **87**, 3153 (1983).
- Outcalt, S.L. and McLinden, M.O., in: Thermophysical Properties of HFC-143a and HFC-152a, Final Report to the Air-Conditioning and Refrigeration Technology Institute, Arlington, VA, Report No. DOE/CE/23810-30 (1994).
- Outcalt, S.L. and McLinden, M.O., *Int. J. Thermophysics* **16**, 79 (1995).
- Takashima, H. and Higashi, Y., Proc. 16th Symp. Thermophysical Props., Hiroshima, Japan **16**, 9 (1995).
- Tillner-Roth, R., Dr.-Ing. Thesis, Institut fur Thermodynamik, Universitat Hannover, Germany (1993).
- Tillner-Roth, R. and Baehr, H.D., *J. Phys. Chem. Ref. Data* **23**, 657 (1994).
- Van Poolen, L.J., Niesen, V.G., Holcomb, C.D., and Outcalt, S.L., *Fluid Phase Equilibria* **97**, 97 (1994).
- Weber, L., *Int. J. Thermophysics* **15**, 461 (1994).
- Widiatmo, J.V., Sato, H., and Watanabe, K., *High Temperatures - High Pressures* **25**, 677 (1993).
- Widiatmo, J.V., Sato, H., and Watanabe, K., *Fluid Phase Equilibria* **19**, 199 (1994).
- Younglove, B.A. and Ely, J.F., *J. Phys. Chem. Ref. Data* **16**, 577 (1987).
- Younglove, B.A. and McLinden, M.O., *J. Phys. Chem. Ref. Data* **23**, 731 (1994).

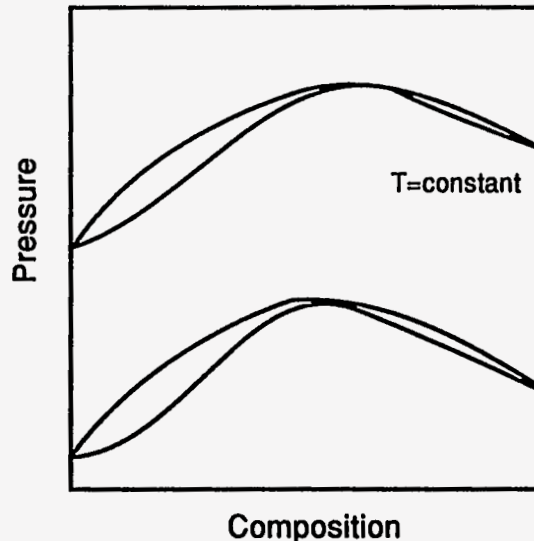
FIGURES

Type I systems have a continuous critical line and can have an azeotrope.



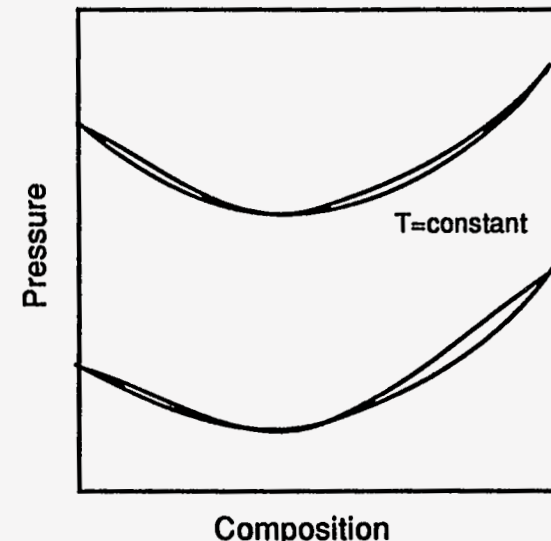
Composition

Type I system with no azeotrope
Examples - R32/134a, R125/134a, R41/744



Composition

Type I system with a positive pressure azeotrope
Examples - R32/125, R32/143a, R143a/134a

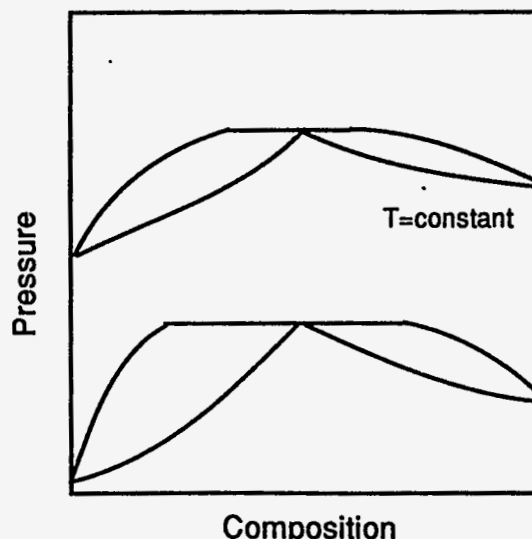


Composition

Type I system with a negative pressure azeotrope
Example - R125/143a

18

Type II systems have a continuous critical line, liquid-liquid immiscibility, and can have an azeotrope.



Composition

Type II system with a positive pressure azeotrope
Examples - R32/290, R125/290, R134a/290

Figure 1. Types of Phase Behavior for the Refrigerant Mixtures Studied in This Project.

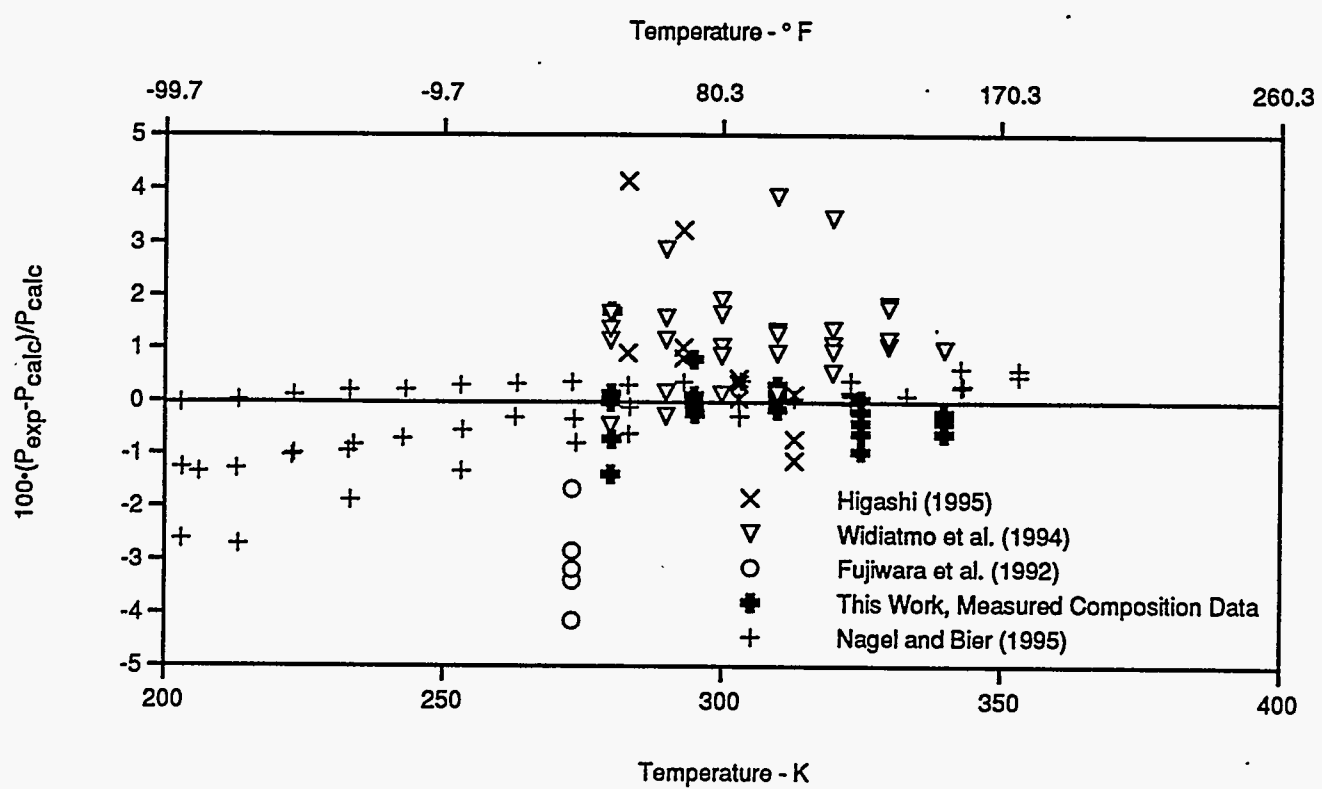


Figure 2. Comparison of Bubble-Point Pressures for the R32/134a System; the Baseline is from the Lemmon-Jacobsen Model in REFPROP 6.0.

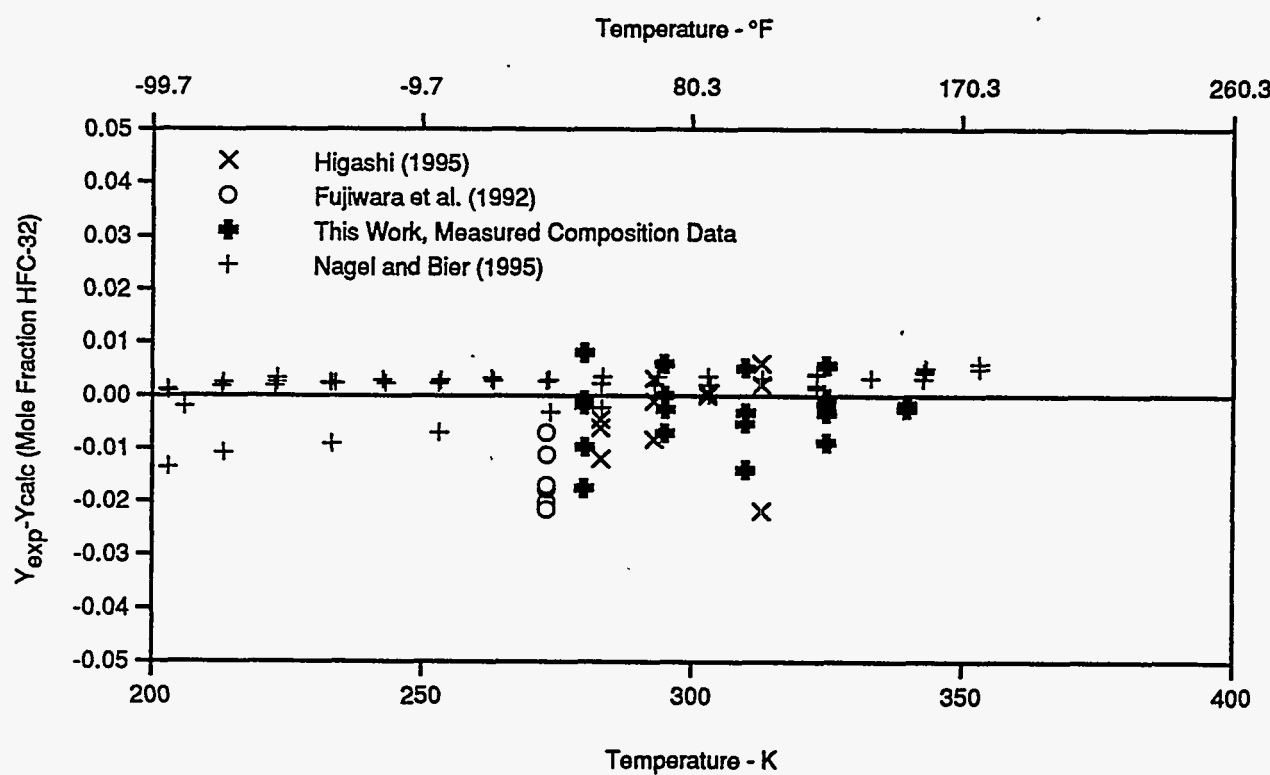


Figure 3. Comparison of Vapor Compositions for the R32/134a System; the Baseline is from the Lemmon-Jacobsen Model in REFPROP 6.0.

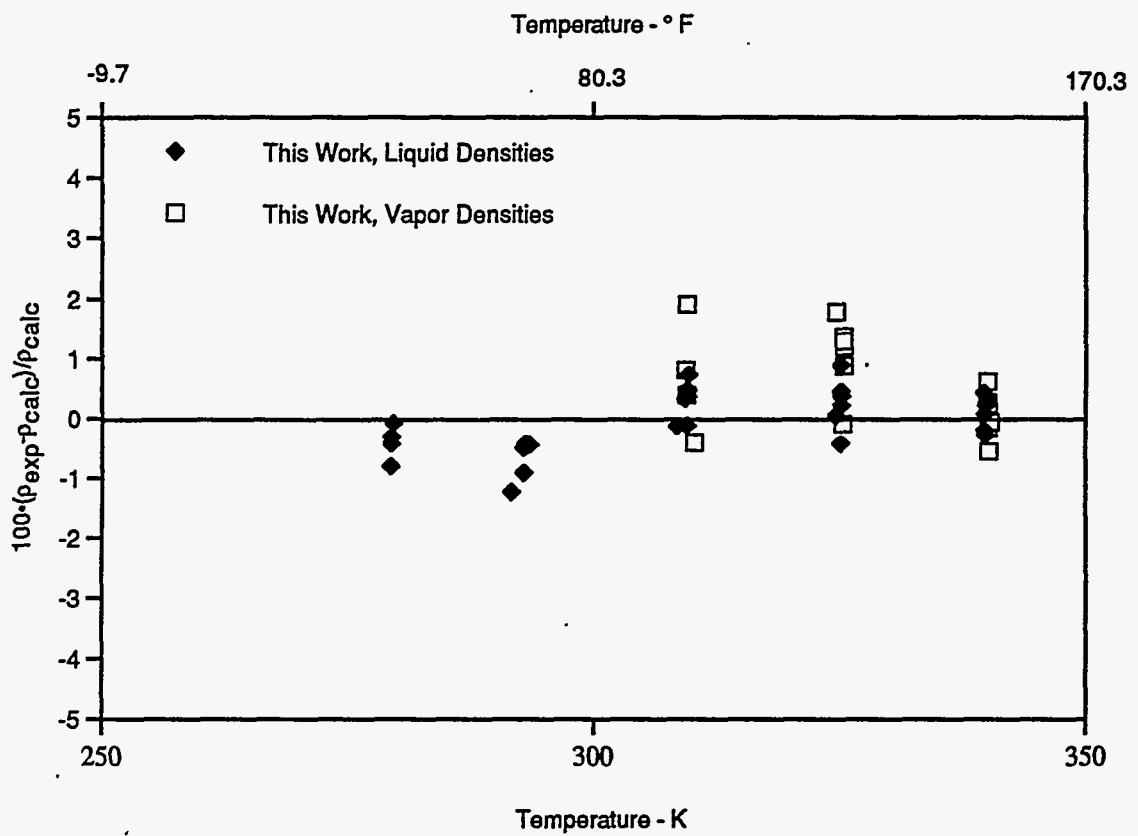


Figure 4. Comparison of Densities for the R32/134a System; the Baseline is from the Lemmon-Jacobsen Model in REFPROP 6.0.

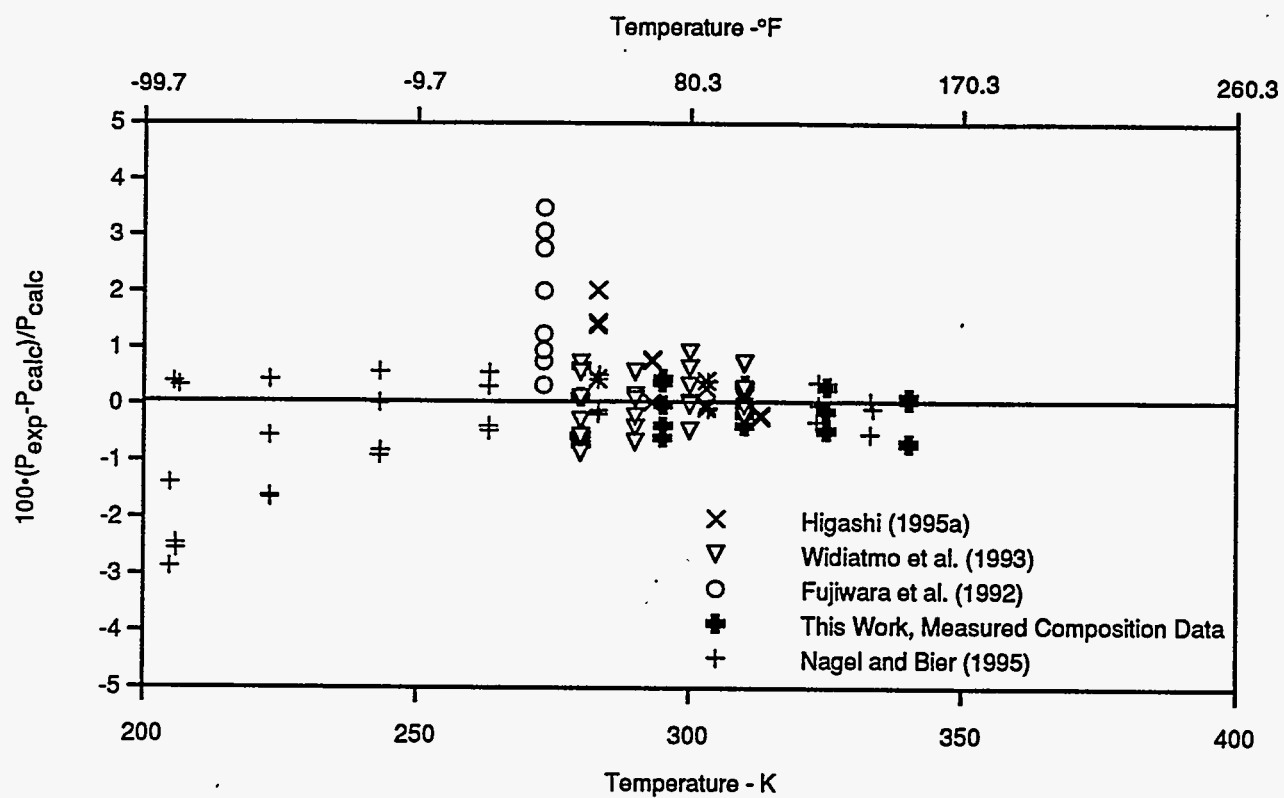


Figure 5. Comparison of Bubble-Point Pressures for the R32/125 System; the Baseline is from the Lemmon-Jacobsen Model in REFPROP 6.0.

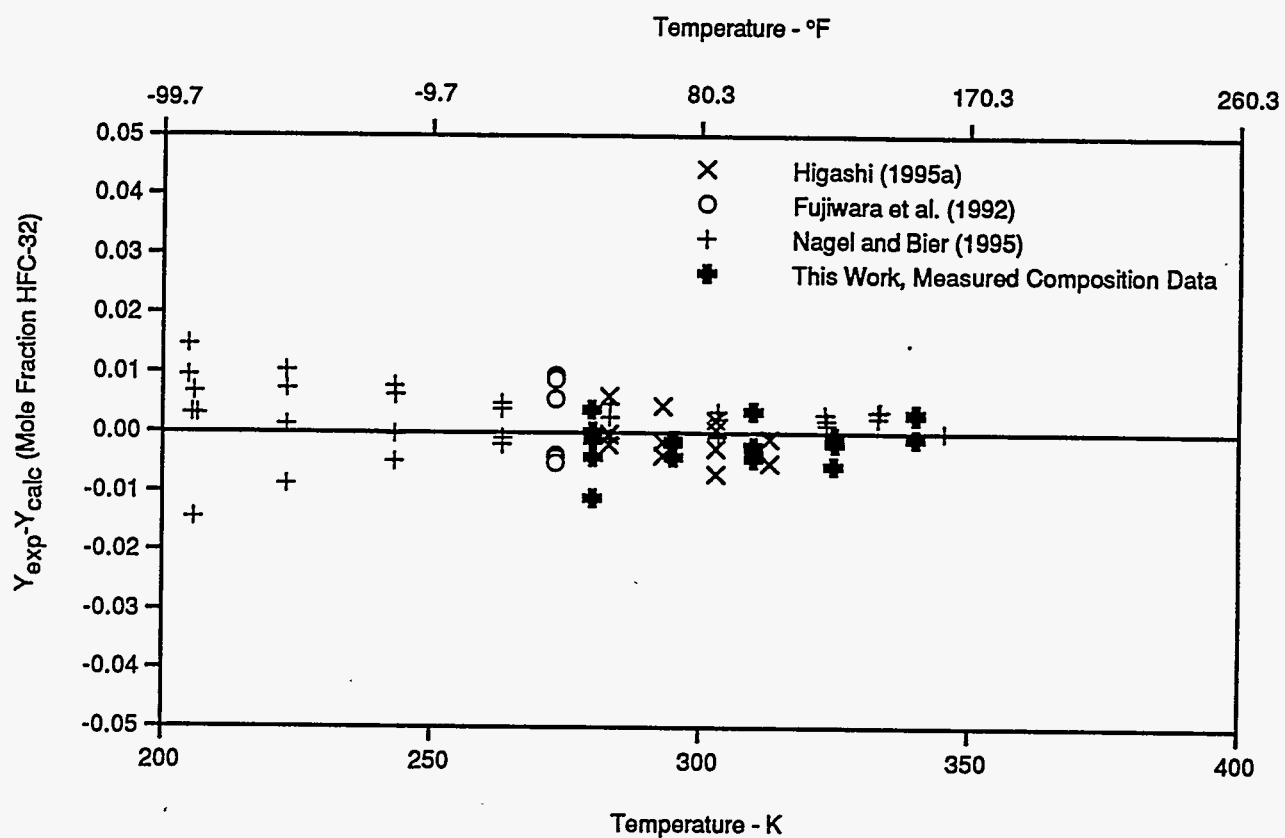


Figure 6. Comparison of Vapor Compositions for the R32/125 System; the Baseline is from the Lemmon-Jacobsen Model in REFPROP 6.0.

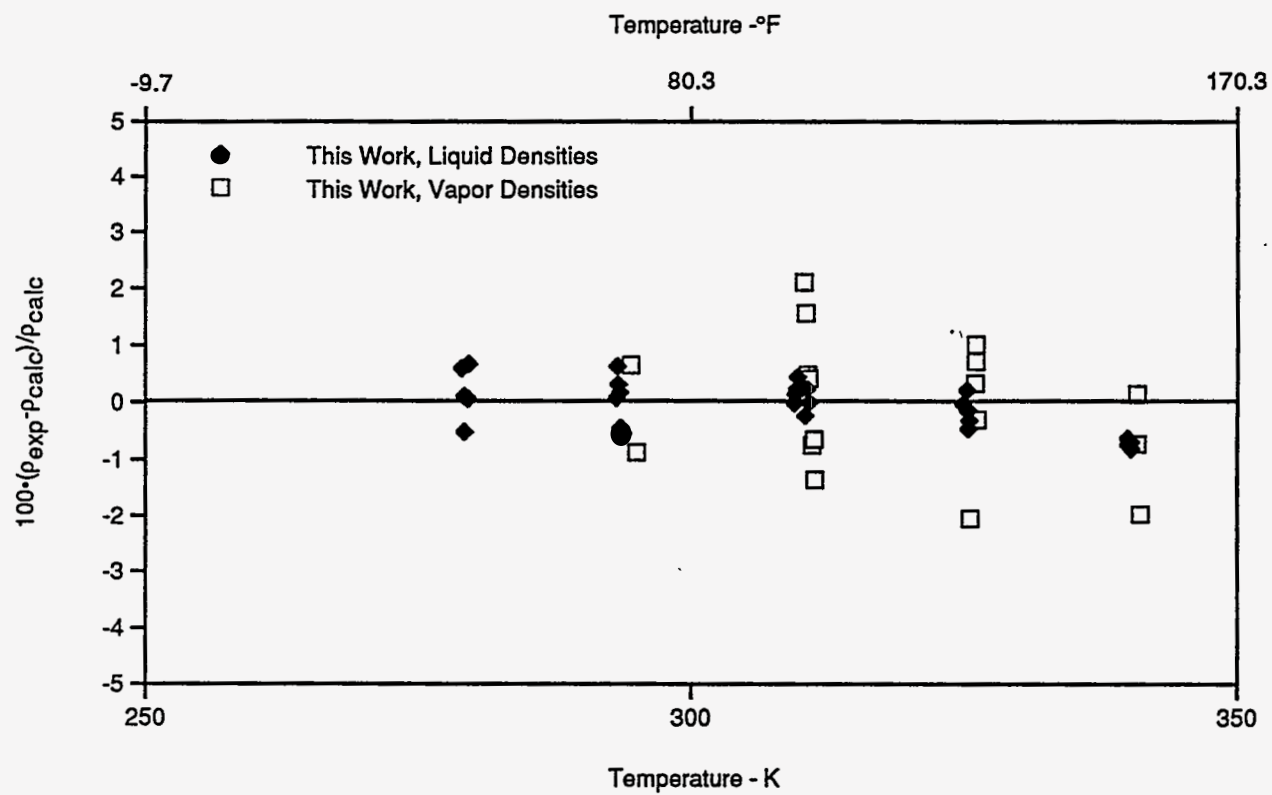


Figure 7. Comparison of Densities for the R32/125 System; the Baseline is from the Lemmon-Jacobsen Model in REFPROP 6.0.

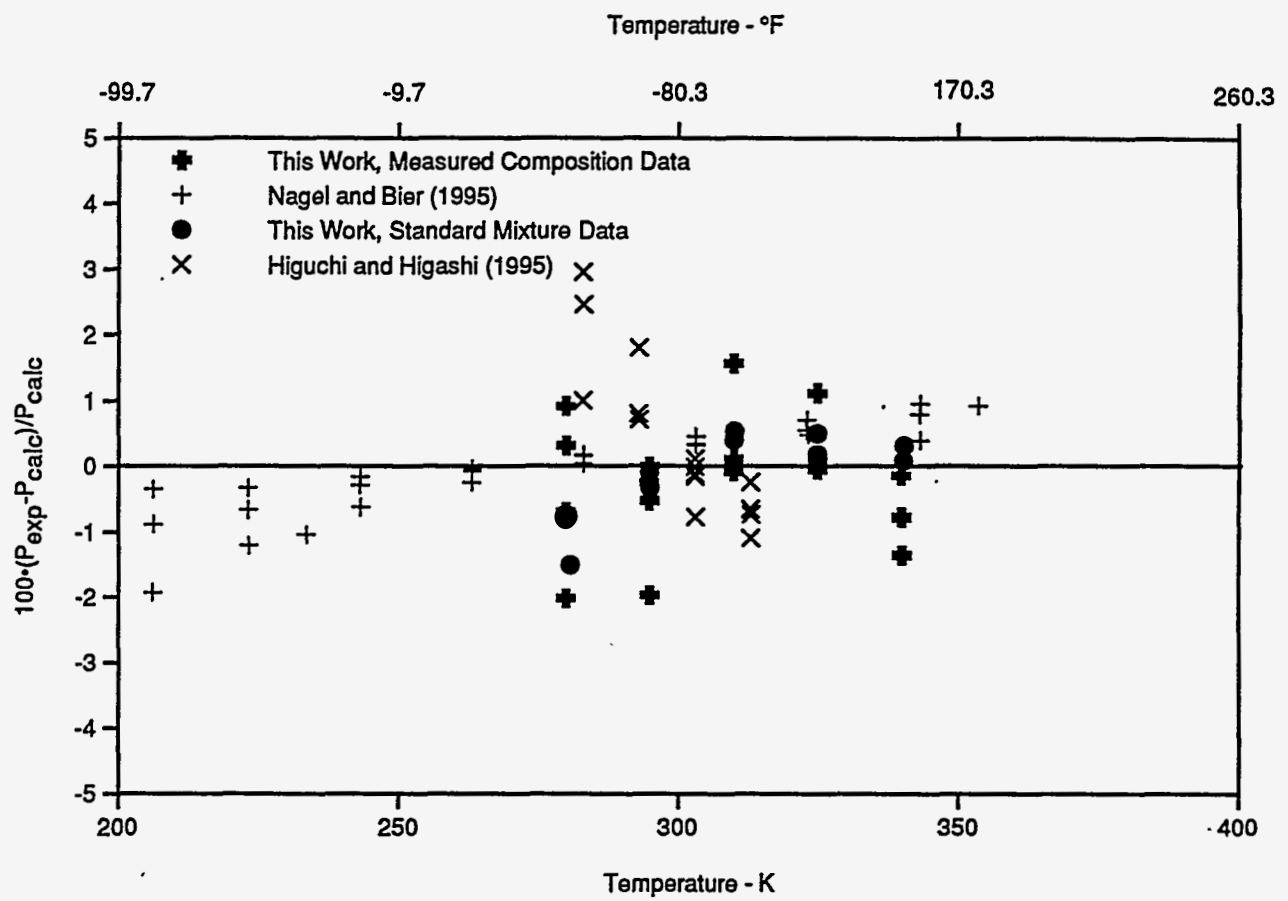


Figure 8. Comparison of Bubble-Point Pressures for the R125/134a System; the Baseline is from the Lemmon-Jacobsen Model in REFPROP 6.0.

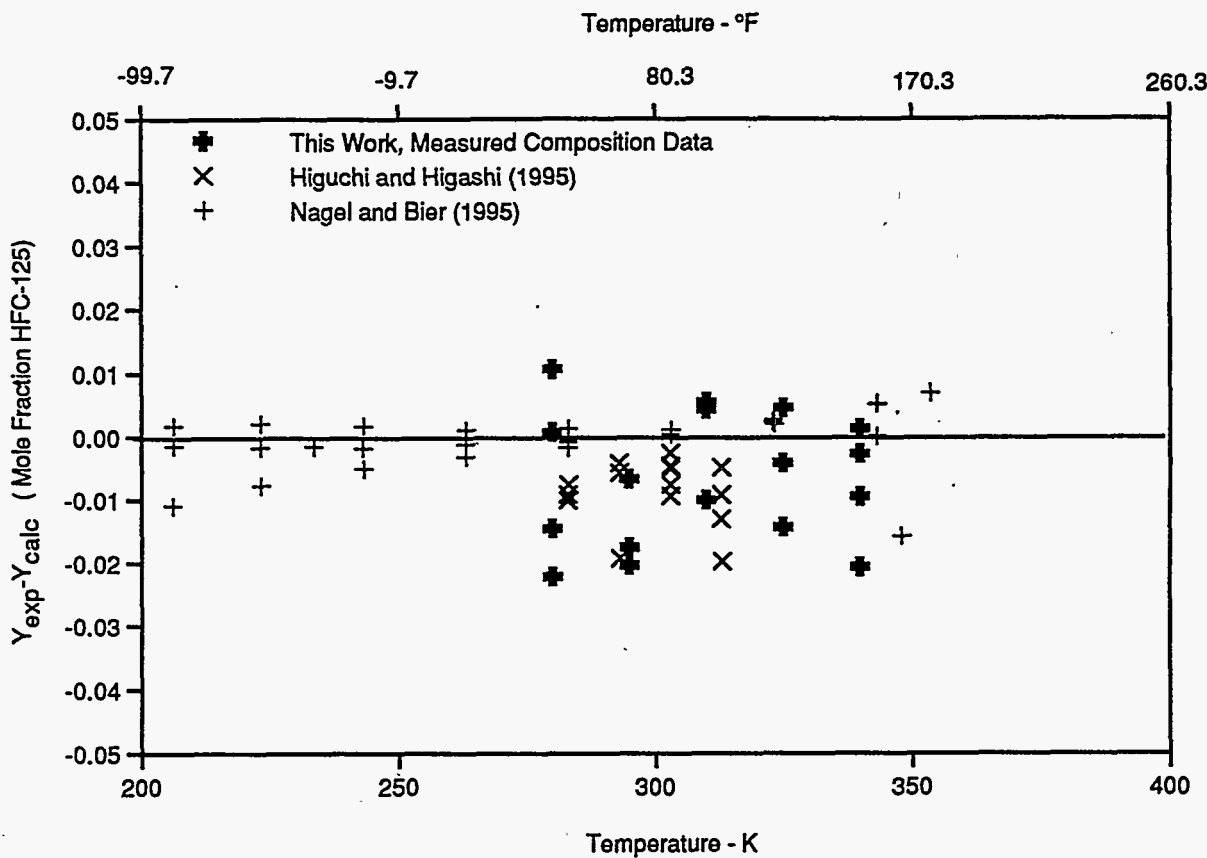


Figure 9. Comparison of Vapor Compositions for the R125/134a System; the Baseline is from the Lemmon-Jacobsen Model in REFPROP 6.0.

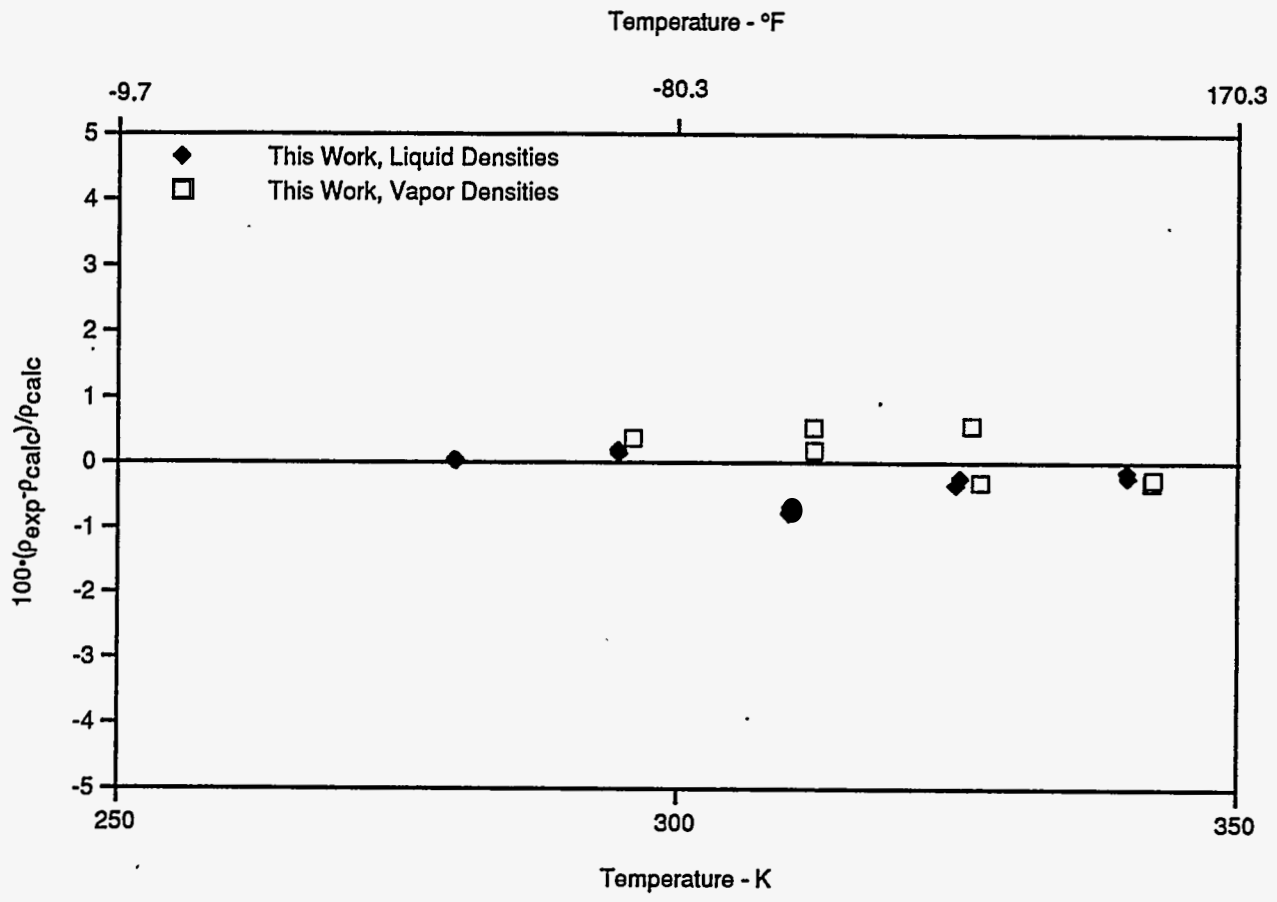


Figure 10. Comparison of Densities for the R125/134a System; the Baseline is from the Lemmon-Jacobsen Model in REPROP 6.0.

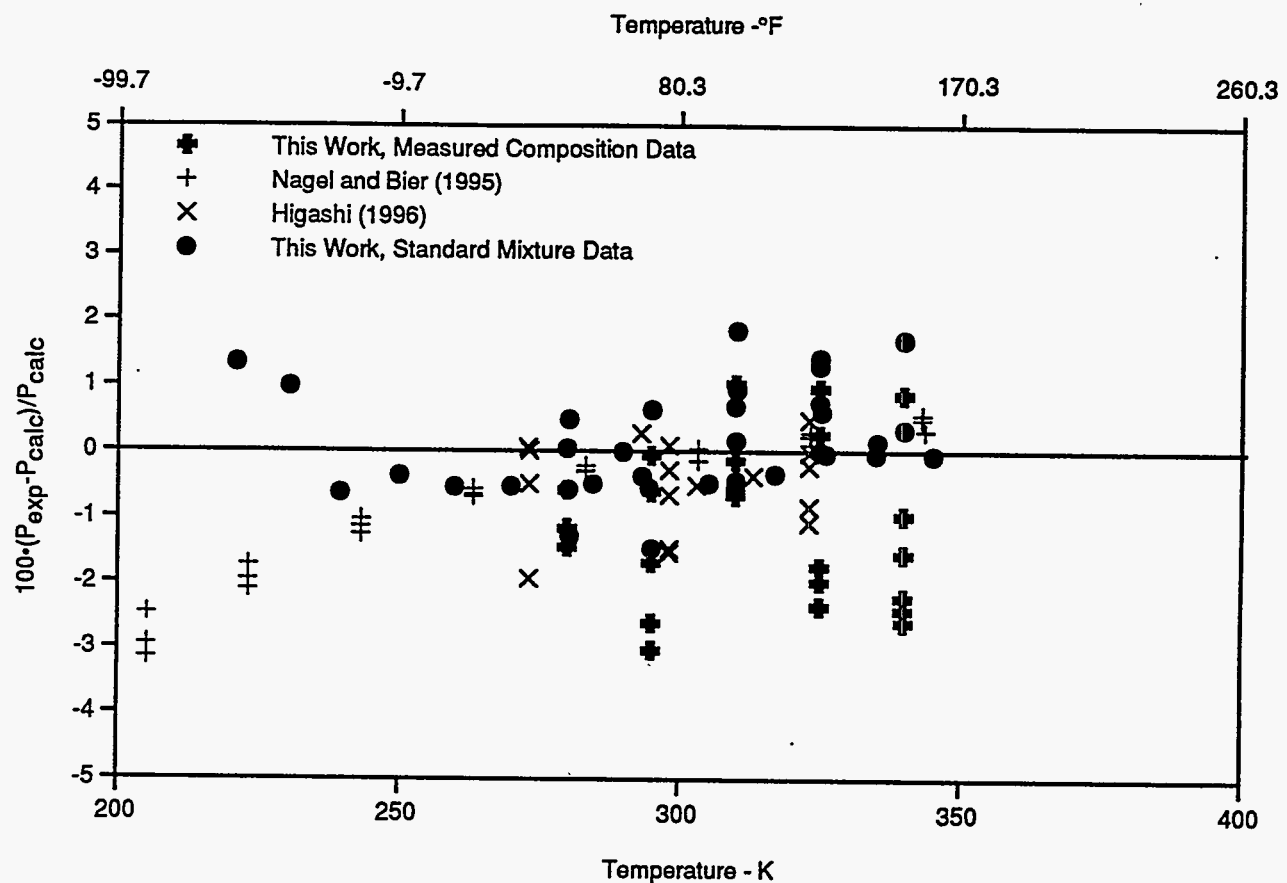


Figure 11. Comparison of Bubble-Point Pressures for the R32/125/134a System; the Baseline is from the Lemmon-Jacobsen Model in REFPROP 6.0.

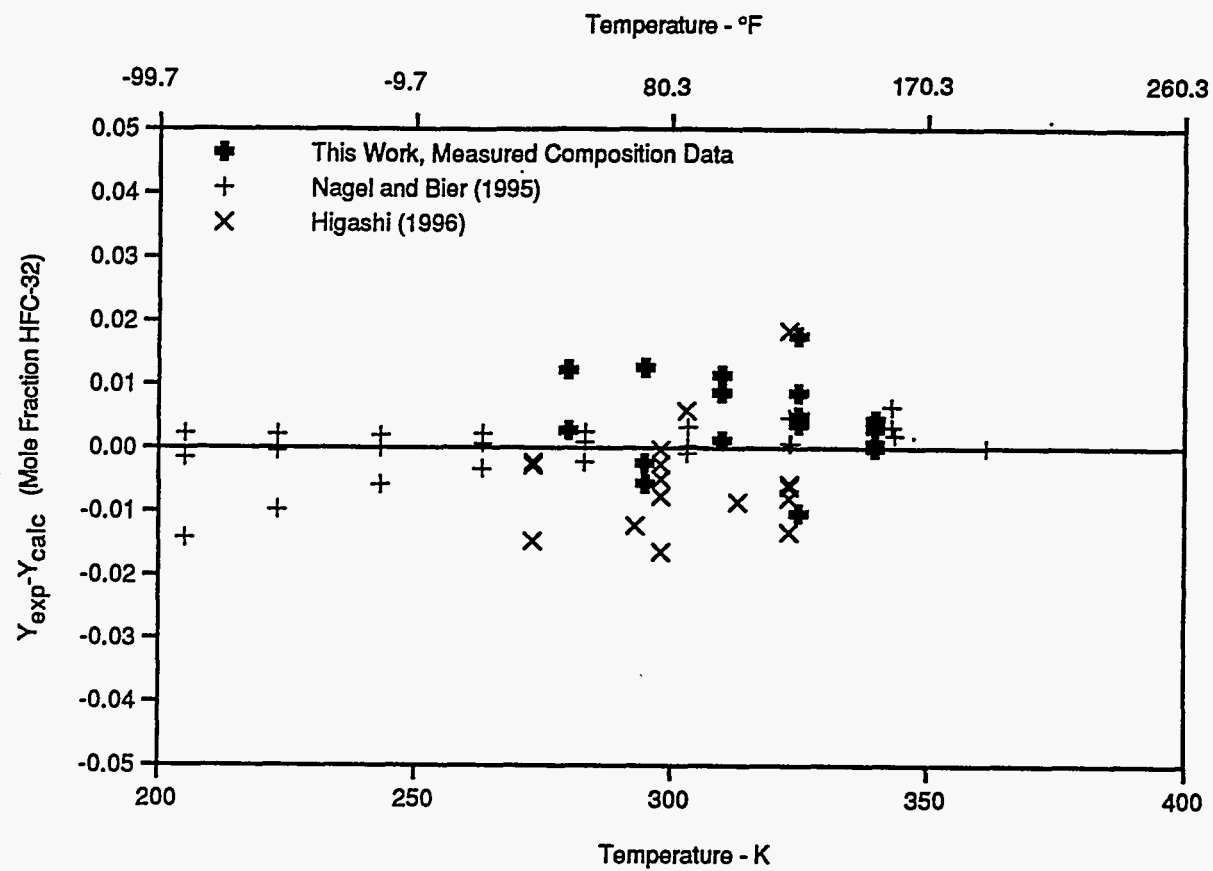


Figure 12. Comparison of Vapor Compositions for the R32/125/134a System; the Baseline is from the Lemmon-Jacobsen Model in REFPROP 6.0.

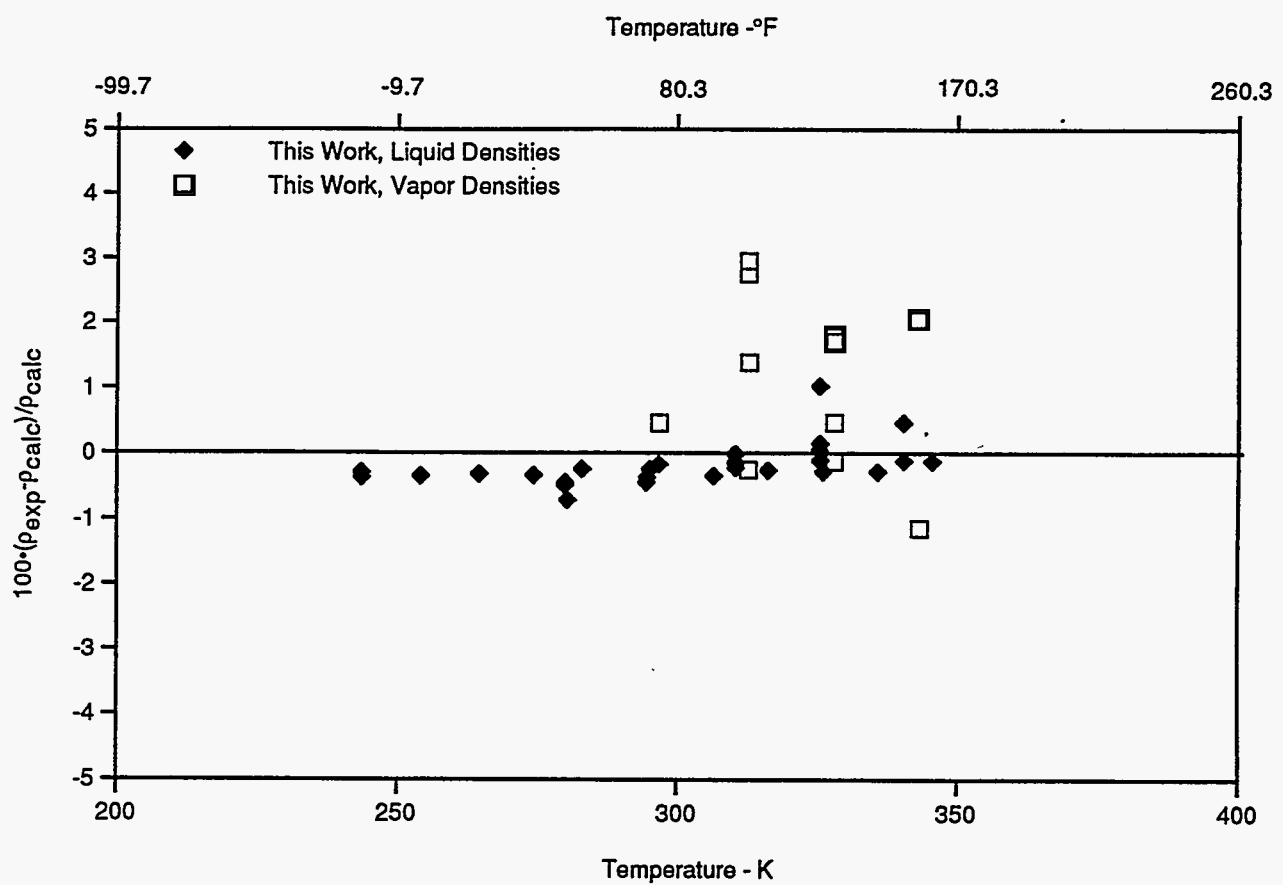


Figure 13. Comparison of Densities for the R32/125/134a System; the Baseline is from the Lemmon-Jacobsen Model in REFPROP 6.0.

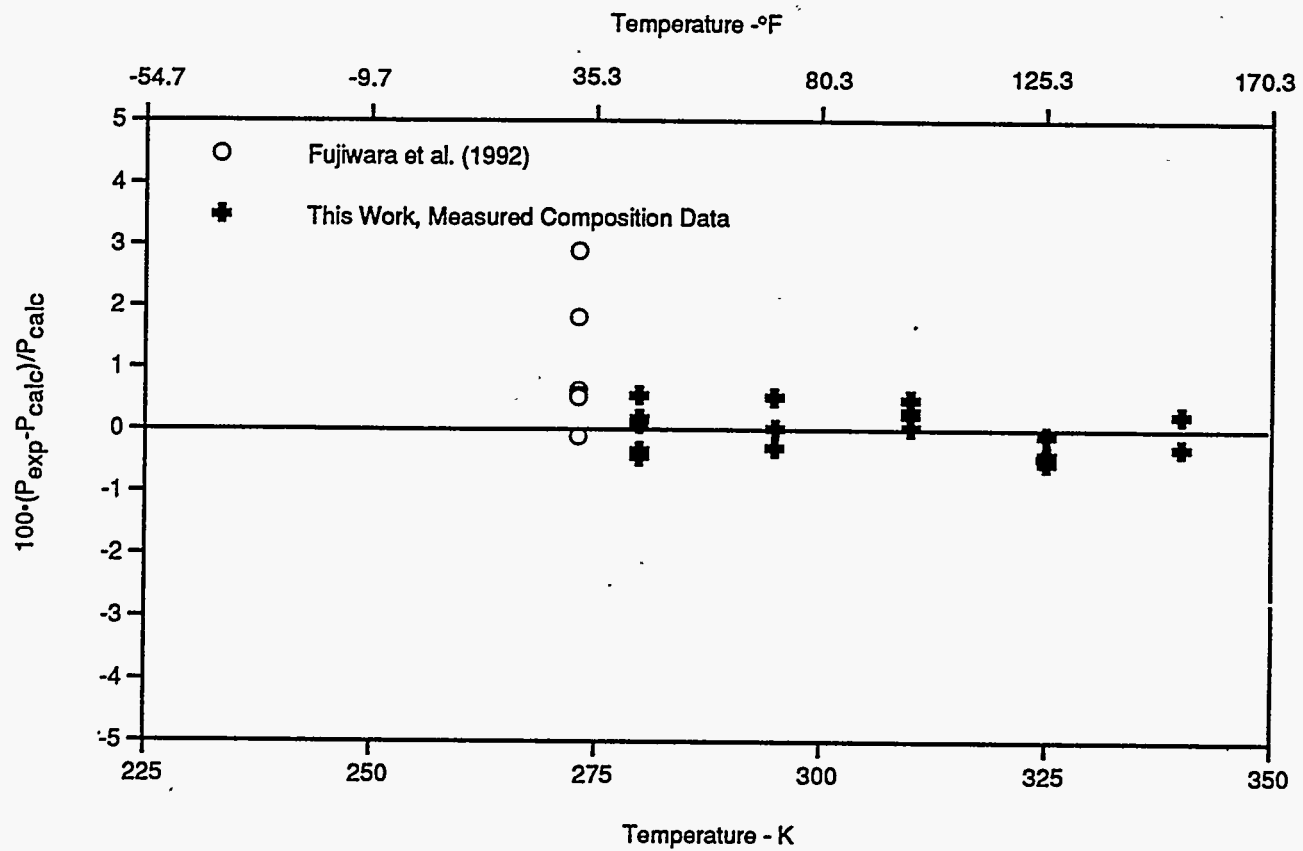


Figure 14. Comparison of Bubble-Point Pressures for the R32/143a System; the Baseline is from the Lemmon-Jacobsen Model in REFPROP 6.0.

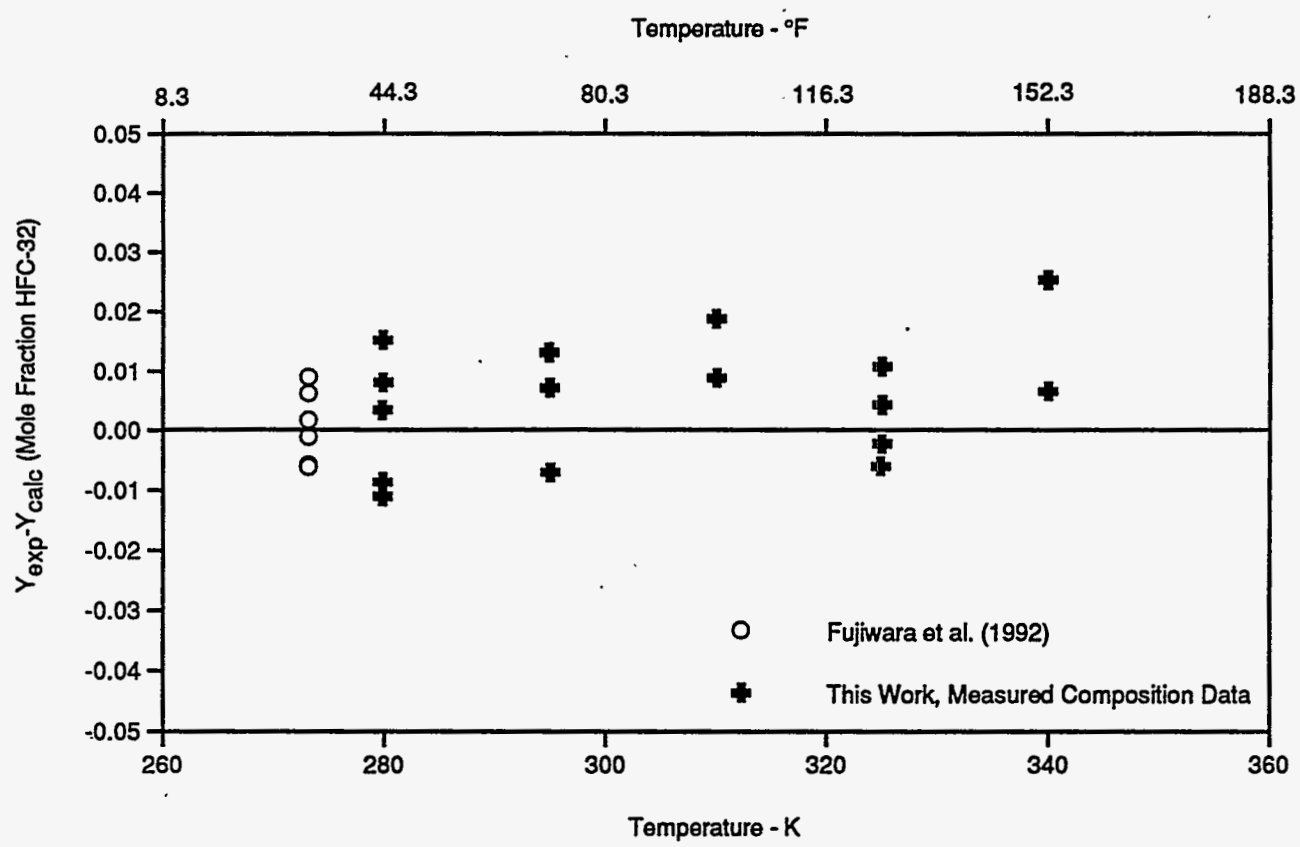


Figure 15. Comparison of Vapor Compositions for the R32/143a System; the Baseline is from the Lemmon-Jacobsen Model in REFPROP 6.0.

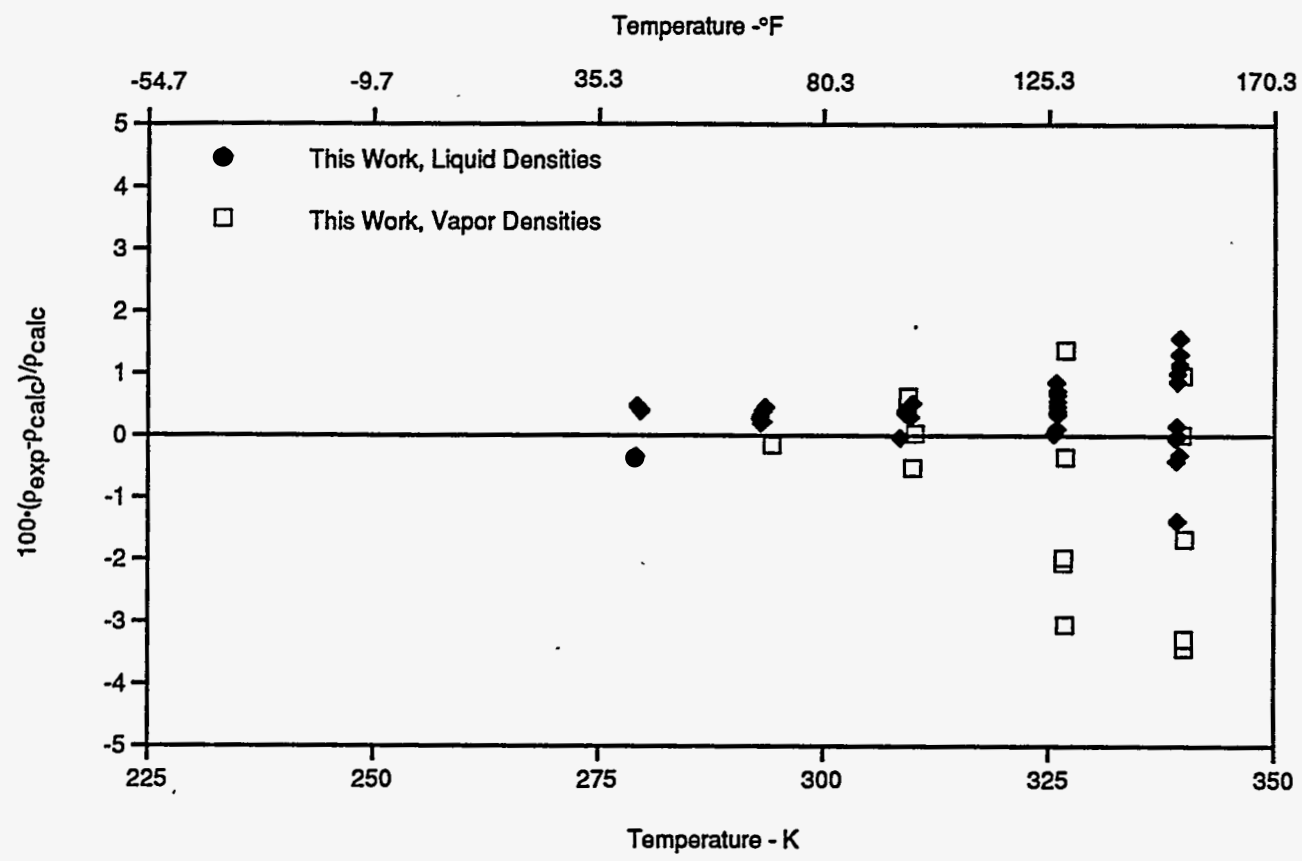


Figure 16. Comparison of Densities for the R32/143a System; the Baseline is from the Lemmon-Jacobsen Model in REFPROP 6.0.

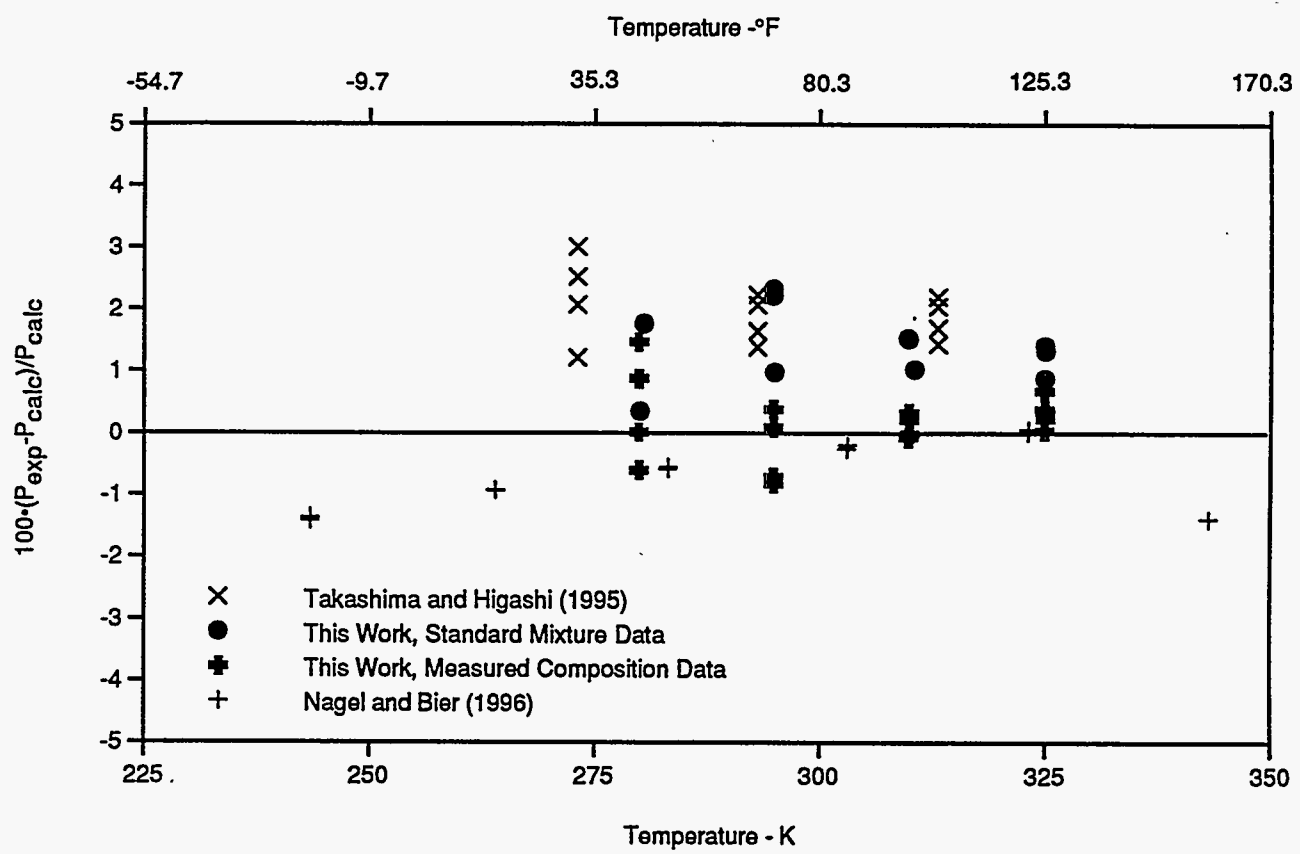


Figure 17. Comparison of Bubble-Point Pressures for the R125/143a System; the Baseline is from the Lemmon-Jacobsen Model in REFPROP 6.0.

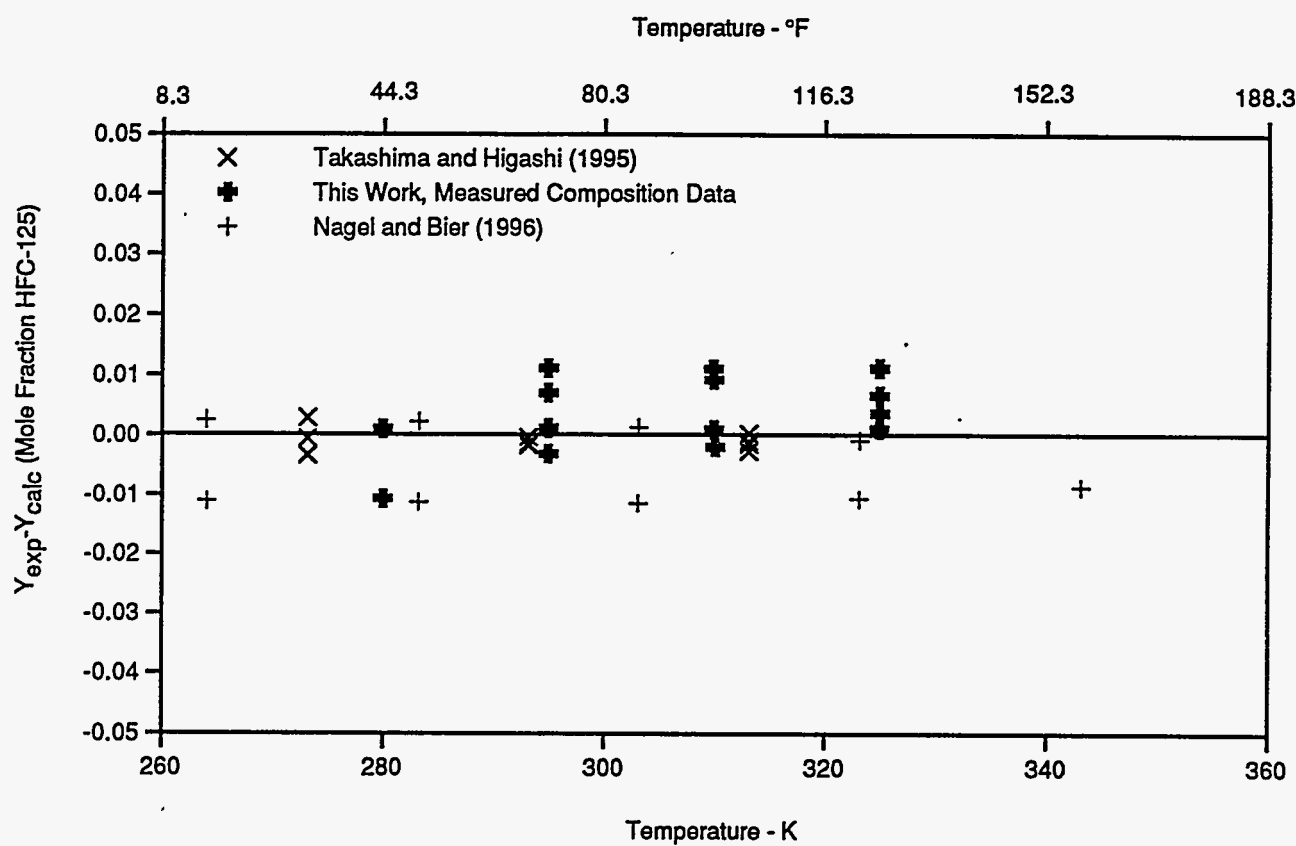


Figure 18. Comparison of Vapor Compositions for the R125/143a System; the Baseline is from the Lemmon-Jacobsen Model in REFPROP 6.0.

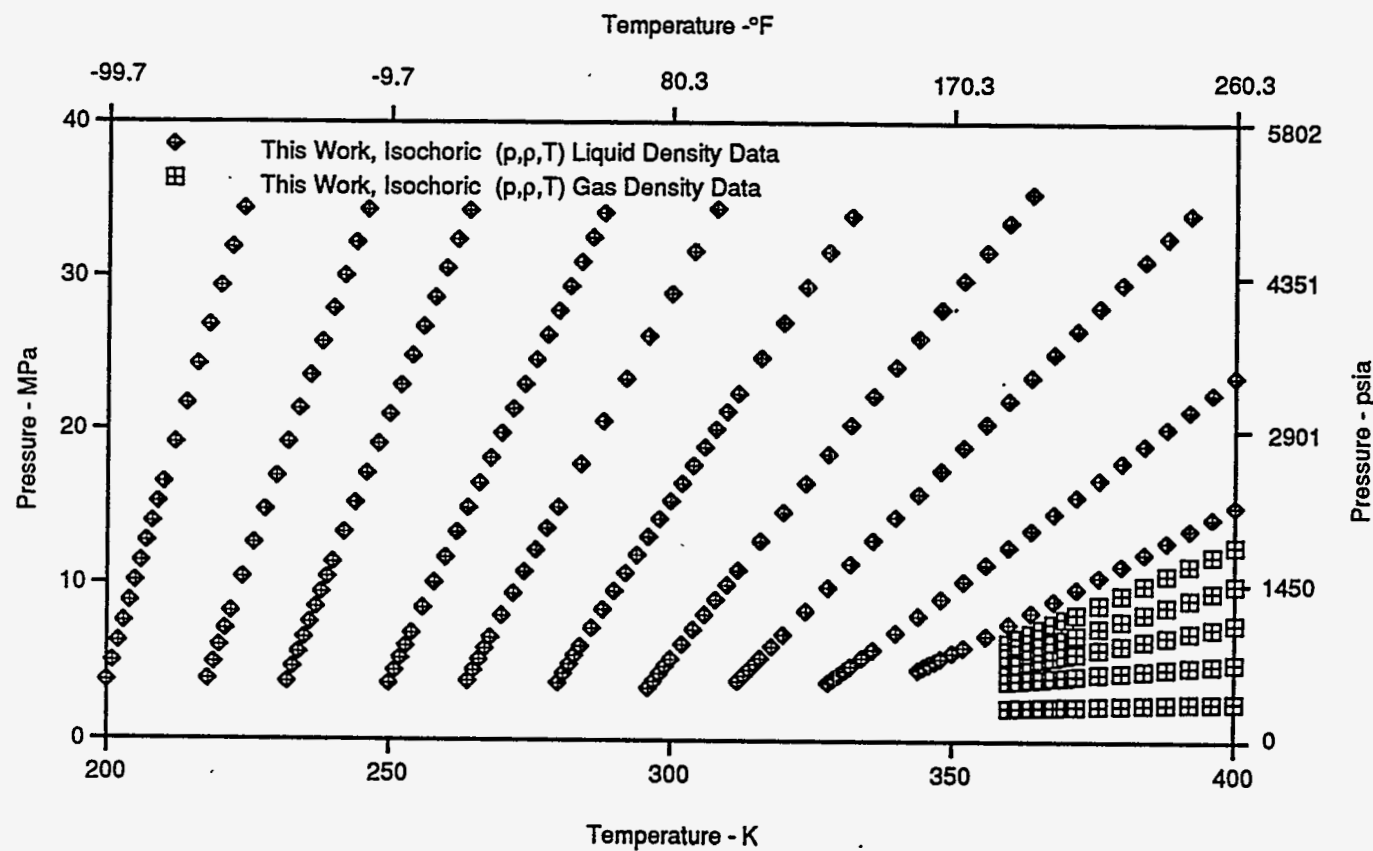


Figure 19. Range of Measured Temperatures and Pressures for Isochoric (p,p,T) Data for a Mixture of R125/143a with $x(\text{R125}) = 0.49996$ Mole Fraction (0.58812 Mass Fraction).

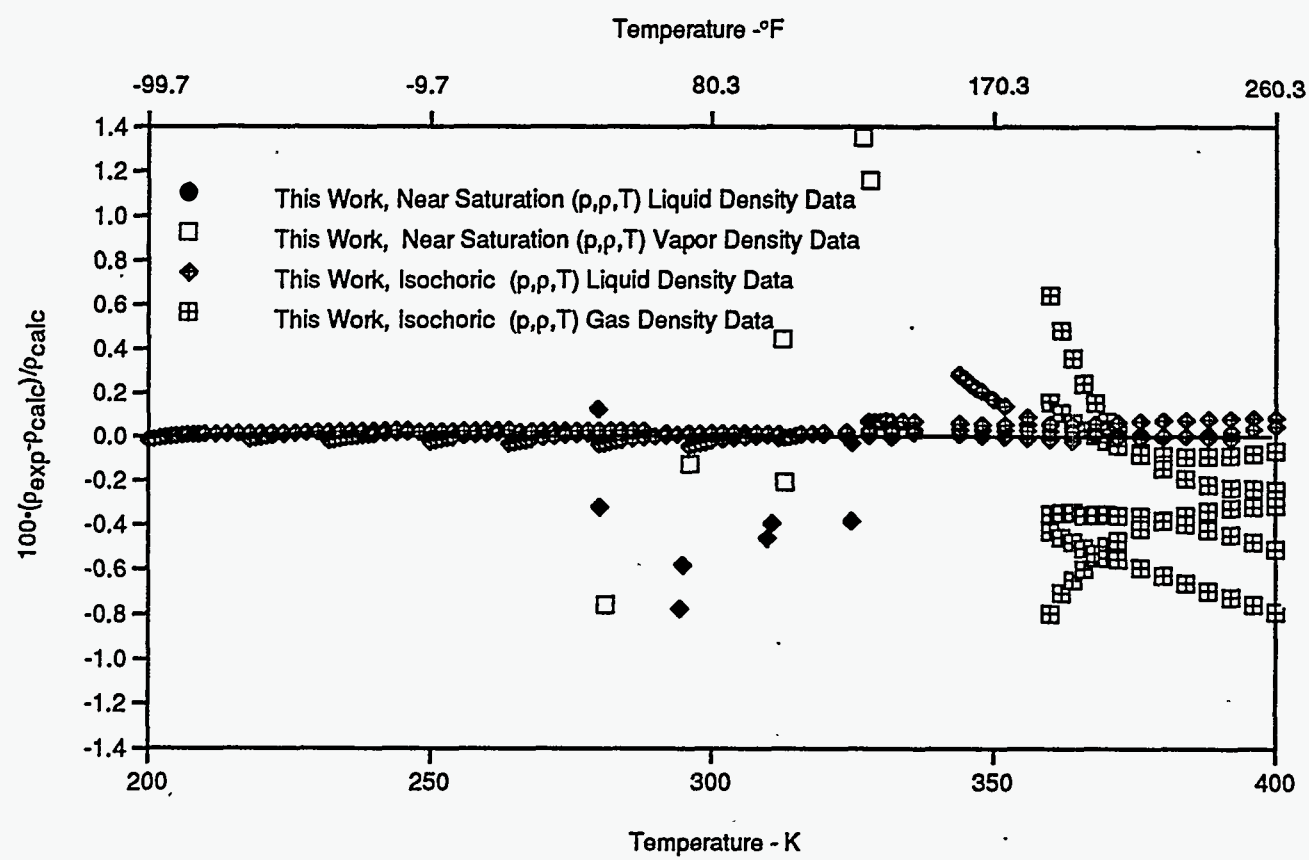


Figure 20. Comparison of Densities for the R125/143a System; the Baseline is from the Lemmon-Jacobsen Model in REFPROP 6.0.

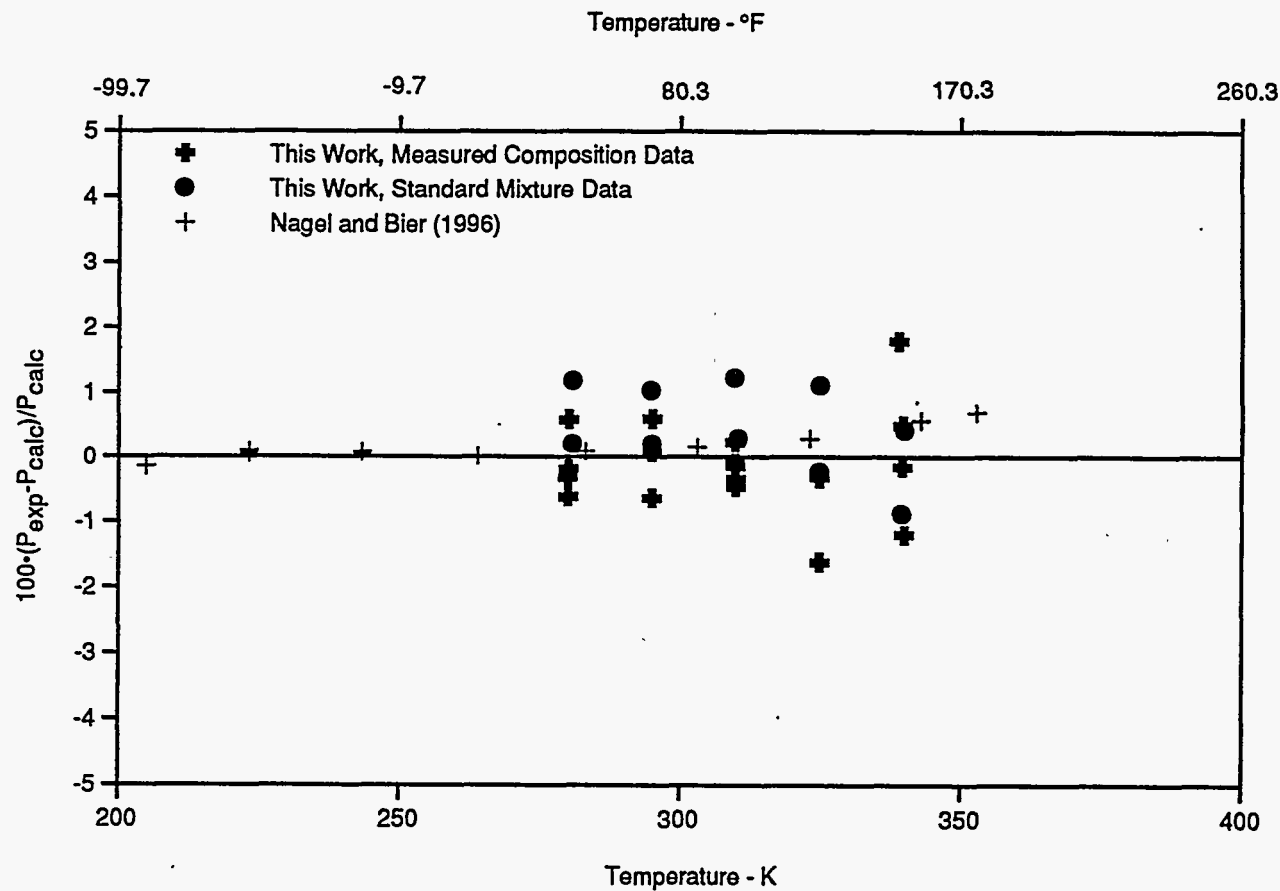


Figure 21. Comparison of Bubble-Point Pressures for the R143a/134a System; the Baseline is from the Lemmon-Jacobsen Model in REFPROP 6.0.

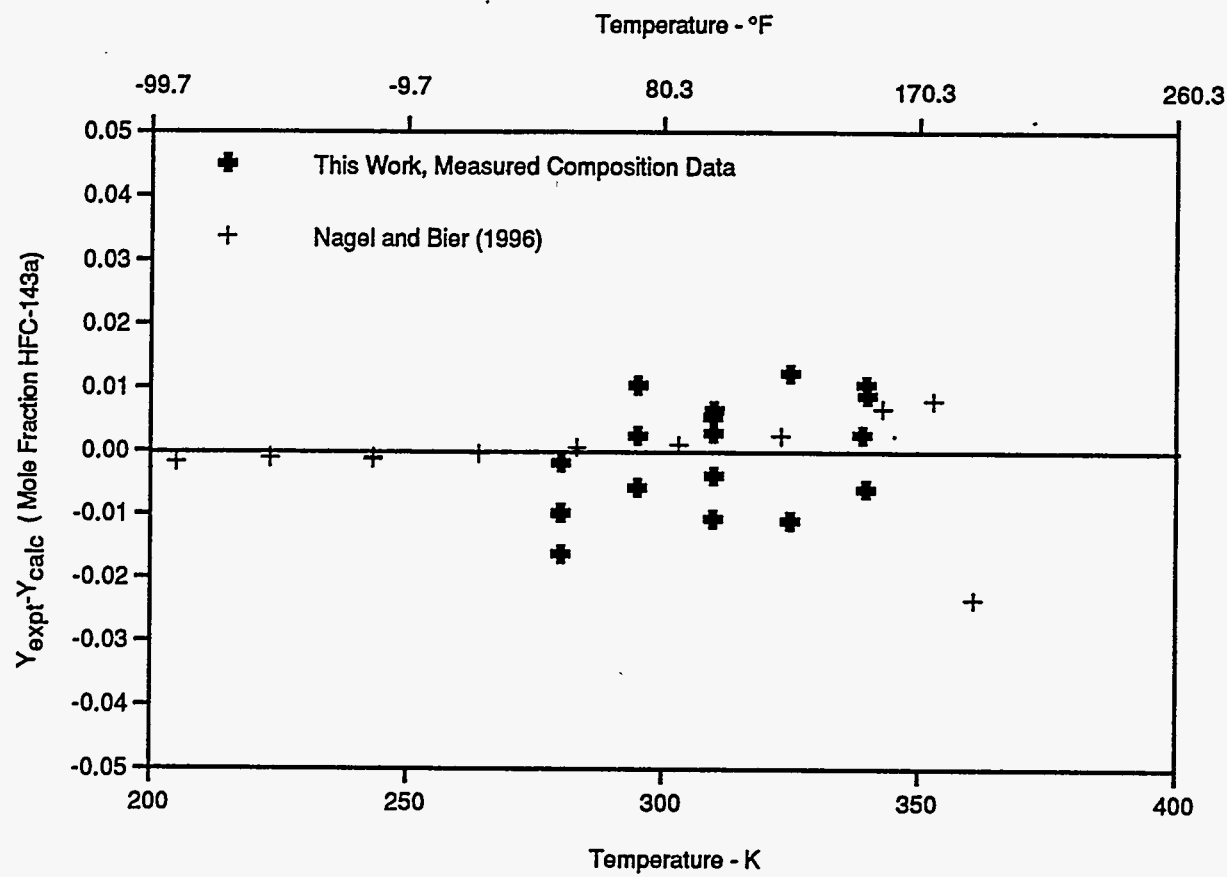


Figure 22. Comparison of Vapor Compositions for the R143a/134a System; the Baseline is from the Lemmon-Jacobsen Model in REFPROP 6.0.

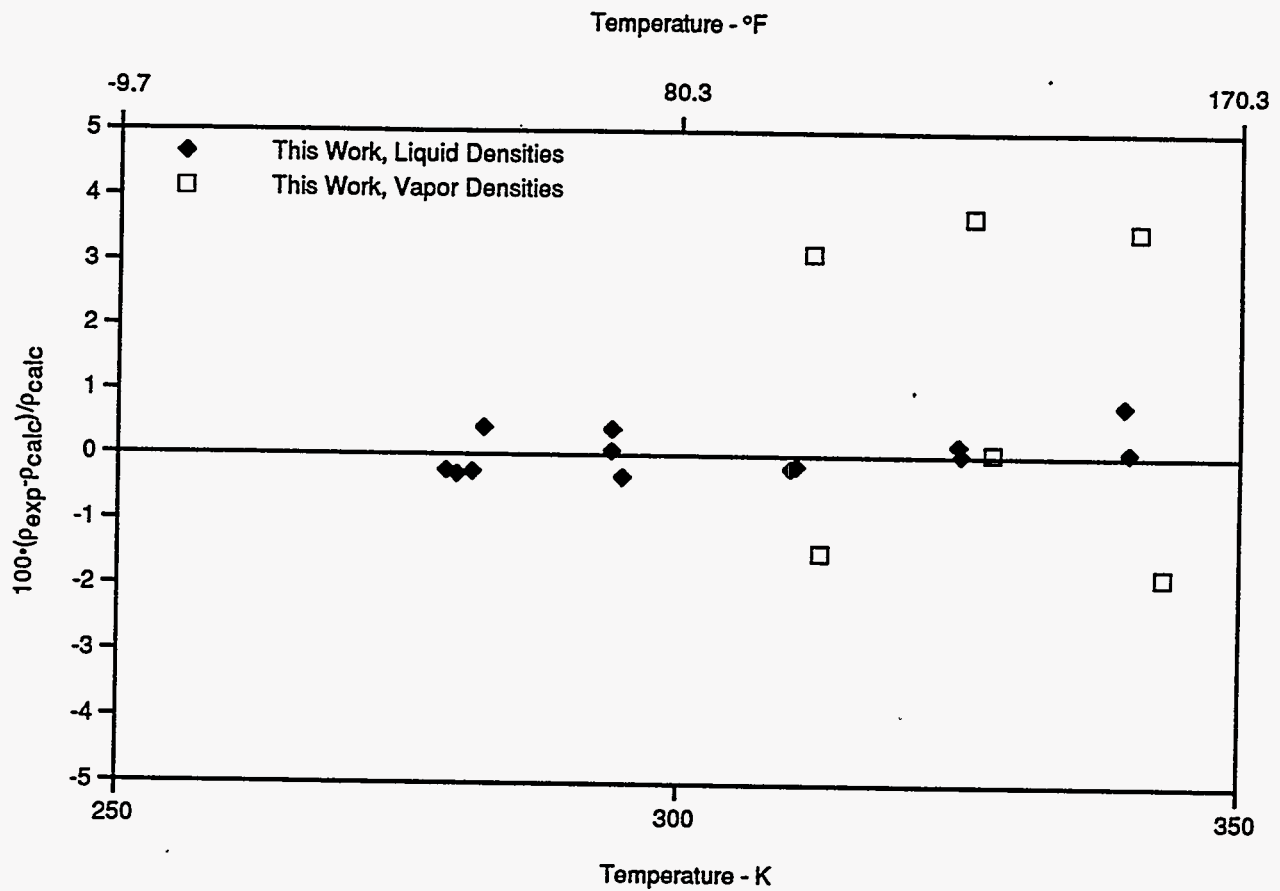


Figure 23. Comparison of Densities for the R143a/134a System; the Baseline is from the Lemmon-Jacobsen Model in REFPROP 6.0.

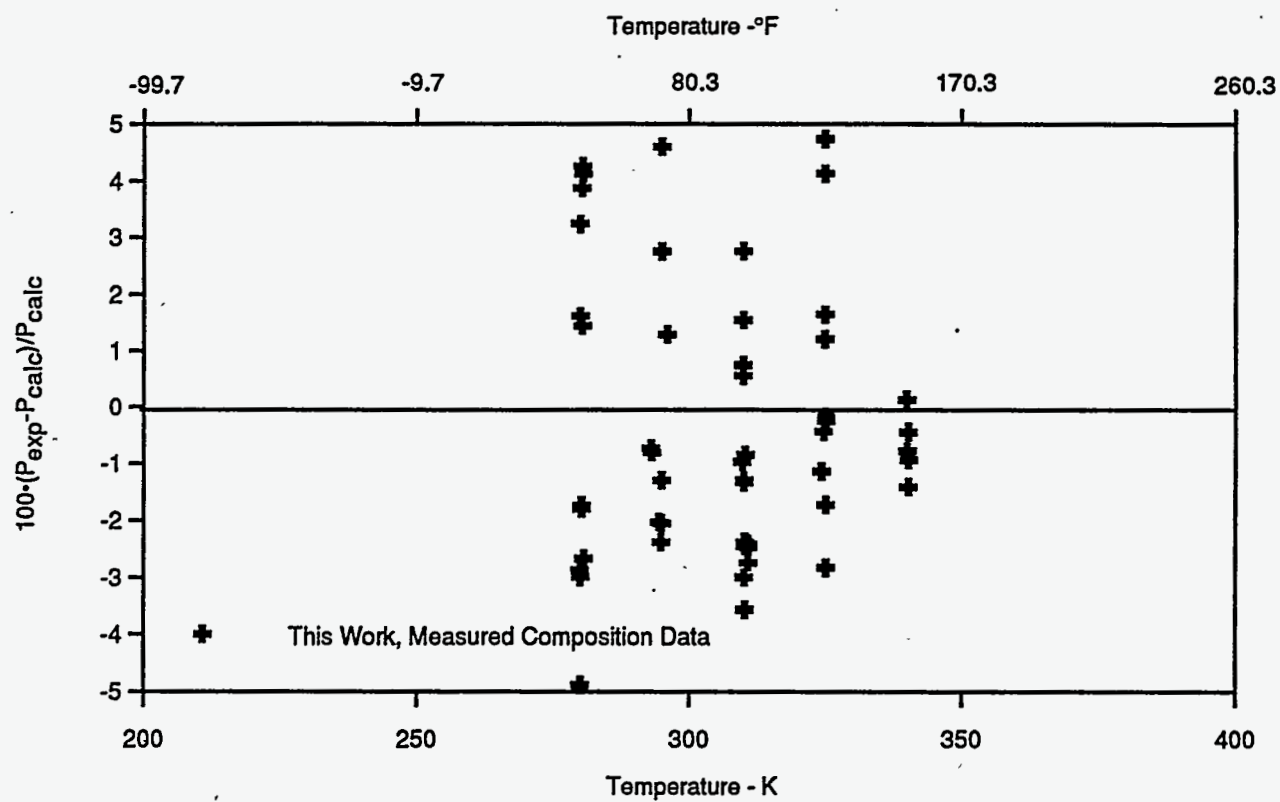


Figure 24. Comparison of Bubble-Point Pressures for the R32/290 System; the Baseline is from the Lemmon-Jacobsen Model in REFPROP 6.0.

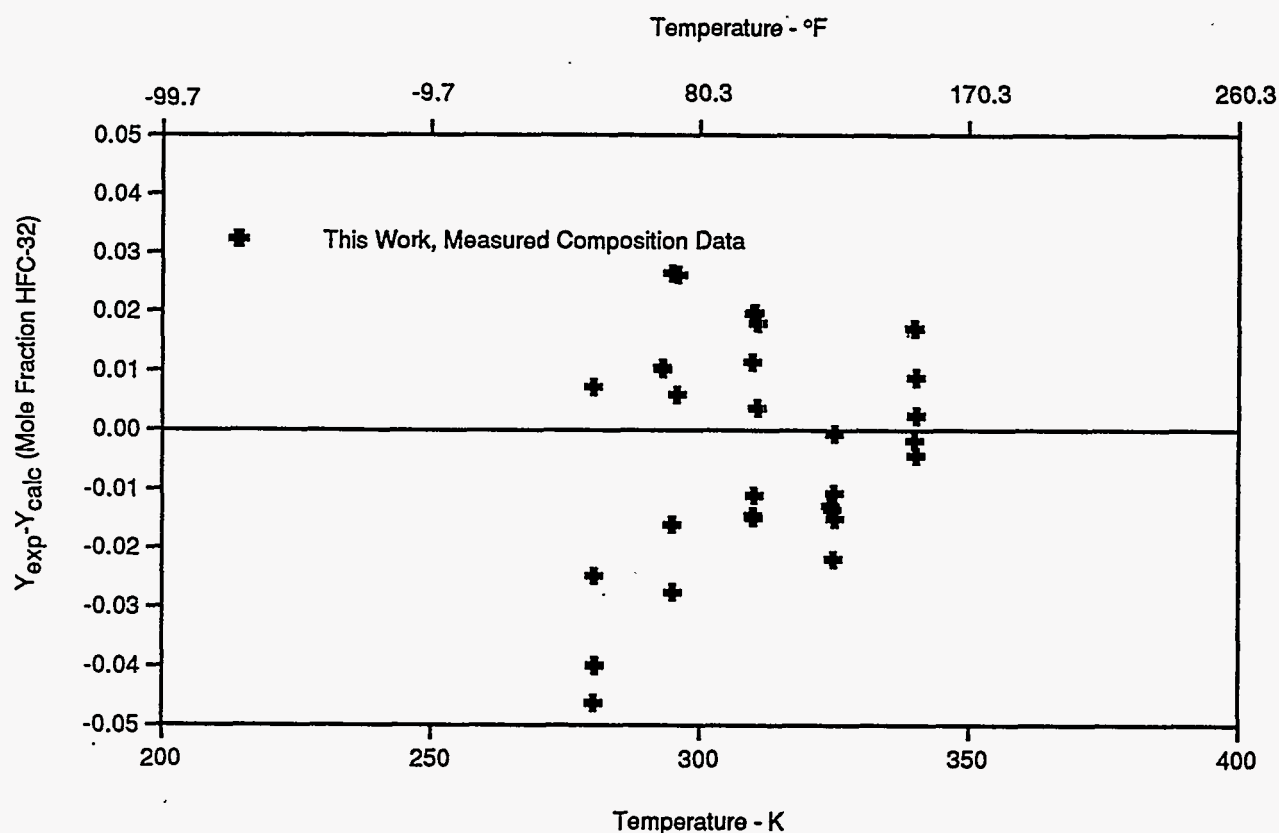


Figure 25. Comparison of Vapor Compositions for the R32/290 System; the Baseline is from the Lemmon-Jacobsen Model in REFPROP 6.0.

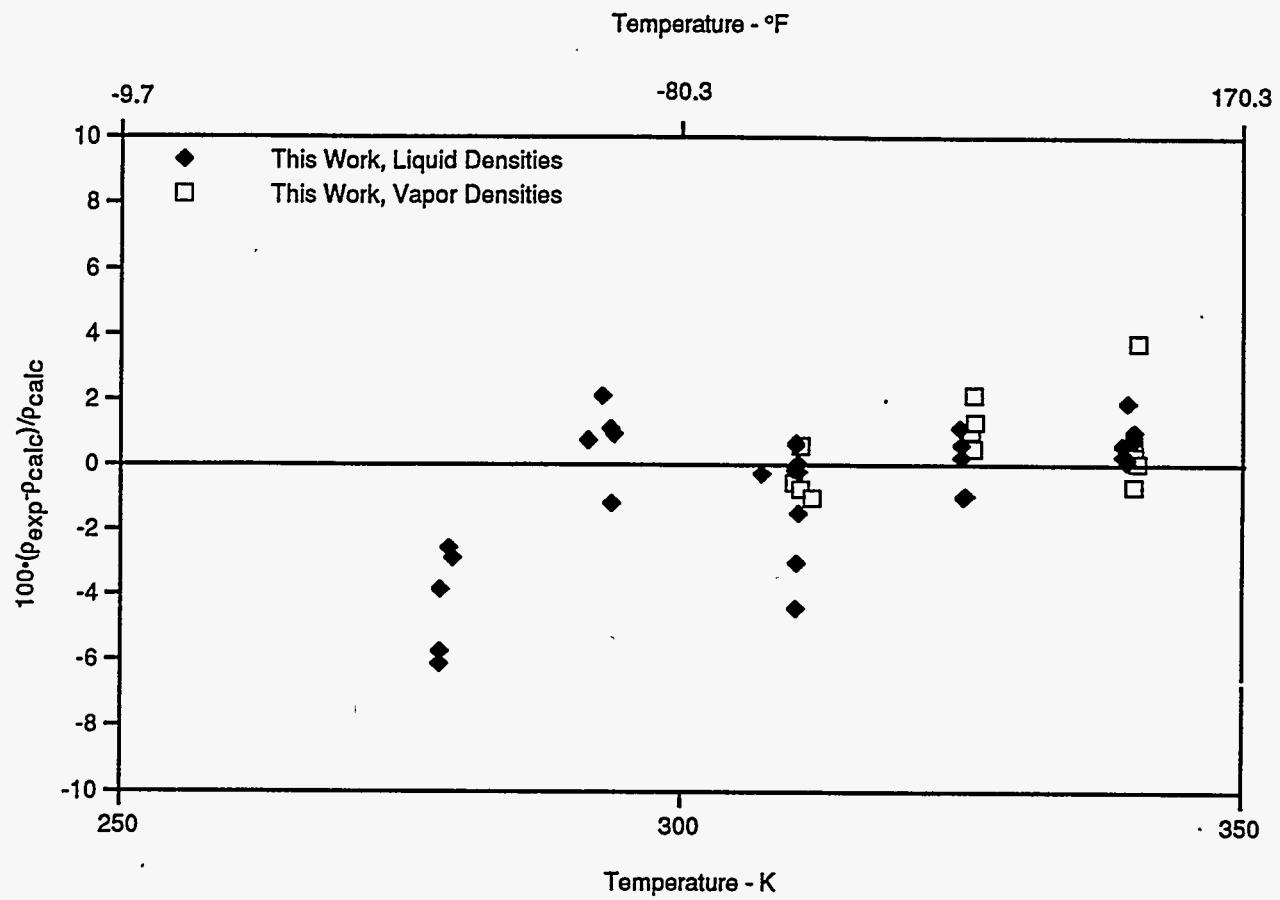


Figure 26. Comparison of Densities for the R32/290 System; the Baseline is from the Lemmon-Jacobsen Model in REFPROP 6.0.

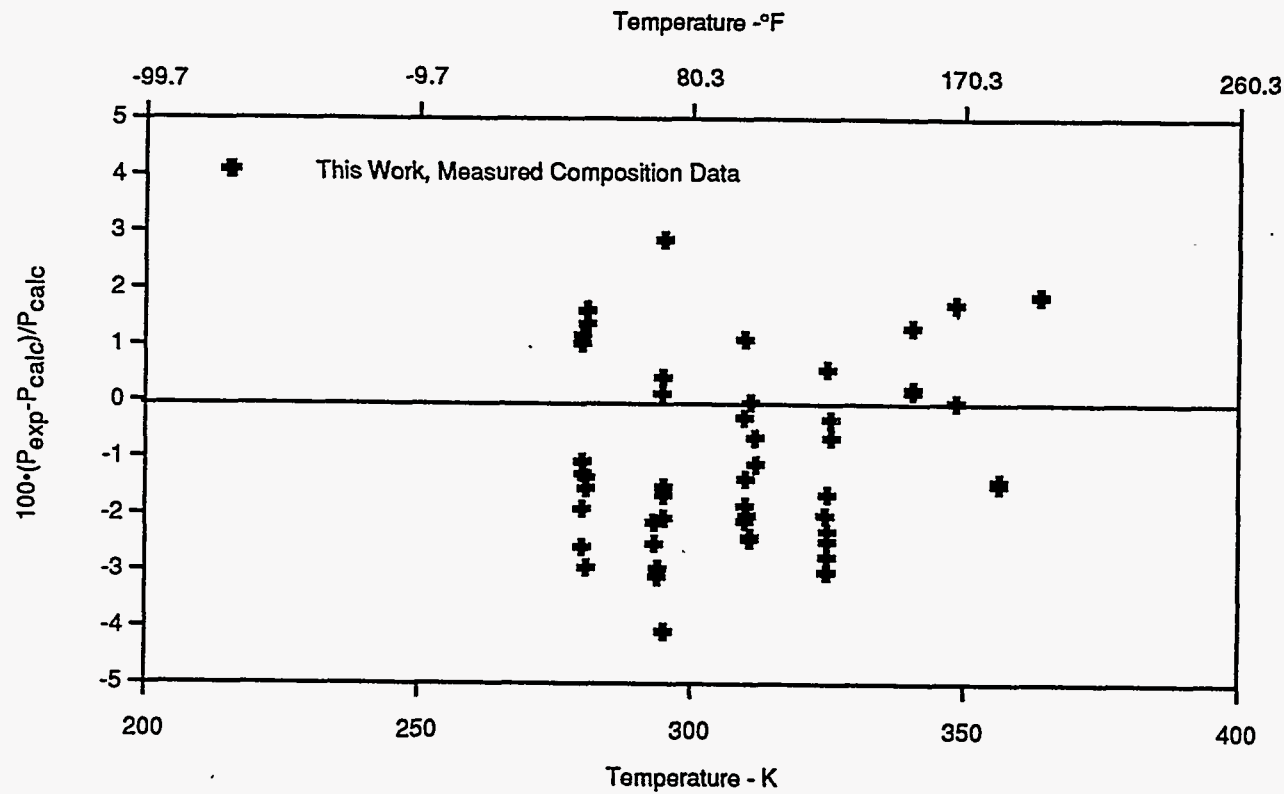


Figure 27. Comparison of Bubble-Point Pressures for the R125/290 System; the Baseline is from the Lemmon-Jacobsen Model in REFPROP 6.0.

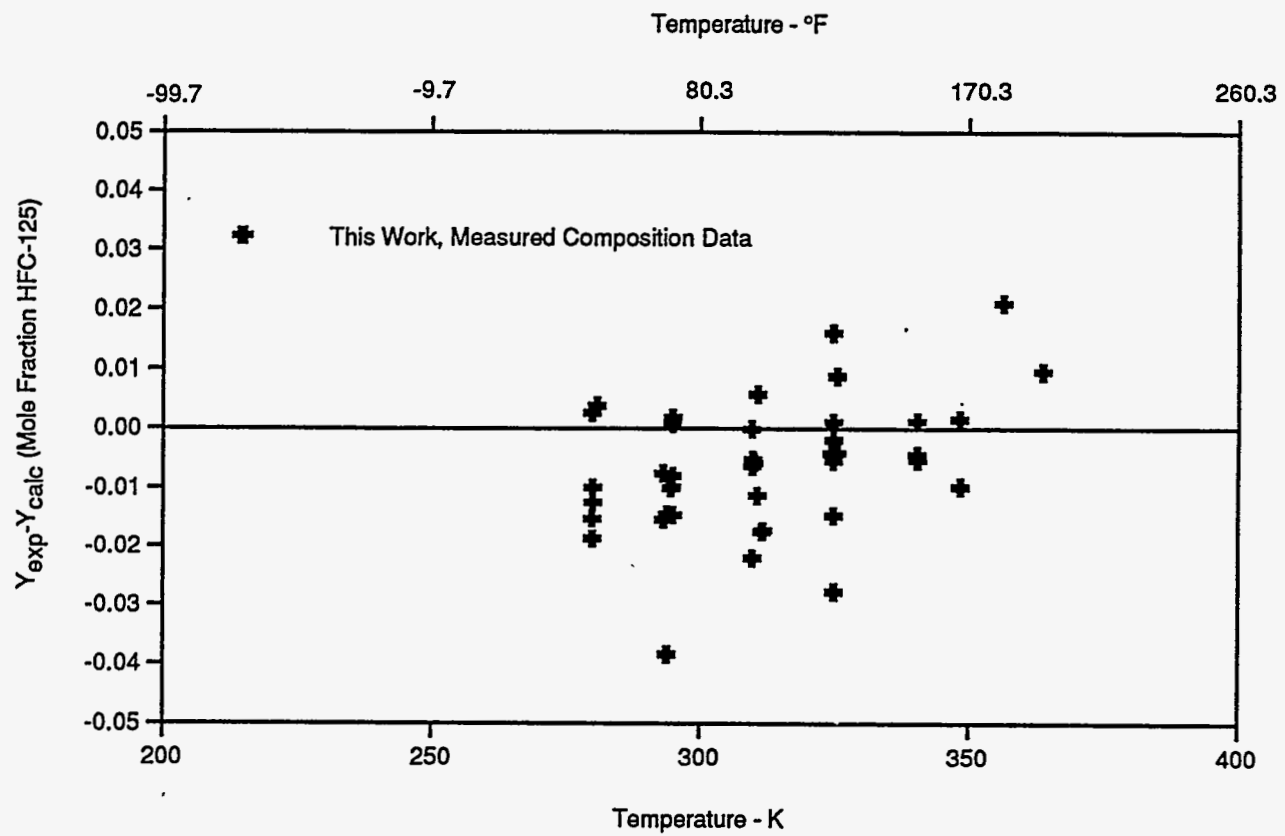


Figure 28. Comparison of Vapor Compositions for the R125/290 System; the Baseline is from the Lemmon-Jacobsen Model in REFPROP 6.0.

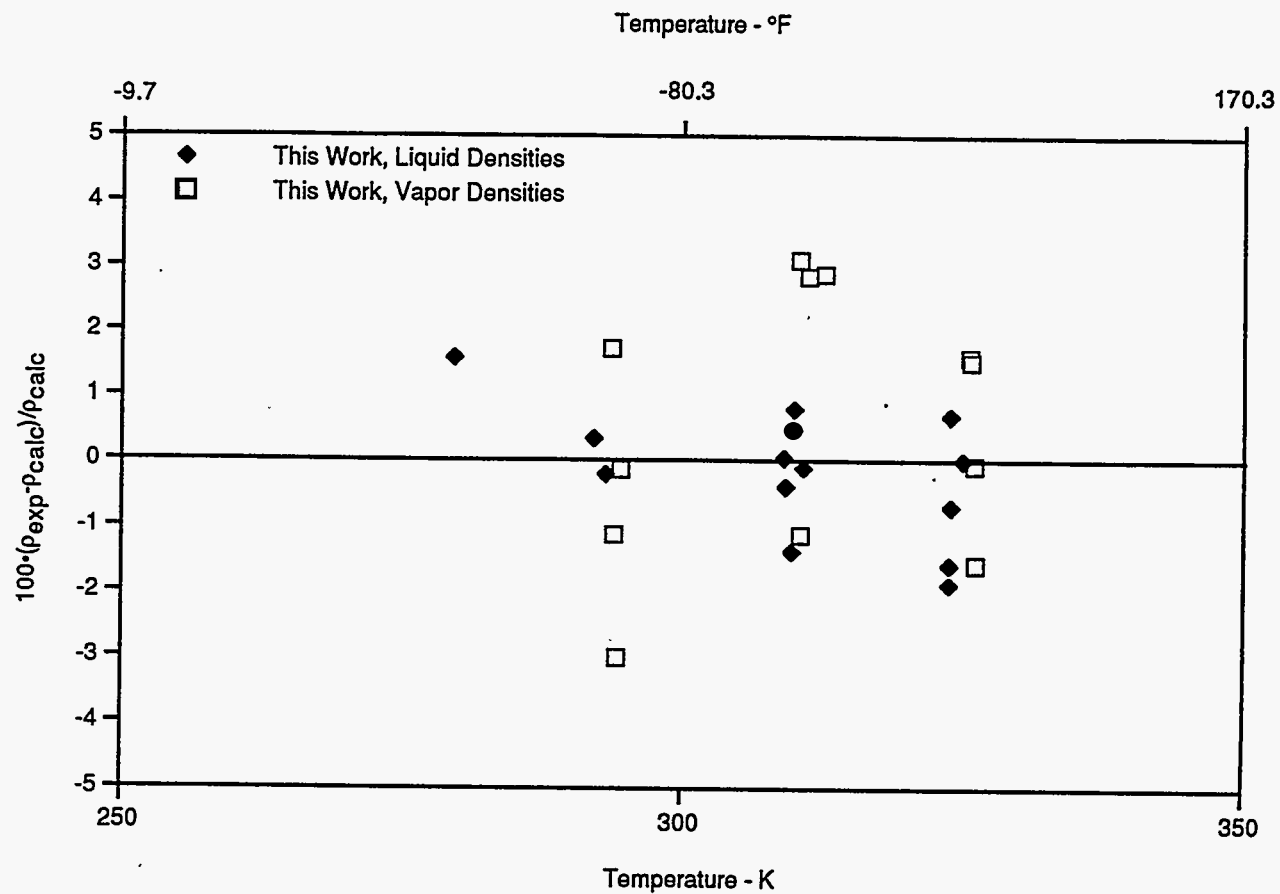


Figure 29. Comparison of Densities for the R125/290 System; the Baseline is from the Lemmon-Jacobsen Model in REFPROP 6.0.

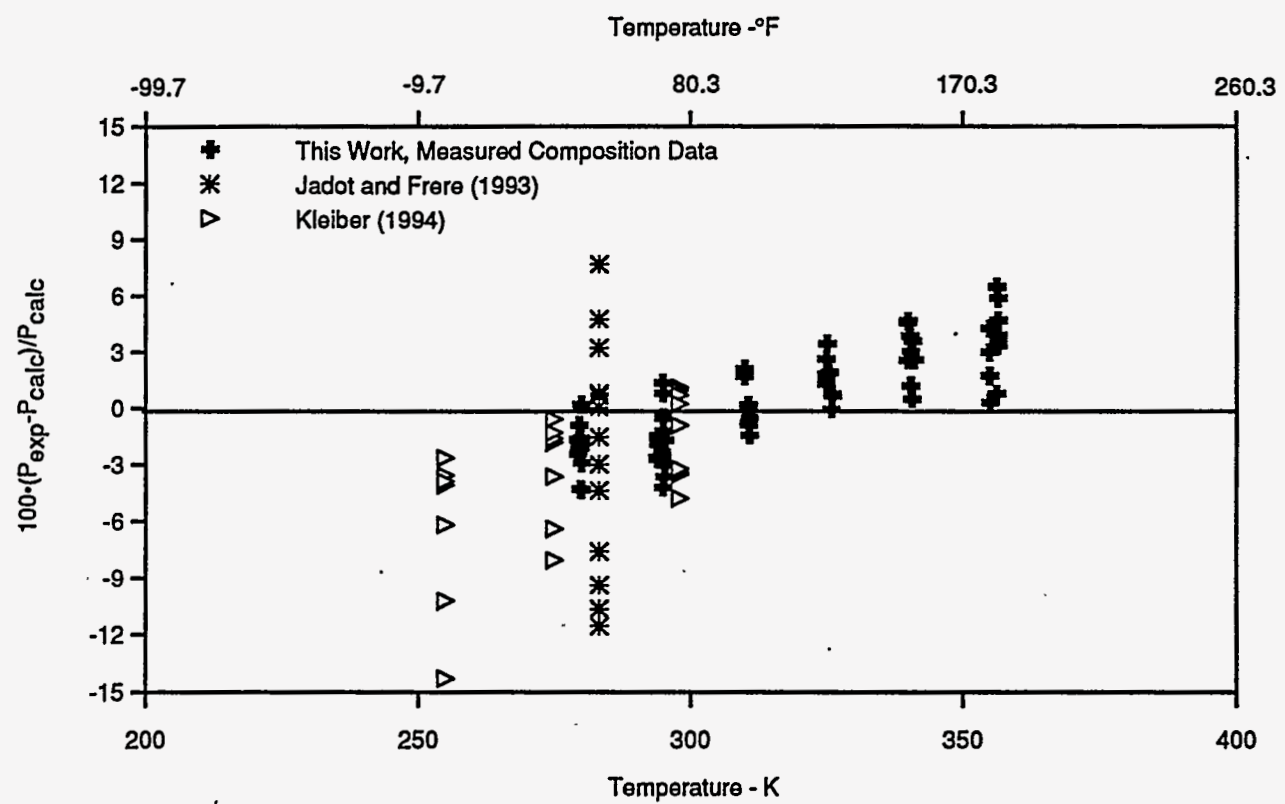


Figure 30. Comparison of Bubble-Point Pressures for the R134a/290 System; the Baseline is from the Lemmon-Jacobsen Model in REFPROP 6.0.

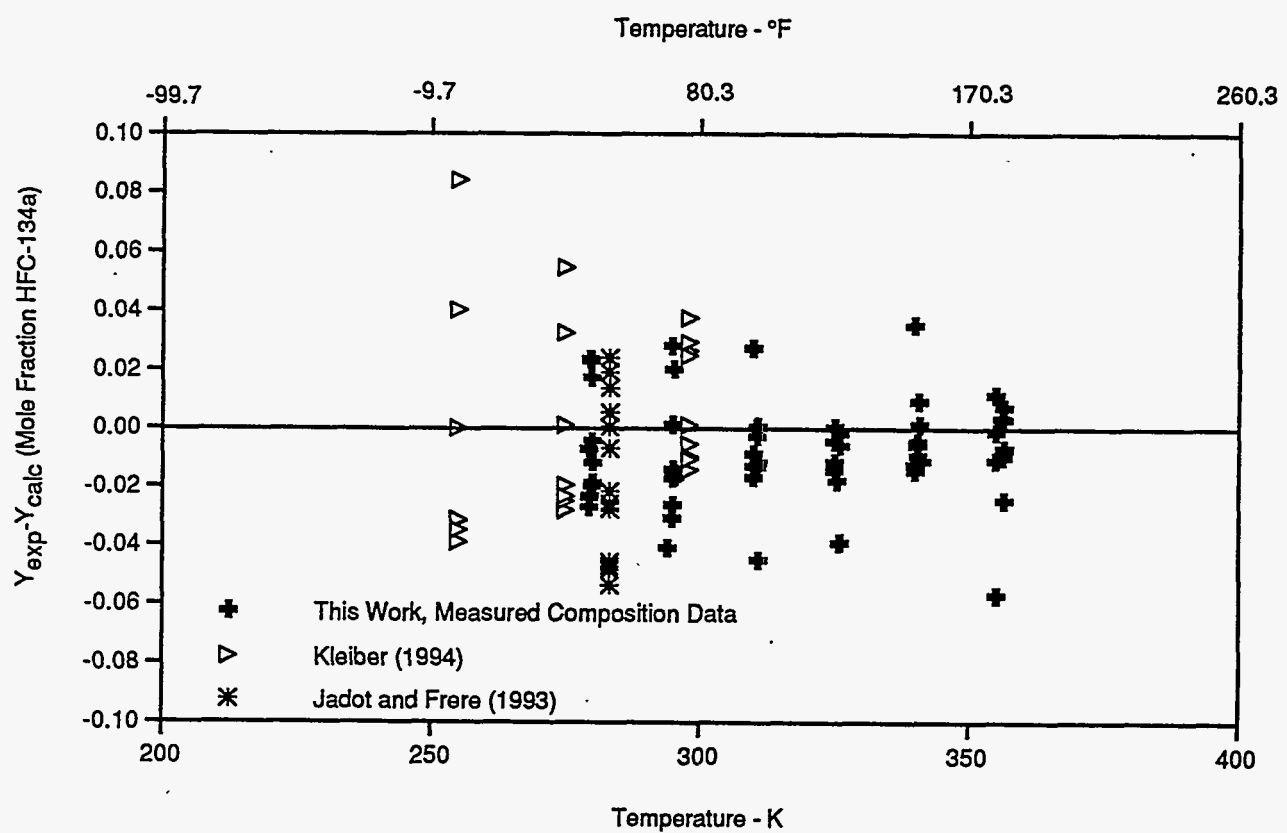


Figure 31. Comparison of Vapor Compositions for the R134a/290 System; the Baseline is from the Lemmon-Jacobsen Model in REFPROP 6.0.

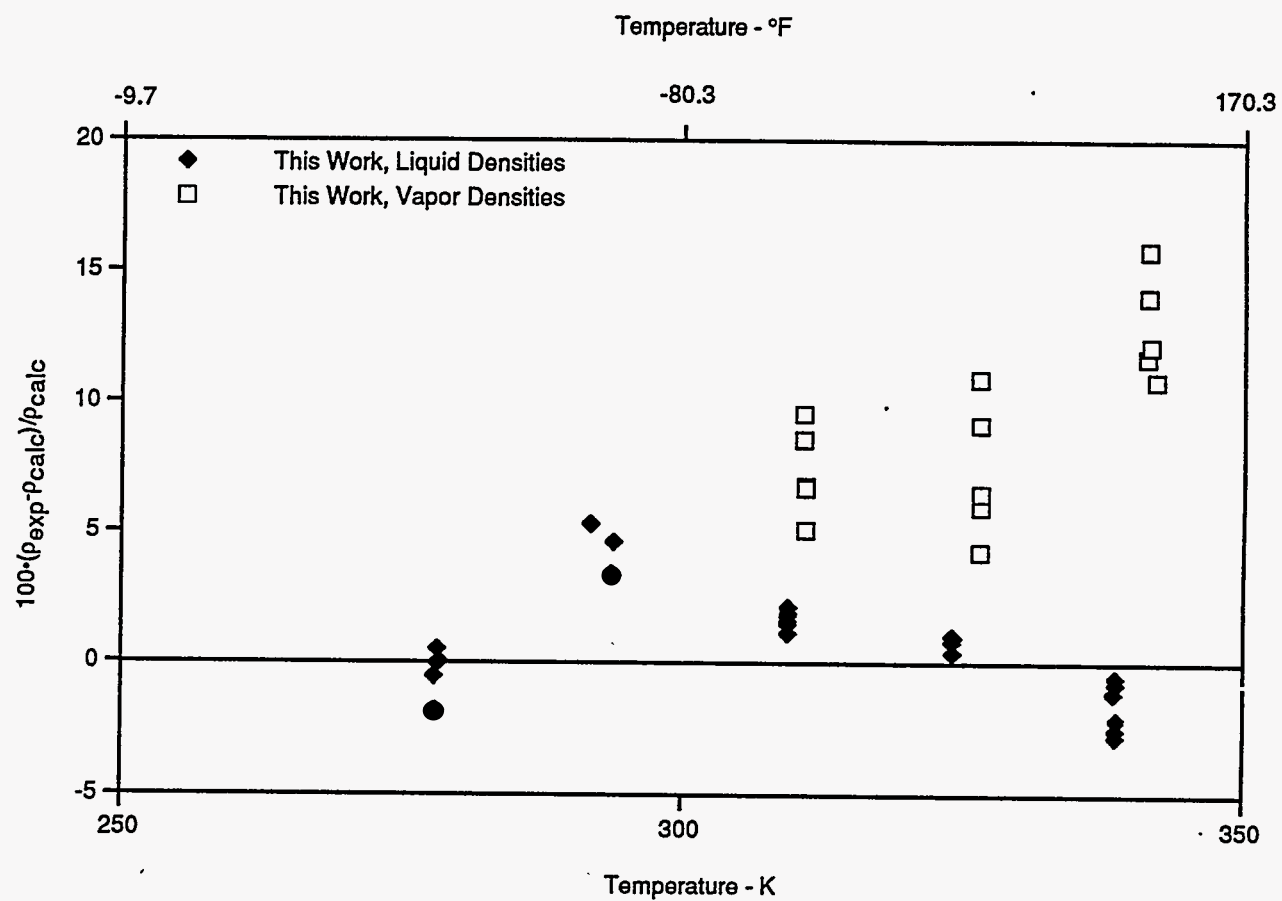


Figure 32. Comparison of Densities for the R134a/290 System; the Baseline is from the Lemmon-Jacobsen Model in REFPROP 6.0.

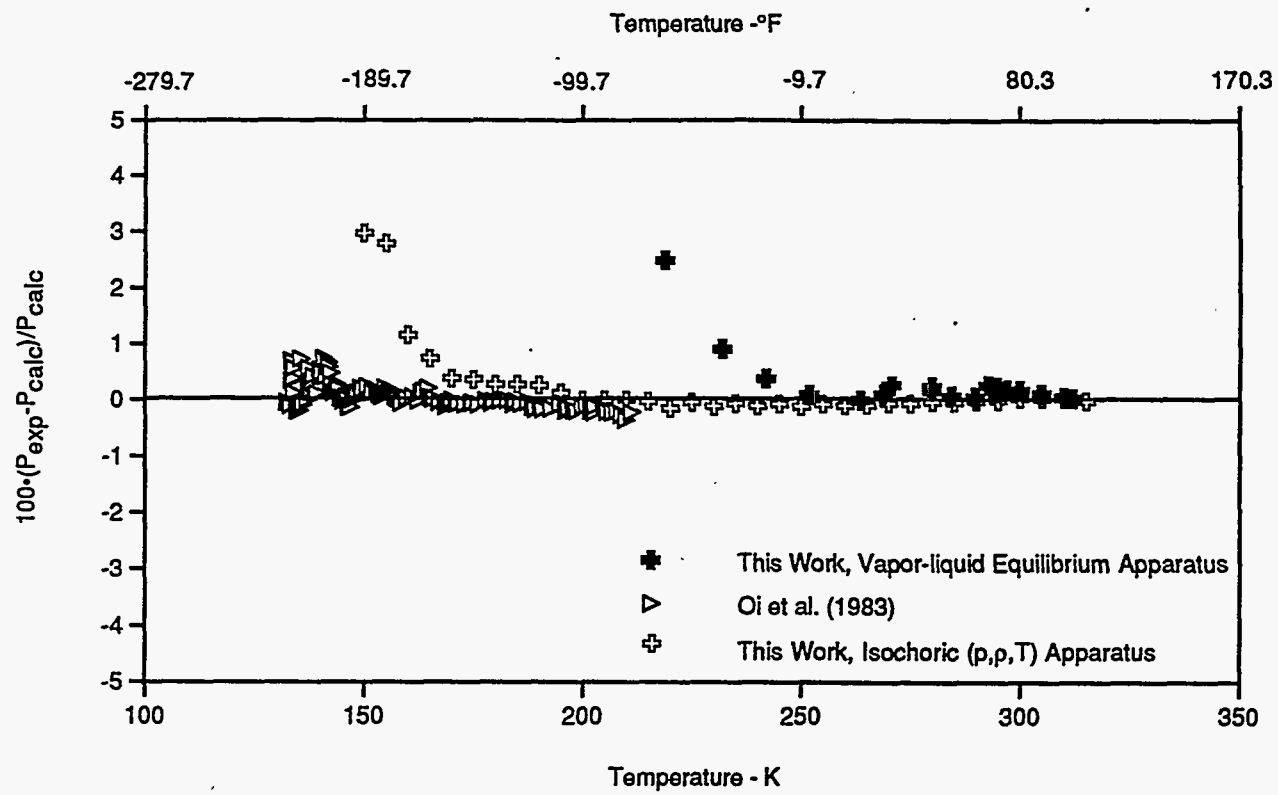


Figure 33. Comparison of Vapor Pressures for HFC-41; the Baseline is from the Ancillary Equation for Vapor Pressure.

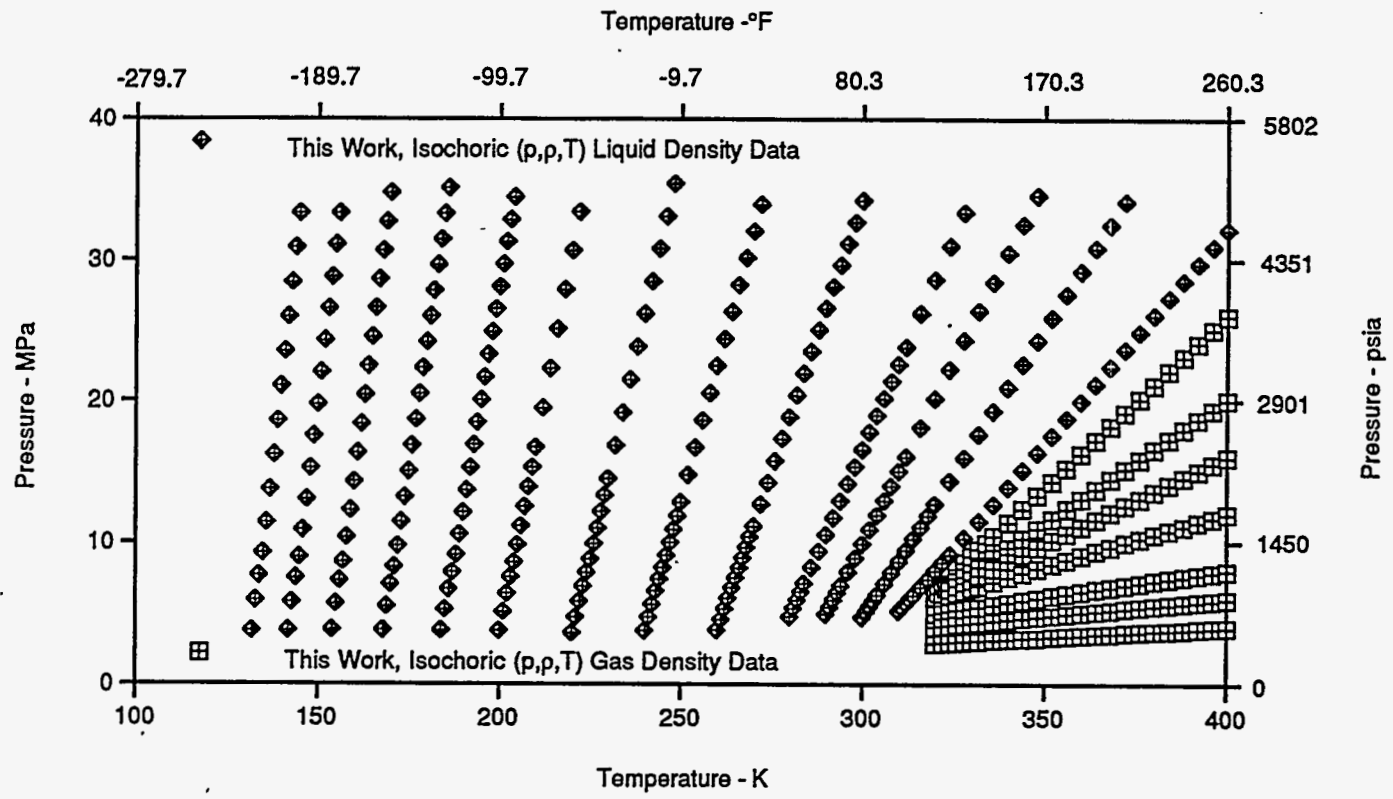


Figure 34. Range of Measured Temperatures and Pressures for Isochoric (p, ρ, T) Data for HFC-41.

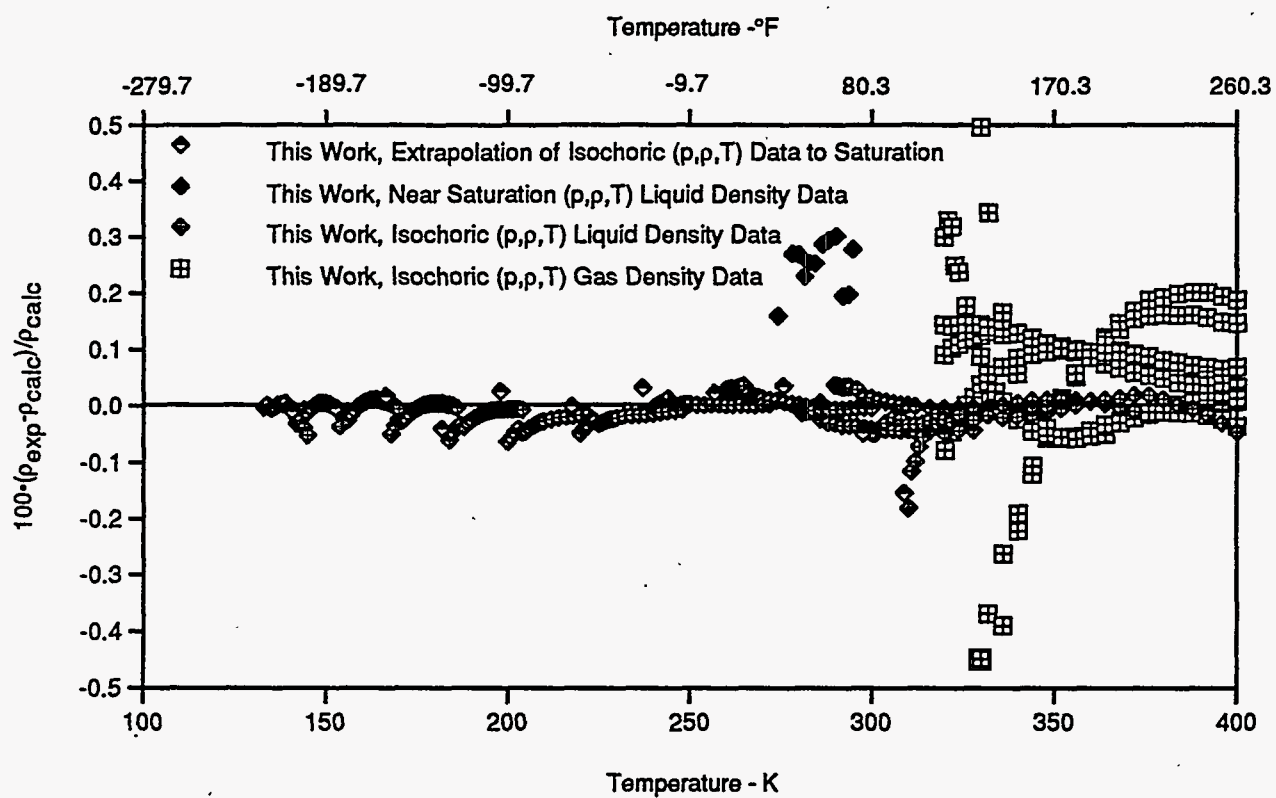


Figure 35. Comparison of Densities for HFC-41; the Baseline is from the MBWR Model in REFPROP 6.0.

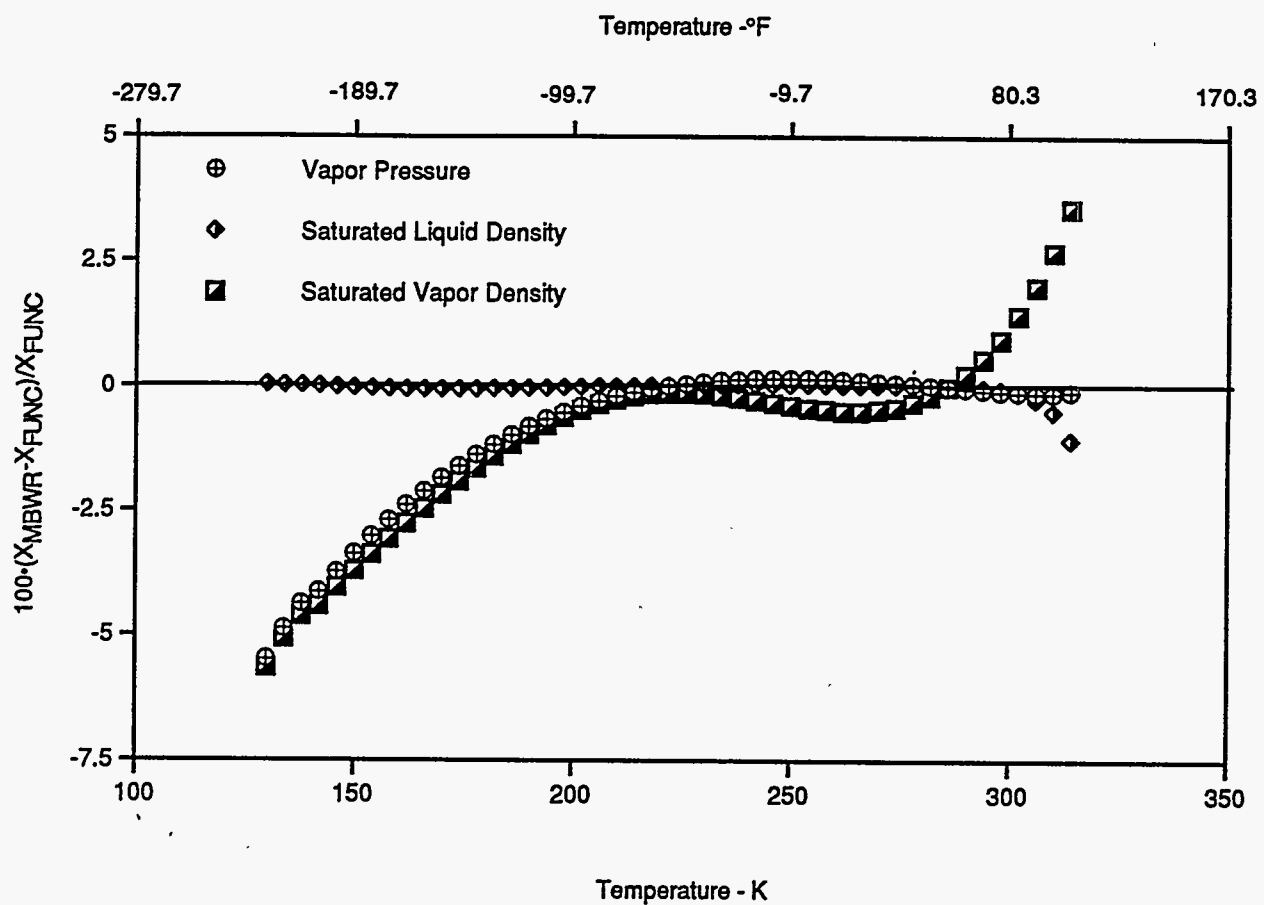


Figure 36. Deviations of the MBWR Equation of State for HFC-41 from Ancillary Equations for Vapor Pressure, Saturated Liquid Density, and Saturated Vapor Density.

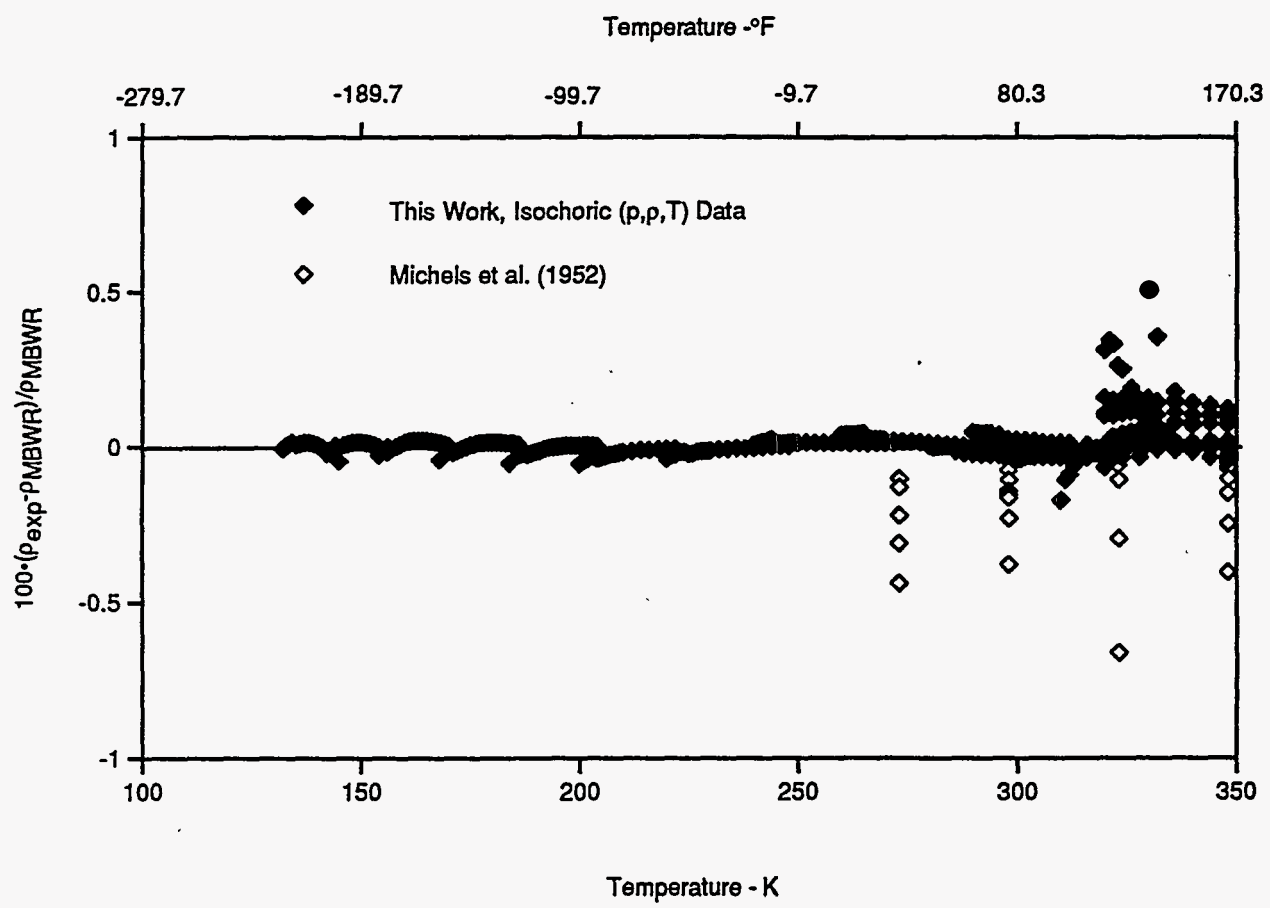


Figure 37. Deviations of the MBWR Equation of State for HFC-41 from Experimental (p,ρ,T) Data.

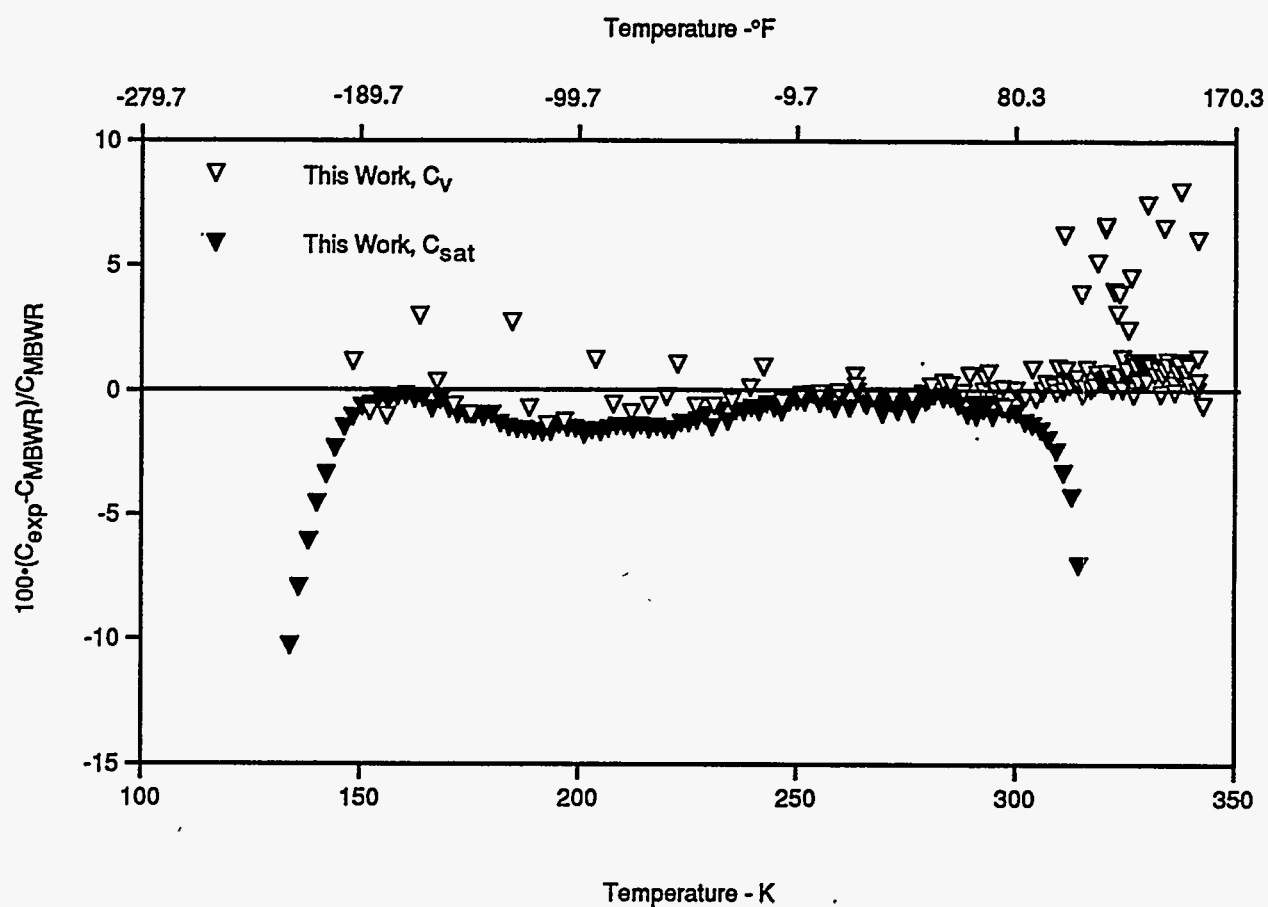


Figure 38. Deviations of the MBWR Equation of State for HFC-41 from Experimental Isochoric Heat Capacity Data at Saturation and in the Single-Phase Liquid Region.

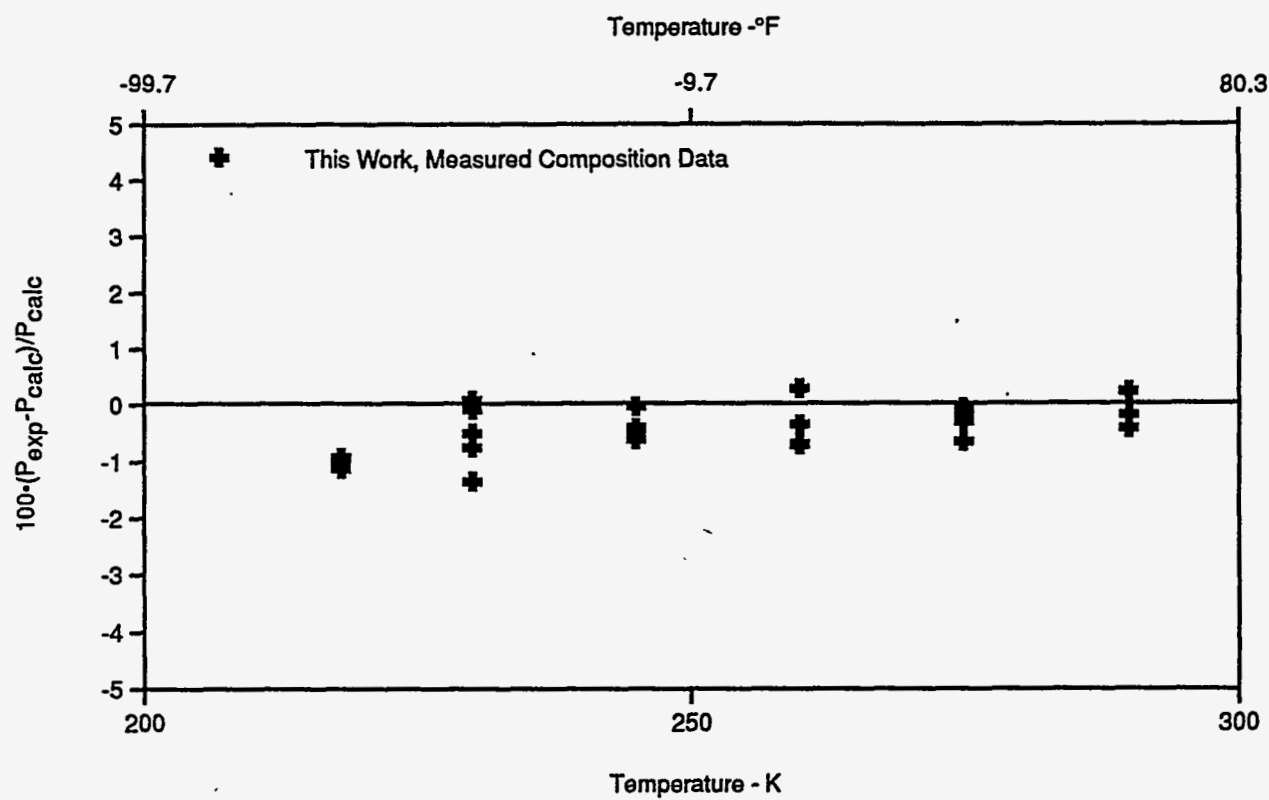


Figure 39. Comparison of Bubble-Point Pressures for the R41/744 System; the Baseline is from the Lemmon-Jacobsen Model in REFPROP 6.0.

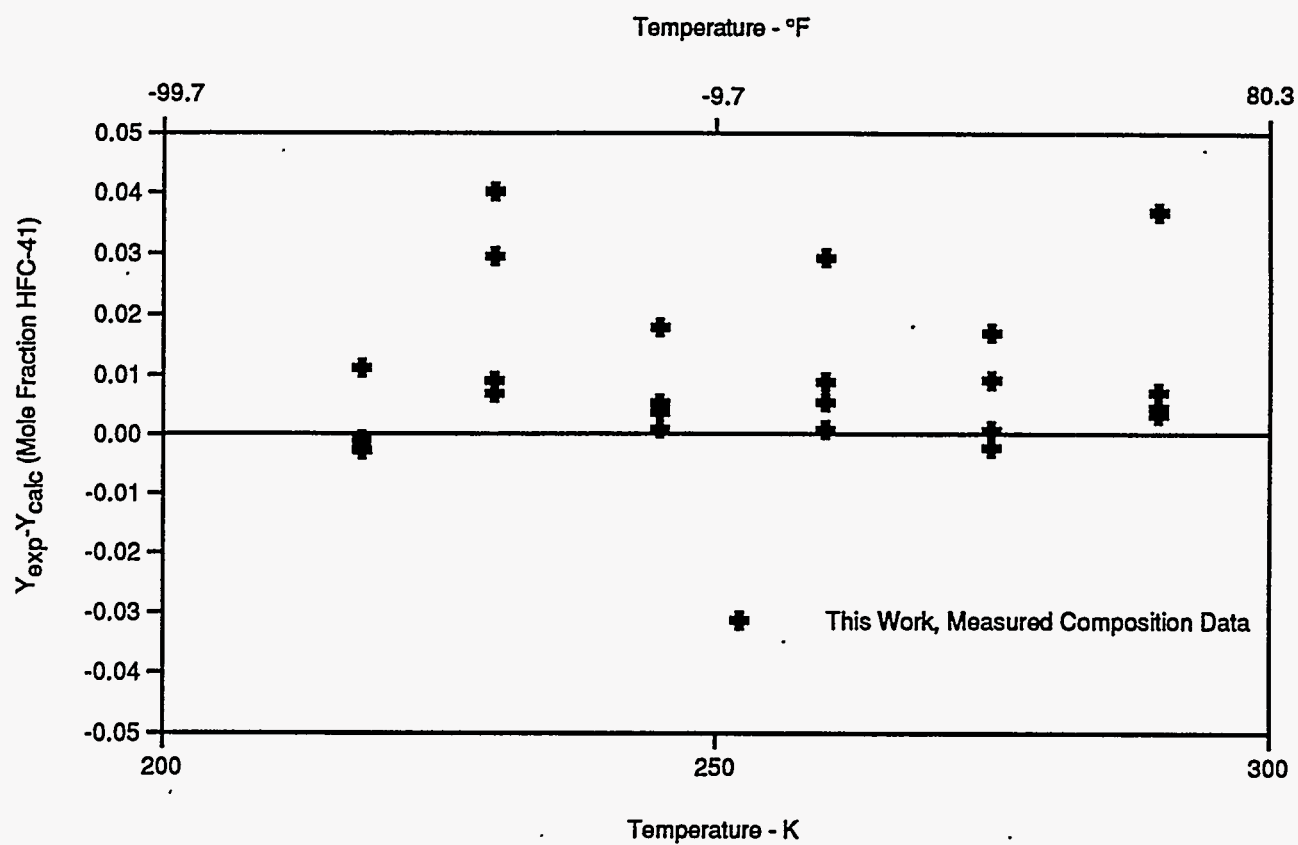


Figure 40. Comparison of Vapor Compositions for the R41/744 System; the Baseline is from the Lemmon-Jacobsen Model in REFPROP 6.0.

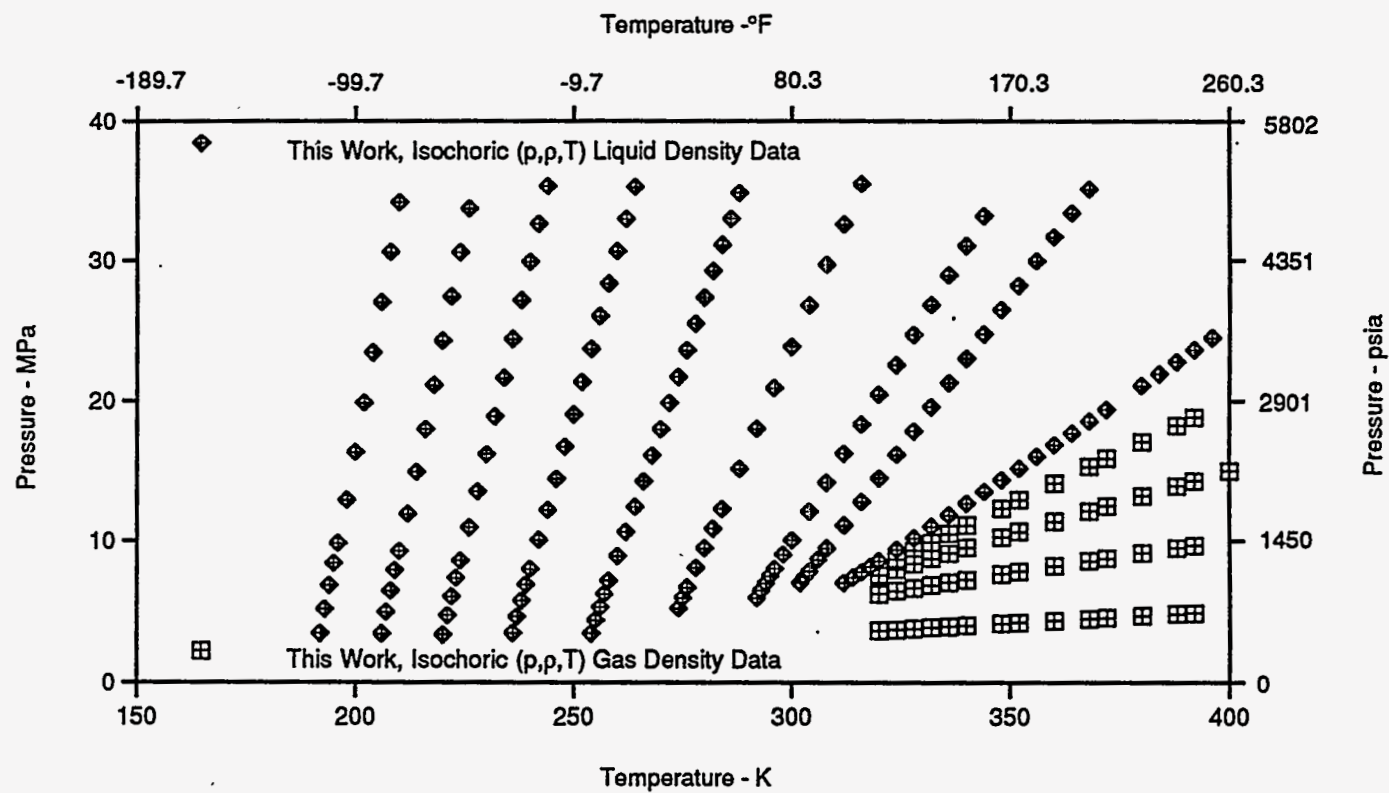


Figure 41. Range of Measured Temperatures and Pressures for Isochoric (p, ρ, T) Data for a Mixture of R41/744 with $x(\text{R41}) = 0.49982$ Mole Fraction (0.43591 Mass Fraction).

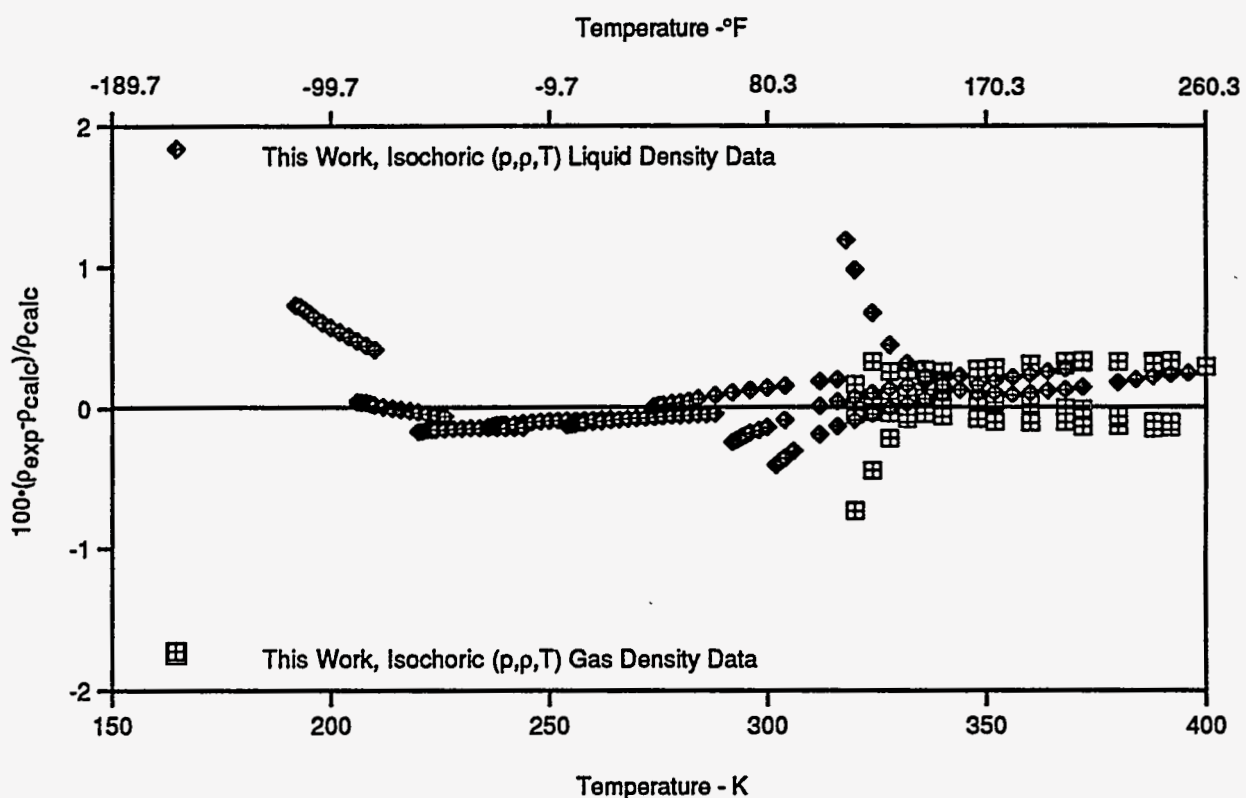
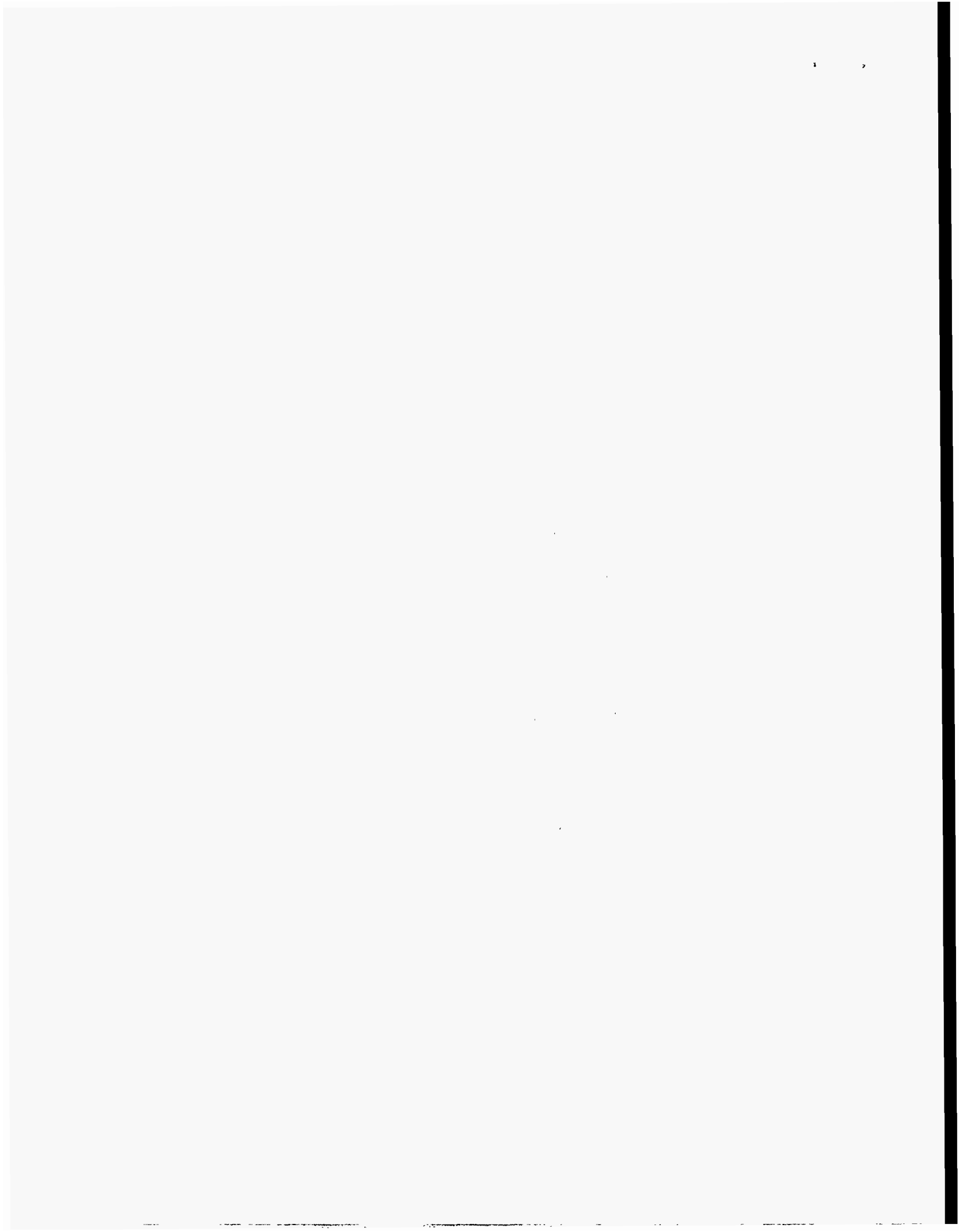


Figure 42. Comparison of Isochoric (p,p,T) Data for the Equimolar Mixture of R41/744; the Baseline is from the Lemmon-Jacobsen Model in REFPROP 6.0.



APPENDIX A:
TABLES OF THERMOPHYSICAL PROPERTY DATA

Table 1. Summary of the Refrigerant Systems Studied, the Properties Measured for Each System, and the Molecular Weights of the Pure Components.

System	Vapor-Liquid Equilibrium Data ¹	Bubble-Point Pressures ²	Near-Saturation (p,ρ,T) Data	Compressed Liquid (p,ρ,T) Data	Compressed Gas (p,ρ,T) Data	Isochoric Heat Capacities	Sound Speed Data
R32/134a	x		x				
R32/125	x		x				
R125/134a	x	x	x				
R32/125/134a	x	x	x				
R32/143a	x		x				
R125/143a	x	x	x	x	x	x	
R143a/134a	x	x	x				
R32/290	x		x				
R125/290	x		x				
R134a/290	x		x				
HFC-41		x ³	x	x	x	x	x
R41/744	x			x	x		

¹ Equilibrium two-phase measurements of the coexisting liquid and vapor compositions, the bubble-point pressures, and the equilibrium temperatures.

² Bubble-point pressures of a standard mixture.

³ Vapor pressure measurements.

Pure Component	Molecular Weight g/mole (lb/lbmole)
HFC-32	52.0237
HFC-125	120.0219
HFC-134a	102.0315
HFC-143a	84.0410
HC-290	44.0965
HFC-41	34.0332
R-744	44.0098

Table 2. Summary of the Experimental Uncertainties for the Apparatus Used in This Project.

Measurement	Pure Component Uncertainty	Mixture Uncertainty
Vapor-Liquid Equilibrium Apparatus		
Temperature	±0.02 K (±0.04°F)	±0.02 K (±0.04°F)
Pressure	+0.001 MPa (±0.15 psia)	+0.001 MPa (±0.15 psia)
Composition		±0.004 Mole Fraction (±0.004 Mass Fraction)
Bubble-Point and Near-Saturation (p,p,T) Apparatus		
Temperature	±0.05 K (±0.09°F)	±0.05 K (±0.09°F)
Density	±0.5 kg/m ³ (±0.03 lb/ft ³)	±0.5 kg/m ³ (±0.03 lb/ft ³)
Pressure	±0.0035 MPa (0.5 psia)	±0.0035 MPa (0.5 psia)
Composition		±0.004 Mole Fraction (±0.004 Mass Fraction)
Isochoric (p,ρ,T) Apparatus		
Temperature	±0.03 K (±0.05°F)	±0.03 K (±0.05°F)
Density	±0.05%	±0.05%
Pressure	±(0.0007 MPa+10 ⁻⁷ P)	±(0.1 psia+1.5x10 ⁻⁵ P)
Composition		±4x10 ⁻⁵ Mole Fraction (±4x10 ⁻⁵ Mass Fraction)
Heat Capacity Apparatus		
Temperature	±0.03 K (±0.05°F)	±0.03 K (±0.05°F)
Density	±0.15%	±0.15%
Pressure	±(0.0007 MPa+10 ⁻⁷ P)	±(0.1 psia+1.5x10 ⁻⁵ P)
Heat Capacity	±0.5%	±0.5%
Composition		±4x10 ⁻⁵ Mole Fraction (±4x10 ⁻⁵ Mass Fraction)
Sound Speed Apparatus		
Temperature	±0.004%	
Pressure	± 0.67%	
Sound Speed	± 0.05%	

Table 3. Vapor-Liquid Equilibrium Data for R32/134a Mixtures from 280 to 340 K (44 to 152°F).

x(R32) Liquid Mole Fraction	Temperature K	Pressure MPa	y(R32) Vapor Mole Fraction	x(R32) Liquid Mass Fraction	Temperature °F	Pressure psia	y(R32) Vapor Mass Fraction
0.000	280.39	0.379	0.000	0.000	45.01	55.0	0.000
0.299	279.98	0.555	0.489	0.179	44.27	80.5	0.328
0.478	280.05	0.674	0.676	0.318	44.41	97.7	0.515
0.604	279.98	0.739	0.757	0.437	44.28	107.2	0.614
0.642	279.98	0.772	0.797	0.478	44.27	111.9	0.667
0.642	280.09	0.774	0.793	0.478	44.47	112.3	0.661
0.650	279.99	0.778	0.805	0.486	44.28	112.9	0.678
0.650	280.19	0.778	0.796	0.486	44.65	112.8	0.665
0.737	280.13	0.852	0.869	0.588	44.54	123.5	0.772
1.000	280.00	1.006	1.000	1.000	44.31	145.9	1.000
0.302	283.02	0.609	0.483	0.181	49.75	88.4	0.323
0.632	283.06	0.840	0.782	0.467	49.81	121.8	0.647
0.640	283.01	0.846	0.795	0.475	49.73	122.7	0.664
0.640	283.08	0.847	0.795	0.475	49.85	122.8	0.664
0.283	289.91	0.746	0.466	0.168	62.15	108.2	0.308
0.637	289.79	1.030	0.782	0.472	61.93	149.4	0.647
0.282	292.93	0.811	0.457	0.167	67.58	117.7	0.300
0.634	292.92	1.124	0.773	0.469	67.56	163.0	0.635
0.000	294.69	0.596	0.000	0.000	70.75	86.5	0.000
0.275	294.95	0.856	0.448	0.162	71.22	124.1	0.293
0.452	294.99	1.018	0.626	0.296	71.29	147.6	0.460
0.529	295.13	1.091	0.696	0.364	71.54	158.3	0.539
0.584	294.94	1.149	0.748	0.417	71.20	166.6	0.602
0.632	294.96	1.187	0.773	0.467	71.24	172.1	0.635
0.720	294.94	1.271	0.838	0.567	71.21	184.3	0.725
1.000	295.48	1.575	1.000	1.000	72.18	228.4	1.000
0.619	299.96	1.357	0.761	0.453	80.24	196.8	0.619
0.262	303.87	1.076	0.403	0.153	87.28	156.1	0.256
0.609	303.07	1.453	0.756	0.443	85.84	210.7	0.612
0.000	309.31	0.913	0.000	0.000	97.07	132.4	0.000
0.181	309.98	1.167	0.292	0.101	98.27	169.3	0.174
0.225	310.00	1.225	0.370	0.129	98.30	177.7	0.230
0.228	309.97	1.215	0.363	0.131	98.26	176.3	0.225
0.360	309.98	1.392	0.515	0.223	98.28	202.0	0.351
0.681	309.99	1.826	0.793	0.521	98.30	264.9	0.661
1.000	309.99	2.294	1.000	1.000	98.29	332.7	1.000

Table 3. Vapor-Liquid Equilibrium Data for R32/134a Mixtures from 280 to 340 K (44 to 152°F) (continued).

x(R32) Liquid Mole Fraction	Temperature K	Pressure MPa	y(R32) Vapor Mole Fraction	x(R32) Liquid Mass Fraction	Temperature °F	Pressure psia	y(R32) Vapor Mass Fraction
0.000	324.50	1.367	0.000	0.000	124.41	198.3	0.000
0.162	325.00	1.643	0.256	0.090	125.32	238.3	0.149
0.294	324.99	1.889	0.422	0.175	125.29	273.9	0.271
0.595	325.00	2.423	0.710	0.428	125.31	351.5	0.555
0.733	324.99	2.698	0.809	0.583	125.29	391.2	0.683
0.783	324.99	2.805	0.860	0.648	125.30	406.9	0.758
1.000	324.99	3.279	1.000	1.000	125.29	475.6	1.000
0.000	340.16	1.986	0.000	0.000	152.60	288.1	0.000
0.466	339.87	3.036	0.569	0.308	152.07	440.4	0.402
0.577	339.93	3.315	0.669	0.410	152.19	480.8	0.508
0.763	339.99	3.807	0.820	0.621	152.12	552.1	0.699
1.000	339.98	4.561	1.000	1.000	152.28	661.5	1.000

A-5

Table 4. Near-Saturation (p,ρ,T) Data for R32/134a Mixtures from 279 to 340 K (43 to 152°F).

x(R32) Liquid Mole Fraction	Temperature K	Pressure MPa	Density kg/m ³	x(R32) Liquid Mass Fraction	Temperature °F	Pressure psia	Density lb/ft ³
0.216	279.63	0.523	1234.7	0.123	43.64	75.9	77.01
0.366	279.40	0.621	1197.5	0.227	43.23	90.1	74.69
0.519	279.45	0.698	1169.8	0.355	43.32	101.2	72.96
0.752	279.42	0.847	1108.9	0.607	43.27	122.9	69.16
0.214	293.49	0.791	1180.6	0.122	68.60	114.7	73.64
0.566	293.04	1.090	1106.8	0.399	67.78	158.1	69.03
0.639	292.88	1.184	1088.3	0.474	67.49	171.7	67.88
0.731	291.67	1.283	1060.3	0.581	65.32	186.0	66.13
0.807	292.93	1.381	1036.9	0.681	67.58	200.2	64.67
0.161	309.55	1.116	1130.6	0.089	97.50	161.9	70.52
0.214	308.46	1.192	1124.7	0.122	95.54	172.8	70.15
0.291	309.55	1.261	1111.0	0.173	97.50	182.9	69.30
0.498	309.62	1.536	1062.8	0.336	97.63	222.8	66.29
0.571	309.60	1.637	1045.8	0.404	97.59	237.4	65.23
0.789	309.70	1.942	987.3	0.656	97.77	281.6	61.58
0.873	309.34	2.085	958.7	0.778	97.13	302.3	59.80
0.130	324.64	1.587	1070.3	0.071	124.66	230.2	66.76
0.236	325.16	1.803	1040.6	0.136	125.59	261.4	64.90
0.387	325.27	2.044	1014.0	0.244	125.79	296.4	63.25
0.658	325.24	2.560	944.2	0.495	125.74	371.3	58.89
0.815	325.22	2.870	900.4	0.692	125.70	416.3	56.16
0.923	325.19	3.115	858.0	0.859	125.65	451.8	53.52
0.140	339.78	2.302	983.2	0.077	151.92	333.8	61.32
0.241	340.07	2.529	963.6	0.139	152.44	366.8	60.10
0.461	339.68	3.017	910.8	0.304	151.74	437.6	56.81
0.592	339.70	3.347	867.3	0.425	151.78	485.5	54.10
0.760	339.67	3.814	816.0	0.618	151.72	553.2	50.90
0.924	339.83	4.288	754.4	0.861	152.01	622.0	47.05

A
6

Table 4. Near-Saturation (p,ρ,T) Data for R32/134a Mixtures from 279 to 340 K (43 to 152°F) (continued).

y(R32)* Vapor Mole Fraction	Temperature K	Pressure MPa	Density kg/m ³	y(R32)* Vapor Mass Fraction	Temperature °F	Pressure psia	Density lb/ft ³
0.652	309.53	1.536	55.9	0.489	97.47	222.8	3.49
0.711	309.40	1.637	57.4	0.556	97.23	237.4	3.58
0.864	310.28	1.942	62.1	0.764	98.82	281.6	3.87
0.917	309.48	2.085	64.5	0.849	97.38	302.3	4.02
0.211	324.69	1.587	74.6	0.120	124.75	230.2	4.65
0.354	325.45	1.803	79.7	0.218	126.12	261.4	4.97
0.522	325.50	2.044	84.1	0.358	126.21	296.4	5.25
0.759	325.50	2.560	93.9	0.616	126.21	371.3	5.86
0.883	325.47	2.870	99.7	0.794	126.15	416.3	6.22
0.973	325.37	3.115	103.4	0.948	125.97	451.8	6.45
0.192	340.31	2.302	114.3	0.108	152.87	333.8	7.13
0.319	340.02	2.529	119.5	0.193	152.35	366.8	7.45
0.562	340.18	3.017	130.2	0.395	152.64	437.6	8.12
0.684	340.10	3.347	139.0	0.525	152.50	485.5	8.67
0.817	340.05	3.814	151.0	0.695	152.41	553.2	9.42
0.920	340.10	4.288	165.9	0.854	152.50	622.0	10.35

*Near-saturation vapor compositions are calculated from the vapor-liquid equilibrium data.

L47

Table 5. Vapor-Liquid Equilibrium Data for R32/125 Mixtures from 280 to 340 K (44 to 152°F).

x(R32) Liquid Mole Fraction	Temperature K	Pressure MPa	y(R32) Vapor Mole Fraction	x(R32) Liquid Mass Fraction	Temperature °F	Pressure psia	y(R32) Vapor Mass Fraction
0.000	280.29	0.830	0.000	0.000	44.83	120.4	0.000
0.346	279.83	0.919	0.398	0.187	44.01	133.3	0.223
0.350	280.02	0.924	0.387	0.189	44.34	134.0	0.215
0.482	280.06	0.955	0.520	0.287	44.41	138.5	0.320
0.650	279.95	0.985	0.676	0.446	44.23	142.9	0.475
0.948	280.07	1.017	0.947	0.888	44.44	147.4	0.886
1.000	280.00	1.008	1.000	1.000	44.31	146.1	1.000
0.000	295.23	1.272	0.000	0.000	71.72	184.5	0.000
0.347	295.01	1.415	0.387	0.187	71.32	205.2	0.215
0.470	295.03	1.461	0.508	0.278	71.37	211.9	0.309
0.653	295.06	1.516	0.676	0.449	71.42	219.9	0.475
0.914	295.03	1.559	0.915	0.822	71.35	226.0	0.824
0.948	294.94	1.556	0.947	0.888	71.20	225.6	0.886
1.000	293.99	1.515	1.000	1.000	69.49	219.8	1.000
0.000	310.61	1.890	0.000	0.000	99.41	274.2	0.000
0.339	310.01	2.080	0.373	0.182	98.32	301.7	0.205
0.465	310.00	2.150	0.498	0.274	98.30	311.8	0.301
0.646	309.96	2.227	0.672	0.442	98.24	323.0	0.470
0.915	310.08	2.303	0.914	0.824	98.45	334.1	0.822
1.000	310.51	2.329	1.000	1.000	99.23	337.8	1.000
0.000	324.89	2.639	0.000	0.000	125.11	382.8	0.000
0.462	325.07	3.058	0.489	0.271	125.43	443.5	0.293
0.644	324.97	3.174	0.661	0.439	125.26	460.3	0.458
0.919	325.17	3.297	0.919	0.831	125.61	478.1	0.831
1.000	325.49	3.318	1.000	1.000	126.19	481.2	1.000
0.000	339.38	3.629	0.000	0.000	151.19	526.4	0.000
0.740	340.18	4.482	0.749	0.552	152.63	650.0	0.564
0.885	340.17	4.572	0.890	0.769	152.62	663.1	0.778
0.919	340.17	4.582	0.919	0.831	152.62	664.5	0.831
1.000	340.08	4.572	1.000	1.000	152.45	663.1	1.000

Table 6. Near-Saturation (p,ρ,T) Data for R32/125 Mixtures from 279 to 341 K (43 to 154°F).

x(R32) Liquid Mole Fraction	Temperature K	Pressure MPa	Density kg/m ³	x(R32) Liquid Mass Fraction	Temperature °F	Pressure psia	Density lb/ft ³
0.250	279.24	0.896	1245.9	0.126	42.94	129.9	77.71
0.494	279.19	0.946	1203.2	0.297	42.85	137.2	75.05
0.797	279.55	1.012	1114.2	0.630	43.50	146.7	69.49
0.875	279.60	1.018	1092.3	0.752	43.59	147.7	68.13
0.956	279.01	1.013	1060.9	0.904	42.53	146.9	66.17
0.237	293.75	1.348	1174.8	0.119	69.07	195.6	73.27
0.460	293.54	1.429	1135.7	0.270	68.69	207.3	70.84
0.801	293.35	1.500	1057.0	0.636	68.33	217.6	65.93
0.801	293.18	1.500	1055.3	0.636	68.04	217.6	65.82
0.890	293.27	1.517	1030.6	0.778	68.19	220.1	64.28
0.947	293.46	1.525	1003.7	0.886	68.55	221.2	62.60
0.270	309.83	2.009	1083.6	0.138	98.01	291.3	67.59
0.509	310.89	2.227	1032.2	0.310	99.92	322.9	64.38
0.745	310.50	2.299	980.8	0.559	99.21	333.5	61.17
0.803	310.66	2.322	969.5	0.639	99.50	336.8	60.47
0.873	309.57	2.296	954.6	0.749	97.54	332.9	59.54
0.916	309.73	2.302	941.1	0.825	97.83	333.9	58.70
0.952	309.52	2.308	927.7	0.896	97.45	334.7	57.86
0.323	324.98	2.969	950.3	0.171	125.27	430.6	59.27
0.456	325.48	3.128	925.7	0.267	126.17	453.7	57.74
0.755	325.40	3.270	883.0	0.572	126.03	474.3	55.07
0.804	325.55	3.303	870.6	0.640	126.30	479.0	54.30
0.867	325.37	3.324	859.8	0.739	125.97	482.1	53.63
0.916	325.35	3.315	851.6	0.825	125.94	480.8	53.12
0.744	340.33	4.581	723.6	0.557	152.91	664.4	45.13
0.873	340.28	4.606	722.0	0.749	152.82	668.0	45.03
0.898	339.99	4.595	724.5	0.792	152.30	666.4	45.19
0.916	339.99	4.598	723.9	0.825	152.30	666.8	45.15

A9

Table 6. Near-Saturation (p, ρ ,T) Data for R32/125 Mixtures from 279 to 341 K (43 to 154°F) (continued).

y(R32)* Vapor Mole Fraction	Temperature K	Pressure MPa	Density kg/m ³	y(R32)* Vapor Mass Fraction	Temperature °F	Pressure psia	Density lb/ft ³
0.275	295.03	1.348	72.9	0.141	71.37	195.6	4.55
0.810	294.49	1.500	53.6	0.649	70.40	217.6	3.34
0.303	310.36	2.009	116.2	0.159	98.96	291.4	7.25
0.541	311.32	2.227	108.6	0.338	100.69	322.9	6.77
0.761	311.11	2.299	89.4	0.580	100.31	333.5	5.58
0.814	311.34	2.322	84.6	0.656	100.72	336.8	5.28
0.879	310.54	2.296	80.7	0.759	99.29	332.9	5.03
0.919	310.82	2.302	76.6	0.831	99.79	333.9	4.78
0.953	310.69	2.308	71.7	0.897	99.56	334.7	4.47
0.349	325.58	2.969	183.6	0.189	126.35	430.6	11.45
0.766	326.12	3.270	143.0	0.586	127.32	474.3	8.92
0.812	326.23	3.303	138.9	0.652	127.52	479.0	8.66
0.872	326.12	3.324	130.1	0.746	127.32	482.1	8.11
0.918	326.10	3.315	121.9	0.829	127.28	480.8	7.60
0.877	341.15	4.606	221.1	0.755	154.39	668.0	13.79
0.901	340.81	4.595	213.3	0.798	153.77	666.4	13.30
0.918	340.81	4.598	197.8	0.830	153.77	666.8	12.34

*Near-saturation vapor compositions are calculated from the vapor-liquid equilibrium data.

Table 7. Vapor-Liquid Equilibrium Data for R125/134a Mixtures from 280 to 340 K (44 to 152°F).

x(R125) Liquid Mole Fraction	Temperature K	Pressure MPa	y(R125) Vapor Mole Fraction	x(R125) Liquid Mass Fraction	Temperature °F	Pressure psia	y(R125) Vapor Mass Fraction
0.000	280.39	0.379	0.000	0.000	45.01	55.0	0.000
0.264	279.98	0.486	0.408	0.297	44.27	70.5	0.448
0.425	279.97	0.574	0.595	0.465	44.27	83.2	0.633
0.521	279.98	0.614	0.690	0.561	44.27	89.0	0.724
0.600	279.98	0.642	0.720	0.638	44.28	93.2	0.752
1.000	280.29	0.830	1.000	1.000	44.83	120.4	1.000
0.000	294.69	0.596	0.000	0.000	70.75	86.5	0.000
0.270	294.93	0.780	0.400	0.303	71.19	113.2	0.440
0.347	294.92	0.835	0.475	0.385	71.17	121.1	0.516
0.383	294.92	0.853	0.523	0.422	71.17	123.8	0.563
0.600	294.84	0.979	0.703	0.638	71.02	142.0	0.736
1.000	295.23	1.272	1.000	1.000	71.73	184.5	1.000
0.000	309.31	0.913	0.000	0.000	97.07	132.4	0.000
0.259	309.97	1.171	0.376	0.291	98.27	169.9	0.415
0.362	309.99	1.263	0.475	0.400	98.29	183.2	0.516
0.454	309.99	1.349		0.494	98.29	195.6	
0.513	309.99	1.423	0.635	0.553	98.30	206.4	0.672
1.000	310.61	1.890	1.000	1.000	99.41	274.2	1.000
0.000	324.50	1.367	0.000	0.000	124.41	198.3	0.000
0.366	324.98	1.824	0.462	0.404	125.27	264.6	0.503
0.406	324.98	1.875	0.492	0.446	125.28	272.0	0.533
0.426	324.97	1.901		0.466	125.25	275.7	
0.511	324.96	2.026	0.610	0.551	125.24	293.9	0.648
1.000	324.89	2.639	1.000	1.000	125.11	382.7	1.000
0.000	340.16	1.986	0.000	0.000	152.60	288.1	0.000
0.361	339.96	2.520	0.438	0.399	152.24	365.5	0.478
0.370	339.91	2.522	0.443	0.409	152.16	365.8	0.483
0.448	339.99	2.664	0.512	0.488	152.29	386.4	0.552
0.493	339.89	2.749	0.543	0.534	152.11	398.7	0.583
1.000	339.38	3.629	1.000	1.000	151.20	526.3	1.000

A-11

Table 8. Bubble-Point Pressures for R125/134a Mixtures from 280 to 340 K (45 to 153°F).

x(R125) Liquid Mole Fraction	Temperature K	Pressure MPa	x(R125) Liquid Mass Fraction	Temperature °F	Pressure psia
0.3498	280.35	0.537	0.3876	44.94	77.9
0.3498	295.09	0.837	0.3876	71.47	121.4
0.3498	310.05	1.260	0.3876	98.40	182.8
0.3498	324.99	1.815	0.3876	125.29	263.3
0.3498	340.26	2.543	0.3876	152.78	368.8
0.3498	340.41	2.546	0.3876	153.05	369.2
0.6491	280.78	0.675	0.6851	45.72	98.0
0.6491	294.99	1.031	0.6851	71.29	149.5
0.6491	310.19	1.541	0.6851	98.65	223.5
0.6491	324.98	2.180	0.6851	125.28	316.2

Table 9. Near-Saturation (p,p,T) Data for R125/134a Mixtures from 280 to 342 K (44 to 157°F).

x(R125) Liquid Mole Fraction	Temperature K	Pressure MPa	Density kg/m ³	x(R125) Liquid Mass Fraction	Temperature °F	Pressure psia	Density lb/ft ³
0.3498	280.09	0.537	1285.2	0.3876	44.47	77.9	80.16
0.3498	294.86	0.837	1226.9	0.3876	71.06	121.4	76.52
0.3498	310.07	1.260	1147.3	0.3876	98.44	182.8	71.56
0.3498	325.34	1.815	1072.4	0.3876	125.92	263.3	66.89
0.3498	340.17	2.543	973.5	0.3876	152.62	368.8	60.72
0.3498	340.24	2.546	972.1	0.3876	152.74	369.2	60.63
0.6491	280.29	0.675	1289.2	0.6851	44.83	98.0	80.41
0.6491	294.76	1.031	1225.4	0.6851	70.88	149.5	76.43
0.6491	310.20	1.541	1134.3	0.6851	98.67	223.5	70.75
0.6491	324.99	2.180	1043.3	0.6851	125.29	316.2	65.07
y(R125)* Vapor Mole Fraction	Temperature K	Pressure MPa	Density kg/m ³	y(R125)* Vapor Mass Fraction	Temperature °F	Pressure psia	Density lb/ft ³
0.426	312.23	1.260	69.7	0.466	102.33	182.8	4.35
0.404	326.34	1.815	105.9	0.444	127.72	263.3	6.61
0.385	342.37	2.543	159.4	0.424	156.58	368.8	9.94
0.385	342.48	2.546	159.6	0.424	156.78	369.2	9.95
0.720	296.07	1.031	60.8	0.752	73.24	149.5	3.79
0.693	312.29	1.541	93.7	0.726	102.43	223.5	5.84
0.673	327.15	2.180	141.3	0.708	129.18	316.2	8.81

*Near-saturation vapor compositions are calculated from the vapor-liquid equilibrium data.

Table 10. Vapor-Liquid Equilibrium Data for R32/125/134a Mixtures from 280 to 340 K (44 to 152°F).

x(R32)	x(R125)	x(R134a)	Temp.	Press.	y(R32)	y(R125)	y(R134a)	x(R32)	x(R125)	x(R134a)	Temp.	Press.	y(R32)	y(R125)	y(R134a)
Liquid Mole Fraction	Liquid Mole Fraction	Liquid Mole Fraction	K	MPa	Vapor Fraction	Vapor Fraction	Vapor Fraction	Liquid Mass Fraction	Liquid Mass Fraction	Liquid Mass Fraction	°F	psia	Vapor Mass Fraction	Vapor Mass Fraction	Vapor Mass Fraction
0.190	0.358	0.452	279.93	0.661	0.294	0.444	0.263	0.100	0.434	0.466	44.19	95.9	0.160	0.558	0.335
0.224	0.261	0.515	279.93	0.641				0.122	0.328	0.550	44.18	92.9			
0.391	0.327	0.282	279.97	0.780	0.495	0.307	0.198	0.230	0.444	0.326	44.25	113.1	0.311	0.445	0.354
0.251	0.214	0.535	294.96	0.987	0.396	0.258	0.346	0.140	0.275	0.585	71.25	143.2	0.237	0.356	0.533
0.263	0.256	0.481	294.96	1.004	0.366	0.306	0.328	0.146	0.329	0.525	71.25	145.6	0.213	0.412	0.477
0.264	0.205	0.531	294.96	0.973	0.464	0.272	0.264	0.148	0.266	0.586	71.24	141.2	0.288	0.390	0.452
0.301	0.230	0.469	294.96	1.036	0.430	0.270	0.300	0.172	0.303	0.525	71.24	150.3	0.262	0.380	0.486
0.495	0.290	0.215	294.94	1.294	0.575	0.265	0.160	0.312	0.422	0.266	71.21	187.6	0.383	0.408	0.339
0.163	0.549	0.288	309.99	1.673	0.212	0.584	0.204	0.082	0.635	0.283	98.29	242.7	0.108	0.688	0.229
0.218	0.506	0.276	309.99	1.722	0.287	0.528	0.185	0.113	0.606	0.281	98.29	249.8	0.154	0.652	0.230
0.303	0.462	0.235	310.00	1.798				0.166	0.583	0.252	98.31	260.8			
0.463	0.308	0.229	309.99	1.903	0.546	0.278	0.178	0.285	0.438	0.277	98.29	276.0	0.355	0.417	0.352
0.203	0.418	0.379	324.99	2.321	0.262	0.476	0.262	0.106	0.505	0.389	125.30	336.6	0.140	0.586	0.319
0.240	0.335	0.425	324.99	2.265	0.315	0.365	0.320	0.130	0.419	0.451	125.29	328.5	0.176	0.472	0.427
0.319	0.193	0.488	324.99	2.174	0.428	0.224	0.348	0.185	0.259	0.556	125.30	315.4	0.263	0.318	0.569
0.428	0.241	0.331	324.98	2.442	0.534	0.245	0.221	0.262	0.340	0.397	125.28	354.1	0.348	0.369	0.434
0.443	0.241	0.316	324.99	2.488	0.523	0.251	0.226	0.274	0.343	0.383	125.30	360.9	0.338	0.375	0.434
0.473	0.253	0.274	324.99	2.562	0.533	0.249	0.198	0.297	0.366	0.337	125.29	371.5	0.356	0.384	0.403
0.045	0.470	0.485	339.96	2.864	0.062	0.508	0.430	0.022	0.521	0.457	152.25	415.3	0.030	0.564	0.418
0.086	0.488	0.466	339.96	2.936	0.111	0.482	0.407	0.040	0.530	0.430	152.24	425.9	0.055	0.550	0.418
0.347	0.326	0.327	339.93	3.331	0.398	0.331	0.271	0.199	0.432	0.368	152.18	483.1	0.235	0.451	0.410
0.452	0.276	0.273	339.93	3.516	0.505	0.273	0.222	0.278	0.392	0.330	152.18	509.9	0.322	0.401	0.409
0.480	0.237	0.283	339.95	3.564	0.533	0.256	0.211	0.303	0.346	0.351	152.23	516.9	0.347	0.384	0.412
0.487	0.255	0.258	339.94	3.564	0.539	0.254	0.207	0.308	0.372	0.320	152.20	516.9	0.352	0.383	0.409

A-14

Table 11. Bubble-Point Pressures for R32/125/134a Mixtures from 221 to 345 K (-62 to 162°F).

x(R32) Liquid Mole Fraction	x(R125) Liquid Mole Fraction	x(R134a) Liquid Mole Fraction	Temp. K	Press. MPa	x(R32) Liquid Mass Fraction	x(R125) Liquid Mass Fraction	x(R134a) Liquid Mass Fraction	Temp. °F	Press. psia
0.3460	0.3005	0.3535	220.93	0.073	0.1997	0.4001	0.4002	-62.02	10.6
0.3460	0.3005	0.3535	230.45	0.116	0.1997	0.4001	0.4002	-44.88	16.9
0.3460	0.3005	0.3535	239.53	0.172	0.1997	0.4001	0.4002	-28.53	25.0
0.3460	0.3005	0.3535	250.06	0.266	0.1997	0.4001	0.4002	-9.58	38.5
0.3460	0.3005	0.3535	259.92	0.383	0.1997	0.4001	0.4002	8.17	55.6
0.3460	0.3005	0.3535	269.95	0.541	0.1997	0.4001	0.4002	26.23	78.5
0.3460	0.3005	0.3535	279.94	0.747	0.1997	0.4001	0.4002	44.20	108.3
0.3460	0.3005	0.3535	289.88	1.000	0.1997	0.4001	0.4002	62.10	145.0
0.3460	0.3005	0.3535	284.50	0.852	0.1997	0.4001	0.4002	52.41	123.5
0.3460	0.3005	0.3535	293.40	1.099	0.1997	0.4001	0.4002	68.43	159.4
0.3460	0.3005	0.3535	305.28	1.504	0.1997	0.4001	0.4002	89.82	218.2
0.3460	0.3005	0.3535	317.09	2.013	0.1997	0.4001	0.4002	111.07	292.0
0.3460	0.3005	0.3535	326.18	2.490	0.1997	0.4001	0.4002	127.44	361.1
0.3460	0.3005	0.3535	335.01	3.020	0.1997	0.4001	0.4002	143.33	438.0
0.3460	0.3005	0.3535	335.33	3.046	0.1997	0.4001	0.4002	143.91	441.8
0.3460	0.3005	0.3535	345.21	3.734	0.1997	0.4001	0.4002	161.69	541.5
0.2004	0.5992	0.2005	280.47	0.794	0.1014	0.6996	0.1990	45.16	115.2
0.2004	0.5992	0.2005	295.07	1.202	0.1014	0.6996	0.1990	71.44	174.4
0.2004	0.5992	0.2005	310.26	1.837	0.1014	0.6996	0.1990	98.78	266.4
0.2004	0.5992	0.2005	325.34	2.584	0.1014	0.6996	0.1990	125.92	374.7
0.5992	0.2006	0.2002	280.25	0.875	0.4119	0.3181	0.2700	44.76	126.9
0.5992	0.2006	0.2002	295.04	1.339	0.4119	0.3181	0.2700	71.38	194.2
0.5992	0.2006	0.2002	310.15	1.986	0.4119	0.3181	0.2700	98.58	288.1
0.5992	0.2006	0.2002	324.96	2.831	0.4119	0.3181	0.2700	125.24	410.5
0.5992	0.2006	0.2002	339.95	3.931	0.4119	0.3181	0.2700	152.22	570.2
0.5992	0.2006	0.2002	325.00	2.830	0.4119	0.3181	0.2700	125.31	410.4
0.5992	0.2006	0.2002	310.00	1.974	0.4119	0.3181	0.2700	98.31	286.3
0.2005	0.1998	0.5997	280.22	0.601	0.1091	0.2509	0.6401	44.71	87.2
0.2005	0.1998	0.5997	294.66	0.921	0.1091	0.2509	0.6401	70.70	133.6
0.2005	0.1998	0.5997	310.07	1.396	0.1091	0.2509	0.6401	98.44	202.5
0.2005	0.1998	0.5997	325.04	2.013	0.1091	0.2509	0.6401	125.38	292.0
0.2005	0.1998	0.5997	340.05	2.791	0.1091	0.2509	0.6401	152.40	404.8
0.2005	0.1998	0.5997	325.15	2.004	0.1091	0.2509	0.6401	125.58	290.6
0.2005	0.1998	0.5997	310.13	1.390	0.1091	0.2509	0.6401	98.55	201.6

A-15

Table 12. Near-Saturation (p,p,T) Data for R32/125/134a Mixtures from 244 to 346 K (-21 to 163°F).

x(R32) Liquid Mole Fraction	x(R125) Liquid Mole Fraction	x(R134a) Liquid Mole Fraction	Temperature K	Pressure MPa	Density kg/m ³	x(R32) Liquid Mass Fraction	x(R125) Liquid Mass Fraction	x(R134a) Liquid Mass Fraction	Temperature °F	Pressure psia	Density lb/ft ³
0.3460	0.3005	0.3535	243.62	0.229	1350.3	0.1997	0.4001	0.4002	-21.17	33.2	84.22
0.3460	0.3005	0.3535	243.62	0.232	1349.3	0.1997	0.4001	0.4002	-21.17	33.6	84.16
0.3460	0.3005	0.3535	254.15	0.329	1313.9	0.1997	0.4001	0.4002	-2.22	47.7	81.95
0.3460	0.3005	0.3535	264.62	0.485	1277.2	0.1997	0.4001	0.4002	16.63	70.4	79.66
0.3460	0.3005	0.3535	274.40	0.664	1240.5	0.1997	0.4001	0.4002	34.23	96.3	77.37
0.3460	0.3005	0.3535	283.04	0.849	1207.6	0.1997	0.4001	0.4002	49.78	123.1	75.32
0.3460	0.3005	0.3535	296.80	1.231	1149.6	0.1997	0.4001	0.4002	74.55	178.6	71.70
0.3460	0.3005	0.3535	306.50	1.595	1101.6	0.1997	0.4001	0.4002	92.01	231.4	68.71
0.3460	0.3005	0.3535	316.24	2.019	1051.2	0.1997	0.4001	0.4002	109.54	292.8	65.57
0.3460	0.3005	0.3535	326.11	2.531	991.3	0.1997	0.4001	0.4002	127.31	367.1	61.83
0.3460	0.3005	0.3535	335.91	3.121	919.5	0.1997	0.4001	0.4002	144.95	452.7	57.35
0.3460	0.3005	0.3535	345.66	3.800	823.6	0.1997	0.4001	0.4002	162.50	551.1	51.37
0.2004	0.5992	0.2005	280.40	0.794	1246.0	0.1014	0.6996	0.1990	45.03	115.2	77.72
0.2004	0.5992	0.2005	294.61	1.202	1184.3	0.1014	0.6996	0.1990	70.61	174.4	73.86
0.2004	0.5992	0.2005	310.46	1.837	1101.9	0.1014	0.6996	0.1990	99.14	266.4	68.73
0.2004	0.5992	0.2005	325.56	2.584	996.5	0.1014	0.6996	0.1990	126.32	374.7	62.15
0.5992	0.2006	0.2002	280.01	0.875	1158.2	0.4119	0.3181	0.2700	44.33	126.9	72.24
0.5992	0.2006	0.2002	295.10	1.339	1097.7	0.4119	0.3181	0.2700	71.49	194.2	68.46
0.5992	0.2006	0.2002	310.49	1.986	1026.2	0.4119	0.3181	0.2700	99.19	288.1	64.01
0.5992	0.2006	0.2002	325.49	2.831	939.5	0.4119	0.3181	0.2700	126.19	410.5	58.60
0.5992	0.2006	0.2002	340.56	3.931	815.8	0.4119	0.3181	0.2700	153.32	570.2	50.88
0.5992	0.2006	0.2002	325.54	2.830	948.2	0.4119	0.3181	0.2700	126.28	410.4	59.14
0.5992	0.2006	0.2002	310.44	1.974	1025.4	0.4119	0.3181	0.2700	99.10	286.3	63.96
0.2005	0.1998	0.5997	279.96	0.601	1240.6	0.1091	0.2509	0.6401	44.24	87.2	77.38
0.2005	0.1998	0.5997	294.50	0.921	1184.3	0.1091	0.2509	0.6401	70.41	133.6	73.87
0.2005	0.1998	0.5997	310.44	1.396	1116.7	0.1091	0.2509	0.6401	99.10	202.5	69.65
0.2005	0.1998	0.5997	325.54	2.013	1039.9	0.1091	0.2509	0.6401	126.28	292.0	64.86
0.2005	0.1998	0.5997	340.45	2.791	948.3	0.1091	0.2509	0.6401	153.12	404.8	59.15
0.2005	0.1998	0.5997	325.56	2.004	1042.4	0.1091	0.2509	0.6401	126.32	290.6	65.02
0.2005	0.1998	0.5997	310.49	1.390	1117.1	0.1091	0.2509	0.6401	99.19	201.6	69.68

A19

Table 12. Near-Saturation (p,p,T) Data for R32/125/134a Mixtures from 244 to 346 K (-21 to 163°F) (continued).

y(R32)* Vapor Mole Fraction	y(R125)* Vapor Mole Fraction	y(R134a)* Vapor Mole Fraction	Temperature K	Pressure MPa	Density kg/m ³	y(R32)* Vapor Mass Fraction	y(R125)* Vapor Mass Fraction	y(R134a)* Vapor Mass Fraction	Temperature °F	Pressure psia	Density lb/ft ³
0.248	0.620	0.132	312.78	1.837	103.6	0.128	0.738	0.134	103.32	266.4	6.46
0.237	0.616	0.147	328.04	2.584	153.7	0.122	0.730	0.148	130.78	374.7	9.59
0.676	0.203	0.121	312.78	1.986	90.7	0.489	0.339	0.172	103.32	288.1	5.66
0.663	0.202	0.135	328.04	2.831	132.4	0.476	0.334	0.190	130.78	410.5	8.26
0.643	0.201	0.156	343.26	3.931	186.8	0.455	0.328	0.217	158.18	570.2	11.65
0.663	0.202	0.135	328.06	2.830	119.6	0.476	0.334	0.190	130.82	410.4	7.46
0.676	0.203	0.121	312.83	1.974	76.7	0.489	0.339	0.172	103.41	286.3	4.78
0.298	0.254	0.448	312.73	1.396	70.4	0.169	0.332	0.498	103.23	202.5	4.39
0.280	0.244	0.476	327.93	2.013	103.0	0.158	0.317	0.526	130.59	292.0	6.42
0.260	0.233	0.507	342.92	2.791	149.7	0.145	0.300	0.555	157.57	404.8	9.34
0.280	0.244	0.476	327.93	2.004	98.0	0.158	0.317	0.526	130.59	290.6	6.11
0.298	0.254	0.448	312.67	1.390	65.2	0.169	0.332	0.498	103.12	201.6	4.07

*Near-saturation vapor compositions are calculated from the vapor-liquid equilibrium data and REFPROP.

Table 13. Vapor-Liquid Equilibrium Data for R32/143a Mixtures from 280 to 340 K (44 to 152°F).

x(R32) Liquid Mole Fraction	Temperature K	Pressure MPa	y(R32) Vapor Mole Fraction	x(R32) Liquid Mass Fraction	Temperature °F	Pressure psia	y(R32) Vapor Mass Fraction
0.000	280.23	0.767	0.000	0.000	44.73	111.3	0.000
0.357	279.88	0.906	0.439	0.256	44.09	131.3	0.326
0.377	279.88	0.912	0.434	0.273	44.10	132.3	0.322
0.605	279.90	0.971	0.652	0.487	44.13	140.8	0.537
0.674	279.86	0.980	0.692	0.561	44.07	142.2	0.582
0.735	279.85	0.992	0.759	0.632	44.04	143.9	0.661
1.000	280.00	1.007	1.000	1.000	44.31	146.1	1.000
0.000	294.11	1.135	0.000	0.000	69.71	164.6	0.000
0.719	294.92	1.517	0.756	0.613	71.16	220.0	0.657
0.414	294.96	1.407	0.479	0.304	71.25	204.0	0.363
0.638	295.03	1.493	0.665	0.522	71.37	216.6	0.551
1.000	293.99	1.515	1.000	1.000	69.49	219.8	1.000
0.000	309.37	1.677	0.000	0.000	97.18	243.2	0.000
0.635	310.10	2.191	0.676	0.519	98.49	317.7	0.564
0.811	310.05	2.266		0.726	98.41	328.7	
0.875	310.07	2.281		0.812	98.43	330.8	
0.912	310.06	2.288	0.936	0.865	98.41	331.9	0.901
1.000	310.51	2.329	1.000	1.000	99.23	337.8	1.000
0.000	326.02	2.467	0.000	0.000	127.15	357.8	0.000
0.818	325.06	3.209	0.841	0.736	125.41	465.5	0.766
0.746	325.05	3.156	0.762	0.645	125.41	457.7	0.665
0.604	325.07	3.067	0.638	0.486	125.44	444.9	0.522
0.547	324.94	3.013	0.575	0.428	125.20	437.0	0.456
1.000	325.49	3.318	1.000	1.000	126.19	481.2	1.000
0.000	340.07	3.318	0.000	0.000	152.44	481.2	0.000
0.543	340.03	4.169	0.570	0.424	152.36	604.7	0.451
0.499	340.01	4.136	0.546	0.381	152.32	599.8	0.427
0.698	340.02	4.345	0.718	0.589	152.35	630.2	0.612
1.000	340.08	4.571	1.000	1.000	152.46	663.0	1.000

A-18

Table 14. Near-Saturation (p,p,T) Data for R32/143a Mixtures from 279 to 340 K (43 to 152°F).

x(R32) Liquid Mole Fraction	Temperature K	Pressure MPa	Density kg/m ³	x(R32) Liquid Mass Fraction	Temperature °F	Pressure psia	Density lb/ft ³
0.271	279.76	0.930	1003.2	0.187	43.87	134.9	62.57
0.271	279.73	0.929	1003.2	0.187	43.83	134.8	62.57
0.542	279.40	0.987	1009.8	0.423	43.23	143.1	62.99
0.952	279.22	1.017	1026.5	0.925	42.90	147.5	64.02
0.203	293.35	1.268	948.9	0.136	68.33	183.9	59.18
0.203	293.14	1.249	949.3	0.136	67.96	181.1	59.21
0.436	293.66	1.417	950.9	0.324	68.89	205.5	59.31
0.619	293.27	1.469	957.8	0.501	68.19	213.1	59.74
0.619	293.35	1.480	957.6	0.501	68.33	214.7	59.73
0.713	293.09	1.491	962.9	0.606	67.87	216.3	60.06
0.861	293.04	1.527	972.9	0.793	67.78	221.5	60.68
0.263	309.22	1.887	877.4	0.181	96.91	273.7	54.72
0.362	309.97	2.022	874.6	0.260	98.26	293.3	54.55
0.635	309.76	2.197	882.6	0.519	97.88	318.7	55.05
0.736	309.22	2.224	892.2	0.633	96.91	322.5	55.65
0.890	308.65	2.343	903.6	0.834	95.88	339.8	56.36
0.172	325.59	2.753	782.1	0.114	126.37	399.3	48.78
0.450	325.90	3.120	786.6	0.336	126.94	452.6	49.06
0.581	326.01	3.204	789.2	0.462	127.12	464.6	49.22
0.596	326.03	3.211	789.2	0.477	127.17	465.7	49.22
0.664	326.01	3.272	793.4	0.550	127.12	474.6	49.49
0.668	326.01	3.269	793.0	0.555	127.12	474.1	49.46
0.728	325.98	3.327	797.8	0.624	127.08	482.5	49.76
0.731	325.98	3.327	797.7	0.627	127.08	482.5	49.75
0.805	325.80	3.331	801.6	0.719	126.75	483.1	50.00
0.787	325.93	3.349	801.1	0.696	126.98	485.7	49.97
0.787	325.93	3.341	801.0	0.696	126.98	484.6	49.96
0.259	339.51	3.796	660.0	0.178	151.43	550.6	41.17
0.267	339.51	3.796	659.6	0.184	151.43	550.5	41.14
0.394	339.49	4.043	665.0	0.287	151.39	586.3	41.48
0.394	339.49	4.044	664.9	0.287	151.39	586.5	41.47
0.467	339.46	4.271	671.0	0.352	151.34	619.5	41.85
0.633	339.25	4.470	677.8	0.516	150.96	648.2	42.28
0.636	339.25	4.396	672.0	0.520	150.96	637.6	41.91
0.715	339.23	4.470	678.0	0.608	150.92	648.2	42.29
0.792	339.12	4.550	689.6	0.702	150.73	659.9	43.01

Table 14. Near-Saturation (p, ρ ,T) Data for R32/143a Mixtures from 279 to 340 K (43 to 152°F) (continued).

x(R32) Liquid Mole Fraction	Temperature K	Pressure MPa	Density kg/m ³	x(R32) liquid Mass Fraction	Temperature °F	Pressure psia	Density lb/ft ³
0.811	339.15	4.555	689.9	0.726	150.78	660.6	43.03
0.887	339.25	4.589	704.8	0.829	150.96	665.6	43.96
y(R32)* Vapor Mole Fraction	Temperature K	Pressure MPa	Density kg/m ³	y(R32)* Vapor Mass Fraction	Temperature °F	Pressure psia	Density lb/ft ³
0.258	294.34	1.249	52.5	0.177	70.13	181.1	3.28
0.408	310.26	2.022	82.6	0.299	98.79	293.3	5.15
0.669	309.95	2.197	78.2	0.550	98.23	318.7	4.88
0.760	309.46	2.224	75.4	0.662	97.34	322.5	4.70
0.190	326.66	2.741	134.9	0.127	128.29	397.5	8.41
0.611	326.89	3.204	133.9	0.492	128.71	464.6	8.35
0.695	326.89	3.269	132.5	0.585	128.71	474.1	8.26
0.658	339.96	4.470	209.8	0.544	152.25	648.2	13.09
0.800	339.78	4.550	198.9	0.712	151.92	659.9	12.40
0.817	339.83	4.555	199.0	0.734	152.01	660.6	12.41
0.888	340.04	4.589	185.8	0.831	152.39	665.6	11.59

*Near-saturation vapor compositions are calculated from the vapor-liquid equilibrium data.

Table 15. Vapor-Liquid Equilibrium Data for R125/143a Mixtures from 280 to 326 K (44 to 127°F).

x(R125) Liquid Mole Fraction	Temperature K	Pressure MPa	y(R125) Vapor Mole Fraction	x(R125) Liquid Mass Fraction	Temperature °F	Pressure psia	y(R125) Vapor Mass Fraction
0.000	280.23	0.767	0.000	0.000	44.73	111.2	0.000
0.287	279.95	0.769		0.365	44.22	111.5	
0.353	279.97	0.779	0.365	0.438	44.26	113.0	0.451
0.425	280.00	0.772	0.428	0.513	44.31	112.0	0.516
0.645	279.95	0.783		0.722	44.22	113.6	
1.000	280.29	0.830	1.000	1.000	44.83	120.4	1.000
0.000	294.11	1.135	0.000	0.000	69.71	164.6	0.000
0.302	294.96	1.176	0.318	0.382	71.24	170.6	0.400
0.353	294.95	1.183	0.365	0.438	71.22	171.6	0.451
0.422	294.95	1.176	0.432	0.510	71.21	170.6	0.521
0.642	294.96	1.199	0.670	0.719	71.24	173.9	0.744
1.000	295.23	1.272	1.000	1.000	71.73	184.5	1.000
0.000	309.37	1.677	0.000	0.000	97.18	243.2	0.000
0.312	309.97	1.727	0.330	0.393	98.26	250.5	0.413
0.354	309.97	1.734	0.365	0.439	98.25	251.5	0.451
0.422	310.08	1.742	0.432	0.510	98.46	252.7	0.521
0.640	309.91	1.792	0.668	0.717	98.15	259.9	0.742
1.000	310.61	1.888	1.000	1.000	99.41	273.8	1.000
0.000	326.02	2.467	0.000	0.000	127.15	357.8	0.000
0.309	324.98	2.450		0.390	125.27	355.3	
0.348	325.00	2.461	0.360	0.432	125.30	356.9	0.445
0.352	324.97	2.461	0.367	0.437	125.26	356.9	0.453
0.419	324.95	2.465	0.430	0.507	125.21	357.5	0.519
0.636	324.95	2.534	0.659	0.714	125.21	367.5	0.734
1.000	324.89	2.636	1.000	1.000	125.11	382.3	1.000

Table 16. Bubble-Point Pressures for R125/143a Mixtures from 280 to 325 K (45 to 125°F).

x(R125) Liquid Mole Fraction	Temperature K	Pressure MPa	x(R125) Liquid Mass Fraction	Temperature °F	Pressure psia
0.3500	280.58	0.800	0.4347	45.36	116.0
0.3500	294.93	1.205	0.4347	71.19	174.8
0.3500	294.97	1.205	0.4347	71.26	174.8
0.3500	309.94	1.753	0.4347	98.20	254.3
0.3500	309.99	1.755	0.4347	98.29	254.5
0.3500	325.01	2.488	0.4347	125.33	360.9
0.3500	325.03	2.476	0.4347	125.37	359.1
0.6500	280.12	0.798	0.7262	44.53	115.7
0.6500	295.06	1.225	0.7262	71.42	177.7
0.6500	310.63	1.823	0.7262	99.45	264.4
0.6500	325.05	2.560	0.7262	125.40	371.3

A-22

Table 17. Near-Saturation (p,p,T) Data for R125/143a Mixtures from 280 to 328 K (44 to 131°F).

x(R125) Liquid Mole Fraction	Temperature K	Pressure MPa	Density kg/m ³	x(R125) Liquid Mass Fraction	Temperature °F	Pressure psia	Density lb/ft ³
0.3500	280.11	0.800	1107.6	0.4347	44.51	116.0	69.08
0.3500	294.92	1.205	1041.4	0.4347	71.17	174.8	64.96
0.3500	310.00	1.755	966.2	0.4347	98.31	254.5	60.27
0.3500	324.89	2.476	869.6	0.4347	125.11	359.1	54.24
0.6500	279.91	0.798	1199.4	0.7262	44.15	115.7	74.81
0.6500	294.40	1.225	1120.6	0.7262	70.23	177.7	69.89
0.6500	310.75	1.823	1032.5	0.7262	99.66	264.4	64.40
0.6500	325.02	2.560	929.4	0.7262	125.35	371.3	57.97
y(R125)* Vapor Mole Fraction	Temperature K	Pressure MPa	Density kg/m ³	y(R125)* Vapor Mass Fraction	Temperature °F	Pressure psia	Density lb/ft ³
0.367	297.57	1.205	59.5	0.453	75.94	174.8	3.71
0.367	313.14	1.755	92.9	0.453	103.96	254.5	5.79
0.367	328.06	2.476	145.4	0.453	130.82	359.1	9.07
0.672	296.22	1.225	70.0	0.745	73.51	177.7	4.37
0.672	312.54	1.823	110.4	0.745	102.88	264.4	6.89
0.672	326.81	2.560	175.1	0.745	128.57	371.3	10.92

*Near-saturation vapor compositions are calculated from the vapor-liquid equilibrium data.

A-23

Table 18. Isochoric (p, ρ ,T) Data from 200 to 400 K (-100 to 260°F) for a Mixture of R125/143a with $x(\text{R125}) = 0.49996$ Mole Fraction (0.58812 Mass Fraction).

Temperature K	Pressure MPa	Density kg/m^3	Temperature °F	Pressure psia	Density lb/ft^3
200.002	3.7506	1436.26	-99.68	543.980	89.663
200.999	4.9935	1435.93	-97.89	724.248	89.642
202.001	6.2613	1435.68	-96.09	908.128	89.627
203.000	7.5391	1435.46	-94.29	1093.458	89.613
204.001	8.8261	1435.25	-92.49	1280.122	89.600
205.001	10.1129	1435.06	-90.69	1466.757	89.588
206.000	11.4026	1434.89	-88.89	1653.813	89.577
206.999	12.6913	1434.71	-87.09	1840.724	89.566
207.998	13.9760	1434.55	-85.29	2027.054	89.556
208.999	15.2691	1434.38	-83.49	2214.603	89.545
210.000	16.5530	1434.22	-81.69	2400.818	89.535
212.000	19.1238	1433.92	-78.09	2773.682	89.517
213.998	21.6852	1433.62	-74.49	3145.183	89.498
216.001	24.2425	1433.32	-70.89	3516.090	89.479
218.002	26.7839	1433.04	-67.28	3884.690	89.462
220.001	29.3202	1432.76	-63.69	4252.550	89.444
222.001	31.8491	1432.48	-60.09	4619.338	89.427
224.001	34.3699	1432.21	-56.49	4984.950	89.410
218.001	3.8638	1384.16	-67.29	560.399	86.410
218.999	4.9311	1383.88	-65.49	715.198	86.393
219.999	6.0153	1383.65	-63.69	872.449	86.378
220.999	7.1022	1383.44	-61.89	1030.091	86.365
222.000	8.1999	1383.26	-60.09	1189.299	86.354
224.000	10.3918	1382.91	-56.49	1507.208	86.332
226.001	12.5889	1382.59	-52.89	1825.872	86.312
228.001	14.7813	1382.29	-49.29	2143.854	86.294
230.000	16.9714	1382.00	-45.69	2461.502	86.275
232.000	19.1605	1381.72	-42.09	2779.005	86.258
234.000	21.3446	1381.45	-38.49	3095.783	86.241
235.999	23.5209	1381.18	-34.89	3411.430	86.224
238.001	25.6902	1380.92	-31.29	3726.061	86.208
239.999	27.8520	1380.65	-27.69	4039.605	86.191
241.998	30.0112	1380.40	-24.09	4352.772	86.176
244.002	32.1628	1380.14	-20.48	4664.836	86.159
246.000	34.3048	1379.89	-16.89	4975.508	86.144

Table 18. Isochoric (p, ρ ,T) Data from 200 to 400 K (-100 to 260°F) for a Mixture of R125/143a
with $x(\text{R125}) = 0.49996$ Mole Fraction (0.58812 Mass Fraction) (continued).

Temperature K	Pressure MPa	Density kg/m ³	Temperature °F	Pressure psia	Density lb/ft ³
232.002	3.7217	1341.20	-42.08	539.789	83.728
233.002	4.6604	1340.93	-40.28	675.936	83.712
233.998	5.6055	1340.70	-38.49	813.012	83.697
235.000	6.5633	1340.51	-36.69	951.930	83.685
236.000	7.5240	1340.33	-34.89	1091.268	83.674
237.000	8.4877	1340.16	-33.09	1231.041	83.663
238.000	9.4505	1340.00	-31.29	1370.684	83.653
238.999	10.4114	1339.84	-29.49	1510.051	83.643
240.000	11.3791	1339.69	-27.69	1650.405	83.634
242.001	13.3040	1339.41	-24.09	1929.589	83.617
244.001	15.2293	1339.13	-20.49	2208.831	83.599
246.000	17.1485	1338.86	-16.89	2487.188	83.582
248.001	19.0670	1338.60	-13.29	2765.444	83.566
250.001	20.9836	1338.34	-9.69	3043.424	83.550
252.000	22.8948	1338.09	-6.09	3320.622	83.534
253.999	24.8013	1337.84	-2.49	3597.137	83.519
256.002	26.7048	1337.59	1.12	3873.217	83.503
258.000	28.5988	1337.35	4.71	4147.920	83.488
260.000	30.4875	1337.11	8.31	4421.853	83.473
262.000	32.3738	1336.86	11.91	4695.439	83.457
263.999	34.2556	1336.62	15.51	4968.372	83.442
250.001	3.6410	1283.22	-9.69	528.084	80.109
250.999	4.4309	1282.97	-7.89	642.650	80.093
252.001	5.2340	1282.76	-6.09	759.130	80.080
253.000	6.0320	1282.58	-4.29	874.871	80.069
253.999	6.8381	1282.41	-2.49	991.786	80.058
256.000	8.4547	1282.10	1.11	1226.255	80.039
257.999	10.0704	1281.82	4.71	1460.593	80.021
259.998	11.6861	1281.55	8.31	1694.931	80.005
262.002	13.3063	1281.29	11.92	1929.922	79.988
263.998	14.9208	1281.03	15.51	2164.087	79.972
265.998	16.5348	1280.79	19.11	2398.178	79.957
268.002	18.1484	1280.54	22.72	2632.212	79.942
269.999	19.7557	1280.31	26.31	2865.332	79.927
271.998	21.3602	1280.07	29.91	3098.046	79.912

A-25

Table 18. Isochoric (p, ρ ,T) Data from 200 to 400 K (-100 to 260°F) for a Mixture of R125/143a with $x(\text{R125}) = 0.49996$ Mole Fraction (0.58812 Mass Fraction) (continued).

Temperature K	Pressure MPa	Density kg/m ³	Temperature °F	Pressure psia	Density lb/ft ³
273.999	22.9642	1279.84	33.51	3330.687	79.898
276.002	24.5672	1279.61	37.12	3563.184	79.883
278.001	26.1621	1279.38	40.71	3794.505	79.869
280.001	27.7544	1279.15	44.31	4025.449	79.855
282.000	29.3470	1278.92	47.91	4256.437	79.840
284.002	30.9361	1278.70	51.52	4486.918	79.827
286.002	32.5217	1278.47	55.12	4716.890	79.812
288.001	34.1018	1278.25	58.71	4946.065	79.799
263.999	3.7705	1235.68	15.51	546.867	77.141
264.998	4.4605	1235.46	17.31	646.943	77.127
266.000	5.1538	1235.28	19.11	747.498	77.116
266.999	5.8503	1235.11	20.91	848.517	77.105
268.001	6.5504	1234.95	22.71	950.059	77.095
270.000	7.9488	1234.66	26.31	1152.880	77.077
272.000	9.3522	1234.39	29.91	1356.427	77.060
274.000	10.7530	1234.13	33.51	1559.596	77.044
276.001	12.1586	1233.89	37.11	1763.462	77.029
277.998	13.5561	1233.65	40.71	1966.153	77.014
279.998	14.9587	1233.41	44.31	2169.584	76.999
284.000	17.7592	1232.95	51.51	2575.763	76.971
287.999	20.5526	1232.51	58.71	2980.913	76.943
291.999	23.3373	1232.06	65.91	3384.801	76.915
295.999	26.1108	1231.64	73.11	3787.065	76.889
300.000	28.8753	1231.20	80.31	4188.023	76.861
304.000	31.6335	1230.78	87.51	4588.067	76.835
308.001	34.3803	1230.35	94.71	4986.458	76.808
280.001	3.6831	1175.50	44.31	534.190	73.384
281.001	4.2625	1175.30	46.11	618.226	73.372
282.000	4.8396	1175.13	47.91	701.927	73.361
283.000	5.4219	1174.97	49.71	786.383	73.351
284.000	6.0052	1174.82	51.51	870.984	73.342
286.001	7.1726	1174.55	55.11	1040.301	73.325
288.001	8.3444	1174.30	58.71	1210.257	73.309
290.001	9.5156	1174.06	62.31	1380.126	73.294

Table 18. Isochoric (p, ρ ,T) Data from 200 to 400 K (-100 to 260°F) for a Mixture of R125/143a
with $x(\text{R125}) = 0.49996$ Mole Fraction (0.58812 Mass Fraction) (continued).

Temperature K	Pressure MPa	Density kg/m ³	Temperature °F	Pressure psia	Density lb/ft ³
292.000	10.6859	1173.82	65.91	1549.864	73.279
294.000	11.8569	1173.59	69.51	1719.704	73.265
296.002	13.0286	1173.37	73.12	1889.645	73.251
297.999	14.1973	1173.16	76.71	2059.151	73.238
300.001	15.3698	1172.94	80.31	2229.209	73.224
302.002	16.5391	1172.73	83.92	2398.802	73.211
304.001	17.7094	1172.52	87.51	2568.540	73.198
306.000	18.8757	1172.31	91.11	2737.698	73.185
308.002	20.0449	1172.11	94.72	2907.277	73.172
310.001	21.2109	1171.90	98.31	3076.392	73.159
311.999	22.3755	1171.70	101.91	3245.303	73.147
316.000	24.7019	1171.29	109.11	3582.720	73.121
319.999	27.0204	1170.89	116.31	3918.991	73.096
324.001	29.3345	1170.49	123.51	4254.624	73.071
328.000	31.6369	1170.09	130.71	4588.560	73.046
332.000	33.9380	1169.69	137.91	4922.308	73.021
296.001	3.3401	1104.63	73.11	484.442	68.960
296.999	3.8033	1104.44	74.91	551.624	68.948
298.000	4.2701	1104.27	76.71	619.328	68.937
298.998	4.7359	1104.12	78.51	686.887	68.928
300.000	5.2037	1103.98	80.31	754.736	68.919
302.000	6.1457	1103.72	83.91	891.362	68.903
304.000	7.0887	1103.48	87.51	1028.133	68.888
306.001	8.0369	1103.25	91.11	1165.658	68.874
308.001	8.9843	1103.03	94.71	1303.067	68.860
310.000	9.9300	1102.82	98.31	1440.230	68.847
312.002	10.8795	1102.61	101.92	1577.944	68.834
316.001	12.7777	1102.21	109.11	1853.255	68.809
320.001	14.6770	1101.81	116.31	2128.726	68.784
324.002	16.5700	1101.44	123.52	2403.284	68.761
328.001	18.4665	1101.07	130.71	2678.349	68.738
332.002	20.3606	1100.71	137.92	2953.066	68.715
336.000	22.2523	1100.33	145.11	3227.435	68.691
340.000	24.1464	1099.96	152.31	3502.151	68.668
344.000	26.0347	1099.58	159.51	3776.027	68.645

A-27

Table 18. Isochoric (p,ρ,T) Data from 200 to 400 K (-100 to 260°F) for a Mixture of R125/143a with x(R125) = 0.49996 Mole Fraction (0.58812 Mass Fraction) (continued).

Temperature K	Pressure MPa	Density kg/m ³	Temperature °F	Pressure psia	Density lb/ft ³
347.999	27.9191	1099.21	166.71	4049.337	68.621
352.000	29.8009	1098.84	173.91	4322.270	68.598
355.999	31.6740	1098.47	181.11	4593.941	68.575
359.998	33.5435	1098.10	188.31	4865.090	68.552
364.000	35.4096	1097.72	195.51	5135.746	68.528
312.000	3.7918	1028.84	101.91	549.956	64.228
313.000	4.1628	1028.70	103.71	603.765	64.220
313.999	4.5353	1028.56	105.51	657.792	64.211
315.000	4.9070	1028.44	107.31	711.703	64.203
316.000	5.2799	1028.32	109.11	765.787	64.196
318.001	6.0293	1028.09	112.71	874.479	64.182
320.002	6.7805	1027.88	116.32	983.432	64.168
323.999	8.2885	1027.47	123.51	1202.149	64.143
327.999	9.8011	1027.09	130.71	1421.534	64.119
332.001	11.3174	1026.72	137.91	1641.456	64.096
335.998	12.8365	1026.35	145.11	1861.783	64.073
340.000	14.3596	1025.99	152.31	2082.691	64.050
344.000	15.8825	1025.64	159.51	2303.570	64.029
348.000	17.4077	1025.29	166.71	2524.782	64.007
352.001	18.9314	1024.94	173.91	2745.777	63.985
356.000	20.4540	1024.59	181.11	2966.612	63.963
360.000	21.9768	1024.25	188.31	3187.476	63.942
363.999	23.4986	1023.90	195.51	3408.196	63.920
367.999	25.0183	1023.56	202.71	3628.610	63.899
372.000	26.5365	1023.21	209.91	3848.807	63.877
376.000	28.0523	1022.87	217.11	4068.656	63.856
380.001	29.5659	1022.52	224.31	4288.186	63.834
383.999	31.0747	1022.18	231.51	4507.020	63.813
388.001	32.5831	1021.83	238.71	4725.796	63.791
392.001	34.0861	1021.48	245.91	4943.788	63.769
328.002	3.7130	919.21	130.72	538.527	57.384
329.001	3.9760	919.09	132.51	576.672	57.377
329.998	4.2397	918.98	134.31	614.919	57.370
331.001	4.5041	918.87	136.11	653.267	57.363

A-28

Table 18. Isochoric (p,p,T) Data from 200 to 400 K (-100 to 260°F) for a Mixture of R125/143a with x(R125) = 0.49996 Mole Fraction (0.58812 Mass Fraction) (continued).

Temperature K	Pressure MPa	Density kg/m ³	Temperature °F	Pressure psia	Density lb/ft ³
331.999	4.7706	918.77	137.91	691.919	57.357
334.002	5.3040	918.57	141.52	769.283	57.344
335.999	5.8395	918.38	145.11	846.951	57.333
340.001	6.9193	918.03	152.31	1003.563	57.311
344.001	8.0054	917.69	159.51	1161.089	57.290
348.001	9.0986	917.36	166.71	1319.645	57.269
352.001	10.1956	917.03	173.91	1478.752	57.248
355.999	11.2964	916.72	181.11	1638.410	57.229
360.002	12.4010	916.40	188.32	1798.619	57.209
363.999	13.5094	916.09	195.51	1959.380	57.190
368.001	14.6199	915.78	202.71	2120.445	57.170
372.000	15.7311	915.47	209.91	2281.611	57.151
376.002	16.8436	915.16	217.12	2442.966	57.132
380.002	17.9569	914.86	224.32	2604.437	57.113
383.999	19.0718	914.55	231.51	2766.140	57.094
388.000	20.1849	914.24	238.71	2927.582	57.074
391.999	21.2995	913.94	245.91	3089.242	57.055
396.001	22.4140	913.63	253.11	3250.887	57.036
399.998	23.5269	913.32	260.31	3412.300	57.017
344.000	4.5684	788.09	159.51	662.593	49.199
344.999	4.7457	788.01	161.31	688.308	49.194
346.000	4.9244	787.93	163.11	714.226	49.189
347.000	5.1033	787.85	164.91	740.174	49.184
348.001	5.2827	787.78	166.71	766.194	49.180
350.001	5.6438	787.63	170.31	818.567	49.170
351.999	6.0069	787.49	173.91	871.230	49.161
356.000	6.7392	787.20	181.11	977.442	49.143
359.999	7.4781	786.92	188.31	1084.610	49.126
364.002	8.2235	786.65	195.52	1192.722	49.109
368.001	8.9734	786.38	202.71	1301.486	49.092
372.000	9.7269	786.11	209.91	1410.772	49.075
376.001	10.4834	785.85	217.11	1520.494	49.059
380.000	11.2428	785.59	224.31	1630.636	49.043
384.002	12.0050	785.32	231.52	1741.184	49.026
388.000	12.7683	785.06	238.71	1851.892	49.010

Table 18. Isochoric (p,ρ,T) Data from 200 to 400 K (-100 to 260°F) for a Mixture of R125/143a with $x(\text{R125}) = 0.49996$ Mole Fraction (0.58812 Mass Fraction) (continued).

Temperature K	Pressure MPa	Density kg/m^3	Temperature °F	Pressure psia	Density lb/ft^3
392.000	13.5340	784.80	245.91	1962.948	48.993
396.001	14.3007	784.54	253.11	2074.148	48.977
399.999	15.0681	784.28	260.31	2185.451	48.961
359.999	6.3326	717.08	188.31	918.469	44.766
361.999	6.6333	716.96	191.91	962.082	44.758
364.001	6.9356	716.83	195.51	1005.927	44.750
365.999	7.2384	716.71	199.11	1049.845	44.743
368.000	7.5426	716.59	202.71	1093.965	44.735
370.000	7.8479	716.47	206.31	1138.246	44.728
372.000	8.1541	716.35	209.91	1182.656	44.720
375.999	8.7690	716.11	217.11	1271.840	44.705
380.000	9.3875	715.87	224.31	1361.547	44.690
384.000	10.0079	715.63	231.51	1451.528	44.675
388.002	10.6302	715.39	238.72	1541.786	44.660
391.999	11.2548	715.15	245.91	1632.376	44.645
396.000	11.8807	714.92	253.11	1723.156	44.631
399.999	12.5078	714.68	260.31	1814.109	44.616
360.001	5.4741	609.87	188.31	793.954	38.073
362.001	5.6949	609.77	191.91	825.978	38.067
364.002	5.9167	609.66	195.52	858.148	38.060
366.000	6.1395	609.56	199.11	890.462	38.054
368.001	6.3631	609.46	202.71	922.893	38.047
370.001	6.5877	609.35	206.31	955.468	38.040
371.998	6.8122	609.25	209.91	988.030	38.034
376.000	7.2640	609.05	217.11	1053.558	38.022
380.002	7.7179	608.84	224.32	1119.391	38.009
384.000	8.1732	608.65	231.51	1185.427	37.997
388.000	8.6302	608.44	238.71	1251.709	37.984
392.000	9.0882	608.24	245.91	1318.137	37.971
396.000	9.5472	608.04	253.11	1384.709	37.959
399.998	10.0079	607.84	260.31	1451.528	37.946
360.000	4.8317	426.20	188.31	700.781	26.607
362.001	4.9666	426.13	191.91	720.347	26.602

Table 18. Isochoric (p,p,T) Data from 200 to 400 K (-100 to 260°F) for a Mixture of R125/143a with x(R125) = 0.49996 Mole Fraction (0.58812 Mass Fraction) (continued).

Temperature K	Pressure MPa	Density kg/m ³	Temperature °F	Pressure psia	Density lb/ft ³
364.000	5.1014	426.06	195.51	739.898	26.598
365.999	5.2360	425.99	199.11	759.420	26.594
367.999	5.3703	425.92	202.71	778.899	26.589
369.999	5.5042	425.86	206.31	798.319	26.586
372.002	5.6386	425.79	209.92	817.813	26.581
376.001	5.9060	425.65	217.11	856.596	26.572
380.001	6.1729	425.51	224.31	895.307	26.564
383.999	6.4393	425.37	231.51	933.945	26.555
388.000	6.7051	425.24	238.71	972.496	26.547
392.002	6.9705	425.10	245.92	1010.989	26.538
396.000	7.2353	424.96	253.11	1049.395	26.529
400.000	7.4996	424.83	260.31	1087.729	26.521
360.002	3.8467	224.68	188.32	557.919	14.026
361.999	3.9073	224.67	191.91	566.708	14.026
364.000	3.9676	224.64	195.51	575.454	14.024
365.999	4.0278	224.61	199.11	584.185	14.022
368.001	4.0875	224.58	202.71	592.844	14.020
369.999	4.1467	224.55	206.31	601.430	14.018
372.000	4.2059	224.51	209.91	610.016	14.016
376.000	4.3232	224.43	217.11	627.029	14.011
379.999	4.4398	224.36	224.31	643.941	14.006
384.000	4.5556	224.29	231.51	660.736	14.002
388.000	4.6706	224.21	238.71	677.416	13.997
392.000	4.7848	224.14	245.91	693.979	13.993
396.001	4.8984	224.06	253.11	710.455	13.988
400.000	5.0114	223.99	260.31	726.845	13.983
359.999	2.1310	90.32	188.31	309.076	5.638
362.000	2.1501	90.30	191.91	311.847	5.637
364.002	2.1691	90.29	195.52	314.602	5.637
366.000	2.1881	90.27	199.11	317.358	5.635
367.999	2.2070	90.25	202.71	320.099	5.634
370.000	2.2258	90.23	206.31	322.826	5.633
372.002	2.2443	90.21	209.92	325.509	5.632
375.999	2.2815	90.17	217.11	330.905	5.629

A-31

Table 18. Isochoric (p, ρ ,T) Data from 200 to 400 K (-100 to 260°F) for a Mixture of R125/143a with $x(\text{R125}) = 0.49996$ Mole Fraction (0.58812 Mass Fraction) (continued).

Temperature K	Pressure MPa	Density kg/m ³	Temperature °F	Pressure psia	Density lb/ft ³
379.999	2.3185	90.14	224.31	336.271	5.627
384.001	2.3553	90.10	231.51	341.609	5.625
388.000	2.3919	90.06	238.71	346.917	5.622
392.000	2.4282	90.02	245.91	352.182	5.620
395.999	2.4644	89.98	253.11	357.432	5.617
400.000	2.5004	89.93	260.31	362.654	5.614

Table 19. Isochoric Heat Capacities (C_v) from 205 to 344 K (-90 to 160°F) for a Mixture of R125/143a with
 $x(\text{R125}) = 0.49996$ Mole Fraction (0.58812 Mass Fraction).

Temperature K	Heat Capacity J/(mole•K)	Density kg/m ³	Pressure MPa	Temperature °F	Heat Capacity BTU/(lb•°F)	Density lb/ft ³	Pressure psia
205.344	79.81	1423.91	5.993	-90.07	0.1815	88.892	869.2
209.396	80.55	1422.62	10.830	-82.78	0.1832	88.811	1570.8
213.409	80.99	1421.37	15.576	-75.55	0.1842	88.733	2259.0
213.471	80.93	1421.35	15.649	-75.44	0.1841	88.732	2269.7
217.471	81.62	1420.11	20.343	-68.24	0.1856	88.655	2950.5
221.438	82.28	1418.89	24.962	-61.10	0.1871	88.578	3620.4
225.368	82.82	1417.69	29.491	-54.03	0.1884	88.504	4277.3
224.591	81.79	1368.69	5.976	-55.42	0.1861	85.445	866.8
228.625	82.40	1367.58	10.114	-48.16	0.1874	85.375	1467.0
232.628	83.25	1366.48	14.190	-40.96	0.1893	85.307	2058.1
236.602	83.77	1365.40	18.201	-33.80	0.1906	85.239	2639.9
240.542	84.51	1364.33	22.140	-26.71	0.1922	85.172	3211.2
244.456	84.77	1363.28	26.015	-19.67	0.1928	85.107	3773.1
248.328	85.63	1362.24	29.806	-12.70	0.1948	85.042	4323.0
242.601	84.18	1312.65	5.503	-23.01	0.1915	81.946	798.2
246.619	84.61	1311.67	9.011	-15.77	0.1925	81.885	1307.0
250.613	85.13	1310.72	12.477	-8.58	0.1936	81.826	1809.6
254.577	85.69	1309.78	15.893	-1.45	0.1949	81.767	2305.2
258.518	86.52	1308.85	19.266	5.64	0.1968	81.709	2794.3
262.438	87.08	1307.93	22.594	12.70	0.1981	81.651	3277.0
266.329	87.44	1307.02	25.871	19.70	0.1988	81.595	3752.3
270.200	88.31	1306.12	29.101	26.67	0.2008	81.538	4220.8
274.049	89.06	1305.22	32.282	33.60	0.2026	81.482	4682.1
263.312	86.95	1244.09	5.209	14.27	0.1978	77.666	755.4
267.338	87.34	1243.28	8.087	21.52	0.1987	77.615	1172.9
271.337	88.18	1242.47	10.935	28.72	0.2006	77.565	1586.0
275.322	88.73	1241.67	13.761	35.89	0.2018	77.515	1995.8
279.279	89.13	1240.89	16.553	43.01	0.2028	77.466	2400.9
283.221	89.51	1240.10	19.319	50.11	0.2036	77.417	2802.0
287.141	90.20	1239.33	22.052	57.17	0.2051	77.369	3198.4
291.048	90.72	1238.56	24.760	64.20	0.2064	77.321	3591.2
294.933	91.20	1237.80	27.436	71.19	0.2074	77.273	3979.3
298.806	92.21	1237.03	30.085	78.16	0.2097	77.225	4363.5

Table 19. Isochoric Heat Capacities (C_v) from 205 to 344 K (-90 to 160°F) for a Mixture of R125/143a with $x(\text{R125}) = 0.49996$ Mole Fraction (0.58812 Mass Fraction) (continued).

Temperature K	Heat Capacity J/(mole•K)	Density kg/m ³	Pressure MPa	Temperature °F	Heat Capacity BTU/(lb•°F)	Density lb/ft ³	Pressure psia
302.674	92.44	1236.27	32.714	85.13	0.2103	77.178	4744.8
283.541	89.92	1169.63	4.960	50.69	0.2046	73.018	719.3
287.598	90.26	1168.95	7.288	57.99	0.2053	72.975	1057.0
291.637	90.58	1168.27	9.602	65.26	0.2060	72.933	1392.7
295.661	91.21	1167.61	11.904	72.50	0.2075	72.892	1726.5
299.678	91.91	1166.95	14.195	79.73	0.2090	72.850	2058.8
303.680	91.96	1166.28	16.470	86.94	0.2091	72.808	2388.8
307.668	92.79	1165.63	18.728	94.11	0.2110	72.768	2716.2
311.647	93.39	1164.98	20.970	101.28	0.2125	72.727	3041.5
315.613	94.11	1164.33	23.195	108.42	0.2141	72.687	3364.2
319.573	94.59	1163.67	25.407	115.54	0.2151	72.646	3685.0
323.529	95.08	1163.03	27.606	122.66	0.2163	72.606	4003.9
327.471	95.67	1162.38	29.788	129.76	0.2176	72.565	4320.5
331.413	96.12	1161.73	31.962	136.86	0.2187	72.524	4635.7
283.602	89.70	1169.62	4.994	50.80	0.2040	73.017	724.4
287.663	90.62	1168.94	7.325	58.11	0.2061	72.975	1062.3
291.722	90.84	1168.26	9.651	65.41	0.2067	72.932	1399.7
295.752	91.29	1167.59	11.956	72.67	0.2076	72.890	1734.1
299.776	91.87	1166.93	14.251	79.91	0.2089	72.849	2066.9
303.783	92.42	1166.27	16.528	87.12	0.2102	72.808	2397.2
307.783	92.95	1165.61	18.793	94.32	0.2114	72.767	2725.6
311.771	93.41	1164.96	21.040	101.50	0.2125	72.726	3051.6
315.755	93.97	1164.31	23.275	108.67	0.2137	72.686	3375.7
319.717	94.50	1163.65	25.487	115.80	0.2149	72.644	3696.6
323.666	94.61	1163.01	27.682	122.91	0.2152	72.604	4014.9
327.618	95.42	1162.36	29.870	130.02	0.2170	72.564	4332.2
331.574	96.49	1161.70	32.051	137.15	0.2195	72.523	4648.6
295.577	91.61	1119.26	4.730	72.35	0.2084	69.873	686.1
299.643	92.44	1118.66	6.738	79.67	0.2103	69.836	977.2
303.695	92.87	1118.07	8.738	86.96	0.2112	69.799	1267.4
307.733	92.90	1117.47	10.732	94.23	0.2113	69.761	1556.5
311.754	93.44	1116.89	12.715	101.47	0.2126	69.725	1844.1
315.766	93.84	1116.31	14.690	108.69	0.2134	69.689	2130.6
319.763	94.34	1115.73	16.652	115.89	0.2146	69.653	2415.2

Table 19. Isochoric Heat Capacities (C_v) from 205 to 344 K (-90 to 160°F) for a Mixture of R125/143a with $x(\text{R125}) = 0.49996$ Mole Fraction (0.58812 Mass Fraction) (continued).

Temperature K	Heat Capacity J/(mole·K)	Density kg/m ³	Pressure MPa	Temperature °F	Heat Capacity BTU/(lb·°F)	Density lb/ft ³	Pressure psia
323.757	94.60	1115.15	18.609	123.07	0.2151	69.617	2699.0
327.714	95.46	1114.58	20.541	130.20	0.2171	69.581	2979.2
331.690	96.10	1113.99	22.476	137.35	0.2186	69.544	3259.9
335.682	96.60	1113.41	24.413	144.54	0.2197	69.508	3540.8
339.691	97.48	1112.83	26.350	151.76	0.2217	69.472	3821.8
343.704	97.55	1112.25	28.283	158.98	0.2219	69.436	4102.1
295.602	91.48	1119.26	4.743	72.40	0.2081	69.873	687.9
299.724	92.12	1118.65	6.777	79.82	0.2095	69.835	983.0
303.838	92.73	1118.04	8.809	87.22	0.2109	69.797	1277.7
307.944	92.88	1117.44	10.836	94.61	0.2112	69.760	1571.6
312.015	93.36	1116.85	12.843	101.94	0.2124	69.723	1862.8
316.079	94.16	1116.26	14.843	109.25	0.2142	69.686	2152.8
320.159	94.42	1115.67	16.847	116.60	0.2148	69.649	2443.4
324.227	94.66	1115.08	18.838	123.92	0.2153	69.612	2732.3
328.290	95.21	1114.49	20.822	131.23	0.2166	69.575	3019.9
332.328	95.58	1113.90	22.786	138.50	0.2174	69.539	3304.9
336.350	95.94	1113.32	24.736	145.74	0.2182	69.502	3587.7
340.383	96.34	1112.74	26.684	153.00	0.2191	69.466	3870.2
344.440	97.26	1112.15	28.636	160.30	0.2212	69.429	4153.3
306.100	93.35	1070.20	4.587	91.29	0.2124	66.810	665.3
310.268	93.49	1069.66	6.361	98.79	0.2127	66.777	922.6
314.448	93.99	1069.12	8.144	106.32	0.2138	66.743	1181.2
318.627	94.40	1068.58	9.929	113.84	0.2148	66.709	1440.0
322.797	94.77	1068.05	11.710	121.35	0.2156	66.676	1698.4
326.970	95.24	1067.51	13.493	128.86	0.2167	66.642	1957.0
331.132	95.79	1066.98	15.269	136.35	0.2179	66.609	2214.6
335.297	96.41	1066.44	17.045	143.85	0.2193	66.576	2472.1
339.464	96.88	1065.91	18.818	151.35	0.2204	66.543	2729.3
343.630	96.90	1065.37	20.587	158.85	0.2204	66.509	2985.8
306.153	94.03	1070.19	4.610	91.39	0.2139	66.810	668.6
310.354	93.95	1069.65	6.398	98.95	0.2137	66.776	927.9
314.537	93.94	1069.11	8.182	106.48	0.2137	66.742	1186.7
318.722	94.31	1068.57	9.969	114.01	0.2146	66.709	1445.9
322.899	94.97	1068.03	11.754	121.53	0.2160	66.675	1704.7
327.073	95.51	1067.50	13.536	129.04	0.2172	66.642	1963.3

Table 19. Isochoric Heat Capacities (C_v) from 205 to 344 K (-90 to 160°F) for a Mixture of R125/143a with $x(\text{R125}) = 0.49996$ Mole Fraction (0.58812 Mass Fraction) (continued).

Temperature K	Heat Capacity J/(mole•K)	Density kg/m ³	Pressure MPa	Temperature °F	Heat Capacity BTU/(lb•°F)	Density lb/ft ³	Pressure psia
331.244	95.82	1066.96	15.317	136.55	0.2180	66.608	2221.5
335.415	95.78	1066.43	17.095	144.06	0.2179	66.575	2479.4
339.571	96.52	1065.89	18.863	151.54	0.2195	66.541	2735.9
343.742	97.07	1065.36	20.634	159.05	0.2208	66.508	2992.7
317.080	95.46	1012.12	4.514	111.06	0.2171	63.185	654.7
321.317	95.94	1011.64	6.025	118.68	0.2182	63.155	873.9
325.544	96.00	1011.17	7.539	126.29	0.2184	63.125	1093.4
329.763	96.35	1010.70	9.053	133.89	0.2191	63.096	1313.1
333.968	96.72	1010.23	10.566	141.45	0.2200	63.067	1532.5
338.182	96.64	1009.77	12.084	149.04	0.2198	63.038	1752.6
342.377	97.38	1009.30	13.596	156.59	0.2215	63.009	1972.0
317.078	95.30	1012.12	4.514	111.05	0.2168	63.185	654.6
321.305	95.82	1011.65	6.021	118.66	0.2180	63.155	873.2
325.537	96.21	1011.17	7.536	126.28	0.2188	63.125	1093.0
329.755	96.46	1010.70	9.051	133.87	0.2194	63.096	1312.7
333.983	96.77	1010.23	10.572	141.48	0.2201	63.067	1533.3
338.205	97.13	1009.76	12.092	149.08	0.2209	63.037	1753.8
342.412	97.47	1009.29	13.609	156.65	0.2217	63.008	1973.8

A-36

Table 20. Vapor-Liquid Equilibrium Data for R143a/134a Mixtures from 280 to 340 K (45 to 152°F).

x(R143a) Liquid Mole Fraction	Temperature K	Pressure MPa	y(R143a) Vapor Mole Fraction	x(R143a) Liquid Mass Fraction	Temperature °F	Pressure psia	y(R143a) Vapor Mass Fraction
0.000	280.39	0.379	0.000	0.000	45.01	55.0	0.000
0.165	280.20	0.441		0.140	44.68	64.0	
0.304	280.17	0.491	0.446	0.265	44.63	71.2	0.399
0.515	280.13	0.569	0.643	0.467	44.54	82.6	0.597
0.578	280.11	0.595	0.703	0.530	44.52	86.3	0.661
1.000	280.23	0.767	1.000	1.000	44.73	111.3	1.000
0.000	294.69	0.596	0.000	0.000	70.75	86.5	0.000
0.194	295.09	0.715	0.294	0.165	71.47	103.8	0.255
0.381	295.10	0.808	0.519	0.336	71.49	117.2	0.471
0.601	295.08	0.935	0.707	0.554	71.46	135.6	0.665
1.000	294.11	1.135	1.000	1.000	69.71	164.6	1.000
0.000	309.31	0.913	0.000	0.000	97.07	132.4	0.000
0.198	309.87	1.072	0.285	0.169	98.07	155.5	0.247
0.237	309.94	1.102	0.330	0.204	98.21	159.9	0.289
0.348	310.02	1.183	0.459	0.305	98.35	171.5	0.411
0.372	310.02	1.202	0.474	0.328	98.36	174.3	0.426
0.595	309.90	1.374	0.679	0.548	98.14	199.2	0.635
1.000	309.37	1.677	1.000	1.000	97.18	243.2	1.000
0.000	324.50	1.367	0.000	0.000	124.41	198.3	0.000
0.290	324.93	1.628	0.382	0.308	125.18	236.2	0.337
0.351	324.88	1.694		0.599	125.10	245.7	
0.645	324.98	2.007	0.704	0.588	125.27	291.1	0.662
1.000	326.02	2.467	1.000	1.000	127.15	357.8	1.000
0.000	340.16	1.986	0.000	0.000	152.6	288.1	0.000
0.261	340.00	2.263	0.328	0.225	152.31	328.2	0.287
0.351	339.79	2.405	0.426	0.308	151.94	348.8	0.379
0.480	339.76	2.554	0.538	0.432	151.87	370.5	0.490
0.634	339.07	2.774	0.690	0.588	150.64	402.3	0.647
1.000	340.07	3.318	1.000	1.000	152.44	481.2	1.000

A37

Table 21. Bubble-Point Pressures for R143a/134a Mixtures from 281 to 340 K (46 to 153°F).

x(R143a) Liquid Mole Fraction	Temperature K	Pressure MPa	x(R143a) Liquid Mass Fraction	Temperature °F	Pressure psia
0.3500	280.85	0.522	0.3072	45.84	75.7
0.3500	294.48	0.786	0.3072	70.38	114.0
0.3500	295.10	0.798	0.3072	71.49	115.7
0.3500	310.43	1.203	0.3072	99.09	174.5
0.3500	324.96	1.709	0.3072	125.24	247.8
0.3500	339.62	2.361	0.3072	151.63	342.4
0.6502	280.92	0.648	0.6049	45.97	94.0
0.6502	295.00	0.970	0.6049	71.31	140.6
0.6502	309.88	1.427	0.6049	98.10	207.0
0.6502	325.04	2.042	0.6049	125.38	296.2
0.6502	340.12	2.818	0.6049	152.53	408.7

Table 22. Near-Saturation (p,p,T) Data for R143a/134a Mixtures from 280 to 343 K (45 to 158°F).

x(R143a) Liquid Mole Fraction	Temperature K	Pressure MPa	Density kg/m ³	x(R143a) Liquid Mass Fraction	Temperature °F	Pressure psia	Density lb/ft ³
0.3500	282.63	0.522	1173.5	0.3072	49.05	75.7	73.19
0.3500	294.07	0.786	1131.7	0.3072	69.64	114.0	70.59
0.3500	294.07	0.798	1128.0	0.3072	69.63	115.7	70.36
0.3500	310.56	1.203	1059.1	0.3072	99.32	174.5	66.06
0.3500	324.99	1.709	994.8	0.3072	125.29	247.8	62.05
0.3500	339.67	2.361	915.5	0.3072	151.72	342.4	57.10
0.6502	280.22	0.648	1092.7	0.6049	44.71	94.0	68.15
0.6502	294.99	0.970	1038.1	0.6049	71.29	140.6	64.75
0.6502	310.05	1.427	976.6	0.6049	98.40	207.0	60.91
0.6502	325.23	2.042	902.5	0.6049	125.73	296.2	56.29
0.6502	340.17	2.818	803.3	0.6049	152.62	408.8	50.10
y(R143a)* Vapor Mole Fraction	Temperature K	Pressure MPa	Density kg/m ³	y(R143a)* Vapor Mass Fraction	Temperature °F	Pressure psia	Density lb/ft ³
0.471	311.90	1.203	61.9	0.423	101.73	174.5	3.86
0.463	326.21	1.709	86.1	0.415	127.49	247.8	5.37
0.417	340.88	2.361	129.0	0.371	153.90	342.4	8.04
0.708	312.70	1.427	65.4	0.666	103.17	207.0	4.08
0.718	327.98	2.042	100.1	0.678	130.68	296.2	6.25
0.668	343.23	2.818	152.4	0.624	158.13	408.8	9.51

*Near-saturation vapor compositions are calculated from the vapor-liquid equilibrium data.

Table 23. Vapor-Liquid Equilibrium Data for R32/290 Mixtures from 280 to 341 K (44 to 154°F).
 (LL- Possibly in a Liquid-Liquid Immiscibility Region)

x(R32) Liquid Mole Fraction	Temperature K	Pressure MPa	y(R32) Vapor Mole Fraction	x(R32) Liquid Mass Fraction	Temperature °F	Pressure psia	y(R32) Vapor Mass Fraction
0.000	280.00	0.580	0.000	0.000	44.31	84.1	0.000
0.097	279.97	0.970		0.112	44.25	140.7	
0.204	279.97	1.121		0.232	44.25	162.6	
0.366	280.25	1.260	0.643	0.405	44.78	182.7	0.680
0.348	280.66	1.255	0.655	0.386	45.51	181.9	0.691
LL	280.37	1.299	0.686	LL	44.99	188.4	0.720
LL	280.39	1.293	0.687	LL	45.03	187.5	0.721
LL	280.21	1.289	0.722	LL	44.71	186.9	0.754
LL	280.32	1.284	0.687	LL	44.90	186.2	0.721
LL	280.03	1.270	0.705	LL	44.38	184.2	0.738
LL	280.00	1.269	0.735	LL	44.33	184.0	0.766
0.755	279.96	1.246		0.784	44.24	180.7	
0.843	280.26	1.262	0.739	0.864	44.80	183.1	0.770
0.907	280.33	1.242	0.770	0.920	44.92	180.2	0.798
0.935	280.31	1.226	0.790	0.944	44.89	177.9	0.816
0.978	280.49	1.135	0.890	0.981	45.21	164.6	0.905
0.978	280.42	1.134	0.890	0.981	45.08	164.5	0.905
0.982	279.96	1.096		0.985	44.23	159.0	
1.000	280.00	1.006	1.000	1.000	44.31	145.9	1.000
0.000	294.80	0.873	0.000	0.000	70.95	126.6	0.000
0.084	294.96	1.413	0.300	0.098	71.23	205.0	0.336
0.135	295.93	1.533	0.437	0.156	73.01	222.4	0.478
0.180	294.95	1.670		0.206	71.23	242.2	
0.232	294.95	1.742		0.263	71.23	252.7	
0.337	294.46	1.767	0.622	0.375	70.37	256.2	0.6601
LL	294.70	1.883	0.700	LL	70.78	273.0	0.734
LL	294.80	1.884	0.703	LL	70.96	273.2	0.736
LL	294.52	1.879	0.692	LL	70.47	272.6	0.726
0.857	293.15	1.778	0.778	0.876	68.01	257.8	0.805
0.857	293.01	1.773	0.778	0.876	67.74	257.1	0.805
0.935	295.82	1.681	0.869	0.944	72.81	243.8	0.887
0.962	294.91	1.644		0.968	71.16	238.5	
1.000	295.48	1.575	1.000	1.000	72.18	228.4	1.000
0.000	309.49	1.259	0.000	0.000	97.39	182.6	0.000
0.112	310.81	1.916	0.337	0.130	99.79	277.9	0.375

Table 23. Vapor-Liquid Equilibrium Data for R32/290 Mixtures from 280 to 341 K (44 to 154°F) (continued).
(LL- Possibly in a Liquid-Liquid Immiscibility Region)

x(R32) Liquid Mole Fraction	Temperature K	Pressure MPa	y(R32) Vapor Mole Fraction	x(R32) Liquid Mass Fraction	Temperature °F	Pressure psia	y(R32) Vapor Mass Fraction
0.127	310.16	1.937	0.347	0.146	98.62	281.0	0.385
0.120	309.94	1.982		0.139	98.21	287.4	
0.026	309.94	1.498		0.031	98.21	217.3	
0.306	309.93	2.530		0.342	98.19	366.9	
0.306	310.25	2.448		0.342	98.78	355.1	
0.306	310.24	2.446		0.342	98.76	354.8	
0.395	309.93	2.641		0.435	98.18	383.1	
0.618	310.07	2.710	0.637	0.656	98.46	393.1	0.674
0.667	310.10	2.767	0.694	0.703	98.51	401.4	0.728
0.667	310.08	2.767	0.694	0.703	98.48	401.4	0.728
0.707	310.84	2.781	0.713	0.740	99.84	403.3	0.746
0.707	310.79	2.779	0.713	0.740	99.75	403.1	0.746
0.833	310.32	2.722	0.795	0.855	98.91	394.7	0.821
0.930	309.83	2.513	0.887	0.94	98.03	364.5	0.903
1.000	309.98	2.294	1.000	1.000	98.28	332.7	1.000
0.000	324.69	1.775	0.000	0.000	124.75	257.4	0.000
0.112	325.13	2.549	0.290	0.130	125.56	369.7	0.325
0.136	324.95	2.843		0.157	125.22	412.3	
0.219	324.95	3.204		0.249	125.23	464.7	
0.341	325.07	3.353	0.486	0.379	125.46	486.3	0.527
0.397	324.96	3.626		0.437	125.23	525.9	
0.449	324.95	3.706	0.535	0.490	125.23	537.6	0.576
0.559	324.39	3.724	0.604	0.599	124.23	540.2	0.643
0.808	324.76	3.794	0.761	0.832	124.90	550.3	0.790
0.914	325.22	3.634	0.860	0.926	125.73	527.1	0.879
0.914	325.23	3.638	0.860	0.926	125.74	527.6	0.879
1.000	324.98	3.279	1.000	1.000	125.28	475.6	1.000
0.000	341.17	2.493	0.000	0.000	154.42	361.5	0.000
0.163	340.31	3.660	0.302	0.187	152.89	530.9	0.338
0.202	340.09	3.884		0.230	152.49	563.4	
0.224	340.33	4.004	0.366	0.254	152.92	580.7	0.405
0.255	340.31	4.167	0.397	0.288	152.89	604.4	0.437
0.255	340.30	4.167	0.397	0.288	152.87	604.3	0.437
0.430	340.01	4.811		0.471	152.35	697.8	
0.493	339.97	4.583	0.574	0.534	152.25	664.7	0.614

A-41

Table 23. Vapor-Liquid Equilibrium Data for R32/290 Mixtures from 280 to 341 K (44 to 154°F) (continued).
 (LL- Possibly in a Liquid-Liquid Immiscibility Region)

x(R32) Liquid Mole Fraction	Temperature K	Pressure MPa	y(R32) Vapor Mole Fraction	x(R32) Liquid Mass Fraction	Temperature °F	Pressure psia	y(R32) Vapor Mass Fraction
0.538	340.04	4.738		0.579	152.38	687.2	
0.873	339.62	5.140	0.801	0.890	151.65	745.5	0.826
0.918	339.74	4.953	0.876	0.930	151.86	718.3	0.893
0.971	340.00	4.731	0.958	0.975	152.32	686.1	0.964
1.000	339.96	4.561	1.000	1.000	152.24	661.5	1.000

Table 24. Near-Saturation (p,ρ,T) Data for R32/290 Mixtures from 278 to 341 K (42 to 153°F).

x(R32) Liquid Mole Fraction	Temperature K	Pressure MPa	Density kg/m ³	x(R32) Liquid Mass Fraction	Temperature °F	Pressure psia	Density lb/ft ³
0.843	278.55	1.262	849.5	0.864	41.70	183.1	52.99
0.907	278.53	1.242	886.4	0.920	41.66	180.2	55.29
0.935	278.48	1.226	908.5	0.944	41.57	177.8	56.67
0.978	279.32	1.134	983.6	0.981	43.09	164.5	61.35
0.997	279.65	1.120	999.6	0.997	43.69	162.4	62.35
0.857	291.75	1.773	855.7	0.876	65.46	257.1	53.37
0.135	293.76	1.533	532.8	0.156	69.08	222.4	33.23
0.337	292.99	1.767	590.6	0.375	67.69	256.2	36.84
0.445	294.04	1.846	615.6	0.486	69.58	267.8	38.39
0.935	293.83	1.681	900.7	0.944	69.21	243.8	56.18
0.112	310.51	1.916	488.9	0.130	99.24	277.9	30.49
0.127	310.17	1.937	492.4	0.147	98.62	281.0	30.71
0.306	310.33	2.448	529.5	0.342	98.91	355.1	33.03
0.618	310.33	2.710	596.4	0.656	98.91	393.1	37.20
0.833	310.49	2.722	753.4	0.855	99.19	394.7	46.99
0.667	310.36	2.767	628.1	0.703	98.96	401.4	39.18
0.707	310.54	2.779	658.8	0.740	99.28	403.1	41.09
0.930	307.25	2.513	848.3	0.940	93.37	364.5	52.91
0.112	325.04	2.549	458.7	0.130	125.39	369.7	28.61
0.341	325.04	3.353	489.7	0.379	125.39	486.3	30.54
0.559	324.91	3.724	540.4	0.599	125.16	540.2	33.70
0.808	325.25	3.794	650.6	0.832	125.77	550.3	40.58
0.914	325.40	3.634	734.6	0.926	126.03	527.1	45.82
0.163	340.33	3.660	421.0	0.187	152.91	530.9	26.26
0.163	339.70	3.660	421.0	0.187	151.76	530.9	26.26
0.202	339.77	3.884	421.7	0.230	151.91	563.4	26.30
0.224	340.35	4.004	423.3	0.254	152.94	580.7	26.40
0.255	340.33	4.167	423.2	0.288	152.91	604.4	26.39
0.255	339.72	4.167	423.1	0.288	151.81	604.3	26.39
0.430	339.80	4.811	430.1	0.471	151.95	697.7	26.83
0.517	339.33	5.109	441.2	0.558	151.10	741.0	27.52
0.711	339.36	5.239	474.7	0.744	151.15	759.9	29.61
0.873	339.49	5.140	551.5	0.890	151.39	745.5	34.40
0.918	339.51	4.953	618.8	0.930	151.43	718.3	38.59
0.918	339.78	4.953	618.6	0.930	151.92	718.3	38.58

Table 24. Near-Saturation (p, ρ ,T) Data for R32/290 Mixtures from 278 to 341 K (42 to 153°F) (continued).

y(R32)* Vapor Mole Fraction	Temperature K	Pressure MPa	Density kg/m ³	y(R32)* Vapor Mass Fraction	Temperature °F	Pressure psia	Density lb/ft ³
0.848	296.04	1.681	50.5	0.868	73.19	243.8	3.15
0.600	310.73	2.722	81.3	0.639	99.63	394.7	5.07
0.625	310.73	2.767	82.2	0.663	99.63	401.3	5.13
0.760	311.71	2.779	81.8	0.789	101.40	403.1	5.10
0.881	310.13	2.513	73.0	0.897	98.55	364.5	4.55
0.263	326.03	2.549	64.2	0.296	127.17	369.7	4.00
0.599	325.90	3.724	119.5	0.638	126.93	540.2	7.46
0.755	326.11	3.794	126.1	0.784	127.31	550.3	7.87
0.869	326.24	3.634	118.1	0.887	127.54	527.1	7.37
0.302	340.33	3.660	105.2	0.338	152.91	530.9	6.56
0.362	340.35	4.004	122.7	0.401	152.94	580.7	7.65
0.391	340.33	4.167	128.6	0.431	152.91	604.4	8.02
0.595	340.64	5.109	222.4	0.634	153.47	741.0	13.87
0.850	340.65	5.140	217.8	0.870	153.48	745.5	13.58
0.876	340.65	4.953	198.5	0.893	153.48	718.3	12.38

*Near-saturation vapor compositions are calculated from the vapor-liquid equilibrium data.

Table 25. Vapor-Liquid Equilibrium Data for R125/290 Mixtures from 280 to 364 K (44 to 195°F).

x(R125) Liquid Mole Fraction	Temperature K	Pressure MPa	y(R125) Vapor Mole Fraction	x(R125) Liquid Mass Fraction	Temperature °F	Pressure psia	y(R125) Vapor Mass Fraction
0.000	280.47	0.590	0.000	0.000	45.16	85.6	0.000
0.154	280.07	0.845	0.345	0.331	44.44	122.6	0.589
0.195	279.92	0.881	0.387	0.397	44.18	127.8	0.633
0.204	280.83	0.916	0.413	0.411	45.82	132.9	0.657
0.293	280.82	0.979		0.530	45.80	142.0	
0.293	280.87	0.978		0.530	45.89	141.8	
0.316	279.98	0.943	0.473	0.557	44.27	136.8	0.710
0.407	280.75	0.995		0.651	45.68	144.3	
0.434	280.74	1.001		0.676	45.66	145.1	
0.648	280.05	1.003	0.631	0.834	44.40	145.5	0.823
0.772	279.98	0.979	0.711	0.902	44.28	142.0	0.870
1.000	280.29	0.830	1.000	1.000	44.83	120.4	1.000
0.000	294.80	0.873	0.000	0.000	70.95	126.6	0.000
0.175	294.96	1.286	0.340	0.366	71.24	186.5	0.584
0.219	294.74	1.306	0.389	0.433	70.87	189.4	0.634
0.219	294.64	1.299	0.389	0.433	70.67	188.4	0.634
0.347	293.92	1.345	0.478	0.591	69.38	195.1	0.714
0.347	293.21	1.333	0.478	0.591	68.12	193.3	0.714
0.470	293.82	1.398	0.520	0.707	69.20	202.8	0.747
0.568	293.23	1.410	0.599	0.782	68.14	204.5	0.803
0.644	294.95	1.492	0.638	0.802	71.22	216.4	0.828
0.725	294.95	1.487	0.694	0.878	71.22	215.7	0.861
0.767	294.96	1.468	0.723	0.900	71.23	212.9	0.877
1.000	295.23	1.272	1.000	1.000	71.73	184.5	1.000
0.000	309.49	1.259	0.000	0.000	97.39	182.6	0.000
0.186	309.79	1.797	0.317	0.383	97.93	260.6	0.558
0.263	310.74	1.898	0.397	0.493	99.66	275.2	0.642
0.263	310.74	1.897	0.397	0.493	99.66	275.1	0.642
0.294	310.83	1.990	0.438	0.531	99.83	288.7	0.680
0.376	311.62	2.106	0.470	0.621	101.25	305.4	0.707
0.376	311.82	2.105	0.470	0.621	101.61	305.3	0.707
0.472	309.76	2.101	0.548	0.709	97.90	304.8	0.767
0.529	309.83	2.095	0.575	0.754	98.03	303.9	0.786
0.604	310.22	2.140	0.620	0.806	98.73	310.4	0.816
0.641	309.99	2.148	0.643	0.829	98.29	311.5	0.831
0.722	309.94	2.129	0.697	0.876	98.20	308.8	0.863

Table 25. Vapor-Liquid Equilibrium Data for R125/290 Mixtures from 280 to 364 K (44 to 195°F) (continued).

x(R125) Liquid Mole Fraction	Temperature K	Pressure MPa	y(R125) Vapor Mole Fraction	x(R125) Liquid Mass Fraction	Temperature °F	Pressure psia	y(R125) Vapor Mass Fraction
1.000	310.61	1.888	1.000	1.000	99.41	273.8	1.000
0.000	324.69	1.775	0.000	0.000	124.75	257.4	0.000
0.178	324.94	2.430	0.295	0.371	125.21	352.4	0.533
0.255	324.94	2.538	0.372	0.482	125.20	368.1	0.617
0.263	324.85	2.531	0.397	0.493	125.05	367.0	0.642
0.315	324.95	2.631	0.423	0.556	125.23	381.6	0.666
0.483	325.61	2.969	0.547	0.718	126.42	430.6	0.767
0.574	325.61	3.030	0.597	0.786	126.42	439.4	0.801
0.615	324.99	2.978	0.603	0.813	125.30	431.9	0.805
0.633	324.94	2.955	0.642	0.824	125.2-	428.6	0.830
0.730	324.60	2.944	0.714	0.880	124.60	427.0	0.872
0.734	324.94	2.942	0.707	0.883	125.21	426.7	0.868
1.000	324.89	2.636	1.000	1.000	125.11	382.4	1.000
0.000	341.17	2.494	0.000	0.000	154.44	361.7	0.000
0.146	340.64	3.148	0.225	0.318	153.49	456.5	0.441
0.243	340.57	3.470	0.320	0.466	153.36	503.2	0.562
0.327	340.54	3.737	0.391	0.569	153.31	542.0	0.636
1.000	339.38	3.629	1.000	1.000	151.22	526.3	1.000
0.000	347.99	2.848	0.000	0.000	166.71	413.0	0.000
0.166	348.56	3.700	0.220	0.351	167.74	536.7	0.434
0.166	348.54	3.699	0.220	0.351	167.70	536.5	0.434
0.133	348.42	3.615	0.198	0.295	167.49	524.3	0.402
0.000	355.73	3.297	0.000	0.000	180.64	478.1	0.000
0.165	356.43	4.175	0.188	0.350	181.90	605.6	0.387
0.165	356.43	4.178	0.188	0.350	181.90	606.0	0.387
0.000	363.52	3.792	0.000	0.000	194.66	550.0	0.000
0.003	363.78	3.899	0.014	0.008	195.13	565.5	0.037

Table 26. Near-Saturation (p,p,T) Data for R125/290 Mixtures from 280 to 326 K (44 to 128°F).

x(R125) Liquid Mole Fraction	Temperature K	Pressure MPa	Density kg/m ³	x(R125) Liquid Mass Fraction	Temperature °F	Pressure psia	Density lb/ft ³
0.204	279.68	0.916	675.3	0.411	43.73	132.9	42.12
0.219	293.24	1.299	642.2	0.433	68.15	188.4	40.05
0.347	292.16	1.333	727.9	0.591	66.20	193.3	45.40
0.263	309.89	1.897	614.1	0.493	98.12	275.1	38.30
0.294	310.05	1.990	643.7	0.531	98.40	288.7	40.15
0.376	310.88	2.106	675.9	0.621	99.89	305.4	42.16
0.472	309.17	2.101	733.7	0.709	96.81	304.8	45.76
0.529	309.30	2.095	759.8	0.754	97.05	303.9	47.39
0.604	309.94	2.140	805.4	0.806	98.21	310.4	50.23
0.263	323.90	2.531	562.8	0.493	123.33	367.0	35.10
0.315	323.90	2.631	584.9	0.556	123.33	381.6	36.48
0.574	325.10	3.030	681.8	0.786	125.48	439.4	42.53
0.615	324.06	2.978	703.2	0.813	123.61	431.9	43.86
0.730	323.98	2.944	774.1	0.880	123.47	427.0	48.28

y(R125)* Vapor Mole Fraction	Temperature K	Pressure MPa	Density kg/m ³	y(R125)* Vapor Mass Fraction	Temperature °F	Pressure psia	Density lb/ft ³
0.467	293.70	1.333	58.9	0.705	68.96	193.3	3.67
0.542	294.55	1.398	64.5	0.763	70.50	202.7	4.03
0.593	293.98	1.410	67.9	0.799	69.48	204.5	4.23
0.691	294.24	1.435	74.1	0.859	69.94	208.1	4.62
0.459	312.70	2.106	100.2	0.698	103.17	305.4	6.25
0.525	310.45	2.101	108.0	0.751	99.11	304.8	6.74
0.562	310.63	2.095	111.2	0.777	99.44	303.9	6.94
0.620	311.25	2.140	117.8	0.816	100.56	310.4	7.35
0.385	325.67	2.531	108.8	0.630	126.51	367.0	6.79
0.432	325.74	2.631	121.4	0.675	126.65	381.6	7.57
0.551	326.21	2.969	179.0	0.770	127.50	430.6	11.16
0.605	326.11	3.030	199.6	0.806	127.31	439.4	12.45
0.730	325.69	2.944	103.3	0.880	126.56	427.0	6.44

*Near-saturation vapor compositions are calculated from the vapor-liquid equilibrium data.

**Table 27. Vapor-Liquid Equilibrium Data for R134a/290 Mixtures from 279 to 357 K (43 to 182°F).
(LL- Possibly in a Liquid-Liquid Immiscibility Region)**

x(R134a) Liquid Mole Fraction	Temperature K	Pressure MPa	y(R134a) Vapor Mole Fraction	x(R134a) Liquid Mass Fraction	Temperature °F	Pressure psia	y(R134a) Vapor Mass Fraction
0.000	280.00	0.580	0.000	0.000	44.31	84.1	0.000
0.079	279.95	0.660	0.163	0.166	44.23	95.7	0.310
LL	279.54	0.716	0.342	LL	43.50	103.8	0.546
LL	279.88	0.717	0.358	LL	44.11	104.0	0.563
LL	279.85	0.717	0.358	LL	44.06	104.0	0.563
0.558	279.97	0.701	0.407	0.745	44.26	101.7	0.614
0.662	279.98	0.677	0.441	0.819	44.27	98.2	0.646
0.692	279.42	0.675	0.437	0.839	43.28	97.9	0.642
0.774	279.29	0.646	0.487	0.888	43.05	93.8	0.687
0.786	279.35	0.648	0.474	0.895	43.16	93.9	0.676
0.913	279.80	0.535	0.656	0.960	43.97	77.6	0.815
0.972	279.73	0.438	0.843	0.988	43.84	63.5	0.926
0.972	279.60	0.437	0.843	0.988	43.61	63.4	0.926
1.000	280.39	0.379	1.000	1.000	45.01	55.0	1.000
0.000	294.99	0.878	0.000	0.000	71.29	127.3	0.000
0.109	294.92	1.018	0.194	0.221	71.17	147.6	0.357
0.262	295.33	1.067	0.308	0.451	71.93	154.7	0.507
LL	295.33	1.063	0.354	LL	71.93	154.2	0.559
0.558	294.95	1.066	0.433	0.745	71.23	154.6	0.639
0.578	294.95	1.054	0.443	0.760	71.22	152.9	0.648
0.602	294.85	1.032	0.494	0.778	71.05	149.6	0.693
0.727	295.17	0.986	0.541	0.860	71.63	143.0	0.732
0.802	294.95	0.977	0.542	0.904	71.22	141.7	0.733
0.831	294.95	0.938		0.919	71.22	136.0	
1.000	294.70	0.596	1.000	1.000	70.77	86.5	1.000
0.000	309.99	1.274	0.000	0.000	98.29	184.8	0.000
0.112	309.96	1.468	0.209	0.227	98.25	212.9	0.380
0.197	309.96	1.532	0.259	0.362	98.24	222.2	0.448
0.200	310.70	1.534	0.267	0.367	99.59	222.5	0.457
0.273	309.96	1.568	0.312	0.465	98.24	227.4	0.512
0.337	310.58	1.575	0.351	0.540	99.38	228.4	0.556
0.354	309.96	1.579	0.357	0.559	98.23	229.0	0.562
0.450	310.63	1.563	0.423	0.654	99.47	226.6	0.629
0.570	310.85	1.536	0.434	0.754	99.86	222.7	0.640
0.748	310.84	1.453	0.578	0.873	99.84	210.7	0.760

A48

Table 27. Vapor-Liquid Equilibrium Data for R134a/290 Mixtures from 279 to 357 K (43 to 182°F)
 (continued). (LL- Possibly in a Liquid-Liquid Immiscibility Region)

x(R134a) Liquid Mole Fraction	Temperature K	Pressure MPa	y(R134a) Vapor Mole Fraction	x(R134a) Liquid Mass Fraction	Temperature °F	Pressure psia	y(R134a) Vapor Mass Fraction
0.671	310.76	1.498	0.518	0.825	99.70	217.2	0.713
1.000	309.31	0.910	1.000	1.000	97.07	132.0	1.000
0.000	324.99	1.786	0.000	0.000	125.29	259.1	0.000
0.134	326.09	2.076	0.190	0.264	127.28	301.2	0.352
0.354	325.01	2.204	0.361	0.559	125.33	319.7	0.567
0.364	325.14	2.229	0.380	0.570	125.57	323.2	0.586
0.446	325.01	2.188	0.414	0.651	125.33	317.3	0.621
0.504	325.51	2.201	0.444	0.702	126.24	319.3	0.649
0.552	325.02	2.150	0.477	0.741	125.35	311.8	0.679
0.603	325.93	2.138	0.480	0.779	127.00	310.0	0.681
0.688	325.01	2.071	0.566	0.836	125.33	300.4	0.751
0.720	326.04	2.069	0.589	0.856	127.19	300.1	0.768
1.000	324.50	1.364	1.000	1.000	124.41	197.9	1.000
0.000	339.98	2.435	0.000	0.000	152.28	353.2	0.000
0.068	339.95	2.659	0.135	0.144	152.23	385.7	0.265
0.213	340.89	2.955	0.258	0.385	153.94	428.6	0.446
0.290	341.17	3.000	0.311	0.486	154.44	435.1	0.511
0.375	340.46	3.002	0.377	0.581	153.16	435.4	0.583
0.457	340.37	3.021	0.437	0.661	153.00	438.1	0.642
0.546	339.99	2.992	0.487	0.736	152.29	434.0	0.687
0.589	339.94	2.961	0.518	0.769	152.21	429.5	0.713
0.610	340.71	2.872	0.555	0.784	153.61	416.5	0.743
0.706	340.51	2.786	0.611	0.847	153.25	404.1	0.784
1.000	340.16	1.984	1.000	1.000	152.60	287.7	1.000
0.000	354.98	3.251	0.000	0.000	179.28	471.5	0.000
0.026	356.23	3.421	0.025	0.058	181.54	496.1	0.056
0.175	356.21	3.948	0.209	0.329	181.50	572.6	0.379
0.685	354.96	3.775	0.638	0.835	179.23	547.5	0.803
0.717	356.48	3.814	0.660	0.854	181.99	553.2	0.818
0.778	356.52	3.693	0.720	0.890	182.06	535.6	0.856
0.827	356.46	3.608	0.755	0.917	181.95	523.3	0.877
0.841	354.93	3.415	0.763	0.925	179.19	495.3	0.882
0.842	356.47	3.609	0.754	0.925	181.97	523.4	0.876
0.897	356.45	3.351	0.837	0.953	181.94	486.0	0.922
0.937	354.97	3.064	0.839	0.972	179.25	444.4	0.924

A-49

Table 27. Vapor-Liquid Equilibrium Data for R134a/290 Mixtures from 279 to 357 K (43 to 182°F)
 (continued). (LL- Possibly in a Liquid-Liquid Immiscibility Region)

x(R134a) Liquid Mole Fraction	Temperature K	Pressure MPa	y(R134a) Vapor Mole Fraction	x(R134a) Liquid Mass Fraction	Temperature °F	Pressure psia	y(R134a) Vapor Mass Fraction
0.897	356.46	3.361	0.837	0.953	181.95	487.5	0.922
0.980	355.04	2.845	0.963	0.991	179.38	412.6	0.984
1.000	355.02	2.745	1.000	1.000	179.35	398.1	1.000

Table 28. Near-Saturation (p,p,T) Data for R134a/290 Mixtures from 278 to 357 K (40 to 183°F).

x(R134a) Liquid Mole Fraction	Temperature K	Pressure MPa	Density kg/m ³	x(R134a) Liquid Mass Fraction	Temperature °F	Pressure psia	Density lb/ft ³
0.692	277.86	0.675	937.7	0.839	40.46	97.9	58.49
0.774	277.94	0.646	1022.1	0.888	40.60	93.8	63.75
0.786	278.04	0.647	1019.5	0.895	40.78	93.9	63.59
0.913	278.22	0.535	1176.1	0.960	41.10	77.6	73.35
0.972	278.45	0.438	1240.9	0.988	41.52	63.5	77.40
0.262	293.81	1.067	654.4	0.451	69.17	154.7	40.82
0.602	293.76	1.032	871.6	0.778	69.08	149.6	54.37
0.727	293.91	0.986	982.4	0.860	69.35	143.0	61.28
0.872	291.85	0.788	1138.5	0.940	65.65	114.3	71.01
0.200	309.53	1.534	579.5	0.367	97.47	222.5	36.14
0.337	309.50	1.575	650.6	0.540	97.42	228.4	40.58
0.450	309.48	1.562	710.3	0.654	97.37	226.6	44.30
0.570	309.53	1.535	793.0	0.754	97.47	222.7	49.46
0.671	309.50	1.497	860.6	0.825	97.42	217.2	53.68
0.748	309.50	1.453	920.5	0.873	97.42	210.7	57.41
0.134	324.13	2.076	511.1	0.264	123.75	301.2	31.88
0.364	324.13	2.229	621.2	0.570	123.75	323.2	38.75
0.504	324.24	2.201	698.8	0.702	123.94	319.3	43.59
0.603	324.24	2.138	759.7	0.779	123.94	310.0	47.38
0.720	324.19	2.069	837.0	0.856	123.85	300.1	52.20
0.213	338.47	2.955	497.6	0.385	149.55	428.6	31.04
0.290	338.75	3.000	525.2	0.486	150.06	435.1	32.76
0.375	338.65	3.002	562.2	0.581	149.88	435.4	35.07
0.457	338.65	3.021	600.6	0.661	149.88	438.1	37.46
0.610	338.65	2.872	697.7	0.784	149.88	416.5	43.52
0.706	338.65	2.786	760.9	0.847	149.88	404.1	47.46
0.026	355.81	3.421	368.5	0.058	180.77	496.1	22.99
0.175	355.73	3.948	392.4	0.329	180.63	572.6	24.47
0.717	355.86	3.814	517.4	0.854	180.86	553.2	32.27
0.778	355.89	3.693	592.2	0.890	180.91	535.6	36.94
0.827	355.86	3.608	718.0	0.917	180.86	523.3	44.78
0.842	355.89	3.609	718.1	0.925	180.91	523.4	44.79
0.897	355.91	3.361	789.6	0.953	180.96	487.5	49.25

A-51

Table 28. Near-Saturation (p, ρ ,T) Data for R134a/290 Mixtures from 278 to 357 K (40 to 183°F) (continued).

y(R134a)* Vapor Mole Fraction	Temperature K	Pressure MPa	Density kg/m ³	y(R134a)* Vapor Mass Fraction	Temperature °F	Pressure psia	Density lb/ft ³
0.345	311.07	1.575	53.9	0.549	100.23	228.4	3.36
0.369	310.89	1.562	56.0	0.575	99.91	226.6	3.50
0.397	310.89	1.535	58.0	0.603	99.91	222.7	3.62
0.444	311.07	1.497	58.6	0.649	100.23	217.2	3.66
0.508	311.04	1.453	58.8	0.705	100.19	210.7	3.67
0.184	326.55	2.076	62.8	0.343	128.10	301.2	3.91
0.368	326.49	2.229	82.2	0.574	128.00	323.2	5.13
0.446	326.58	2.201	86.4	0.651	128.15	319.3	5.39
0.505	326.60	2.138	86.3	0.703	128.20	310.0	5.38
0.596	326.60	2.069	87.6	0.773	128.20	300.1	5.46
0.285	341.64	2.955	107.4	0.480	155.26	428.6	6.70
0.350	342.14	3.000	115.6	0.555	156.16	435.1	7.21
0.408	341.43	3.002	123.5	0.605	154.88	435.4	7.70
0.457	341.45	2.872	130.1	0.661	154.93	416.5	8.11
0.547	341.35	2.786	130.5	0.736	154.74	404.1	8.14
0.051	357.03	3.421	101.2	0.110	182.97	496.1	6.31
0.247	357.16	3.948	180.0	0.432	183.21	572.6	11.22
0.625	357.01	3.814	238.9	0.794	182.92	553.2	14.90
0.680	357.03	3.608	228.0	0.831	182.97	523.3	14.22

*Near-saturation vapor compositions are calculated from the vapor-liquid equilibrium data.

Table 29. Vapor Pressures for HFC-41 from 219 to 312 K (-66 to 102°F) Using the Vapor-Liquid Equilibrium Apparatus.

Temperature K	Vapor Pressure MPa	Temperature °F	Vapor Pressure psia
218.69	0.330	-66.05	47.8
231.96	0.554	-42.16	80.4
241.92	0.790	-24.22	114.6
251.86	1.096	-6.35	159.0
251.90	1.097	-6.28	159.1
251.96	1.099	-6.17	159.4
263.62	1.566	14.83	227.1
268.80	1.817	24.14	263.5
270.66	1.916	27.49	277.9
279.93	2.456	44.18	356.2
279.92	2.454	44.17	355.9
284.42	2.751	52.27	399.0
289.88	3.150	62.10	456.9
292.78	3.387	67.32	491.2
292.83	3.391	67.41	491.8
294.85	3.558	71.04	516.1
294.85	3.558	71.04	516.1
294.93	3.561	71.18	516.5
297.02	3.742	74.95	542.8
299.99	4.010	80.29	581.6
304.86	4.480	89.05	649.8
309.93	5.016	98.18	727.4
311.92	5.241	101.77	760.1

A-53

**Table 30. Vapor Pressures for HFC-41 Using 132 to 317 K (-222 to 111°F)
Using the Isochoric (p, ρ ,T) Apparatus.**

Temperature K	Vapor Pressure MPa	Temperature °F	Vapor Pressure psia
132.00	0.0005785	-222.09	0.0839
136.00	0.0008884	-214.89	0.1289
140.00	0.0013645	-207.69	0.1979
145.00	0.002299	-198.69	0.3334
150.00	0.0037764	-189.69	0.5477
155.00	0.006083	-180.69	0.8823
160.00	0.0093391	-171.69	1.3545
165.00	0.014073	-162.69	2.0411
170.00	0.020646	-153.69	2.9945
175.00	0.029642	-144.69	4.2992
180.00	0.041581	-135.69	6.0308
185.00	0.057194	-126.69	8.2953
190.00	0.077194	-117.69	11.1961
195.00	0.10231	-108.69	14.8389
200.00	0.13348	-99.69	19.3597
205.00	0.17194	-90.69	24.9379
210.00	0.21855	-81.69	31.6981
215.00	0.27436	-72.69	39.7927
220.00	0.34027	-63.69	49.3522
225.00	0.41862	-54.69	60.7159
230.00	0.50925	-45.69	73.8607
235.00	0.61479	-36.69	89.1681
240.00	0.73545	-27.69	106.6684
245.00	0.87379	-18.69	126.7330
250.00	1.03005	-9.69	149.3966
255.00	1.2074	-0.69	175.1192
260.00	1.40572	8.31	203.8832
265.00	1.62797	17.31	236.1179
270.00	1.87591	26.31	272.0787
275.00	2.15015	35.31	311.8540
280.00	2.45422	44.31	355.9558
285.00	2.7885	53.31	404.4391
290.00	3.15708	62.31	457.8973
295.00	3.56141	71.31	516.5406
300.00	4.00546	80.31	580.9449

Table 30. Vapor Pressures for HFC-41 Using 132 to 317 K (-222 to 111°F)
Using the Isochoric (p,ρ,T) Apparatus (continued).

Temperature K	Vapor Pressure MPa	Temperature °F	Vapor Pressure psia
305.00	4.49047	89.31	651.2899
310.00	5.02212	98.31	728.3995
315.00	5.60592	107.31	813.0728
317.00	5.86166	110.91	850.1649

Table 31. Vapor Pressures for HFC-41 Calculated from the Vapor Pressure Correlation.

Temperature °K	Vapor Pressure MPa	Temperature K	Vapor Pressure MPa
131.35	0.00043	230.00	0.50910
140.00	0.00126	240.00	0.73523
150.00	0.00367	250.00	1.03002
160.00	0.00923	260.00	1.40572
170.00	0.02056	270.00	1.87558
180.00	0.04143	280.00	2.45416
190.00	0.07691	290.00	3.15794
200.00	0.13332	300.00	4.00640
210.00	0.21823	310.00	5.02477
220.00	0.34027	317.28	5.89700

Temperature °F	Vapor Pressure psia	Temperature °F	Vapor Pressure psia
-223.24	0.062	-40.00	83.197
-200.00	0.294	-20.00	123.537
-180.00	0.889	0.00	177.089
-160.00	2.278	20.00	246.381
-140.00	5.118	40.00	334.197
-120.00	10.338	60.00	443.691
-100.00	19.153	80.00	578.614
-80.00	33.046	100.00	743.912
-60.00	53.746	111.43	855.288

A-56

Table 32. Near-Saturation (p,ρ,T) Data for HFC-41 from 274 to 296 K (34 to 73°F)

Temperature K	Pressure MPa	Density kg/m ³	Temperature °F	Pressure psia	Density lb/ft ³
274.38	2.195	675.6	34.20	318.4	42.14
278.42	2.460	662.2	41.47	356.8	41.30
280.06	2.564	656.2	44.42	371.9	40.93
281.65	2.681	650.1	47.28	388.9	40.55
282.94	2.775	645.4	49.60	402.5	40.25
284.66	2.906	638.8	52.70	421.5	39.84
286.58	3.053	631.4	56.16	442.7	39.38
288.28	3.186	624.5	59.22	462.1	38.95
290.44	3.349	615.3	63.10	485.8	38.37
292.21	3.497	606.9	66.29	507.1	37.85
293.86	3.644	599.5	69.26	528.5	37.39
294.89	3.728	595.1	71.11	540.7	37.12
278.32	2.339	50.0	41.29	339.3	3.12
280.14	2.460	53.3	44.56	356.8	3.33
281.76	2.564	56.7	47.48	371.9	3.53
283.40	2.681	60.7	50.43	388.9	3.79
284.71	2.775	63.2	52.79	402.5	3.94
286.46	2.906	66.8	55.94	421.5	4.17
288.36	3.053	71.0	59.36	442.7	4.43
290.12	3.186	76.7	62.53	462.1	4.78
292.07	3.349	81.5	66.04	485.8	5.09
294.11	3.497	88.5	69.71	507.1	5.52
295.35	3.644	97.4	71.94	528.5	6.07
295.89	3.728	106.4	72.91	540.7	6.64

A-57

Table 33. Comparisons of Critical Point Parameters for HFC-41.

	Critical Temperature	Critical Pressure	Critical Density
This Work	$317.28 \pm 0.08\text{K}$ ($111.43 \pm 0.014^\circ\text{F}$)	$5.897 \pm 0.01 \text{ MPa}$ ($855.3 \pm 1.4 \text{ psia}$)	$316.5 \pm 1.5 \text{ kg/m}^3$ ($19.74 \pm 0.9 \text{ lb/ft}^3$)
Bominaar et al. (1987)	317.38 K (111.61°F)	5.87 MPa (851 psia)	311.4 kg/m^3 (19.40 lb/ft^3)
Biswas et al. (1989)	317.40 K (111.65°F)	5.875 MPa (852.1 psia)	312.3 kg/m^3 (19.48 lb/ft^3)

Table 34. Isochoric (p,p,T) Data for HFC-41 from 132 to 400 K (-222 to 260°F).

Temperature K	Pressure MPa	Density kg/m ³	Temperature °F	Pressure psia	Density lb/ft ³
132.000	3.7947	1007.73	-222.09	550.4	62.911
132.999	5.9677	1007.38	-220.29	865.5	62.889
134.000	7.6985	1006.73	-218.49	1116.6	62.848
135.000	9.2786	1005.85	-216.69	1345.8	62.793
136.000	11.4361	1005.48	-214.89	1658.7	62.770
136.999	13.7673	1005.23	-213.09	1996.8	62.754
138.000	16.1748	1005.03	-211.29	2346.0	62.742
138.999	18.6070	1004.85	-209.49	2698.7	62.731
139.999	21.0494	1004.69	-207.69	3053.0	62.721
140.999	23.5062	1004.54	-205.89	3409.3	62.711
142.000	25.9595	1004.39	-204.09	3765.1	62.702
143.000	28.4095	1004.25	-202.29	4120.5	62.693
143.999	30.8687	1004.11	-200.49	4477.1	62.685
144.999	33.3136	1003.98	-198.69	4831.8	62.676
142.000	3.8165	989.01	-204.09	553.5	61.742
142.999	5.8434	988.68	-202.29	847.5	61.721
144.000	7.5402	988.11	-200.49	1093.6	61.686
144.999	8.9768	987.22	-198.69	1302.0	61.630
145.999	10.9159	986.82	-196.89	1583.2	61.605
146.999	13.0556	986.57	-195.09	1893.6	61.590
148.001	15.2637	986.37	-193.29	2213.8	61.577
149.000	17.5065	986.20	-191.49	2539.1	61.566
150.000	19.7567	986.04	-189.69	2865.5	61.556
151.000	22.0135	985.89	-187.89	3192.8	61.547
152.000	24.2862	985.74	-186.09	3522.4	61.538
153.000	26.5428	985.61	-184.29	3849.7	61.530
154.000	28.8015	985.48	-182.49	4177.3	61.522
155.000	31.0703	985.35	-180.69	4506.4	61.513
156.001	33.3213	985.22	-178.89	4832.9	61.505
154.000	3.8535	966.31	-182.49	558.9	60.325
155.000	5.7194	966.01	-180.69	829.5	60.306
155.999	7.3427	965.52	-178.89	1065.0	60.275
157.001	8.6648	964.63	-177.09	1256.7	60.220
157.999	10.3772	964.20	-175.29	1505.1	60.193
158.999	12.2980	963.94	-173.49	1783.7	60.177

A-59

Table 34. Isochoric (p, ρ ,T) Data for HFC-41 from 132 to 400 K (-222 to 260°F) (continued).

Temperature K	Pressure MPa	Density kg/m ³	Temperature °F	Pressure psia	Density lb/ft ³
159.999	14.3003	963.74	-171.69	2074.1	60.164
160.999	16.3194	963.57	-169.89	2366.9	60.154
161.999	18.3586	963.41	-168.09	2662.7	60.144
163.000	20.4124	963.27	-166.29	2960.6	60.135
163.999	22.4542	963.13	-164.49	3256.7	60.126
165.000	24.5189	963.00	-162.69	3556.2	60.118
165.999	26.5634	962.87	-160.89	3852.7	60.110
166.998	28.6067	962.75	-159.09	4149.1	60.103
168.000	30.6602	962.63	-157.29	4446.9	60.095
168.999	32.6986	962.51	-155.49	4742.5	60.088
170.000	34.7485	962.40	-153.69	5039.9	60.081
167.998	3.8483	939.30	-157.29	558.2	58.639
168.999	5.5291	939.03	-155.49	801.9	58.622
169.999	7.0744	938.63	-153.69	1026.1	58.597
170.998	8.3010	937.80	-151.89	1204.0	58.545
172.000	9.7689	937.29	-150.09	1416.9	58.513
173.000	11.4618	937.02	-148.29	1662.4	58.496
173.999	13.2224	936.82	-146.49	1917.8	58.484
174.999	15.0243	936.65	-144.69	2179.1	58.473
175.999	16.8417	936.49	-142.89	2442.7	58.463
176.999	18.6613	936.35	-141.09	2706.6	58.454
177.999	20.4950	936.22	-139.29	2972.6	58.446
179.000	22.3201	936.09	-137.49	3237.3	58.438
179.999	24.1515	935.97	-135.69	3502.9	58.431
180.998	25.9775	935.85	-133.89	3767.7	58.423
181.999	27.8011	935.74	-132.09	4032.2	58.416
182.999	29.6298	935.63	-130.29	4297.5	58.409
184.000	31.4503	935.52	-128.49	4561.5	58.403
184.999	33.2697	935.41	-126.69	4825.4	58.396
185.999	35.0874	935.30	-124.89	5089.0	58.389
184.000	3.8192	907.68	-128.49	553.9	56.665
185.000	5.3156	907.44	-126.69	771.0	56.650
186.000	6.7440	907.11	-124.89	978.1	56.629
187.000	7.9183	906.46	-123.09	1148.5	56.588
188.001	9.1419	905.80	-121.29	1325.9	56.547

Table 34. Isochoric (p,p,T) Data for HFC-41 from 132 to 400 K (-222 to 260°F) (continued).

Temperature K	Pressure MPa	Density kg/m ³	Temperature °F	Pressure psia	Density lb/ft ³
189.001	10.5886	905.50	-119.49	1535.8	56.529
190.001	12.1260	905.29	-117.69	1758.7	56.515
191.001	13.6949	905.12	-115.89	1986.3	56.505
192.000	15.2734	904.97	-114.09	2215.2	56.495
193.000	16.8728	904.83	-112.29	2447.2	56.487
194.000	18.4663	904.70	-110.49	2678.3	56.479
195.001	20.0674	904.58	-108.69	2910.5	56.471
196.000	21.6675	904.47	-106.89	3142.6	56.464
197.000	23.2669	904.35	-105.09	3374.6	56.457
198.000	24.8753	904.24	-103.29	3607.9	56.450
198.999	26.4733	904.14	-101.49	3839.6	56.444
200.001	28.0748	904.03	-99.69	4071.9	56.437
201.000	29.6684	903.93	-97.89	4303.0	56.431
202.001	31.2603	903.83	-96.09	4533.9	56.424
203.000	32.8550	903.73	-94.29	4765.2	56.418
204.000	34.4410	903.63	-92.49	4995.3	56.412
200.000	3.7884	874.87	-99.69	549.5	54.616
201.000	5.1415	874.66	-97.89	745.7	54.603
202.000	6.4328	874.38	-96.09	933.0	54.586
203.001	7.5796	873.91	-94.29	1099.3	54.556
204.000	8.6144	873.17	-92.49	1249.4	54.510
205.000	9.8458	872.81	-90.69	1428.0	54.488
206.000	11.1682	872.58	-88.89	1619.8	54.473
207.001	12.5291	872.41	-87.09	1817.2	54.463
207.999	13.9092	872.26	-85.29	2017.4	54.453
209.001	15.2923	872.13	-83.49	2218.0	54.445
210.000	16.6913	872.00	-81.69	2420.9	54.437
211.999	19.4853	871.77	-78.09	2826.1	54.423
214.000	22.2776	871.56	-74.49	3231.1	54.410
216.001	25.0812	871.36	-70.89	3637.7	54.397
218.001	27.8685	871.17	-67.29	4042.0	54.385
220.002	30.6434	870.98	-63.68	4444.5	54.374
222.001	33.4180	870.80	-60.09	4846.9	54.362
220.002	3.6347	831.14	-63.68	527.2	51.886
221.000	4.7578	830.97	-61.89	690.1	51.876

Table 34. Isochoric (p,ρ,T) Data for HFC-41 from 132 to 400 K (-222 to 260°F) (continued).

Temperature K	Pressure MPa	Density kg/m ³	Temperature °F	Pressure psia	Density lb/ft ³
222.001	5.8830	830.75	-60.09	853.3	51.862
222.999	6.9410	830.46	-58.29	1006.7	51.844
224.000	7.8843	829.90	-56.49	1143.5	51.809
224.999	8.8290	829.31	-54.69	1280.5	51.772
226.001	9.9027	829.02	-52.89	1436.3	51.754
227.001	11.0226	828.82	-51.09	1598.7	51.742
228.002	12.1643	828.67	-49.28	1764.3	51.732
229.001	13.3203	828.53	-47.49	1931.9	51.723
230.000	14.4766	828.41	-45.69	2099.7	51.716
232.000	16.8051	828.18	-42.09	2437.4	51.702
234.000	19.1419	827.98	-38.49	2776.3	51.689
236.001	21.4772	827.79	-34.89	3115.0	51.677
238.001	23.8124	827.61	-31.29	3453.7	51.666
239.999	26.1386	827.43	-27.69	3791.1	51.655
242.002	28.4583	827.26	-24.08	4127.5	51.644
244.002	30.7777	827.09	-20.48	4463.9	51.634
246.001	33.0881	826.92	-16.89	4799.0	51.623
248.002	35.4018	826.76	-13.28	5134.6	51.613
240.000	3.8003	783.97	-27.69	551.2	48.942
241.001	4.7476	783.82	-25.89	688.6	48.932
241.999	5.6800	783.64	-24.09	823.8	48.921
243.000	6.5951	783.41	-22.29	956.5	48.907
244.000	7.4483	783.06	-20.49	1080.3	48.885
245.000	8.2413	782.44	-18.69	1195.3	48.846
246.000	9.0950	782.04	-16.89	1319.1	48.821
247.000	10.0074	781.82	-15.09	1451.5	48.807
247.999	10.9381	781.65	-13.29	1586.4	48.797
249.000	11.8837	781.51	-11.49	1723.6	48.788
249.998	12.8368	781.39	-9.69	1861.8	48.781
252.001	14.7587	781.17	-6.09	2140.6	48.767
253.999	16.6777	780.97	-2.49	2418.9	48.754
255.998	18.5953	780.79	1.11	2697.0	48.743
258.000	20.5214	780.62	4.71	2976.4	48.733
260.000	22.4456	780.46	8.31	3255.5	48.723
261.999	24.3658	780.29	11.91	3534.0	48.712
264.000	26.2848	780.14	15.51	3812.3	48.703

Table 34. Isochoric (p,p,T) Data for HFC-41 from 132 to 400 K (-222 to 260°F) (continued).

Temperature K	Pressure MPa	Density kg/m ³	Temperature °F	Pressure psia	Density lb/ft ³
265.999	28.2029	779.98	19.11	4090.5	48.693
268.002	30.1190	779.83	22.72	4368.4	48.683
270.002	32.0287	779.68	26.32	4645.4	48.674
271.999	33.9325	779.53	29.91	4921.5	48.664
260.000	3.8305	729.90	8.31	555.6	45.566
261.001	4.5921	729.77	10.11	666.0	45.558
261.998	5.3514	729.63	11.91	776.2	45.549
263.000	6.1075	729.46	13.71	885.8	45.539
263.999	6.8400	729.25	15.51	992.1	45.526
265.000	7.5401	728.91	17.31	1093.6	45.504
266.001	8.2129	728.37	19.11	1191.2	45.471
266.999	8.9132	728.01	20.91	1292.8	45.448
268.001	9.6499	727.79	22.71	1399.6	45.434
269.000	10.3986	727.63	24.51	1508.2	45.424
270.000	11.1601	727.50	26.31	1618.6	45.416
272.001	12.6898	727.28	29.91	1840.5	45.403
273.999	14.2226	727.09	33.51	2062.8	45.391
275.999	15.7612	726.92	37.11	2286.0	45.380
277.999	17.3033	726.75	40.71	2509.6	45.370
280.002	18.8483	726.60	44.32	2733.7	45.360
281.999	20.3912	726.45	47.91	2957.5	45.351
283.998	21.9356	726.30	51.51	3181.5	45.341
286.000	23.4783	726.16	55.11	3405.2	45.333
288.000	25.0172	726.01	58.71	3628.4	45.323
289.999	26.5552	725.88	62.31	3851.5	45.315
292.000	28.0941	725.74	65.91	4074.7	45.306
294.000	29.6266	725.60	69.51	4297.0	45.298
296.000	31.1562	725.47	73.11	4518.8	45.290
298.000	32.6880	725.34	76.71	4741.0	45.282
299.999	34.2158	725.20	80.31	4962.6	45.273
280.001	4.7980	669.23	44.31	695.9	41.779
281.000	5.3963	669.11	46.11	782.7	41.771
281.999	5.9836	668.97	47.91	867.8	41.762
283.002	6.5694	668.81	49.72	952.8	41.752
283.999	7.1428	668.60	51.51	1036.0	41.739

A-63

Table 34. Isochoric (p,ρ,T) Data for HFC-41 from 132 to 400 K (-222 to 260°F) (continued).

Temperature K	Pressure MPa	Density kg/m ³	Temperature °F	Pressure psia	Density lb/ft ³
285.999	8.2455	667.81	55.11	1195.9	41.690
287.999	9.3867	667.31	58.71	1361.4	41.659
289.999	10.5647	667.04	62.31	1532.3	41.642
292.002	11.7576	666.84	65.92	1705.3	41.629
294.002	12.9527	666.66	69.52	1878.6	41.618
295.998	14.1466	666.50	73.11	2051.8	41.608
297.999	15.3500	666.35	76.71	2226.3	41.599
300.001	16.5543	666.21	80.31	2401.0	41.590
301.999	17.7579	666.07	83.91	2575.6	41.581
304.001	18.9619	665.94	87.51	2750.2	41.573
306.002	20.1678	665.81	91.12	2925.1	41.565
308.002	21.3725	665.68	94.72	3099.8	41.557
309.999	22.5758	665.55	98.31	3274.4	41.549
311.999	23.7842	665.43	101.91	3449.6	41.541
315.999	26.1888	665.19	109.11	3798.4	41.526
319.999	28.6007	664.94	116.31	4148.2	41.511
324.002	30.9990	664.70	123.52	4496.0	41.496
327.999	33.3941	664.47	130.71	4843.4	41.482
290.000	4.9719	631.25	62.31	721.1	39.408
291.000	5.4774	631.15	64.11	794.4	39.401
292.000	5.9816	631.02	65.91	867.6	39.393
293.001	6.4815	630.88	67.71	940.1	39.385
294.001	6.9806	630.71	69.51	1012.5	39.374
296.001	7.9414	630.10	73.11	1151.8	39.336
297.999	8.9106	629.50	76.71	1292.4	39.298
299.999	9.9103	629.20	80.31	1437.4	39.280
302.000	10.9257	629.00	83.91	1584.6	39.267
303.998	11.9428	628.82	87.51	1732.2	39.256
306.000	12.9682	628.66	91.11	1880.9	39.246
308.000	13.9931	628.52	94.71	2029.5	39.237
310.000	15.0194	628.38	98.31	2178.4	39.228
312.002	16.0497	628.25	101.92	2327.8	39.220
316.000	18.1104	628.00	109.11	2626.7	39.205
320.000	20.1735	627.76	116.31	2925.9	39.190
323.999	22.2349	627.52	123.51	3224.9	39.175
328.000	24.2980	627.29	130.71	3524.1	39.160

Table 34. Isochoric (p,p,T) Data for HFC-41 from 132 to 400 K (-222 to 260°F) (continued).

Temperature K	Pressure MPa	Density kg/m ³	Temperature °F	Pressure psia	Density lb/ft ³
332.000	26.3637	627.07	137.91	3823.7	39.147
336.002	28.4230	626.84	145.12	4122.4	39.132
340.000	30.4830	626.62	152.31	4421.2	39.119
344.002	32.5415	626.40	159.52	4719.8	39.105
348.000	34.5921	626.18	166.71	5017.2	39.091
300.001	4.7418	576.77	80.31	687.7	36.007
300.999	5.1390	576.68	82.11	745.3	36.001
302.000	5.5349	576.59	83.91	802.8	35.995
303.000	5.9330	576.49	85.71	860.5	35.989
304.001	6.3276	576.38	87.51	917.7	35.982
306.001	7.1170	576.09	91.11	1032.2	35.964
308.000	7.8936	575.57	94.71	1144.9	35.932
310.002	8.6734	575.02	98.32	1258.0	35.897
312.000	9.4679	574.73	101.91	1373.2	35.879
314.000	10.2710	574.53	105.51	1489.7	35.867
315.999	11.0811	574.36	109.11	1607.2	35.856
317.999	11.8932	574.22	112.71	1725.0	35.847
319.999	12.7079	574.08	116.31	1843.1	35.839
324.001	14.3409	573.83	123.51	2080.0	35.823
328.001	15.9858	573.60	130.71	2318.6	35.809
331.999	17.6232	573.42	137.91	2556.0	35.797
336.000	19.2728	573.20	145.11	2795.3	35.784
340.000	20.9259	572.99	152.31	3035.1	35.771
344.002	22.5808	572.79	159.52	3275.1	35.758
348.001	24.2362	572.58	166.71	3515.2	35.745
352.000	25.8912	572.38	173.91	3755.2	35.733
356.000	27.5489	572.18	181.11	3995.6	35.720
360.000	29.2040	571.98	188.31	4235.7	35.708
363.999	30.8587	571.78	195.51	4475.7	35.695
367.999	32.5115	571.58	202.71	4715.4	35.683
372.000	34.1636	571.39	209.91	4955.0	35.671
310.000	5.1991	501.26	98.31	754.1	31.293
310.999	5.4742	501.19	100.11	794.0	31.288
311.998	5.7550	501.12	101.91	834.7	31.284
313.000	6.0360	501.04	103.71	875.5	31.279

A-65

Table 34. Isochoric (p, ρ ,T) Data for HFC-41 from 132 to 400 K (-222 to 260°F) (continued).

Temperature K	Pressure MPa	Density kg/m ³	Temperature °F	Pressure psia	Density lb/ft ³
314.000	6.3180	500.96	105.51	916.3	31.274
316.001	6.8842	500.75	109.11	998.5	31.261
318.002	7.4523	500.47	112.72	1080.9	31.243
320.000	8.0197	500.00	116.31	1163.2	31.214
322.001	8.5905	499.60	119.91	1245.9	31.189
324.001	9.1656	499.37	123.51	1329.4	31.175
327.998	10.3330	499.06	130.71	1498.7	31.155
332.001	11.5146	498.82	137.91	1670.1	31.140
336.000	12.7046	498.60	145.11	1842.7	31.127
340.000	13.9017	498.39	152.31	2016.3	31.113
343.999	15.1044	498.20	159.51	2190.7	31.102
347.999	16.3116	498.01	166.71	2365.8	31.090
352.001	17.5233	497.83	173.91	2541.6	31.079
356.001	18.7375	497.65	181.11	2717.6	31.067
360.001	19.9543	497.47	188.31	2894.1	31.056
363.999	21.1726	497.29	195.51	3070.8	31.045
368.000	22.3931	497.12	202.71	3247.9	31.034
372.002	23.6127	496.95	209.92	3424.7	31.024
376.002	24.8337	496.78	217.12	3601.8	31.013
380.001	26.0567	496.60	224.31	3779.2	31.002
384.000	27.2806	496.43	231.51	3956.7	30.991
387.998	28.5023	496.26	238.71	4133.9	30.981
392.002	29.7240	496.09	245.92	4311.1	30.970
396.000	30.9428	495.92	253.11	4487.9	30.959
399.998	32.1613	495.75	260.31	4664.6	30.949
319.998	6.8061	446.36	116.31	987.1	27.865
321.000	7.0279	446.27	118.11	1019.3	27.860
322.001	7.2522	446.16	119.91	1051.8	27.853
322.998	7.4800	446.02	121.71	1084.9	27.844
323.999	7.7051	445.85	123.51	1117.5	27.834
325.999	8.1587	445.45	127.11	1183.3	27.809
327.998	8.6162	445.14	130.71	1249.7	27.789
330.000	9.0776	444.93	134.31	1316.6	27.776
332.000	9.5419	444.77	137.91	1383.9	27.766
334.002	10.0099	444.64	141.52	1451.8	27.758
335.999	10.4781	444.52	145.11	1519.7	27.750

Table 34. Isochoric (p,p,T) Data for HFC-41 from 132 to 400 K (-222 to 260°F) (continued).

Temperature K	Pressure MPa	Density kg/m ³	Temperature °F	Pressure psia	Density lb/ft ³
340.001	11.4237	444.30	152.31	1656.9	27.737
344.000	12.3754	444.11	159.51	1794.9	27.725
347.999	13.3328	443.93	166.71	1933.8	27.714
351.998	14.2941	443.76	173.91	2073.2	27.703
356.000	15.2600	443.59	181.11	2213.3	27.692
360.001	16.2277	443.43	188.31	2353.6	27.682
364.001	17.1980	443.27	195.51	2494.4	27.672
368.002	18.1715	443.11	202.72	2635.6	27.662
372.000	19.1458	442.95	209.91	2776.9	27.652
376.000	20.1219	442.80	217.11	2918.4	27.643
379.999	21.0988	442.64	224.31	3060.1	27.633
384.000	22.0772	442.49	231.51	3202.0	27.624
387.999	23.0554	442.34	238.71	3343.9	27.614
391.999	24.0344	442.18	245.91	3485.9	27.604
395.999	25.0129	442.03	253.11	3627.8	27.595
399.999	25.9923	441.88	260.31	3769.9	27.586
320.001	6.3260	366.39	116.31	917.5	22.873
320.998	6.4852	366.34	118.11	940.6	22.870
321.998	6.6445	366.29	119.91	963.7	22.867
323.001	6.8068	366.23	121.71	987.2	22.863
323.999	6.9689	366.16	123.51	1010.8	22.859
326.000	7.2960	365.99	127.11	1058.2	22.848
328.000	7.6251	365.77	130.71	1105.9	22.834
330.000	7.9559	365.47	134.31	1153.9	22.816
332.002	8.2891	365.19	137.92	1202.2	22.798
335.999	8.9586	364.82	145.11	1299.3	22.775
339.999	9.6346	364.57	152.31	1397.4	22.759
343.999	10.3154	364.38	159.51	1496.1	22.748
348.000	10.9998	364.21	166.71	1595.4	22.737
351.998	11.6867	364.05	173.91	1695.0	22.727
356.001	12.3767	363.90	181.11	1795.1	22.718
360.002	13.0684	363.76	188.32	1895.4	22.709
363.999	13.7619	363.62	195.51	1996.0	22.700
368.002	14.4558	363.48	202.72	2096.6	22.691
372.000	15.1518	363.35	209.91	2197.6	22.683
376.001	15.8485	363.22	217.11	2298.6	22.675

A-67

Table 34. Isochoric (p, ρ ,T) Data for HFC-41 from 132 to 400 K (-222 to 260°F) (continued).

Temperature K	Pressure MPa	Density kg/m ³	Temperature °F	Pressure psia	Density lb/ft ³
379.998	16.5453	363.09	224.31	2399.7	22.667
383.999	17.2436	362.96	231.51	2501.0	22.659
388.000	17.9423	362.84	238.71	2602.3	22.651
392.001	18.6407	362.71	245.91	2703.6	22.643
395.999	19.3387	362.58	253.11	2804.9	22.635
399.999	20.0367	362.46	260.31	2906.1	22.628
320.002	6.2317	286.65	116.32	903.8	17.895
321.999	6.4775	286.58	119.91	939.5	17.891
324.000	6.7234	286.50	123.51	975.2	17.886
326.000	6.9691	286.40	127.11	1010.8	17.879
327.999	7.2144	286.29	130.71	1046.4	17.873
330.000	7.4597	286.14	134.31	1081.9	17.863
332.000	7.7045	285.95	137.91	1117.4	17.851
336.001	8.1936	285.51	145.11	1188.4	17.824
339.999	8.6829	285.18	152.31	1259.3	17.803
344.001	9.1724	284.96	159.51	1330.3	17.789
347.999	9.6620	284.79	166.71	1401.4	17.779
352.000	10.1518	284.64	173.91	1472.4	17.769
356.000	10.6405	284.49	181.11	1543.3	17.760
360.000	11.1298	284.36	188.31	1614.2	17.752
364.001	11.6195	284.25	195.51	1685.3	17.745
367.999	12.1082	284.14	202.71	1756.2	17.738
371.998	12.5965	284.03	209.91	1827.0	17.731
376.001	13.0847	283.92	217.11	1897.8	17.725
380.000	13.5727	283.82	224.31	1968.6	17.718
384.002	14.0606	283.71	231.52	2039.3	17.711
388.002	14.5475	283.61	238.72	2109.9	17.705
392.002	15.0340	283.51	245.92	2180.5	17.699
396.000	15.5201	283.41	253.11	2251.0	17.693
399.998	16.0054	283.31	260.31	2321.4	17.686
319.999	6.0003	193.24	116.31	870.3	12.064
321.998	6.1630	193.20	119.91	893.9	12.061
323.999	6.3243	193.15	123.51	917.3	12.058
325.999	6.4842	193.10	127.11	940.5	12.055
328.000	6.6433	193.05	130.71	963.5	12.052

Table 34. Isochoric (p,p,T) Data for HFC-41 from 132 to 400 K (-222 to 260°F) (continued).

Temperature K	Pressure MPa	Density kg/m ³	Temperature °F	Pressure psia	Density lb/ft ³
330.000	6.8009	192.99	134.31	986.4	12.048
331.999	6.9578	192.93	137.91	1009.2	12.044
335.998	7.2690	192.79	145.11	1054.3	12.035
340.001	7.5768	192.59	152.31	1098.9	12.023
343.999	7.8812	192.33	159.51	1143.1	12.007
347.999	8.1832	192.06	166.71	1186.9	11.990
351.999	8.4835	191.84	173.91	1230.4	11.976
355.999	8.7831	191.67	181.11	1273.9	11.966
360.002	9.0816	191.53	188.32	1317.2	11.957
364.001	9.3782	191.42	195.51	1360.2	11.950
367.999	9.6739	191.31	202.71	1403.1	11.943
372.000	9.9686	191.22	209.91	1445.8	11.937
376.000	10.2623	191.13	217.11	1488.4	11.932
380.001	10.5551	191.04	224.31	1530.9	11.926
384.001	10.8468	190.96	231.51	1573.2	11.921
388.001	11.1377	190.88	238.71	1615.4	11.916
392.000	11.4275	190.80	245.91	1657.4	11.911
396.000	11.7165	190.72	253.11	1699.3	11.906
399.999	12.0047	190.65	260.31	1741.1	11.902
320.002	4.9891	110.22	116.32	723.6	6.881
322.001	5.0712	110.20	119.91	735.5	6.880
323.998	5.1527	110.18	123.51	747.3	6.878
326.000	5.2341	110.15	127.11	759.1	6.876
328.001	5.3149	110.13	130.71	770.9	6.875
330.000	5.3952	110.10	134.31	782.5	6.873
332.000	5.4752	110.08	137.91	794.1	6.872
336.000	5.6338	110.03	145.11	817.1	6.869
340.000	5.7910	109.97	152.31	839.9	6.865
344.001	5.9470	109.92	159.51	862.5	6.862
348.002	6.1017	109.87	166.72	885.0	6.859
352.000	6.2552	109.81	173.91	907.2	6.855
356.000	6.4073	109.75	181.11	929.3	6.851
360.000	6.5585	109.69	188.31	951.2	6.848
364.002	6.7082	109.62	195.52	973.0	6.843
368.002	6.8569	109.56	202.72	994.5	6.840
372.000	7.0042	109.48	209.91	1015.9	6.835

Table 34. Isochoric (p,ρ,T) Data for HFC-41 from 132 to 400 K (-222 to 260°F) (continued).

Temperature K	Pressure MPa	Density kg/m ³	Temperature °F	Pressure psia	Density lb/ft ³
376.000	7.1510	109.40	217.11	1037.2	6.830
379.998	7.2966	109.31	224.31	1058.3	6.824
384.000	7.4407	109.22	231.51	1079.2	6.818
387.999	7.5835	109.11	238.71	1099.9	6.812
392.001	7.7250	108.98	245.91	1120.4	6.803
396.002	7.8648	108.84	253.12	1140.7	6.795
400.000	8.0044	108.71	260.31	1160.9	6.787
319.999	4.0606	76.13	116.31	588.9	4.753
322.001	4.1127	76.11	119.91	596.5	4.751
324.000	4.1646	76.10	123.51	604.0	4.751
326.000	4.2162	76.09	127.11	611.5	4.750
327.998	4.2676	76.07	130.71	619.0	4.749
329.998	4.3187	76.06	134.31	626.4	4.748
331.998	4.3695	76.04	137.91	633.7	4.747
336.000	4.4710	76.01	145.11	648.5	4.745
340.001	4.5714	75.98	152.31	663.0	4.743
344.000	4.6712	75.95	159.51	677.5	4.741
348.000	4.7703	75.92	166.71	691.9	4.740
352.001	4.8687	75.89	173.91	706.2	4.738
356.001	4.9663	75.86	181.11	720.3	4.736
360.000	5.0632	75.83	188.31	734.4	4.734
364.001	5.1589	75.80	195.51	748.2	4.732
368.001	5.2550	75.76	202.71	762.2	4.730
372.001	5.3504	75.73	209.91	776.0	4.728
376.001	5.4452	75.70	217.11	789.8	4.726
380.000	5.5397	75.66	224.31	803.5	4.723
384.000	5.6336	75.63	231.51	817.1	4.721
388.000	5.7272	75.60	238.71	830.7	4.720
392.000	5.8203	75.56	245.91	844.2	4.717
395.999	5.9130	75.52	253.11	857.6	4.715
400.000	6.0051	75.49	260.31	871.0	4.713
320.000	2.8997	47.14	116.31	420.6	2.943
321.999	2.9290	47.13	119.91	424.8	2.942
323.999	2.9581	47.12	123.51	429.0	2.942
326.000	2.9871	47.11	127.11	433.2	2.941

A-70

Table 34. Isochoric (p,p,T) Data for HFC-41 from 132 to 400 K (-222 to 260°F) (continued).

Temperature K	Pressure MPa	Density kg/m ³	Temperature °F	Pressure psia	Density lb/ft ³
327.999	3.0160	47.10	130.71	437.4	2.940
330.000	3.0448	47.10	134.31	441.6	2.940
332.000	3.0736	47.09	137.91	445.8	2.940
336.000	3.1307	47.07	145.11	454.1	2.938
340.000	3.1875	47.06	152.31	462.3	2.938
343.999	3.2440	47.04	159.51	470.5	2.937
348.000	3.3002	47.02	166.71	478.7	2.935
351.998	3.3560	47.01	173.91	486.8	2.935
355.999	3.4116	46.99	181.11	494.8	2.933
359.999	3.4668	46.97	188.31	502.8	2.932
363.998	3.5221	46.96	195.51	510.8	2.932
368.000	3.5769	46.94	202.71	518.8	2.930
371.998	3.6315	46.92	209.91	526.7	2.929
376.000	3.6858	46.90	217.11	534.6	2.928
379.998	3.7399	46.89	224.31	542.4	2.927
383.998	3.7939	46.87	231.51	550.3	2.926
388.001	3.8476	46.85	238.71	558.0	2.925
392.001	3.9011	46.83	245.91	565.8	2.924
395.998	3.9544	46.82	253.11	573.5	2.923
399.999	4.0076	46.80	260.31	581.3	2.922

A71

Table 35. Saturated Liquid Densities for HFC-41 from 131 to 309 K (-224 to 96°F) Extrapolated from Isochoric (p, ρ ,T) Data.

Temperature K	Vapor Pressure MPa	Density kg/m ³	Temperature °F	Vapor Pressure psia	Density lb/ft ³
130.785	0.0004	1007.747	-224.275	0.058	62.8551
140.784	0.0014	988.908	-206.277	0.203	61.6801
152.713	0.0048	966.101	-184.805	0.696	60.2576
166.519	0.0158	939.357	-159.954	2.292	58.5895
181.998	0.0472	907.781	-132.092	6.846	56.6200
197.962	0.1198	875.030	-103.356	17.376	54.5773
217.537	0.3000	831.220	-68.121	43.511	51.8448
236.983	0.6603	784.123	-33.119	95.769	48.9072
256.759	1.2743	730.022	2.478	184.822	45.5329
275.799	2.1968	669.316	36.750	318.620	41.7465
285.861	2.8503	631.151	54.862	413.403	39.3661
297.612	3.7895	576.839	76.014	549.622	35.9786
308.959	4.9099	501.276	96.438	712.123	31.2655

A-72

Table 36. Isochoric Heat Capacities (C_v) for HFC-41 from 148 to 343 K (-193 to 157°F).

Temperature K	Heat Capacity J/(mole•K)	Density kg/m ³	Pressure MPa	Temperature °F	Heat Capacity BTU/(lb•°F)	Density lb/ft ³	Pressure psia
148.371	47.40	980.16	10.157	-192.62	0.3327	61.189	1473.2
152.215	46.44	978.95	18.001	-185.70	0.3259	61.114	2610.8
156.062	46.40	977.77	25.835	-178.78	0.3257	61.040	3747.0
163.611	45.63	951.78	9.859	-165.19	0.3203	59.418	1429.9
167.527	44.88	950.65	17.045	-158.14	0.3150	59.347	2472.2
171.441	44.75	949.55	24.197	-151.10	0.3141	59.278	3509.5
175.337	44.75	948.47	31.183	-144.08	0.3141	59.211	4522.8
184.739	44.12	910.91	9.211	-127.16	0.3097	56.866	1336.0
188.751	42.89	909.89	15.479	-119.94	0.3010	56.803	2245.0
192.773	42.73	908.90	21.785	-112.70	0.2999	56.741	3159.7
196.773	42.81	907.93	27.948	-105.50	0.3005	56.680	4053.5
203.880	42.42	873.03	9.122	-92.70	0.2977	54.501	1323.1
207.990	41.75	872.11	14.702	-85.31	0.2930	54.444	2132.4
212.090	41.62	871.22	20.261	-77.93	0.2921	54.388	2938.6
216.170	41.70	870.35	25.725	-70.58	0.2927	54.334	3731.2
220.240	41.78	869.50	31.092	-63.26	0.2932	54.281	4509.6
222.687	41.45	833.49	8.794	-58.85	0.2909	52.033	1275.4
226.888	40.77	832.66	13.692	-51.29	0.2862	51.981	1985.8
231.072	40.76	831.87	18.566	-43.76	0.2861	51.932	2692.8
235.239	40.79	831.10	23.370	-36.26	0.2863	51.884	3389.5
239.396	40.96	830.34	28.110	-28.77	0.2875	51.836	4077.0
242.409	40.83	788.80	8.494	-23.35	0.2866	49.243	1232.0
246.712	40.27	788.08	12.709	-15.61	0.2826	49.198	1843.3
250.996	40.37	787.39	16.904	-7.89	0.2833	49.155	2451.7
255.277	40.38	786.71	21.066	-0.19	0.2834	49.113	3055.3
259.537	40.38	786.05	25.169	7.48	0.2834	49.072	3650.4
263.547	40.47	785.42	28.999	14.70	0.2840	49.032	4206.0
263.247	40.58	736.81	8.432	14.16	0.2848	45.998	1222.9
267.655	40.26	736.20	11.944	22.09	0.2826	45.959	1732.4
272.049	40.26	735.62	15.444	30.00	0.2826	45.923	2239.9
276.430	40.26	735.04	18.921	37.89	0.2826	45.887	2744.3

A-73

Table 36. Isochoric Heat Capacities (C_v) for HFC-41 from 148 to 343 K (-193 to 157°F) (continued).

Temperature K	Heat Capacity J/(mole•K)	Density kg/m ³	Pressure MPa	Temperature °F	Heat Capacity BTU/(lb•°F)	Density lb/ft ³	Pressure psia
280.813	40.44	734.48	22.380	45.78	0.2838	45.852	3245.9
285.180	40.48	733.91	25.804	53.64	0.2841	45.817	3742.6
289.533	40.67	733.36	29.196	61.47	0.2854	45.782	4234.5
293.880	40.77	732.80	32.559	69.30	0.2862	45.747	4722.2
283.493	40.90	675.15	7.865	50.60	0.2871	42.148	1140.7
288.047	40.71	674.64	10.682	58.80	0.2857	42.116	1549.3
292.599	40.72	674.16	13.505	66.99	0.2858	42.086	1958.8
297.149	40.75	673.69	16.326	75.18	0.2860	42.057	2367.9
301.697	40.60	673.22	19.140	83.37	0.2850	42.028	2776.0
306.230	40.76	672.76	21.937	91.53	0.2861	41.999	3181.7
310.776	40.91	672.30	24.732	99.71	0.2871	41.970	3587.1
315.313	40.79	671.83	27.511	107.88	0.2863	41.941	3990.1
319.841	41.12	671.37	30.274	116.03	0.2886	41.912	4390.8
324.356	41.58	670.92	33.018	124.15	0.2918	41.884	4788.8
293.035	41.38	640.69	7.687	67.77	0.2904	39.997	1114.9
297.659	40.84	640.23	10.159	76.10	0.2866	39.968	1473.5
302.286	40.97	639.80	12.650	84.43	0.2876	39.941	1834.8
306.910	41.17	639.39	15.142	92.75	0.2890	39.916	2196.1
311.533	41.37	638.97	17.629	101.07	0.2904	39.890	2556.9
316.156	41.39	638.56	20.113	109.39	0.2905	39.864	2917.1
320.758	41.35	638.15	22.580	117.68	0.2902	39.838	3274.9
325.353	41.44	637.74	25.039	125.95	0.2909	39.813	3631.7
329.979	41.60	637.32	27.512	134.27	0.2920	39.787	3990.3
334.592	41.75	636.91	29.972	142.58	0.2930	39.761	4347.1
339.218	41.83	636.50	32.428	150.90	0.2936	39.735	4703.3
295.409	41.16	640.45	8.953	72.05	0.2889	39.982	1298.6
300.041	41.10	640.01	11.441	80.39	0.2885	39.955	1659.4
304.682	40.93	639.59	13.941	88.74	0.2873	39.928	2022.0
309.317	41.01	639.17	16.437	97.08	0.2878	39.902	2384.0
313.958	41.24	638.75	18.932	105.44	0.2895	39.876	2745.9
318.600	41.33	638.34	21.423	113.79	0.2901	39.850	3107.2
323.245	41.32	637.92	23.911	122.15	0.2900	39.824	3468.1
327.885	41.28	637.51	26.393	130.51	0.2897	39.798	3828.0
332.520	41.57	637.10	28.868	138.85	0.2918	39.773	4186.9
337.158	41.76	636.68	31.336	147.20	0.2931	39.747	4545.0

Table 36. Isochoric Heat Capacities (C_v) for HFC-41 from 148 to 343 K (-193 to 157°F) (continued).

Temperature K	Heat Capacity J/(mole·K)	Density kg/m ³	Pressure MPa	Temperature °F	Heat Capacity BTU/(lb·°F)	Density lb/ft ³	Pressure psia
303.889	42.30	594.11	7.584	87.31	0.2969	37.089	1100.0
308.581	41.87	593.72	9.641	95.76	0.2939	37.065	1398.4
313.273	41.86	593.35	11.714	104.20	0.2938	37.042	1699.0
317.975	41.67	593.00	13.800	112.67	0.2925	37.020	2001.5
322.667	41.73	592.65	15.887	121.11	0.2929	36.998	2304.2
327.369	41.89	592.30	17.981	129.57	0.2940	36.976	2607.9
336.793	41.76	591.59	22.177	146.54	0.2931	36.932	3216.5
341.521	41.64	591.24	24.281	155.05	0.2923	36.910	3521.7
306.150	41.84	593.91	8.574	91.38	0.2937	37.077	1243.5
310.881	41.74	593.54	10.656	99.90	0.2930	37.053	1545.5
315.625	41.69	593.18	12.756	108.44	0.2926	37.031	1850.2
320.366	41.77	592.82	14.863	116.97	0.2932	37.009	2155.7
325.118	41.75	592.46	16.978	125.52	0.2930	36.986	2462.5
329.870	41.94	592.11	19.095	134.08	0.2944	36.964	2769.5
334.633	41.87	591.75	21.216	142.65	0.2939	36.942	3077.1
339.387	41.88	591.40	23.331	151.21	0.2939	36.920	3383.9
309.790	43.06	559.96	7.340	97.93	0.3022	34.957	1064.6
314.617	42.51	559.61	9.162	106.62	0.2984	34.935	1328.8
319.442	42.43	559.28	11.001	115.31	0.2978	34.915	1595.6
324.290	42.12	558.96	12.862	124.03	0.2956	34.895	1865.5
329.127	42.40	558.64	14.727	132.74	0.2976	34.875	2135.9
333.993	42.20	558.32	16.608	141.50	0.2962	34.855	2408.9
338.842	42.27	558.00	18.488	150.23	0.2967	34.835	2681.5
312.334	42.64	559.77	8.297	102.51	0.2993	34.945	1203.5
317.173	42.37	559.43	10.134	111.22	0.2974	34.924	1469.9
322.028	42.19	559.11	11.993	119.96	0.2961	34.904	1739.4
326.891	41.95	558.79	13.864	128.71	0.2944	34.884	2010.8
331.759	42.17	558.47	15.744	137.48	0.2960	34.864	2283.5
336.630	42.21	558.15	17.630	146.25	0.2963	34.844	2557.0
341.522	42.30	557.83	19.529	155.05	0.2969	34.824	2832.4
320.500	50.98	423.52	6.618	117.21	0.3578	26.439	959.8
325.616	48.15	423.26	7.654	126.42	0.3379	26.423	1110.1
330.826	46.68	423.04	8.737	135.80	0.3276	26.410	1267.2
336.080	45.67	422.84	9.848	145.26	0.3205	26.397	1428.4
341.380	44.92	422.63	10.985	154.80	0.3153	26.384	1593.2

A-75

Table 36. Isochoric Heat Capacities (C_v) for HFC-41 from 148 to 343 K (-193 to 157°F) (continued).

Temperature K	Heat Capacity J/(mole•K)	Density kg/m ³	Pressure MPa	Temperature °F	Heat Capacity BTU/(lb•°F)	Density lb/ft ³	Pressure psia
323.108	48.86	423.37	7.142	121.91	0.3429	26.430	1035.9
328.289	47.10	423.15	8.207	131.23	0.3306	26.416	1190.3
333.528	46.14	422.94	9.306	140.66	0.3238	26.403	1349.8
338.817	45.54	422.73	10.433	150.18	0.3196	26.390	1513.2
320.394	56.41	199.30	6.069	117.02	0.3959	12.442	880.2
326.669	51.63	198.94	6.590	128.32	0.3624	12.419	955.9
333.055	49.26	198.80	7.111	139.81	0.3457	12.411	1031.4
339.500	47.94	198.69	7.630	151.41	0.3365	12.404	1106.6
323.568	53.97	199.06	6.334	122.74	0.3788	12.427	918.7
329.857	50.33	198.86	6.851	134.05	0.3533	12.414	993.7
336.255	48.52	198.75	7.369	145.57	0.3405	12.408	1068.8
342.711	46.86	198.64	7.886	157.19	0.3289	12.401	1143.8
311.056	43.63	59.86	3.237	100.21	0.3062	3.737	469.5
318.622	42.18	59.83	3.387	113.83	0.2960	3.735	491.3
326.203	41.15	59.80	3.535	127.48	0.2888	3.733	512.7
333.816	41.30	59.77	3.682	141.18	0.2899	3.731	534.0
341.451	40.61	59.75	3.827	154.92	0.2850	3.730	555.0
314.884	42.14	59.84	3.314	107.10	0.2958	3.736	480.6
322.429	41.31	59.81	3.462	120.68	0.2899	3.734	502.1
329.997	41.97	59.79	3.609	134.31	0.2946	3.733	523.4
337.588	41.60	59.76	3.754	147.97	0.2920	3.731	544.4

A-76

Table 37. Two-Phase Heat Capacities for HFC-41 from 136 to 314 K (-215 to 106°F).

Temperature K	$C_v^{(2)}$ J/(mole•K)	C_σ J/(mole•K)	Density kg/m ³	Pressure MPa	Temperature °F	$C_v^{(2)}$ BTU/(lb•°F)	C_σ BTU/(lb•°F)	Density lb/ft ³	Pressure psia
136.023	71.859	71.835	997.70	0.001	-214.85	0.5044	0.5042	62.284	0.1
140.144	71.514	71.478	990.09	0.001	-207.43	0.5019	0.5017	61.809	0.2
144.237	71.289	71.240	982.47	0.002	-200.06	0.5004	0.5000	61.334	0.3
148.312	71.075	71.008	974.82	0.003	-192.73	0.4989	0.4984	60.856	0.4
152.365	70.819	70.730	967.14	0.005	-185.43	0.4971	0.4964	60.377	0.7
156.398	70.613	70.499	959.43	0.007	-178.17	0.4956	0.4948	59.895	1.0
160.407	70.659	70.515	951.69	0.010	-170.96	0.4959	0.4949	59.412	1.4
164.402	70.594	70.416	943.91	0.013	-163.76	0.4955	0.4942	58.926	1.9
168.369	70.638	70.422	936.10	0.018	-156.62	0.4958	0.4943	58.439	2.6
172.320	70.388	70.129	928.24	0.024	-149.51	0.4940	0.4922	57.948	3.5
176.242	70.515	70.211	920.37	0.032	-142.45	0.4949	0.4928	57.457	4.7
180.148	70.683	70.331	912.43	0.042	-135.42	0.4961	0.4936	56.961	6.1
184.031	70.500	70.096	904.45	0.054	-128.43	0.4948	0.4920	56.463	7.8
187.886	70.620	70.165	896.44	0.068	-121.49	0.4957	0.4925	55.963	9.8
191.726	70.713	70.205	888.37	0.085	-114.58	0.4963	0.4927	55.459	12.3
195.542	71.121	70.561	880.24	0.105	-107.71	0.4992	0.4952	54.952	15.2
199.339	71.218	70.609	872.05	0.129	-100.88	0.4999	0.4956	54.440	18.7
203.109	71.371	70.716	863.81	0.156	-94.09	0.5009	0.4963	53.926	22.7
206.860	71.658	70.962	855.50	0.188	-87.34	0.5029	0.4981	53.407	27.3
210.586	71.967	71.237	847.14	0.224	-80.63	0.5051	0.5000	52.885	32.5
214.292	72.244	71.489	838.68	0.265	-73.96	0.5071	0.5018	52.357	38.5
217.979	72.501	71.730	830.14	0.312	-67.33	0.5089	0.5035	51.824	45.3
221.639	72.709	71.935	821.54	0.364	-60.74	0.5103	0.5049	51.287	52.9
225.276	73.237	72.475	812.83	0.423	-54.19	0.5140	0.5087	50.744	61.3
228.890	73.810	73.078	804.04	0.488	-47.69	0.5180	0.5129	50.194	70.7
232.486	74.336	73.653	795.13	0.559	-41.21	0.5217	0.5169	49.638	81.1
236.059	74.715	74.105	786.10	0.639	-34.78	0.5244	0.5201	49.075	92.6
239.606	75.230	74.719	776.97	0.725	-28.40	0.5280	0.5244	48.504	105.2
243.135	75.801	75.420	767.69	0.820	-22.05	0.5320	0.5293	47.925	118.9
246.639	76.041	75.826	758.27	0.923	-15.74	0.5337	0.5322	47.337	133.8
250.119	76.885	76.877	748.70	1.034	-9.47	0.5396	0.5396	46.740	150.0
253.581	77.607	77.852	738.95	1.155	-3.24	0.5447	0.5464	46.131	167.5
257.022	77.964	78.517	729.00	1.285	2.95	0.5472	0.5511	45.510	186.3
260.436	78.725	79.649	718.86	1.424	9.10	0.5525	0.5590	44.877	206.6
263.838	79.473	80.842	708.46	1.574	15.22	0.5578	0.5674	44.228	228.3
267.218	79.960	81.861	697.81	1.735	21.30	0.5612	0.5746	43.563	251.6
270.576	80.615	83.151	686.86	1.906	27.35	0.5658	0.5836	42.879	276.4

A-77

Table 37. Two-Phase Heat Capacities for HFC-41 from 136 to 314 K (-215 to 106°F) (continued).

Temperature K	$C_v^{(2)}$ J/(mole•K)	C_σ J/(mole•K)	Density kg/m ³	Pressure MPa	Temperature °F	$C_v^{(2)}$ BTU/(lb•°F)	C_σ BTU/(lb•°F)	Density lb/ft ³	Pressure psia
134.063	71.904	71.884	1001.30	0.001	-218.38	0.5047	0.5045	62.509	0.1
138.189	71.598	71.568	993.71	0.001	-210.95	0.5025	0.5023	62.035	0.1
142.294	71.306	71.263	986.09	0.002	-203.56	0.5005	0.5002	61.560	0.2
146.376	71.242	71.184	978.46	0.002	-196.21	0.5000	0.4996	61.083	0.4
150.430	70.987	70.910	970.81	0.004	-188.91	0.4982	0.4977	60.606	0.6
154.472	70.844	70.743	963.12	0.006	-181.64	0.4972	0.4965	60.126	0.8
158.486	70.644	70.515	955.41	0.008	-174.41	0.4958	0.4949	59.644	1.2
162.480	70.561	70.400	947.66	0.011	-167.22	0.4952	0.4941	59.161	1.7
166.453	70.341	70.143	939.88	0.016	-160.07	0.4937	0.4923	58.675	2.3
170.404	70.455	70.217	932.06	0.021	-152.96	0.4945	0.4928	58.187	3.1
174.336	70.438	70.156	924.21	0.028	-145.88	0.4944	0.4924	57.696	4.1
178.248	70.531	70.203	916.30	0.037	-138.84	0.4950	0.4927	57.203	5.4
182.139	70.519	70.141	908.35	0.048	-131.84	0.4950	0.4923	56.707	6.9
186.011	70.526	70.096	900.35	0.061	-124.87	0.4950	0.4920	56.207	8.8
189.859	70.661	70.178	892.31	0.076	-117.94	0.4959	0.4926	55.705	11.1
193.687	70.820	70.285	884.20	0.095	-111.05	0.4971	0.4933	55.199	13.8
197.488	71.136	70.551	876.06	0.117	-104.21	0.4993	0.4952	54.691	16.9
201.278	71.138	70.505	867.83	0.142	-97.39	0.4993	0.4949	54.177	20.7
205.036	71.427	70.750	859.56	0.172	-90.62	0.5013	0.4966	53.661	24.9
208.772	71.857	71.143	851.23	0.206	-83.90	0.5043	0.4993	53.140	29.9
212.489	72.005	71.261	842.81	0.245	-77.21	0.5054	0.5002	52.615	35.5
216.176	72.285	71.520	834.34	0.289	-70.57	0.5073	0.5020	52.086	41.9
219.846	72.570	71.796	825.77	0.338	-63.97	0.5093	0.5039	51.551	49.0
223.485	73.065	72.295	817.14	0.393	-57.42	0.5128	0.5074	51.012	57.0
227.111	73.476	72.726	808.39	0.455	-50.89	0.5157	0.5104	50.466	66.0
230.712	73.661	72.950	799.54	0.523	-44.41	0.5170	0.5120	49.914	75.9
234.282	74.211	73.561	790.62	0.598	-37.98	0.5209	0.5163	49.357	86.8
237.841	74.912	74.348	781.54	0.681	-31.57	0.5258	0.5218	48.790	98.8
241.373	75.328	74.878	772.34	0.771	-25.22	0.5287	0.5255	48.216	111.9
244.886	75.919	75.616	763.01	0.870	-18.89	0.5329	0.5307	47.633	126.2
248.378	76.573	76.457	753.52	0.977	-12.61	0.5374	0.5366	47.040	141.7
251.850	77.099	77.211	743.85	1.093	-6.36	0.5411	0.5419	46.437	158.5
255.299	77.597	77.988	734.01	1.218	-0.15	0.5446	0.5474	45.823	176.7
258.728	78.020	78.750	723.97	1.353	6.02	0.5476	0.5527	45.196	196.2
262.135	78.639	79.775	713.71	1.498	12.16	0.5519	0.5599	44.555	217.2
265.520	79.458	81.079	703.20	1.653	18.25	0.5577	0.5691	43.900	239.7
268.889	80.187	82.389	692.41	1.818	24.31	0.5628	0.5783	43.226	263.7

Table 37. Two-Phase Heat Capacities for HFC-41 from 136 to 314 K (-215 to 106°F) (continued).

Temperature K	$C_v^{(2)}$ J/(mole•K)	C_σ J/(mole•K)	Density kg/m ³	Pressure MPa	Temperature °F	$C_v^{(2)}$ BTU/(lb•°F)	C_σ BTU/(lb•°F)	Density lb/ft ³	Pressure psia
272.233	80.826	83.721	681.32	1.995	30.33	0.5673	0.5876	42.533	289.3
275.556	81.672	85.396	669.88	2.183	36.31	0.5732	0.5994	41.819	316.6
278.862	82.742	87.463	658.04	2.382	42.26	0.5807	0.6139	41.080	345.5
282.203	78.873	84.818	645.54	2.598	48.28	0.5536	0.5953	40.300	376.8
266.017	81.680	81.191	701.63	1.676	19.14	0.5733	0.5699	43.801	243.1
269.584	82.253	82.254	690.14	1.854	25.56	0.5773	0.5773	43.084	268.9
273.123	83.252	83.867	678.30	2.044	31.93	0.5843	0.5886	42.345	296.4
276.637	84.147	85.529	666.07	2.246	38.26	0.5906	0.6003	41.581	325.8
280.107	85.658	87.991	653.45	2.461	44.50	0.6012	0.6176	40.794	356.9
283.555	86.814	90.338	640.30	2.689	50.71	0.6093	0.6341	39.973	390.0
286.972	87.740	92.759	626.56	2.931	56.86	0.6158	0.6510	39.115	425.1
290.361	89.099	96.017	612.11	3.186	62.96	0.6254	0.6739	38.213	462.1
293.728	90.551	99.925	596.76	3.456	69.02	0.6355	0.7013	37.255	501.3
297.066	91.970	104.586	580.32	3.741	75.03	0.6455	0.7341	36.228	542.6
269.553	88.268	82.604	690.24	1.852	25.51	0.6195	0.5798	43.090	268.7
273.526	89.745	84.364	676.92	2.066	32.66	0.6299	0.5921	42.259	299.7
277.459	91.364	86.439	663.13	2.296	39.74	0.6413	0.6067	41.398	333.0
281.353	93.156	88.909	648.78	2.542	46.75	0.6538	0.6240	40.502	368.7
285.212	94.859	91.588	633.74	2.804	53.69	0.6658	0.6428	39.563	406.7
289.028	96.172	94.278	617.90	3.084	60.56	0.6750	0.6617	38.574	447.3
292.794	98.441	98.484	601.13	3.380	67.34	0.6909	0.6912	37.527	490.2
296.528	101.003	103.816	583.06	3.694	74.06	0.7089	0.7287	36.399	535.8
300.215	103.408	110.276	563.39	4.027	80.70	0.7258	0.7740	35.172	584.0
303.854	106.086	119.181	541.51	4.377	87.25	0.7446	0.8365	33.806	634.9
307.438	109.485	132.956	516.40	4.746	93.70	0.7684	0.9332	32.237	688.4
310.958	113.465	157.099	485.90	5.133	100.04	0.7964	1.1026	30.334	744.4
314.409	117.980	218.689	443.79	5.537	106.25	0.8281	1.5349	27.705	803.1
271.694	89.023	83.493	683.14	1.966	29.36	0.6248	0.5860	42.647	285.1
275.649	90.590	85.430	669.56	2.188	36.48	0.6358	0.5996	41.799	317.4
279.565	92.180	87.589	655.46	2.427	43.53	0.6470	0.6148	40.919	351.9
283.438	94.020	90.257	640.76	2.681	50.50	0.6599	0.6335	40.001	388.9
287.281	95.855	93.271	625.28	2.953	57.42	0.6728	0.6546	39.035	428.3
291.080	97.212	96.287	608.92	3.242	64.26	0.6823	0.6758	38.014	470.3
294.827	99.430	100.851	591.50	3.548	71.00	0.6979	0.7078	36.926	514.6
298.541	102.148	106.966	572.59	3.873	77.69	0.7169	0.7508	35.746	561.7
302.199	104.668	114.563	551.83	4.215	84.27	0.7346	0.8041	34.450	611.3
305.807	107.922	125.921	528.37	4.575	90.77	0.7575	0.8838	32.985	663.6

Table 37. Two-Phase Heat Capacities for HFC-41 from 136 to 314 K (-215 to 106°F) (continued).

Temperature K	$C_v^{(2)}$ J/(mole•K)	C_σ J/(mole•K)	Density kg/m ³	Pressure MPa	Temperature °F	$C_v^{(2)}$ BTU/(lb•°F)	C_σ BTU/(lb•°F)	Density lb/ft ³	Pressure psia
309.361	111.724	144.228	500.71	4.954	97.16	0.7842	1.0123	31.258	718.5
312.838	116.880	182.168	465.35	5.350	103.42	0.8203	1.2786	29.051	775.9
138.763	75.233	74.270	992.64	0.001	-209.91	0.5280	0.5213	61.969	0.2
148.037	76.372	74.280	975.34	0.003	-193.22	0.5360	0.5213	60.888	0.4
156.991	77.949	74.005	958.29	0.007	-177.10	0.5471	0.5194	59.824	1.0
165.677	80.255	73.576	941.41	0.015	-161.47	0.5633	0.5164	58.770	2.1
174.111	83.666	73.261	924.66	0.028	-146.29	0.5872	0.5142	57.724	4.0
182.312	88.959	73.782	908.00	0.048	-131.53	0.6244	0.5179	56.684	7.0
190.301	94.984	73.980	891.38	0.078	-117.15	0.6667	0.5192	55.647	11.4
198.079	101.839	73.994	874.79	0.121	-103.15	0.7148	0.5193	54.611	17.5
205.655	109.735	74.093	858.19	0.177	-89.51	0.7702	0.5200	53.575	25.7
213.032	118.544	74.232	841.57	0.251	-76.23	0.8320	0.5210	52.537	36.4
220.229	129.115	75.322	824.87	0.344	-63.28	0.9062	0.5287	51.495	49.8
227.244	139.503	75.499	808.06	0.457	-50.65	0.9791	0.5299	50.446	66.3
234.091	150.323	75.427	791.10	0.594	-38.32	1.0551	0.5294	49.386	86.2
240.771	163.031	76.616	773.93	0.755	-26.30	1.1443	0.5377	48.315	109.5
247.295	175.671	77.124	756.48	0.943	-14.56	1.2330	0.5413	47.226	136.7
253.662	189.611	78.343	738.72	1.158	-3.10	1.3308	0.5499	46.117	167.9
259.881	203.752	79.153	720.53	1.401	8.10	1.4301	0.5556	44.981	203.2
265.970	218.536	79.940	701.78	1.674	19.06	1.5338	0.5611	43.811	242.8
271.914	234.463	81.197	682.40	1.977	29.76	1.6456	0.5699	42.601	286.8
277.712	252.595	83.936	662.22	2.311	40.19	1.7729	0.5891	41.341	335.2

Table 38. Vapor-Phase Sound Speed Data for HFC-41 from 249.5 to 350 K (-11 to 170°F).

Temperature K	Pressure MPa	Sound Speed m/s	Temperature °F	Pressure psia	Sound Speed ft/s
249.500	0.6914	262.52	-10.588	100.3	861.30
249.500	0.5423	267.17	-10.588	78.7	876.56
249.500	0.4104	271.09	-10.588	59.5	889.40
249.500	0.2770	274.87	-10.588	40.2	901.79
249.500	0.1382	278.66	-10.589	20.0	914.22
249.500	0.0984	279.70	-10.588	14.3	917.66
269.500	1.3738	259.94	25.412	199.3	852.84
269.500	1.0335	268.98	25.412	149.9	882.48
269.499	0.6893	277.39	25.411	100.0	910.06
269.501	0.3505	284.97	25.413	50.8	934.95
269.500	0.1712	288.69	25.412	24.8	947.14
269.500	0.1051	290.04	25.412	15.2	951.57
309.998	2.7334	269.68	98.308	396.5	884.79
310.000	2.4120	275.29	98.312	349.8	903.19
310.000	2.0706	280.96	98.312	300.3	921.77
310.000	1.7286	286.38	98.312	250.7	939.57
310.000	1.3719	291.79	98.312	199.0	957.33
310.000	1.0366	296.62	98.312	150.3	973.17
310.000	0.6857	301.57	98.312	99.5	989.41
310.000	0.5148	303.93	98.312	74.7	997.15
310.000	0.3435	306.25	98.312	49.8	1004.77
330.000	3.4382	278.00	134.312	498.7	912.09
330.000	2.7587	286.97	134.312	400.1	941.51
330.000	1.3797	303.88	134.312	200.1	996.98
330.000	0.6914	311.73	134.312	100.3	1022.72
330.000	0.5044	313.78	134.312	73.2	1029.47
330.000	0.3370	315.64	134.312	48.9	1035.57
330.000	0.1707	317.49	134.312	24.8	1041.64
350.000	3.4419	294.73	170.312	499.2	966.96
350.000	2.7612	301.47	170.312	400.5	989.08
350.000	2.0509	308.37	170.312	297.5	1011.72
350.000	1.3758	314.75	170.311	199.5	1032.64
350.000	1.0242	318.03	170.312	148.6	1043.40
350.000	0.6875	321.16	170.312	99.7	1053.68
350.000	0.5206	322.71	170.312	75.5	1058.75
350.000	0.3410	324.35	170.312	49.5	1064.14
350.000	0.1789	325.85	170.312	25.9	1069.07

A-81

Table 39. Coefficients of the MBWR Equation of State for HFC-41 [Units are K, bar, L, mol, R = 8.314471 J/(mol • K)].

$$P = \sum_{i=1}^9 a_i(T) \rho^i + \exp \left[-\left(\frac{\rho}{\rho_c} \right)^2 \right] \sum_{i=10}^{15} a_i(T) \rho^{2i-17}$$

$$\begin{aligned} a_1 &= RT \\ a_2 &= b_1 T + b_2 T^{0.5} + b_3 + b_4/T + b_5/T^2 \\ a_3 &= b_6 T + b_7 + b_8/T + b_9/T^2 \\ a_4 &= b_{10} T + b_{11} + b_{12}/T \\ a_5 &= b_{13} \\ a_6 &= b_{14}/T + b_{15}/T^2 \\ a_7 &= b_{16}/T \\ a_8 &= b_{17}/T + b_{18}/T^2 \end{aligned}$$

$$\begin{aligned} a_9 &= b_{19}/T^2 \\ a_{10} &= b_{20}/T^2 + b_{21}/T^3 \\ a_{11} &= b_{22}/T^2 + b_{23}/T^4 \\ a_{12} &= b_{24}/T^2 + b_{25}/T^3 \\ a_{13} &= b_{26}/T^2 + b_{27}/T^4 \\ a_{14} &= b_{28}/T^2 + b_{29}/T^3 \\ a_{15} &= b_{30}/T^2 + b_{31}/T^3 + b_{32}/T^4 \end{aligned}$$

b_1	-0.326441485138 x 10 ⁻¹	b_2	0.338620074694 x 10	b_3	-0.831696847103 x 10 ²	b_4	0.139589938388 x 10 ⁵
b_5	-0.156113972752 x 10 ⁷	b_6	-0.165160386413 x 10 ⁻²	b_7	0.118821153813 x 10	b_8	-0.137311604695 x 10 ³
b_9	0.176999573025 x 10 ⁶	b_{10}	0.164945271187 x 10 ⁻⁴	b_{11}	0.595329911829 x 10 ⁻¹	b_{12}	-0.341969857376 x 10 ²
b_{13}	-0.168552064750 x 10 ⁻²	b_{14}	-0.758216269071 x 10 ⁻²	b_{15}	-0.134800586220 x 10 ²	b_{16}	0.311348265418 x 10 ⁻²
b_{17}	-0.651499088798 x 10 ⁻⁴	b_{18}	0.184033192190 x 10 ⁻¹	b_{19}	-0.281459127843 x 10 ⁻³	b_{20}	-0.186344956951 x 10 ⁶
b_{21}	0.110422095705 x 10 ⁸	b_{22}	-0.147526754027 x 10 ⁴	b_{23}	0.261603025982 x 10 ⁸	b_{24}	-0.744431617418 x 10
b_{25}	0.782355157170 x 10 ³	b_{26}	-0.562784094508 x 10 ⁻²	b_{27}	-0.843317187588 x 10 ³	b_{28}	-0.600934897964 x 10 ⁻⁴
b_{29}	0.145050417148 x 10 ⁻¹	b_{30}	0.222324172533 x 10 ⁻⁷	b_{31}	-0.204419971811 x 10 ⁻⁴	b_{32}	0.245556593457 x 10 ⁻³

Critical Parameters for HFC-41 for Use with the MBWR Equation of State.

T_c	317.28 K
P_c	58.97 bar
ρ_c	316.51 kg/m ³

Ideal Gas Heat Capacity Auxiliary equation and its Coefficients for HFC-41 [Units are K and J/(mol • K)].

$$\frac{C_p^0}{R} = c_0 + c_1 T + c_2 T^2 + c_3 T^3$$

$$c_0 \quad 4.58643 \qquad c_1 \quad -9.48588 \times 10^{-3} \qquad c_2 \quad 3.96059 \times 10^{-5} \qquad c_3 \quad -2.85616 \times 10^{-8}$$

Table 40. Vapor-Liquid Equilibrium Data for R41/744 Mixtures from 218 to 290 K (-68 to 62°F).

x(R41) Liquid Mole Fraction	Temperature K	Pressure MPa	y(R41) Vapor Mole Fraction	x(R41) Liquid Mass Fraction	Temperature °F	Pressure psia	y(R41) Vapor Mass Fraction
0.000	218.00	0.551	0.000	0.000	-67.29	79.9	0.000
0.014	217.97	0.540	0.010	0.011	-67.35	78.3	0.008
0.153	217.97	0.502	0.080	0.123	-67.35	72.8	0.063
0.319	217.94	0.457	0.215	0.266	-67.40	66.2	0.175
0.433	217.99	0.430	0.316	0.371	-67.31	62.4	0.263
1.000	217.54	0.306	1.000	1.000	-68.12	44.5	1.000
0.000	230.00	0.893	0.000	0.000	-45.69	129.5	0.000
0.440	229.98	0.703	0.319	0.378	-45.73	102.0	0.266
0.473	229.97	0.693	0.350	0.410	-45.73	100.6	0.294
0.553	229.97	0.664	0.427	0.489	-45.73	96.3	0.366
0.590	229.97	0.645	0.465	0.527	-45.74	93.6	0.402
0.636	229.98	0.625	0.521	0.575	-45.73	90.7	0.457
1.000	230.00	0.509	1.000	1.000	-45.69	73.8	1.000
0.000	245.00	1.517	0.000	0.000	-18.69	220.0	0.000
0.327	244.94	1.279	0.235	0.273	-18.79	185.5	0.192
0.448	244.94	1.205	0.325	0.386	-18.80	174.7	0.271
0.520	244.94	1.155	0.408	0.456	-18.79	167.5	0.348
0.640	244.94	1.079	0.531	0.579	-18.80	156.4	0.467
1.000	245.00	0.873	1.000	1.000	-18.69	126.6	1.000
0.000	260.00	2.416	0.000	0.000	8.31	350.4	0.000
0.325	259.95	2.047	0.244	0.271	8.22	296.9	0.200
0.410	259.95	1.980		0.350	8.22	287.1	
0.555	259.95	1.824	0.449	0.491	8.23	264.5	0.387
0.666	259.95	1.711	0.569	0.607	8.22	248.1	0.505
1.000	260.00	1.406	1.000	1.000	8.31	203.9	1.000
0.000	275.00	3.655	0.000	0.000	35.31	530.1	0.000
0.410	274.94	3.003	0.316	0.350	35.21	435.6	0.263
0.489	274.94	2.883	0.409	0.425	35.21	418.2	0.349
0.586	274.94	2.738	0.502	0.523	35.21	397.2	0.438
0.672	274.94	2.605	0.584	0.613	35.21	377.8	0.520
1.000	275.00	2.150	1.000	1.000	35.31	311.9	1.000

A-83

Table 40. Vapor-Liquid Equilibrium Data for R41/744 Mixtures from 218 to 290 K (-68 to 62°F) (continued).

x(R41) Liquid Mole Fraction	Temperature K	Pressure MPa	y(R41) Vapor Mole Fraction	x(R41) Liquid Mass Fraction	Temperature °F	Pressure psia	y(R41) Vapor Mass Fraction
0.000	290.00	5.312	0.000	0.000	62.31	770.4	0.000
0.229	289.98	4.777	0.182	0.187	62.28	692.8	0.147
0.338	289.98	4.528	0.280	0.283	62.28	656.7	0.231
0.295	289.98	4.621	0.243	0.244	62.28	670.2	0.199
0.441	289.98	4.337		0.379	62.27	629.0	
1.000	289.00	3.158	1.000	1.000	60.51	458.0	1.000

Table 41. Isochoric (p, ρ ,T) Data from 192 to 400 K (-114 to 260°F) for a Mixture of R41/744 with $x(\text{R41}) = 0.49982$ Mole Fraction (0.43591 Mass Fraction).

Temperature K	Pressure MPa	Density kg/m ³	Temperature °F	Pressure psia	Density lb/ft ³
192.000	3.437	1076.33	-114.09	498.5	67.193
193.001	5.145	1076.07	-112.29	746.3	67.177
194.001	6.824	1075.73	-110.49	989.8	67.156
195.000	8.419	1075.27	-108.69	1221.1	67.127
196.001	9.851	1074.58	-106.89	1428.8	67.084
198.000	12.922	1073.63	-103.29	1874.2	67.025
200.001	16.361	1073.13	-99.69	2373.0	66.993
202.000	19.892	1072.75	-96.09	2885.1	66.970
204.001	23.450	1072.43	-92.49	3401.2	66.950
206.000	27.011	1072.13	-88.89	3917.6	66.931
207.999	30.571	1071.85	-85.29	4433.9	66.914
210.001	34.127	1071.58	-81.69	4949.7	66.897
A-85	206.002	3.417	1039.65	-88.88	64.903
	206.999	4.953	1039.41	-87.09	64.888
	208.001	6.448	1039.12	-85.29	64.870
	209.001	7.914	1038.74	-83.49	64.847
	210.002	9.273	1038.18	-81.68	64.811
	211.999	11.934	1037.13	-78.09	64.746
	214.000	14.930	1036.59	-74.49	64.712
	216.000	18.024	1036.21	-70.89	64.689
	218.000	21.152	1035.90	-67.29	64.669
	220.001	24.288	1035.61	-63.69	64.651
	221.999	27.420	1035.34	-60.09	64.634
	223.999	30.551	1035.08	-56.49	64.618
	225.998	33.676	1034.84	-52.89	64.603
	220.001	3.352	1000.69	-63.69	62.471
	221.000	4.707	1000.47	-61.89	62.458
	222.000	6.029	1000.23	-60.09	62.442
	223.000	7.340	999.93	-58.29	62.423
	224.000	8.600	999.51	-56.49	62.398
	225.999	10.951	998.42	-52.89	62.329
	227.999	13.522	997.81	-49.29	62.291
	229.999	16.207	997.42	-45.69	62.267
	232.002	18.931	997.10	-42.08	62.240

**Table 41. Isochoric (p,ρ,T) Data from 192 to 400 K (-114 to 260°F) for a Mixture of R41/744 with x(R41) = 0.49982 Mole Fraction (0.43591 Mass Fraction)
(continued).**

Temperature K	Pressure MPa	Density kg/m ³	Temperature °F	Pressure psia	Density lb/ft ³
234.001	21.667	996.82	-38.49	3142.5	62.229
236.001	24.403	996.56	-34.89	3539.4	62.213
238.000	27.139	996.31	-31.29	3936.1	62.198
240.001	29.876	996.08	-27.69	4333.2	62.183
242.001	32.606	995.85	-24.09	4729.1	62.169
244.001	35.320	995.63	-20.49	5122.8	62.155
236.002	3.454	952.92	-34.88	501.0	59.489
237.002	4.606	952.73	-33.08	668.0	59.477
238.000	5.733	952.52	-31.29	831.5	59.464
239.001	6.870	952.27	-29.49	996.5	59.448
240.000	7.980	951.96	-27.69	1157.4	59.429
242.001	10.066	950.99	-24.09	1459.9	59.369
243.999	12.188	950.28	-20.49	1767.7	59.324
246.000	14.447	949.85	-16.89	2095.4	59.297
248.001	16.744	949.53	-13.29	2428.6	59.277
250.000	19.057	949.26	-9.69	2764.0	59.260
252.001	21.371	949.00	-6.09	3099.6	59.244
254.001	23.690	948.77	-2.49	3436.0	59.230
256.000	26.008	948.55	1.11	3772.1	59.216
258.000	28.319	948.33	4.71	4107.3	59.202
260.001	30.631	948.12	8.31	4442.7	59.189
261.999	32.938	947.92	11.91	4777.3	59.177
264.000	35.241	947.72	15.51	5111.4	59.164
253.999	3.425	891.98	-2.49	496.8	55.685
255.002	4.364	891.83	-0.68	633.0	55.675
256.000	5.294	891.66	1.11	767.8	55.664
257.001	6.216	891.47	2.91	901.5	55.652
258.000	7.137	891.24	4.71	1035.1	55.638
259.998	8.921	890.61	8.31	1294.0	55.599
262.002	10.637	889.76	11.92	1542.8	55.546
264.000	12.423	889.23	15.51	1801.8	55.513
266.000	14.262	888.87	19.11	2068.6	55.490
268.000	16.124	888.59	22.71	2338.6	55.473

A-86

Table 41. Isochoric (p,p,T) Data from 192 to 400 K (-114 to 260°F) for a Mixture of R41/744 with x(R41) = 0.49982 Mole Fraction (0.43591 Mass Fraction)
(continued).

Temperature K	Pressure MPa	Density kg/m ³	Temperature °F	Pressure psia	Density lb/ft ³
270.000	17.990	888.34	26.31	2609.3	55.457
272.000	19.861	888.11	29.91	2880.6	55.443
273.998	21.734	887.90	33.51	3152.3	55.430
275.999	23.608	887.70	37.11	3424.0	55.417
278.001	25.479	887.50	40.71	3695.4	55.405
280.001	27.350	887.31	44.31	3966.8	55.393
282.000	29.220	887.12	47.91	4238.0	55.381
284.002	31.088	886.94	51.52	4509.0	55.370
286.000	32.952	886.76	55.11	4779.3	55.359
287.999	34.811	886.59	58.71	5048.9	55.348
274.000	5.219	821.73	33.51	757.0	51.299
275.000	5.939	821.58	35.31	861.4	51.290
276.000	6.661	821.41	37.11	966.1	51.279
277.999	8.087	820.99	40.71	1172.9	51.253
280.000	9.480	820.35	44.31	1375.0	51.213
282.000	10.853	819.69	47.91	1574.0	51.171
284.002	12.259	819.26	51.52	1778.0	51.145
288.001	15.134	818.70	58.71	2195.1	51.110
292.000	18.034	818.28	65.91	2615.7	51.083
296.001	20.945	817.90	73.11	3037.8	51.060
299.999	23.855	817.55	80.31	3459.9	51.038
304.001	26.773	817.21	87.51	3883.1	51.017
308.001	29.679	816.89	94.71	4304.6	50.997
312.000	32.583	816.58	101.91	4725.8	50.977
316.000	35.479	816.27	109.11	5145.9	50.958
292.000	5.946	730.54	65.91	862.4	45.606
293.000	6.461	730.42	67.71	937.1	45.598
294.001	6.976	730.28	69.51	1011.8	45.590
294.999	7.491	730.13	71.31	1086.5	45.580
296.000	8.002	729.96	73.11	1160.6	45.570
297.998	9.025	729.51	76.71	1308.9	45.542
300.000	10.036	728.95	80.31	1455.6	45.507
304.001	12.082	728.18	87.51	1752.4	45.459

A-87

Table 41. Isochoric (p, ρ ,T) Data from 192 to 400 K (-114 to 260°F) for a Mixture of R41/744 with $x(\text{R41}) = 0.49982$ Mole Fraction (0.43591 Mass Fraction)
(continued).

Temperature K	Pressure MPa	Density kg/m ³	Temperature °F	Pressure psia	Density lb/ft ³
308.002	14.158	727.76	94.72	2053.4	45.433
312.001	16.254	727.39	101.91	2357.5	45.409
316.000	18.361	727.06	109.11	2663.0	45.389
320.000	20.476	726.75	116.31	2969.9	45.369
324.000	22.588	726.44	123.51	3276.1	45.350
328.002	24.706	726.16	130.72	3583.3	45.333
332.001	26.825	725.88	137.91	3890.6	45.315
336.000	28.945	725.61	145.11	4198.1	45.298
340.001	31.063	725.34	152.31	4505.4	45.282
344.000	33.180	725.08	159.51	4812.4	45.265
302.000	7.012	670.78	83.91	1017.0	41.876
303.000	7.423	670.66	85.71	1076.7	41.868
304.000	7.835	670.51	87.51	1136.4	41.859
306.000	8.657	670.18	91.11	1255.6	41.838
307.999	9.480	669.74	94.71	1375.0	41.810
312.000	11.120	668.98	101.91	1612.8	41.763
316.002	12.794	668.50	109.12	1855.6	41.733
320.000	14.485	668.13	116.31	2100.8	41.710
324.000	16.186	667.82	123.51	2347.6	41.690
328.000	17.889	667.51	130.71	2594.6	41.671
331.999	19.607	667.23	137.91	2843.7	41.654
336.002	21.325	666.97	145.12	3093.0	41.638
340.002	23.046	666.72	152.32	3342.6	41.622
344.000	24.768	666.47	159.51	3592.3	41.606
348.001	26.491	666.22	166.71	3842.2	41.591
352.001	28.215	665.98	173.91	4092.2	41.576
356.001	29.938	665.74	181.11	4342.2	41.561
360.000	31.663	665.50	188.31	4592.3	41.546
364.000	33.385	665.26	195.51	4842.1	41.531
368.001	35.106	665.03	202.71	5091.7	41.516
312.000	7.002	468.43	101.91	1015.6	29.243
313.999	7.386	468.30	105.51	1071.2	29.235
315.998	7.774	468.16	109.11	1127.6	29.226

A-88

Table 41. Isochoric (p, ρ ,T) Data from 192 to 400 K (-114 to 260°F) for a Mixture of R41/744 with $x(\text{R41}) = 0.49982$ Mole Fraction (0.43591 Mass Fraction)
(continued).

Temperature K	Pressure MPa	Density kg/m ³	Temperature °F	Pressure psia	Density lb/ft ³
317.999	8.171	468.00	112.71	1185.2	29.216
319.998	8.571	467.81	116.31	1243.2	29.204
324.000	9.379	467.36	123.51	1360.3	29.176
327.999	10.195	466.87	130.71	1478.7	29.146
332.000	11.017	466.48	137.91	1597.9	29.121
336.000	11.845	466.17	145.11	1717.9	29.102
340.002	12.678	465.91	152.32	1838.8	29.086
344.002	13.514	465.68	159.52	1960.1	29.072
348.000	14.353	465.47	166.71	2081.8	29.059
352.000	15.193	465.28	173.91	2203.6	29.046
355.999	16.038	465.09	181.11	2326.2	29.034
360.000	16.882	464.90	188.31	2448.5	29.023
364.002	17.727	464.73	195.52	2571.1	29.012
368.001	18.574	464.55	202.71	2693.9	29.001
372.002	19.420	464.38	209.92	2816.6	28.990
379.999	21.113	464.04	224.31	3062.2	28.969
384.000	21.959	463.88	231.51	3184.9	28.959
388.000	22.804	463.71	238.71	3307.5	28.949
392.000	23.650	463.55	245.91	3430.2	28.939
395.999	24.497	463.39	253.11	3553.0	28.928
400.001	25.341	463.23	260.31	3675.4	28.918
320.000	8.116	374.46	116.31	1177.1	23.377
324.002	8.714	374.20	123.52	1263.9	23.361
328.000	9.316	373.86	130.71	1351.1	23.339
332.001	9.916	373.49	137.91	1438.2	23.316
336.001	10.516	373.16	145.11	1525.3	23.295
340.001	11.117	372.88	152.31	1612.4	23.278
348.001	12.317	372.45	166.71	1786.4	23.251
352.001	12.917	372.27	173.91	1873.5	23.240
360.001	14.116	371.93	188.31	2047.3	23.219
367.999	15.313	371.63	202.71	2221.0	23.200
372.002	15.909	371.48	209.92	2307.4	23.191
379.999	17.102	371.20	224.31	2480.4	23.173
388.000	18.293	370.93	238.71	2653.2	23.156

A-80

Table 41. Isochoric (p,p,T) Data from 192 to 400 K (-114 to 260°F) for a Mixture of R41/744 with x(R41) = 0.49982 Mole Fraction (0.43591 Mass Fraction)
(continued).

Temperature K	Pressure MPa	Density kg/m ³	Temperature °F	Pressure psia	Density lb/ft ³
392.001	18.886	370.79	245.91	2739.2	23.148
400.001	20.070	370.52	260.31	2910.9	23.131
319.999	7.575	262.49	116.31	1098.6	16.387
324.000	7.972	262.35	123.51	1156.2	16.378
328.001	8.364	262.18	130.71	1213.1	16.367
332.000	8.753	261.99	137.91	1269.5	16.356
336.001	9.138	261.77	145.11	1325.3	16.342
340.001	9.520	261.54	152.31	1380.7	16.327
347.999	10.274	261.07	166.71	1490.2	16.298
352.000	10.648	260.88	173.91	1544.4	16.286
360.001	11.391	260.55	188.31	1652.1	16.265
368.000	12.127	260.26	202.71	1758.8	16.248
372.002	12.493	260.14	209.92	1811.9	16.240
379.999	13.221	259.90	224.31	1917.6	16.225
388.002	13.945	259.68	238.72	2022.5	16.211
392.000	14.304	259.57	245.91	2074.7	16.205
400.000	15.021	259.37	260.31	2178.6	16.192
320.000	6.242	154.33	116.31	905.4	9.634
324.000	6.447	154.42	123.51	935.1	9.640
328.000	6.650	154.35	130.71	964.5	9.636
332.000	6.850	154.28	137.91	993.6	9.631
336.000	7.049	154.20	145.11	1022.4	9.627
340.000	7.246	154.13	152.31	1050.9	9.622
348.000	7.634	153.96	166.71	1107.3	9.612
352.001	7.827	153.88	173.91	1135.2	9.606
360.001	8.206	153.70	188.31	1190.2	9.595
368.001	8.580	153.50	202.71	1244.4	9.583
372.001	8.765	153.40	209.91	1271.3	9.576
379.999	9.132	153.16	224.31	1324.5	9.562
388.001	9.494	152.91	238.71	1376.9	9.546
392.002	9.673	152.79	245.92	1402.9	9.538
400.001	10.028	152.55	260.31	1454.4	9.523

Table 41. Isochoric (p, ρ ,T) Data from 192 to 400 K (-114 to 260°F) for a Mixture of R41/744 with $x(\text{R41}) = 0.49982$ Mole Fraction (0.43591 Mass Fraction)
(continued).

Temperature K	Pressure MPa	Density kg/m ³	Temperature °F	Pressure psia	Density lb/ft ³
320.001	3.637	67.16	116.31	527.5	4.193
324.002	3.710	67.14	123.52	538.1	4.191
328.000	3.782	67.11	130.71	548.6	4.190
332.000	3.854	67.09	137.91	559.0	4.188
336.001	3.925	67.07	145.11	569.3	4.187
340.001	3.996	67.04	152.31	579.6	4.185
348.002	4.137	67.00	166.72	600.0	4.182
352.001	4.207	66.97	173.91	610.1	4.181
360.001	4.345	66.92	188.31	630.2	4.178
368.001	4.482	66.88	202.71	650.1	4.175
372.001	4.551	66.85	209.91	660.0	4.173
379.998	4.686	66.80	224.31	679.7	4.170
388.000	4.821	66.75	238.71	699.2	4.167
392.000	4.887	66.72	245.91	708.8	4.165
400.001	5.020	66.67	260.31	728.2	4.162

A-91

Table 42. Summary of the Interaction Parameters for the Lemmon-Jacobsen Model for the Systems Studied in This Project.

System	Interaction Parameters for the Lemmon-Jacobsen Model		
	$k_{T,ij}$	$k_{V,ij}$	F_{ij}
R32/134a	1.0213	0.9733	-0.3737
R32/125	1.1124	0.9657	-0.9662
R125/134a	0.9927	1.0000	0.0856
R32/143a	0.9519	1.0000	-0.1242
R125/143a	1.0080	1.0000	0.0168
R143a/134a	1.0022	1.0048	0.0235
R32/290	0.7587	0.9394	-1.1135
R125/290	0.8021	1.0509	-0.4849
R134a/290	0.9183	1.1113	-3.4374
R41/744	1.0031	0.9995	-0.5329

A-92

APPENDIX B:
EXPERIMENTAL APPARATUS

Four apparatus were used to acquire the data for this project. These apparatus will be described in this section.

Vapor-Liquid Equilibrium Apparatus

A schematic diagram of the vapor-liquid equilibrium apparatus used in this project is presented in Figure B1. The apparatus is designed to allow the liquid and vapor of a fluid to come to equilibrium. Then the equilibrium pressure and temperature are measured. Also, the liquid and vapor phase compositions are measured using a gas chromatograph. The main part of the apparatus consists of an equilibrium cell, two recirculating pumps, and a platinum resistance thermometer that are contained in a dewar filled with silicone oil. The platinum resistance thermometer has been calibrated on the ITS-90. The pressure transducer and feed system are contained in an insulated box with an independent temperature control system to maintain it at a temperature above the temperature of the dewar. The pressure transducer is an oscillating quartz crystal pressure transducer calibrated in our laboratory.

One or more mixture components are introduced into the system using the feed system. The liquid and the vapor are continuously circulated to ensure that the system is well mixed. The liquid and vapor samples are withdrawn through capillary tubing to gas chromatograph sampling valves that are used to inject a small quantity of the sample into a helium stream. The helium stream carries the sample to the gas chromatograph where the mixture components are separated. The procedure for calibrating the gas chromatograph is outlined in Appendix C.

Bubble-Point and Near-Saturation (p, ρ, T) Apparatus

The apparatus used to measure the bubble-point pressures and near-saturation (p, ρ, T) data is similar to the vapor-liquid equilibrium apparatus described above. The main part of the apparatus consists of an equilibrium cell, two pumps, and two vibrating tube densimeters. These components are housed in an oven which is used to control the temperature of the system. Figure B2 shows a schematic diagram of this system. The liquid pump is located outside of the system and is used when the system is above room temperature.

The system can either be filled with a standard mixture of known composition, or the liquid composition can be measured. The liquid and the vapor are continuously circulated to ensure that the system is well mixed. Once the system is equilibrated, the temperatures of the main cell and both densimeters are measured, the pressure of the system is recorded, and both the liquid and vapor densities are recorded. The composition of the vapor phase is calculated from the vapor-liquid equilibrium data from the VLE apparatus described above. It is assumed that the vapor composition is that of the vapor in equilibrium with the liquid which is at the temperature and pressure of the main cell. The reason the vapor composition is not measured directly is because the temperature gradients in this apparatus adversely affect the vapor composition determination.

Isochoric (p, ρ, T) Apparatus

An isochoric technique was employed to measure the single-phase densities in this study. In this method, a sample of fixed mass is confined in a container of nearly fixed volume. The volume of the container is accurately known as a function of pressure and temperature. The temperature is changed in selected increments, and the pressure is measured at each temperature, until the upper limit of either temperature (400 K (260°F)) or pressure (35 MPa (5100 psia)) was attained. When an isochoore is completed, that is, after the upper temperature or pressure limit of the run has been reached, the sample is condensed into a light-weight stainless steel cylinder which is immersed in liquid nitrogen. When the (p, ρ, T) cell and its connecting capillary have been heated to about 20 K (36°F) above the critical temperature of the sample, the cylinder is sealed, warmed to ambient temperature, and weighed. The density of the test fluid is then determined from a knowledge of the cell volume and of the mass difference of the steel cylinder before and after trapping the sample. Allowances to account for the noxious volumes in the system, such as those of the capillaries and the

pressure gauge, are made for each point. A small adjustment to the apparent sample mass was made to account for the change in atmospheric buoyant force acting on the steel cylinder. The density of the sample fluid is then the quotient of the mass of the sample and the volume of the cell at each pressure and temperature.

The sample cell, shown in Figure B3, is a cylindrical piece of electrolytic tough pitch copper containing a cavity with a volume of approximately 28.5 cm^3 (1.74 in^3). It is suspended inside an evacuated cryostat from a thin-walled stainless steel tube used for reflux cooling. High resistance wire wound tightly around the cell is used to heat the cell. The cell temperature is determined with a platinum resistance thermometer (calibrated at NIST relative to the IPTS-68, with temperatures converted to the ITS-90) embedded in a small well at the top of the cell. An ultrastable current source supplies the thermometer with a current of 2 mA. Errors caused by steady-state thermal and contact EMF's are minimized by averaging voltages measured for opposite directions of current flow. The temperatures were controlled and reproduced within 1 mK (0.0018°F). The total uncertainty in the temperature ranged from 10 mK at 100 K to 30 mK at 400 K (0.018°F at -279.7°F to 0.054°F at 260°F).

Pressures are measured by reading the period of vibration, averaged over 10 s, of an oscillating quartz crystal transducer which is connected to the sample cell through a fine diameter (0.2 mm i.d. (0.008 in. i.d.)) capillary. Since the frequency of the transducer varies with temperature, the transducer has been anchored in an insulated aluminum block controlled at $333.15 \pm 0.05 \text{ K}$ ($139.98 \pm 0.09^\circ\text{F}$). The transducer has been calibrated with an oil-lubricated piston gauge, accurate within $\pm 0.01\%$. Calibrations have demonstrated that the transducer is extremely stable over long periods of time. Changes of less than 0.003% were observed over one year. The expanded uncertainty in the pressure measurements is approximately 0.01% for pressure greater than 3 MPa (435 psia), but increases to 0.05% at low pressures (1 MPa (145 psia) and lower) as a result of the transducer resolution, of the fluctuations in the temperature of the pressure transducer, and of the occasional hysteresis in the vibrational frequency of the quartz element.

Adiabatic Constant Volume Calorimeter

The principal components of the calorimeter used for these measurements are shown in Figure B4. A spherical bomb contains a sample of well-established mass. The volume of the bomb, approximately 73 cm^3 (4.6 in^3), is known as a function of temperature and pressure. A platinum resistance thermometer is attached to the bomb for the temperature measurement. Temperatures are reported on the ITS-90, after conversions from the original calibration on the IPTS-68. Pressures are measured with an oscillating quartz crystal pressure transducer with a 0-70 MPa (0-10000 psia) range. Adiabatic conditions are ensured by a high vacuum ($3 \times 10^{-3} \text{ Pa}$ ($4.4 \times 10^{-4} \text{ psia}$)) in the can surrounding the bomb, by a temperature-controlled radiation shield, and by a temperature-controlled guard ring which thermally anchors the filling capillary and the lead wires to the bomb.

For heat capacity measurement, a precisely determined electrical energy (Q) is applied and the resulting temperature rise ($\Delta T = T_2 - T_1$) is measured. We obtain the heat capacity from

$$C_v = \left(\frac{\delta U}{\delta T} \right)_v \approx \frac{Q - Q_0 - W_{pv}}{n\Delta T}, \quad (\text{B1})$$

where U is the internal energy, Q_0 is the energy required to heat the empty calorimeter, W_{pv} is the change-of-volume work due to the slight dilation of the bomb, and n is the number of moles contained in the bomb. In this work, the bomb was charged with sample up to the (p, T) conditions of the highest-density isochore. The bomb and its contents were cooled to a starting temperature in the single-phase liquid region. The measurements were performed with increasing temperature until either the upper temperature (345 K (161°F)) or pressure limit (35 MPa (5076 psia)) was attained. At the completion of a run, a small part of the sample was cryopumped into a lightweight cylinder for

weighing. The next run was started with a smaller density. A maximum of eight runs was measured with one filling of the bomb. When the runs were completed, the remaining sample was discharged and weighed. A series of such runs from different fillings completes the investigation of the (p,T,C_v) surface.

Spherical Resonator Sound Speed Apparatus

Accurate data of the speed of sound of a gas, in our case a refrigerant gas, are obtained from measurements of the resonant frequencies produced in a stainless steel spherical cavity containing the gas. Measurements of several radial modes are taken at a very stable temperature and pressure. The speed of sound is computed from the frequency at each of the modes and an average is taken. The sphere radius used in the computation of the speed of sound is found from similar measurements of the radial modes using argon. Highly accurate properties of argon gas, including the speed of sound, are found in the work of M. Moldover, et al. [Moldover, M. R., Mehl, J. B., and Greenspan, M., *J. Acoust. Soc. Am.* **79**, 2, (1986)]. Also included in this reference is a detailed description of the theory of operation of the spherical resonator.

The spherical steel cavity is mounted in a pressure vessel which also contains the gas. This vessel is surrounded by a temperature shield and is housed in a cryostat which provided cooling for reduced temperatures. The pressure vessel has been designed for operation at pressures up to 3.5 MPa (500 psia) and temperatures from 249 K to 350 K (-11.5 to 170.3°F). Figure B5 shows a schematic diagram of this apparatus.

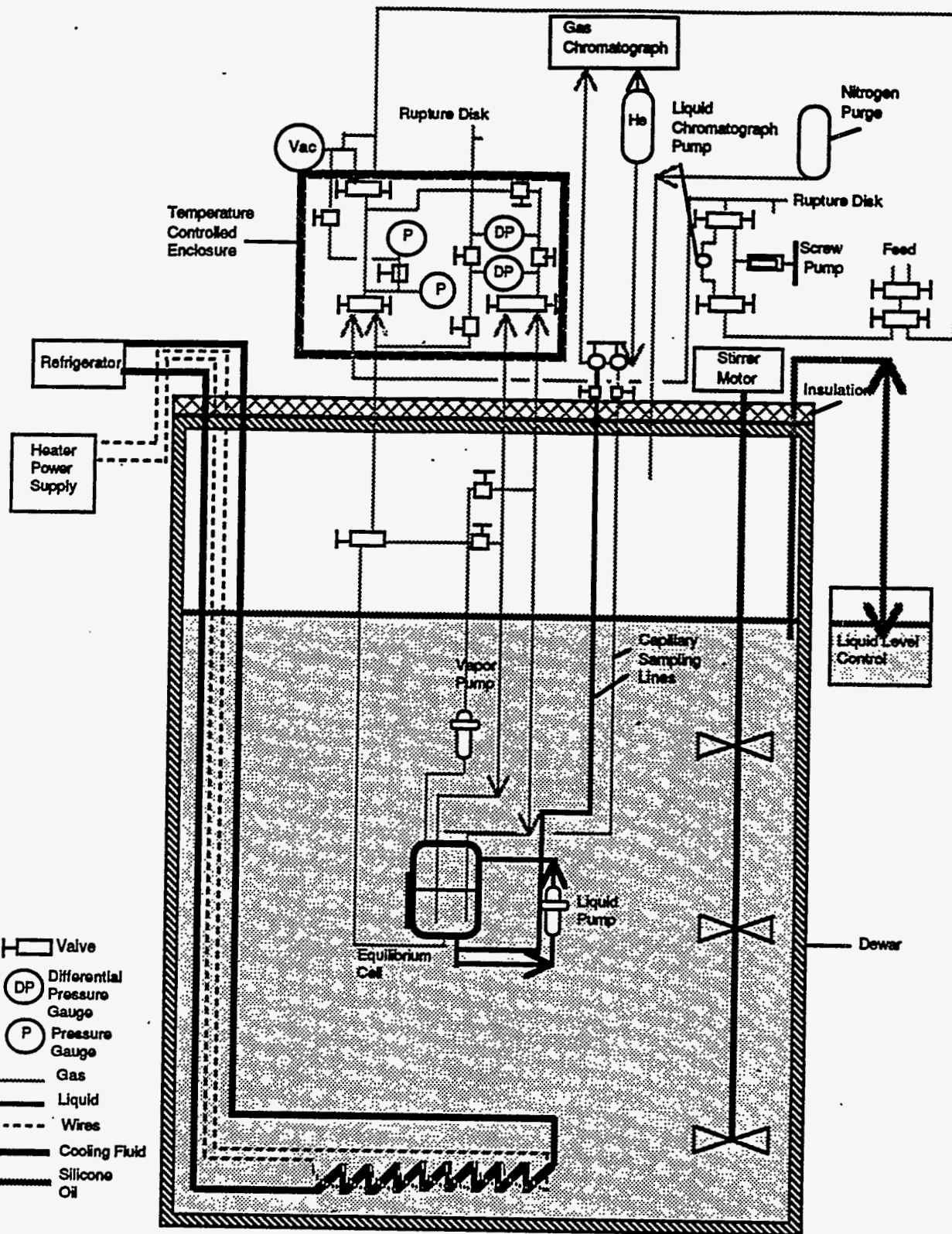


Figure B1. Schematic Diagram of the Dynamic Phase Equilibria Apparatus.

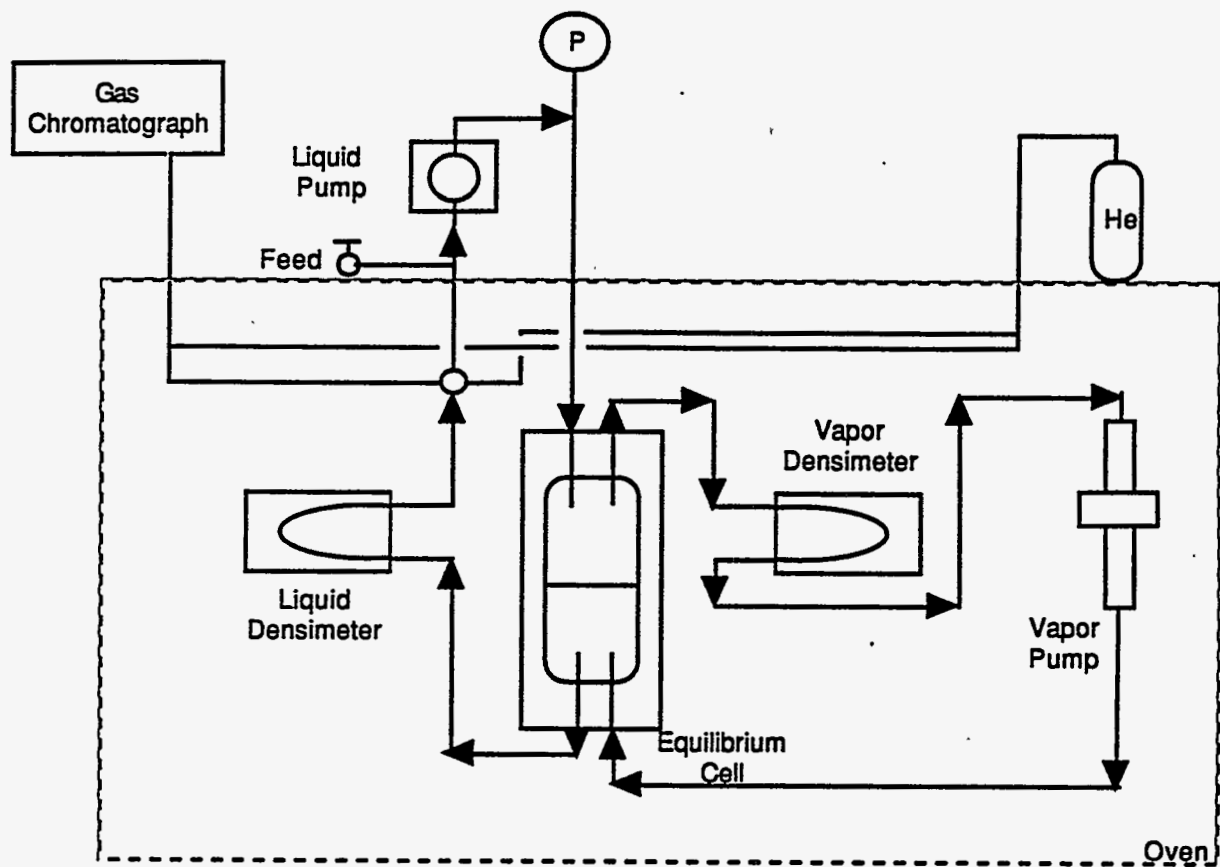


Figure B2. Schematic Drawing of Bubble-Point and Near-Saturation
(p, p, T) Apparatus

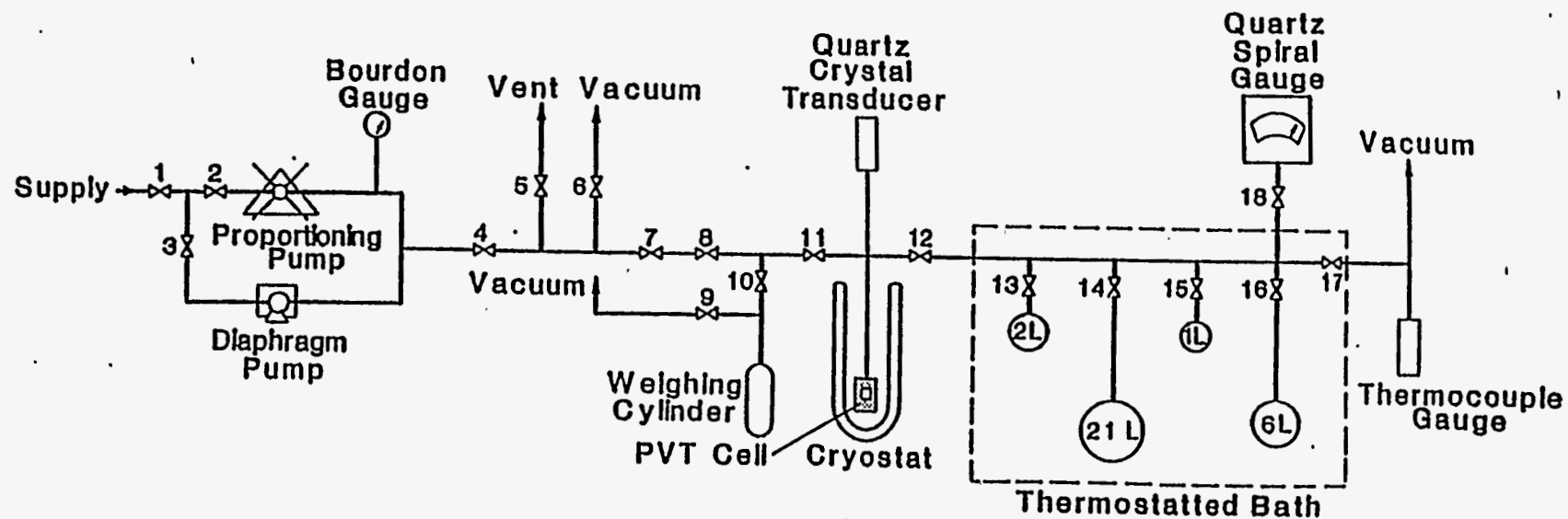


Figure B3. Schematic Diagram of the Isochoric (p,p,T) Apparatus.

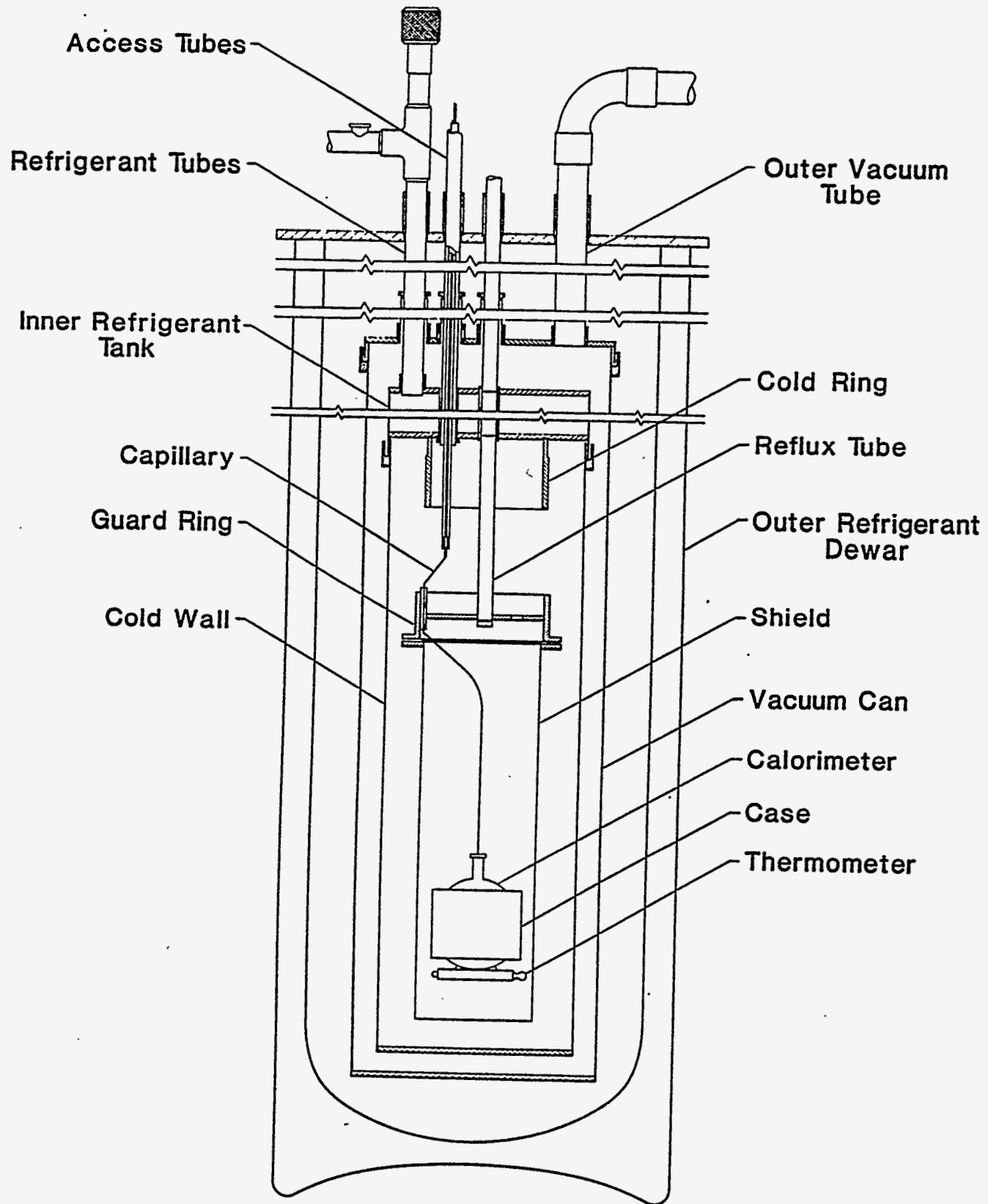


Figure B4. Schematic Diagram of the Calorimeter.

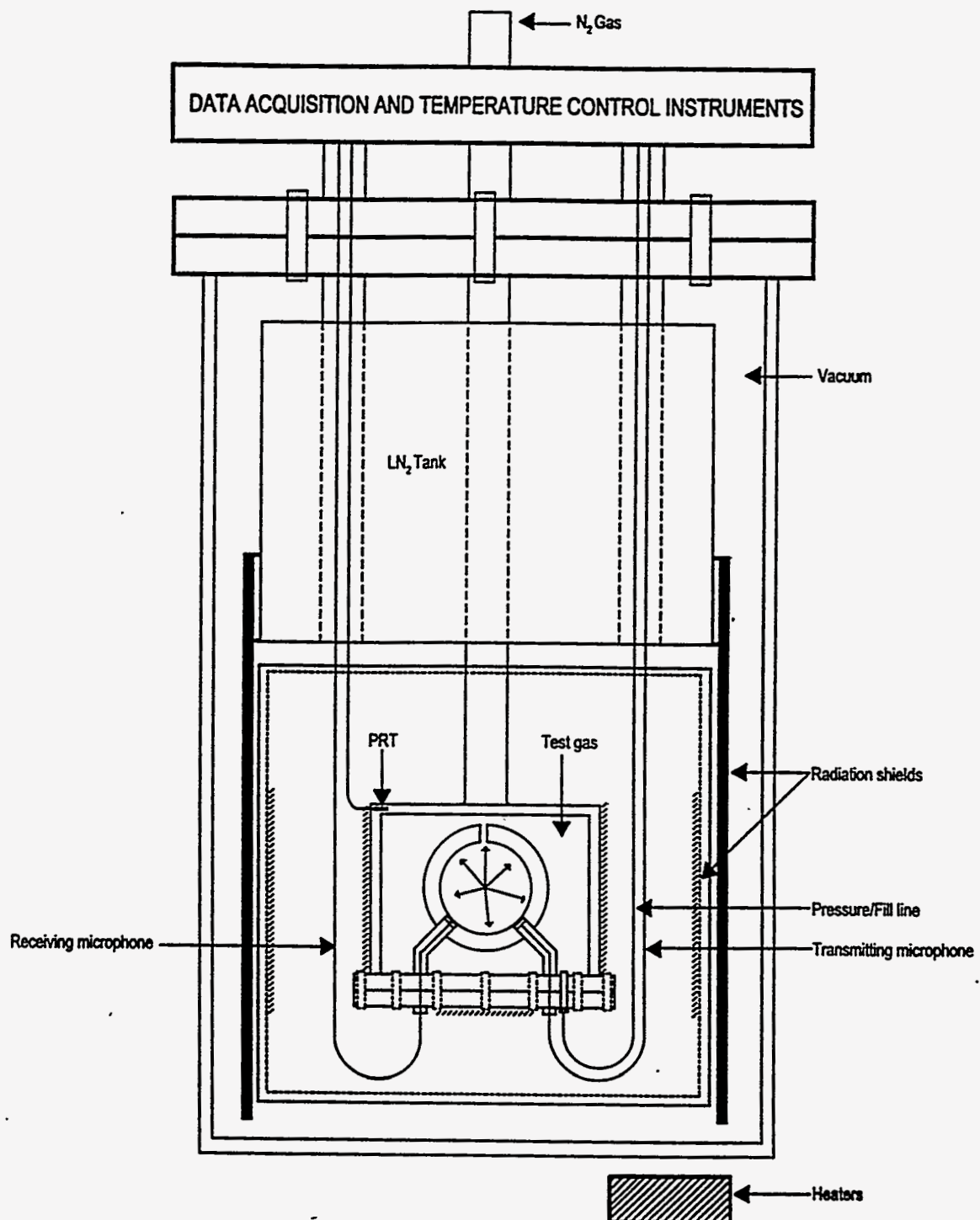
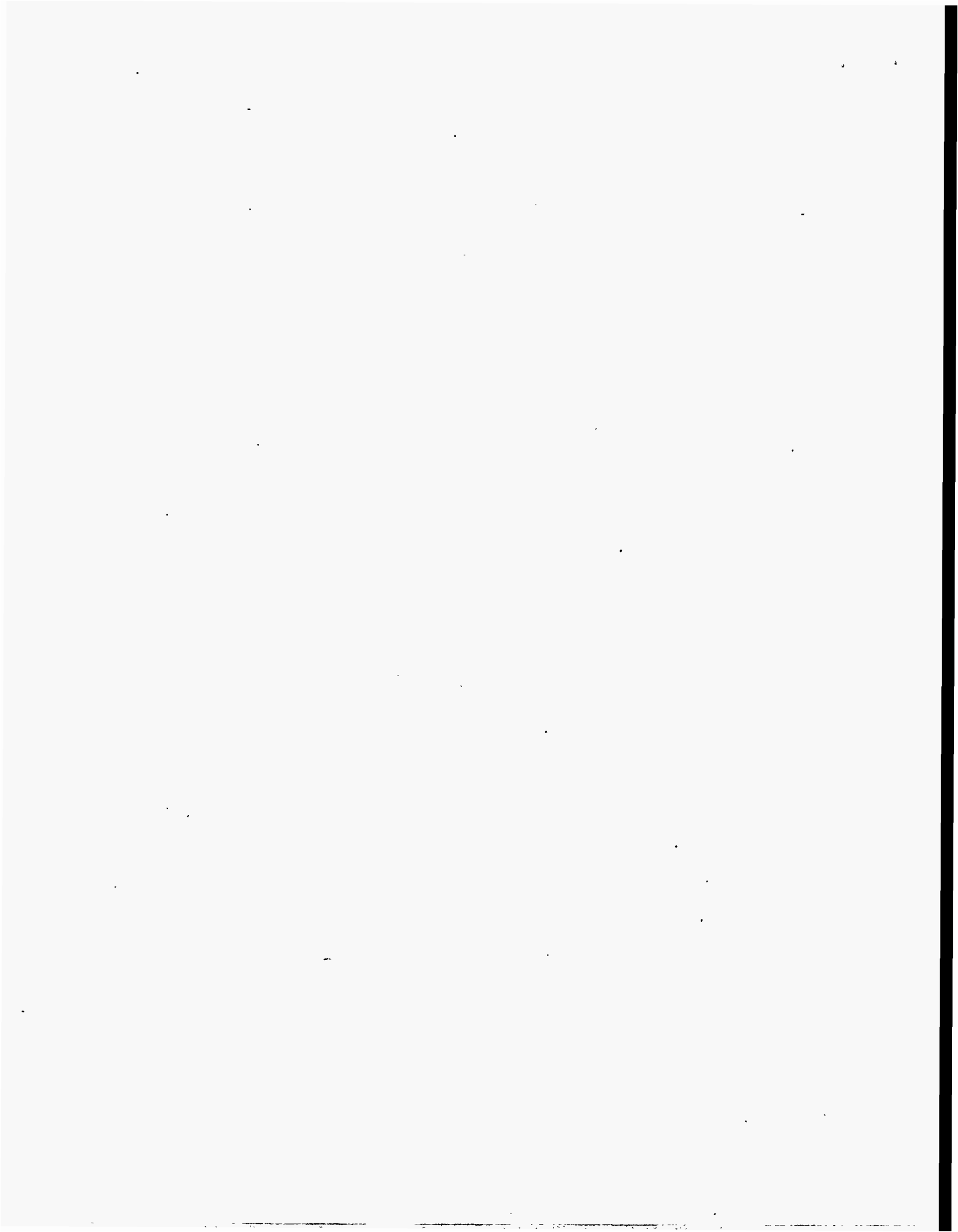


Figure B5. Schematic Diagram of Spherical Resonator Sound Speed Apparatus



APPENDIX C:
ESTIMATES OF STATE-POINT UNCERTAINTIES

A state point is a group of parameters that uniquely specifies a point in a system such that there are no degrees of freedom. For a binary system, if there are two phases in equilibrium and the temperature and liquid composition (the independent parameters) are known, the state point is specified. The bubble-point pressure, vapor composition, densities, viscosity, surface tension, and many other dependent properties are functions only of the temperature and liquid composition along the two-phase boundary. Therefore, any uncertainties in the temperature and liquid composition directly affect the uncertainty of the dependent properties. Unlike the measurement of an individual parameter where the uncertainty is a function of only the calibration and measurement technique, the state-point uncertainty also depends on the relations among the measured parameters.

The bubble-point pressure state-point uncertainty is defined as the uncertainty of the bubble-point pressure given the uncertainty of the liquid composition measurement, the uncertainty of the temperature measurement, the change of the bubble-point pressure with temperature and composition, and the uncertainty in the pressure measurement. The bubble-point pressure state-point uncertainty can be estimated using Equation (C1).

$$\pm \Delta P_{\sigma} = \pm \left[\left| \left(\frac{\delta P_{\sigma}}{\delta x} \right)_T \cdot \Delta x \right| + \left| \left(\frac{\delta P_{\sigma}}{\delta T} \right)_x \cdot \Delta T \right| + |\Delta P| \right] \cdot \frac{100}{P} \quad (C1)$$

where

- P_{σ} = bubble point pressure,
- ΔP_{σ} = bubble-point state-point pressure uncertainty in percent,
- x = measured liquid composition,
- Δx = liquid-composition uncertainty,
- T = measured temperature,
- ΔT = temperature measurement uncertainty,
- P = measured pressure, and
- ΔP = pressure measurement uncertainty.

The partial derivatives can be calculated using either the experimental data or an equation of state.

The uncertainty of the vapor-composition state-point is a function of temperature , liquid composition, and the interdependence of the parameters. It can be determined with a calculation similar to that of the bubble-point pressure state-point uncertainty. The expression for the vapor-composition state-point uncertainty is shown in Equation (C2).

$$\pm \Delta y_{\sigma} = \pm \left[\left| \left(\frac{\delta y_{\sigma}}{\delta x} \right)_T \cdot \Delta x \right| + \left| \left(\frac{\delta y_{\sigma}}{\delta T} \right)_x \cdot \Delta T \right| + |\Delta y| \right] \quad (C2)$$

where

- y_{σ} = equilibrium vapor composition,
- Δy_{σ} = vapor-composition state-point pressure uncertainty,
- x = measured liquid composition,
- Δx = liquid-composition uncertainty,
- T = measured temperature,
- ΔT = temperature measurement uncertainty,
- y = measured vapor composition, and
- Δy = vapor-composition measurement uncertainty.

The uncertainty of the density state point is a function of temperature , composition, and the interdependence of the parameters. It can be determined with a calculation similar to that of the bubble-point pressure state-point uncertainty. The expression for the density state-point uncertainty is shown in Equation (C3).

$$\pm \Delta \rho_{\sigma} = \pm \left[\left| \left(\frac{\delta \rho_{\sigma}}{\delta c} \right)_T \cdot \Delta c \right| + \left| \left(\frac{\delta \rho_{\sigma}}{\delta T} \right)_c \cdot \Delta T \right| + |\Delta \rho| \right] \cdot \frac{100}{\rho} \quad (C3)$$

where

- ρ_{σ} = state-point density,
 $\Delta \rho_{\sigma}$ = density state-point pressure uncertainty in percent,
 c = measured liquid or vapor composition,
 Δc = liquid or vapor composition measurement uncertainty,
 T = measured temperature,
 ΔT = temperature measurement uncertainty,
 ρ = measured density, and
 $\Delta \rho$ = density measurement uncertainty.



APPENDIX D:
GAS CHROMATOGRAPH CALIBRATION PROCEDURES

The gas chromatograph calibration procedure involves six steps. The first step is the preparation of two or three standard mixtures for each system. These mixtures are used to determine which GC column to use, to refine the calibration, and to check the sampling system for adsorption or mixing problems. The number of mixtures needed is dependent on the type of GC column used to separate the two components. A short-packed column usually requires two standard mixtures. A capillary column or long-packed column requires three or more mixtures due to the complex behavior of adsorption and desorption along the length of the column.

In the second step, the standard mixtures are used to determine which GC column best separates the two components and what are the appropriate settings on the GC. Table D1 summarizes the GC columns and settings used for each of the systems in this report.

In the third step of the procedure, density-versus-area data are obtained for the pure components from the GC. A specific volume is chosen for injection of the sample into the GC. This volume is filled at different pressures of the pure fluid in a region where the virial equation for the pure fluid can accurately predict the density. The pressure and temperature of the standard volume are recorded before each injection. The density of the injected gas is calculated from the virial equation of state.

The fourth step of the procedure characterizes any peak interaction or sample size dependence by injecting different quantities of the standard mixtures into the GC. The same sample volume used for the pure fluids is filled to different pressures with the standard mixtures. The area-percent-versus-sample-size data are recorded.

The fifth step is determining the correct calibration equation to use with the calibration data. For short-packed columns the area percent of the GC peaks should be independent of the amount of the standard mixture injected. The calibration equation for this type of column is based on combining the area-versus-density data of the two pure components. Usually the area-versus-density relationships for each of the pure components can be represented by a simple quadratic equation. The standard mixture data is used to optimize the fit and to check the accuracy of the equation.

A capillary column or long-packed column shows a dependence of area percent on the sample size injected. The calibration equations for these systems are more complicated than for short-packed columns because they include a size dependence as well as a composition dependence that requires all of the mixture and pure component data to be used in the fit. The procedure is more complicated than the procedure for a short-packed column, but is necessary in order to obtain accurate results.

The final step checks the sampling system for losses due to adsorption or inhomogeneous sampling. The apparatus is filled with one of the standard mixtures and several samples are analyzed using the sampling system. The composition calculated from the GC should be the same as the composition of the standard mixture. If the composition is not the same as the standard mixture, one of the components may be adsorbing to the walls of the sampling system or the sample is not well mixed before it reaches the GC.

The GC calibration is only accurate within the peak area range of its calibration. If the samples withdrawn from the system are too large or too small, the calculated compositions will be in error. The size of the sample withdrawn from the apparatus must be adjusted to stay within the limits of the calibration.

Table D1. Summary of the Gas Chromatograph Settings, the Separation Columns, and the Standard Reference Mixtures Used for Each Refrigerant System.

System	Column	Column Head Pressure MPa (psi)	Sample Flow cm ³ /min (in ³ /min)	Carrier Flow cm ³ /min (in ³ /min)	Oven Temperature K(°F)	Injector Temperature K(°F)	Detector Temperature K(°F)	Standard Mixtures Mole Fraction(Mass Fraction)	
R32/134a	A	0.35(50.7)	30(1.8)	40(2.4)	283.2(50.1)	373.2(212)	398.2(257)	0.35/0.65(0.22/0.78) 0.65/0.35(0.49/0.51)	
R32/125	A	0.35(50.7)	30(1.8)	40(2.4)	283.2(50.1)	373.2(212)	398.2(257)	0.35/0.65((0.19/0.81) 0.65/0.35(0.45/0.55)	
R125/134a	B	0.25(22)	-	-	323.2(122)	353.2(176)	363.2(194)	0.35/0.65(0.39/0.61) 0.50/0.50(0.54/0.46) 0.65/0.35(0.69/0.31)	
R32/125/134a	B	0.25(22)	-	-	323.2(122)	353.2(176)	363.2(194)	0.20/0.20/0.60(0.11/0.25/0.64) 0.20/0.60/0.20(0.10/0.70/0.20) 0.60/0.20/0.20(0.41/0.32/0.27)	
D-3	R32/143a	A	0.25(50.7)	30(1.8)	40(2.4)	303.2(86.0)	373.2(212)	398.2(257)	0.35/0.65(0.25/0.75) 0.65/0.35(0.53/0.47)
	R125/143a	C+D	0.15(29.2)	25(1.5)	15(0.9)	323.2(122)	353.2(176)	363.2(194)	0.35/0.65(0.43/0.57) 0.50/0.50(0.59/0.41) 0.65/0.35(0.73/0.27)
	R143a/134a	B	0.15(36.7)	-	-	323.2(122)	353.2(176)	363.2(194)	0.35/0.65(0.31/0.69) 0.50/0.50(0.45/0.55) 0.65/0.35(0.60/0.40)
	R32/290	A	0.25(50.7)	30(1.8)	40(2.4)	303.2(86.0)	373.2(212)	398.2(257)	0.35/0.65(0.39/0.61) 0.65/0.35(0.69/0.31)
	R125/290	A	0.25(50.7)	30(1.8)	40(2.4)	283.2(50.1)	373.2(212)	398.2(257)	0.35/0.65(0.59/0.41) 0.65/0.35(0.83/0.17)
	R134a/290	A	0.25(50.7)	30(1.8)	40(2.4)	283.2(50.1)	373.2(212)	398.2(257)	0.35/0.65(0.55/0.45) 0.65/0.35(0.81/0.19)
	R41/744	C	0.35(50.7)	30(1.8)	40(2.4)	293.2(68.0)	373.2(212)	398.2(257)	0.50/0.50(0.44/0.56)

Separation Columns

A - 10 ft x 1/8 in SPAL 5% Fluorcol 60/80 Carbopak B

B - 30 m x 0.32 mm GS(Q)

C - 6 ft x 1/8 in Porapak Q 80/100

D - 2 ft x 1/8 in Carbograph1 60/80

